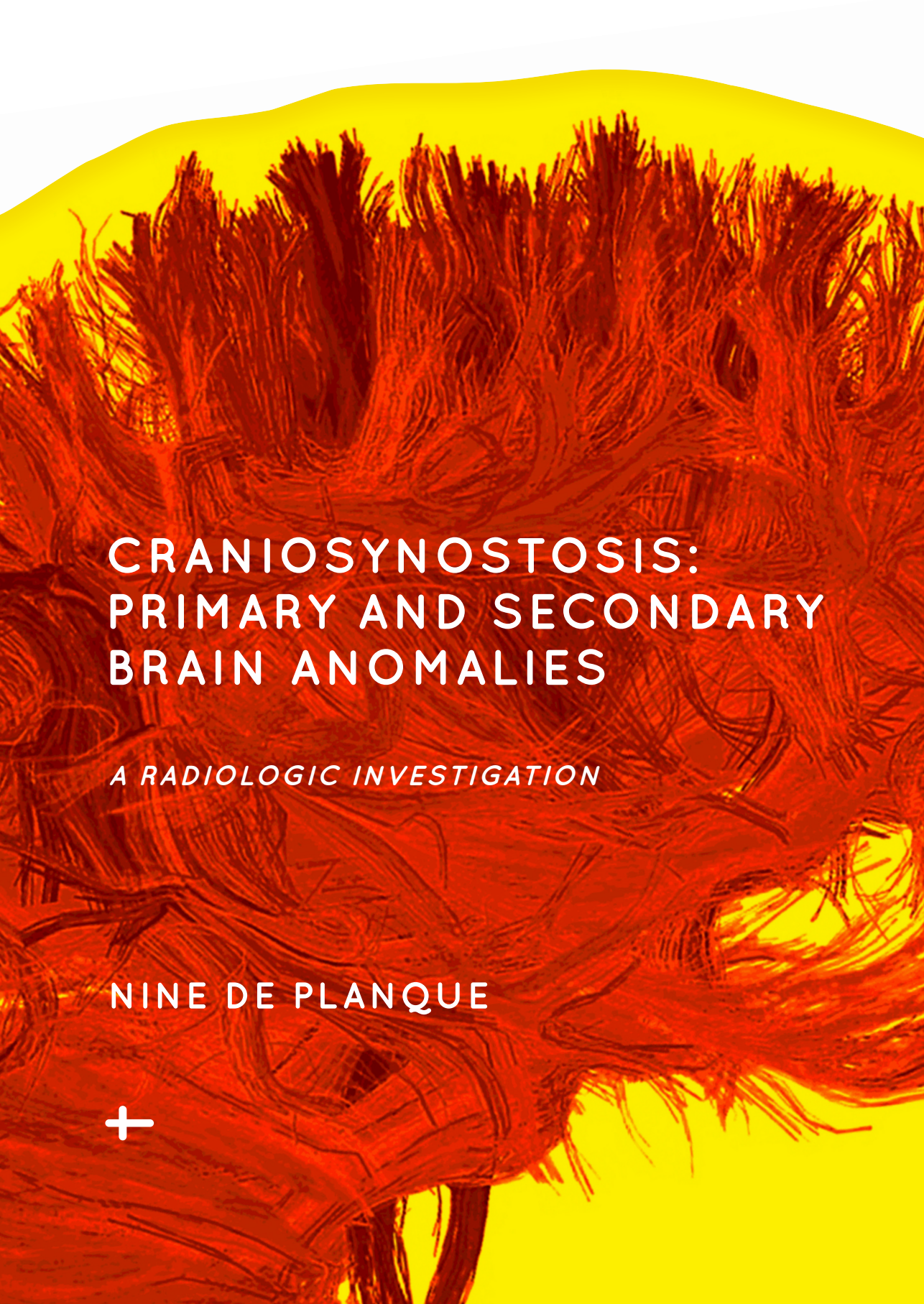

CRANIOSYNOSTOSIS: PRIMARY AND SECONDARY BRAIN ANOMALIES

A RADIOLOGIC INVESTIGATION

NINE DE PLANQUE

Craniosynostosis: primary and secondary brain anomalies

A radiologic investigation

C.A. de Planque

Colofon

The studies described in this academic dissertation were performed at the Craniofacial Research Unit of the Department of Plastic and Reconstructive Surgery, Erasmus University Medical Center, Rotterdam, The Netherlands. The research has been supported by a grant of the Sophia Stichting Wetenschappelijk Onderzoek (project number: B-16-03a). The production of this book has been financially supported by Landelijke Patienten- en Oudervereniging voor Schedel- en/of Aangezichtsaandoeningen (LAPOSA) and the Traumaplatform Foundation.

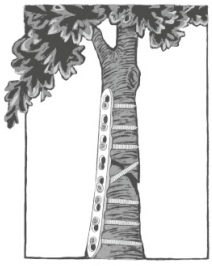

Provided by thesis specialist Ridderprint, ridderprint.nl

Author:	C.A. de Planque
Printing:	Ridderprint
Layout and design:	Eduard Boxem, persoonlijkproefschrift.nl
Book Cover:	Robin Edelkoort
Cover Lay Out:	Robin Edelkoort
ISBN:	978-94-6458-727-2

Craniosynostosis: primary and secondary brain anomalies
A radiologic investigation

Proefschrift

Craniosynostose: intrinsieke en extrinsieke brein afwijkingen
Een radiologisch onderzoek

Ter verkrijging van de graad van doctor aan de Erasmus Universiteit Rotterdam
op gezag van de rector magnificus
prof.dr. A.L. Bredenoord
en volgens besluit van het College voor Promoties

De openbare verdediging zal plaatsvinden op
9 december 2022

door

Catherine Annemiek de Planque
geboren te Rotterdam

Erasmus University Rotterdam

PROMOTIECOMMISSIE

Promotor:	Prof. Dr. I.M.J. Mathijssen
Overige leden:	Prof. Dr. M. de Bruijne
	Prof. Dr. C.M.F. Dirven
	Prof. Dr. R.C. Tasker
Copromotor:	Dr. M.L.C. van Veelen

INDEX

Aan mijn ouders.

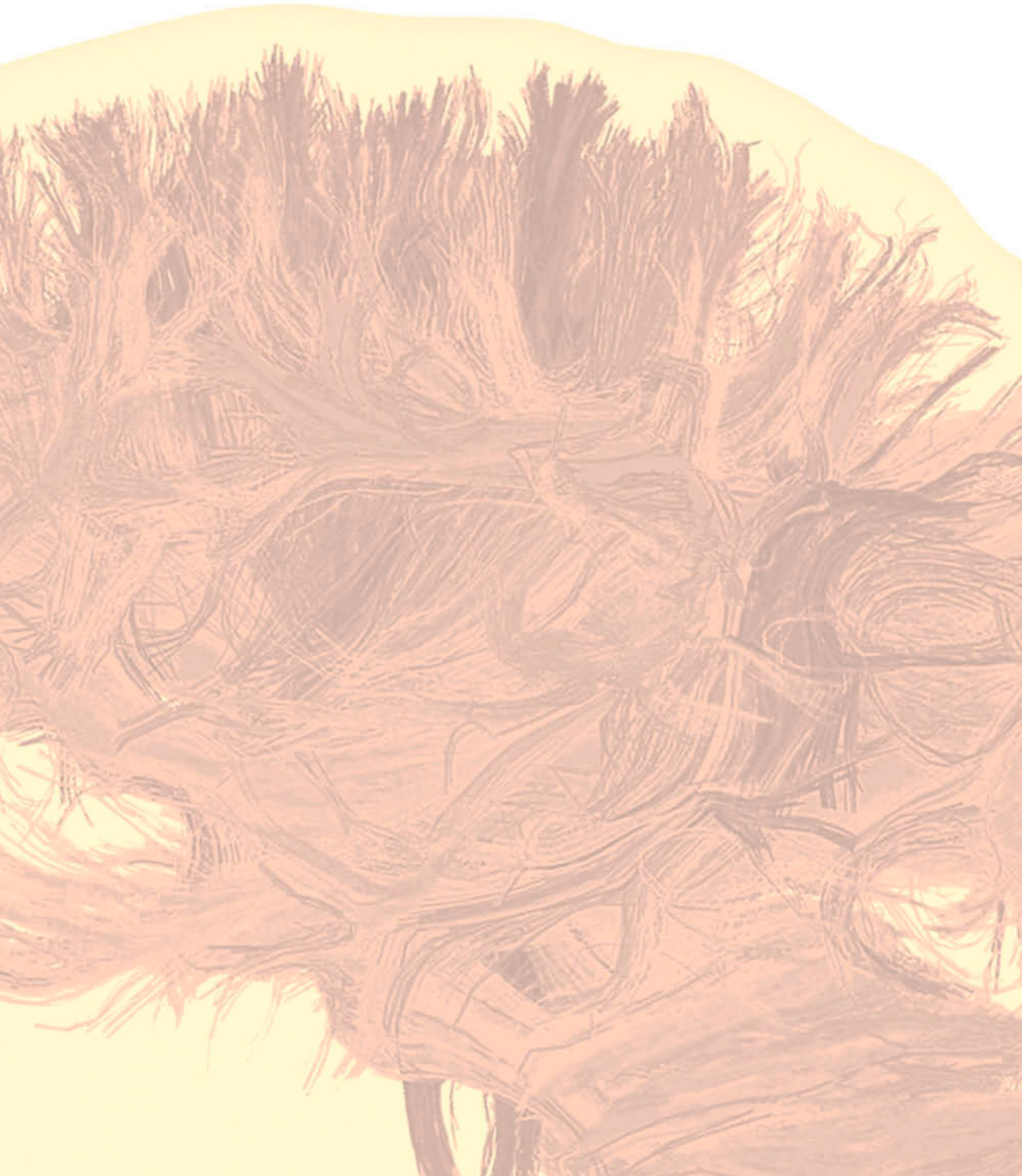

CHAPTER 1

GENERAL INTRODUCTION

INTRODUCTION

This thesis focuses on brain anomalies in children with isolated or syndromic craniosynostosis that arise either as a primary brain development disorder or secondary to disturbed skull growth. Affected children have a higher prevalence of neurocognitive impairment and are at risk to develop intracranial hypertension (ICH), which could further impair cognitive development, cause behavioural issues, and could cause visual loss by damaging the optic nerves.[1-3] [4] The most important aim of surgical treatment is to strive for best possible neurocognitive outcome by reducing the risk of developing ICH. The pathogenesis of ICH and its interconnected problems, such as hydrocephalus and herniation of the cerebellar tonsils through the foramen magnum, is multifactorial and still ill understood.

This thesis seeks to differentiate between primary and secondary brain anomalies in children with craniosynostosis in a search to determine best treatment strategy. Identification of primary, inborn disorders of the brain can prevent overtreatment, as it is unlikely that surgery will be of benefit. On the other hand, the identification of secondary brain disorders and their impact on outcome can guide us to a better screening policy with earlier treatment to prevent these sequelae. Better understanding of the consequences of ICH on brain development will be the scientific basis of treatment protocols, that strive to improve the quality of life of the patients.

This thesis will be focusing on answering the following questions:

- To what extent do primary brain abnormalities exist in non-operated isolated and syndromic craniosynostosis, looking at intracerebral blood flow and brain microstructures? (**Part I**)

- Are there any secondary effects of ICH and treatment on the brain of operated syndromic craniosynostosis patients, focusing on ventriculomegaly, Chiari and cortical thickness? (**Part II**)

In this introduction, craniosynostosis, intracranial hypertension, cognitive outcome and the used types of imaging are set out, finalized by an outline of each study.

Craniosynostosis

A newborns' cranial vault consists of seven bones, which are separated by the metopic, two coronal, the sagittal and two lambdoid sutures.[5] These open sutures allow for transient skull distortion during birth and facilitate future growth of the brain. In the first years of life, brain growth is the main incentive of skull growth. Craniosynostosis refers to this premature closure of the skull sutures, which mainly occurs around the 15th-19th week of gestation resulting in an abnormal skull shape.[6, 7] The prevalence of

craniosynostosis is 7.2 per 10.000 live born children in the Netherlands.[8] There are three types of craniosynostosis: isolated, unisutural craniosynostosis, multisutural/complex craniosynostosis and syndromic craniosynostosis. The majority of craniosynostosis is isolated, defined as the fusion of a single suture without other congenital abnormalities (**Figure 1**).

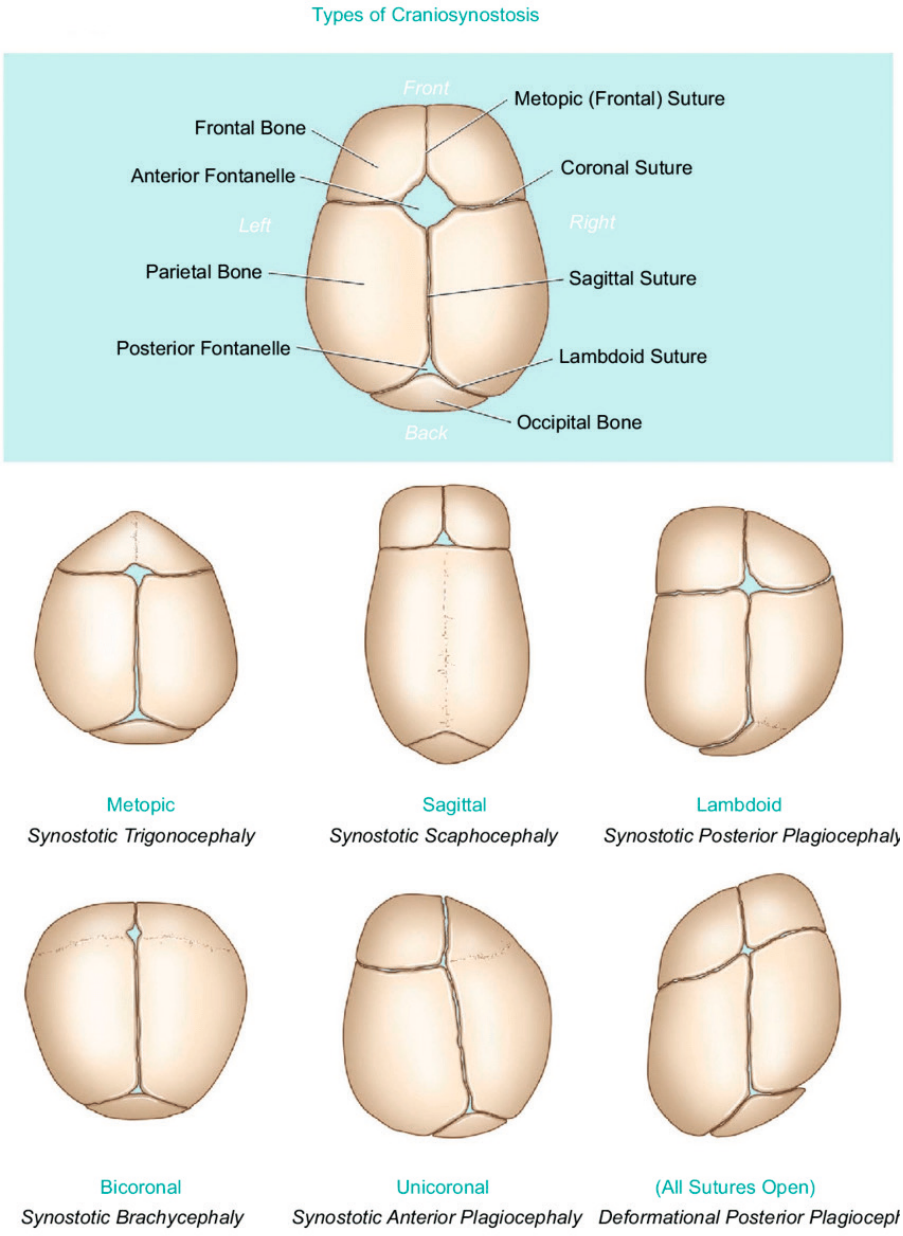

Figure 1. Types of single suture craniosynostosis

Examples of single suture synostosis include scaphocephaly (sagittal suture synostosis), trigonocephaly (metopic suture synostosis) and posterior plagiocephaly (lambdoid suture synostosis). When two of more skull sutures are fused without any other congenital abnormalities, it is defined as multisutural/complex craniosynostosis. In 24% of the cases, craniosynostosis is syndromic, which means single (usually the coronal suture) or multiple skull sutures are fused in combination with additional congenital abnormalities, such as facial anomalies and malformations of the hands and feet.[9] Syndromic craniosynostosis is caused by mutations in various genes.[9] The most distinct craniosynostosis syndromes are: Apert, Crouzon-Pfeiffer, Muenke and Saethre-Chotzen syndromes. The diagnosis of craniosynostosis is primarily made based on the anamnesis and physical examination and confirmed by a 3D-CT scan.[10, 11]

Intracranial pressure

According to the Monro-Kellie doctrine, the cranial vault is a closed box and contains the sum of the 3 main components of intracranial volume: brain tissue, intracerebral blood, and cerebrospinal fluid (CSF) (**Figure 2a**).[12] The intracranial pressure (ICP) represents the net effect of intracranial volume and content, brain compliance, plus blood- and cerebrospinal fluid dynamics in this closed box.[13 14] If there is a conflict between growth in brain volume and skull restriction, it has its effect on the brain, cerebral blood volume (CBV), CSF and in consequence on the ICP.[15-17]

As the brain grows in a fused fault, brain growth and arterial blood supply will be maintained as much as possible, depending on compensatory mechanisms like relocating CSF to the spinal compartment and faster discharge of blood to the extra cranial compartment by collaterals (**Figure 2b**). In patients with craniosynostosis, skull growth may be reduced while both compensatory mechanisms may fail.

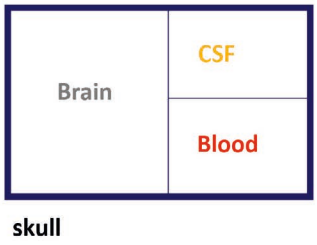

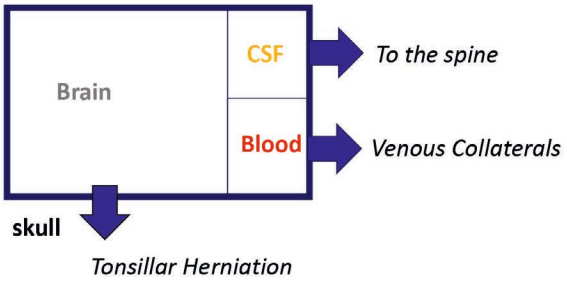

Figure 2a.) Craniosynostosis Brain **Figure 2b.)** Craniosynostosis brain during growth

Intracranial volume

Looking at the skull with its intracranial volume, literature shows that initially the intracranial volume of sCS patients is normal and enlarged in Apert patients, which

makes a small ICV less likely to be associated with ICH.[18-22] However, restricted growth with deviation in the skull OFC growth curve demonstrates to be an important clinical sign that indicates the impending or presence of ICH.[23 21]Also studies on the base of the skull have been undertaken, finding that the foramen magnum is smaller in sCS patients than in controls. This smaller foramen magnum may play a role in the development of ventriculomegaly and ICH. [24-29 30 27, 29]

Brain tissue

Focusing on brain tissue, De Jong et al. showed that brain volumes of sCS patients were not different compared to normative data at ages 1, 4, 8 and 12 years.[31] Also cerebellar volume has been found to be the same in sCS patients compared to control subjects.[20, 27]

Intracranial blood

The cerebral blood volume is a dynamic intracranial compartment, which is under physiological control by autoregulation, but also carbon dioxide level and venous outflow play a role.

Vasodilatation effect of OSA

Obstructive sleep apnea (OSA) is also noticeable contributor to increased cerebral blood volume in children with craniosynostosis.[16 32] OSA leads to carbon dioxide retention during obstructive episodes, which causes vasodilatation and subsequently raised ICP.[16] In children with multisuture or syndromic craniosynostosis, there may be a high prevalence of OSA, around 70%. The prevalence and severity are highest in patients with Apert, Crouzon and Pfeiffer syndrome.[33-38] This moderate-severe OSA occurs mostly in Apert and Crouzon patients, due to midface hypoplasia with/without mandibular hypoplasia.

Impaired venous outflow

The jugular foramina are skull apertures from which blood outflows from the intracranial compartment. The jugular foramina of sCS patients were shown to be smaller than in controls, which could cause impaired intracranial venous outflow and venous vascular collateral adaptation. Apart from Muenke syndrome, this adaption of emissary veins is seen more often in sCS patients than in normal controls. [27, 39, 40] Because patients with Muenke syndrome rarely have ICH, the relation between emissary veins and ICH implies to be more presumable.

The mutation in the fibroblast growth factor receptor *(FGFR)* gene might also contribute to impaired venous outflow, by affecting the premature endothelial proliferation and subsequent differentiation of the sigmoid and jugular sinuses. This results in a narrowed vascular lumen of these sinuses.[41, 42]

Cerebrospinal fluid

As the third component of the intracranial brain volume, we look into CSF. CSF accumulation can occur as the result of more secretion, increased resistance to CSF circulation or reduced resorption. Most evidence of alterations of CSF volume in sCS patients focus on obstruction of outflow of CSF and reduced resorption by elevated venous pressure in the sinus.[43] Both causes can occur at the same time, where several pathogenetic mechanisms can play a role.

Obstruction of CSF

CSF produced in the choroid plexus flows from the intracranial compartment through the foramen magnum around the spinal cord and up to the granulations of Pacchioni back into the sagittal sinus. Potential obstructions of CSF in craniosynostosis patients could be a smaller foramen magnum, compromised CSF spaces of the posterior fossa, a small fourth ventricle and tonsillar herniation. [43-46] In Rijken et al. the smaller foramen magnum was related to premature closure of the anterior and posterior intraoccipital synchondroses.[28] Crowding of the posterior fossa induces a reduction in volume of the CSF cisterns.[47, 48] Because of the compromised fourth ventricle in CT scan studies some authors believe in a aqueduct stenosis, while others dispute this argument based on MRI studies.[49]

Tonsillar herniation, which is commonly observed in Crouzon-Pfeiffer patients, may affect the CSF flow at the level of the craniocervical junction and/or cisterna magna. [43 44] Whether tonsillar herniation develops as a result of elevated ICP or causes the ICP is an ongoing debate, but a higher cerebellar volume / posterior fossa volume ratio has been found to be a predisposing factor for the development of tonsillar herniation. [20, 29] At last, some studies have shown that premature closure of the lambdoid sutures is associated with development of tonsillar herniation.[44, 50]

The theory of mechanical CSF outflow obstruction remains challenged by the fact that posterior fossa decompressions could fail to sufficiently restore normal CSF circulation and, in several cases, tonsillar herniation arises without ventriculomegaly.[45, 46]

Reduced resorption of CSF

Venous hypertension leads directly to ICH via increased cerebral blood volume and indirectly via venous hypertension-induced diminution of CSF absorption and an increase in brain interstitial fluid volume.[14, 43] Normally the CSF pressure is slightly higher than the venous capillary bed pressure to maintain a gradient to drive the reabsorption of CSF. Increased venous pressure impairs this reabsorption of CSF.[51] Impaired CSF absorption due to venous hypertension typically causes general dilatation of the inner and outer CSF spaces and progressive head enlargement if the skull is still capable of expanding. At the same time compensatory mechanisms as venous collaterals will develop or expand. In patients with craniosynostosis, the fused sutures do not allow

any ventricular dilatation, what could result in high CSF pressure with normal or even small ventricles. [14] If the skull then is opened by a vault expansion, a 'pseudo-tumour' /hydrocephalus of venous origin could occur postoperatively.

Prevalence of Intracranial hypertension

Isolated craniosynostosis

Based on invasive ICP measurement or the presence of papilledema, the prevalence of ICH in isolated synostosis has been described.[52-59] The prevalence of preoperatively increased ICP in sagittal suture synostosis probably ranges from 2.5 to 14% and increases with age. The prevalence of preoperatively increased ICP in metopic suture synostosis probably ranges from 2 to 8%, and for isolated coronal suture synostosis around 16%.[8, 52-58, 60] The prevalence of increased ICP during follow-up after cranial correction in isolated craniosynostosis probably varies from 2 to 9% for sagittal suture synostosis, and around 1.5% for metopic suture synostosis.[57, 58, 60-62] Corresponding figures for isolated coronal suture synostosis are not known.

Syndromic craniosynostosis

For syndromic craniosynostosis the following studies defined ICH by invasive preoperative ICP measurement, the presence of papilledema, an abnormal VEP, a deflecting head circumference curve or extensive endocortical erosion on CT images. [53, 63-68] One study uses a set of symptoms to determine increased ICP, namely papilledema, an abnormal VEP scan, a tense fontanel, progressive ventriculomegaly and invasive ICP measurement. [69]

The prevalence of increased ICP in syndromic craniosynostosis before cranial surgery is likely to be 9 to 83% for Apert, 53 to 64% for Crouzon, 19 to 43% for Saethre-Chotzen and 0 to 4% for Muenke syndrome.[64, 65, 67-69] The prevalence of increased ICP in syndromic craniosynostosis after cranial surgery is likely to be 35 to 45% for Apert, 20 to 47% for Crouzon, 17 to 42% for Saethre-Chotzen and 0 to 5% for Muenke syndrome, 58 to 67% for multisuture craniosynostosis and around 31% for bicoronal synostosis.[53, 63-65, 68, 69]

Signs and screening on Intracranial Hypertension

Because ICH could impair cognitive development, cause behavioural issues, and visual loss by damaging the optic nerves, it is important to recognize signs of ICH as early as possible.[1-3] [4] Raised ICP is defined as increased pressure on invasive measurement, but to avoid invasive measurement a set of indicators is used to assess the risk of ICH, namely hydrocephalus, papilledema, and indirect signs on radiological images.[70] At the Erasmus MC depending on suture involvement and syndromic/nonsyndromic synostosis, head circumference, fundoscopy or optical coherence tomography (OCT) are used to screen for ICH.

On radiologic images intrinsic pressure from the brain could be seen by resorption of the bone, resulting in scalloping of the inner cortex and ultimately leading to full thickness defects. Also, herniation of the cerebellar tonsils through the foramen magnum and prominent venous collaterals could arise. At last, a decrease in central and peripheral CSF spaces could be seen as a sign of intrinsic pressure. **Figure 3** shows an radiologic images of each of these examples.

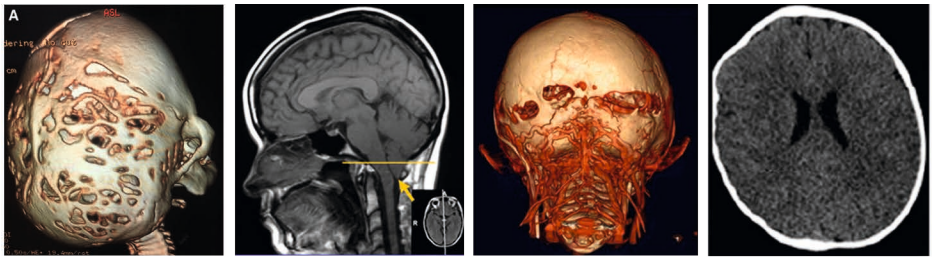

Figure 3. a.) scalloping skull b.) tonsillar herniation c.) venous collaterals. D) decrease of CSF central and peripheral

Treatment

To prevent/treat ICH is the main goal of surgical intervention in craniosynostosis.[53, 71, 72] The timing of surgery is therefore diagnosis dependent.

At the Erasmus MC, patients are surgically treated within their first year of life. Within our clinical protocol patients with Apert and Crouzon-Pfeiffer will be surgically treated by a vault expansion at the age of 6 months. An occipital expansion with springs is the primary choice because it allows to maximally increase the ICV and preserves the facial profile which facilitates a monobloc advancement, Le Fort III or facial bipartition in a later stage.[73] In patients with severe exorbitism, a monobloc advancement with distraction is considered as first cranial vault expansion.

In Saethre Chotzen and Muenke patients, retrusion of the orbital bar is a main clinical feature and therefore a fronto-orbital advancement will be performed in their first year of life: Saethre-Chotzen between 6-9 months of age, and Muenke between 9-12 months of age. Muenke patients have a low risk of developing ICH and therefore a better esthetical outcome of the facial appearance will be when operated at a later age.[74-76] Occasionally Saethre-Chotzen patients need an additional vault expansion such as an occipital expansion or biparietal widening.

In patients with complex craniosynostosis the choice of the procedure depends on the sutures that are involved. If coronal sutures have closed prematurely, a fronto-orbital advancement is the procedure of first choice, while in patients with involvement of

lambdoid sutures, an occipital vault expansion is typically performed. Nevertheless, in case of severe exorbitism, visual loss and/or severe OSA, a monobloc advancement with distraction should be performed as first procedure.

If there is proof of elevated intracranial pressure, surgery will be performed at an earlier stage in all patients. Treatment focuses on the cause which appears to be clinically the major contributor to the increase in intracranial pressure. As described above, causes for syndromic patients could be a too small intracranial volume, moderate to severe obstructive sleep apnea, hydrocephalus and venous intracranial hypertension or a combination of these factors.[4, 23, 77]

Cognitive outcome

sCs patients are at risk of developing intellectual disabilities and problems in behavioral and emotional function. Most patients with Crouzon-Pfeiffer and Saethre-Chotzen have a long-term intellectual outcome within the normal limits, while patients with Apert Syndrome have typically an IQ below the norm.[68] In addition, a large group of patients within all 3 syndromes has an IQ that is 2SD or more below the normal limits. This means that a large proportion of patients cannot work and live independently.

Trigonocephaly patients are at risk of developing mental deficiencies/disorders, behavioral problems, delays in speech and language.[78, 79] However, preoperatively less than 2% of the trigonocephaly patients have papilledema as a sign of intracranial hypertension.[59] Whether these derangements are caused by a primary disturbances in brain development or arise secondarily due to the synostosis is unknown.[5] Is this neurocognitive disorder a consequence of mechanical distortion of the brain due to abnormal shape, ventriculomegaly and/or cerebellar tonsillar herniation, or does this finding reflect an intrinsic inborn brain problem? [80-85]

While the most important aim of surgical treatment is to strive for best possible neurocognitive outcome by treating and reducing the risk of developing ICH, it remains unknown what the added value of surgery is in particularly trigonocephaly with respect to future brain development.

To answer the questions in this thesis regarding to the intrinsic brain abnormalities and the potential effect of ICH, MRI brain imaging techniques have been used in both non-operated as operated craniosynostosis patients to investigate cerebral blood flow, microstructures, and cortical thickness. In the next chapter the used MRI brain imaging techniques are set out.

MRI physics used in the upcoming studies

Magnetic resonance imaging (MRI) is an imaging technique which can be used as a tool to image and investigate body regions or tissues, including the brain. MRI scanners

use strong magnetic fields and radio waves to generate images, which in this thesis will be used to investigate images of the brain in children with craniosynostosis.

Figure 4. T1-weighted image.

T1 weighted image

A T1-weighted (T1W) image is a basic MRI pulse sequence and depicts differences in signal based upon intrinsic T1 relaxation time of various tissues (**Figure 4**). Clinically, T1-weighted images are used for depicting the anatomy of the brain, where tissue fluid characteristics are presented in grey scale differences. In the upcoming studies we will use T1w images to measure anatomical structures i.e. the size of ventricles, the herniation of the cerebellar tonsils and the thickness of the cortex.

Arterial spin labeling

Two studies will use Arterial Spin Labeling (ASL). ASL is a MRI technique that provides injection-free measurements of the absolute brain perfusion by magnetically labelling water protons in the blood vessels of the patient.[11] ASL is used for several pediatric imaging applications, for example in vascular diseases, tumors, epilepsy and seizures, to detect cortical hyper perfusion or hypoperfusion.[86] The main advantage of the ASL technique is that it measures absolute brain perfusion and that it is does not require administration of an exogenous contrast agent.[87]

ASL magnetically labels arterial blood water when it flows through the neck perpendicular to the cervical arteries. By a radiofrequency pulse the water protons in the blood will get inverted; the blood will get a negative magnetization.[88, 89] After a post-labeling delay (PLD) in which the labelled blood flows into brain tissue, an image of the brain will be acquired (**Figure 5**).[90] As depicted in **Figure 6**, by making two images a third image can be provided with the weighted perfusion.[91] The control image is the image without labelling of the blood. The second image contains both the normal stationary blood as well as the negative magnetization from the inflowing labeled blood.[92] Therefore, an ASL image is weighted for the cerebral blood flow (CBF), i.e. the volume of blood that flows through 100 grams of brain tissue each minute (mL/100g/min).

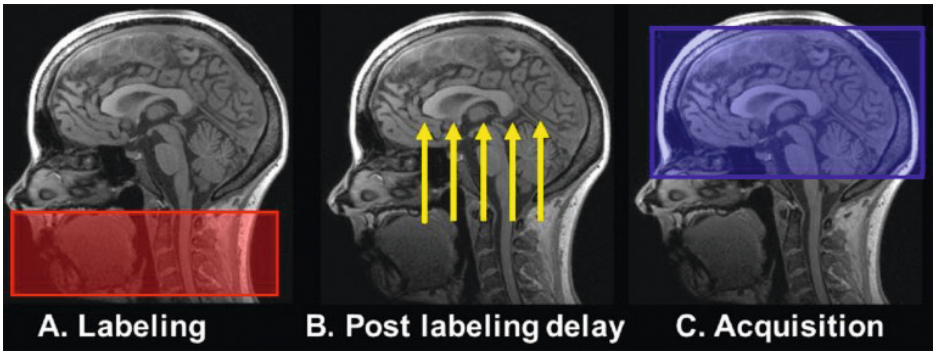

Figure 5. Principle for arterial spin labeling acquisition.

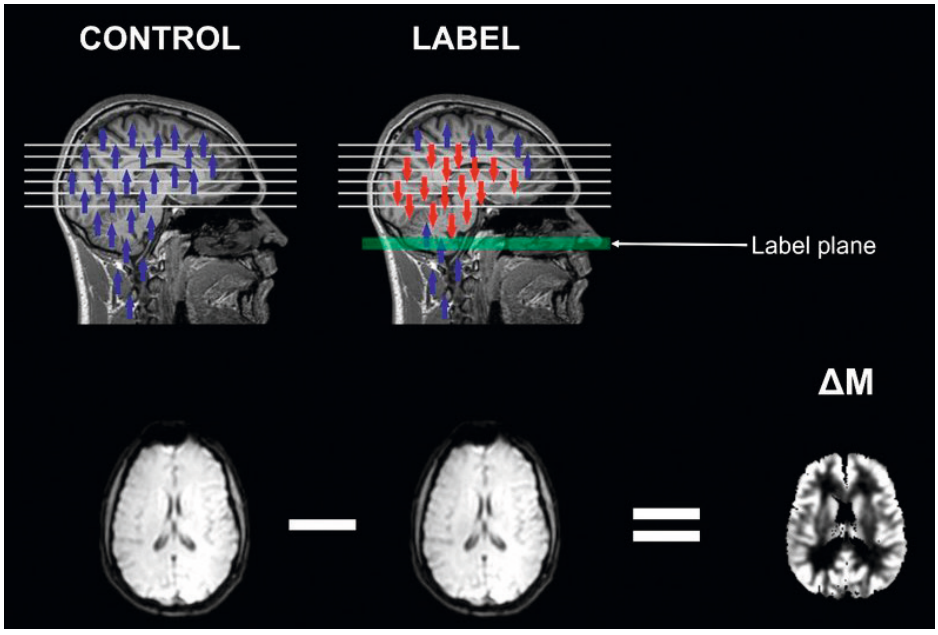

Figure 6. In ASL, a perfusion-weighted (**Δ**M) image is obtained by subtraction of a labeled from a control image.

Diffusion Tensor Imaging

To investigate the microstructure of the white matter of the brain, we will use Diffusion Tensor Imaging (DTI). DTI is a MRI technique that uses movement of water molecules in the brain to produce neural tract images. By evaluating and quantifying diffusion restriction and limited movement of water in white matter of the brain the pattern of neural networks in the brain could be revealed (**Figure 7**). In this way, the microarchitecture of the white matter tracts in the brain can be investigated.

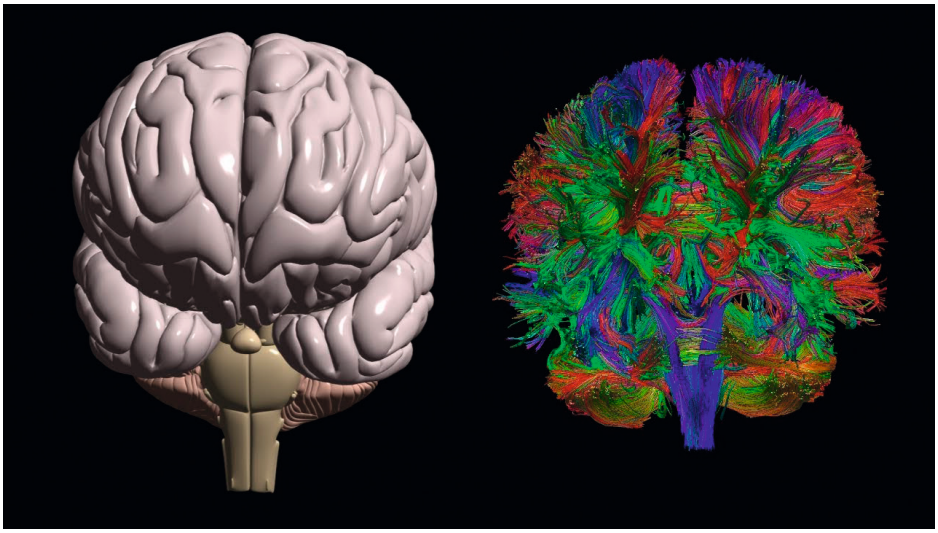

Figure 7. Tractography of bundles of axons in the brain. The main direction of diffusion is encoded in the colour of tracks with blue representing tracts coursing up and down, green representing tracts coursing from front-to-back and left representing tracts coursing left to right.

To understand the technique behind DTI, we have to zoom into diffusion. In general, diffusion movement in all directions (for example in a glass of pure water) is called **isotropy**. Diffusion in tissues varies with direction, which is called **anisotropy**. In white matter of the brain, the diffusion anisotropy is primarily caused by cellular membranes, with some contribution from myelination and the packing of axons. Anisotropic diffusion can indicate the underlying tissue orientation (**Figure 8**).

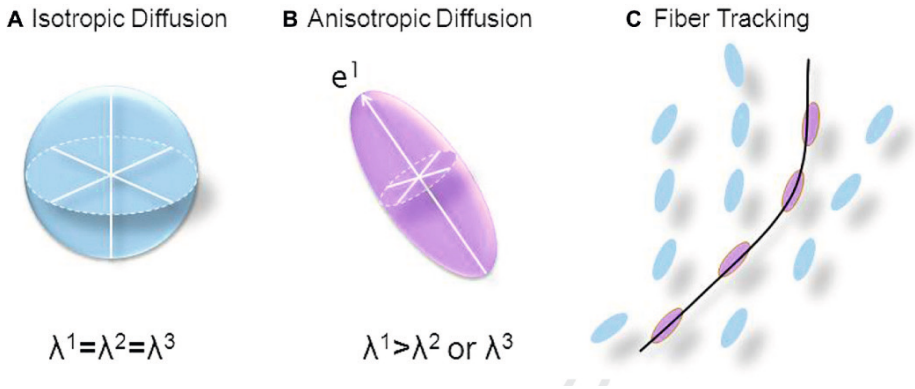

Figure 8. Representation of A.) diffusion as an isotropic shape of the corresponding diffusion lengths (λ1, λ2, and λ3), the eigenvalues. B.) diffusion as an anisotropic shape of the corresponding eigenvalues C.) fibre tracking by using the different voxels.

The white matter metrics from DTI, voxel-by-voxel, are mathematically based on 3 mutually perpendicular eigenvectors, whose magnitude is given by 3 corresponding eigenvalues sorted in order of decreasing magnitude as λ1, λ2 and λ3. An ellipsoid is created by the long axis of λ_1, and the small axes λ_2 and λ_3, from where the measured length of the three axes are the eigenvalues.

DTI describes the magnitude, the degree and orientation of diffusion anisotropy. These eigenvalues are used to generate quantitative maps of fractional anisotropy (FA), the derivation of axial diffusivity (AD), radial diffusivity (RD) and mean diffusivity (MD). FA represents the amount of diffusional asymmetry in a voxel, which is presented from 0 (infinite isotropy) to 1 (infinite anisotropy). AD stands for the diffusivity along the neural tract: λ_1. The diffusivity of the minor axes, λ_2 and λ_3, is called the perpendicular or radial diffusivity. The mean of these diffusivity λ_1, λ_2 and λ_3 is known as MD. FA, MD, AD and RD are used as indirect markers of white matter microstructure of these young patients.[93]

To summarize, DTI maps the course of the neural axon bundles in the brain. With DTI we obtain a sufficient number of gradient directions to determine the tensor components per voxel. We determine eigenvalues and eigenvectors which indicate the major and minor directions of the diffusion movement down the axonal bundles. This measurement of diffusion of water in tissue could be used to investigate the microarchitecture of the white matter of the brain and produce white matter tracts.

Aim and outline of this thesis

The aim of this thesis is to get more understanding about the extent and the origin of brain abnormalities in children with craniosynostosis by using brain imaging. Specifically, the potential effect of mechanical causes due to shape and pressure are addressed and compared to intrinsic or genetic causes in isolated and syndromic synostosis before and after treatment.

Part I Brain imaging in non-operated infants with isolated and syndromic craniosynostosis

Arterial spin labeling (ASL) is a MRI technique which could be used to measure the absolute brain perfusion. In **Chapter 2** a new approach of using ASL on trigonocephaly patients will be validated. In **Chapter 3** blood perfusion of the frontal lobe in non-operated trigonocephaly patients is analyzed. In **Chapter 4** we respond on a letter to the editor focused on the ASL article. The microstructural properties of the frontal lobe of non-operated patients with trigonocephaly patients will be assessed in comparison to controls in **Chapter 5. Chapter 6** the microstructural characteristics of the non-operated syndromic craniosynostosis brain are described. By diffusion tensor imaging (DTI) fiber tractography diffusion parameters of multiple white matter tracts between craniosynostosis patients in comparison to controls are evaluated.

Part II Brain imaging during follow-up of operated children with isolated and syndromic craniosynostosis

Chapter 7 assesses the cortical thickness of the brain in Crouzon syndrome after surgical treatment. In **Chapter 8** the interaction of ventriculomegaly and cerebellar tonsillar position over time and the association between abnormal anatomy of the skull base and cerebellar tonsillar position are investigated. **Chapter 9** dives into the rare and severe course of patients with Crouzon syndrome and acanthosis nigricans. Treatment protocols of three international centers are reviewed in this cohort.

REFERENCES

1. Bartels MC, Vaandrager JM, de Jong TH, et al. Visual loss in syndromic craniosynostosis with papilledema but without other symptoms of intracranial hypertension. *J Craniofac Surg* 2004;15:1019-1022; discussion 1023-1014
2. Tay T, Martin F, Rowe N, et al. Prevalence and causes of visual impairment in craniosynostotic syndromes. *Clin Exp Ophthalmol* 2006;34:434-440
3. Mathijssen IMJ, Working Group Guideline C. Updated Guideline on Treatment and Management of Craniosynostosis. *J Craniofac Surg* 2021;32:371-450
4. Hayward R, Britto J, Dunaway D, et al. Connecting raised intracranial pressure and cognitive delay in craniosynostosis: many assumptions, little evidence. *J Neurosurg Pediatr* 2016;18:242-250
5. Morriss-Kay GM, Wilkie AO. Growth of the normal skull vault and its alteration in craniosynostosis: insights from human genetics and experimental studies. *J Anat* 2005;207:637-653
6. Mathijssen IM, van Splunder J, Vermeij-Keers C, et al. Tracing craniosynostosis to its developmental stage through bone center displacement. *J Craniofac Genet Dev Biol* 1999;19:57-63
7. Connolly JP, Gruss J, Seto ML, et al. Progressive postnatal craniosynostosis and increased intracranial pressure. *Plast Reconstr Surg* 2004;113:1313-1323
8. Cornelissen M, Ottelander B, Rizopoulos D, et al. Increase of prevalence of craniosynostosis. *J Craniomaxillofac Surg* 2016;44:1273-1279
9. Sharma VP, Fenwick AL, Brockop MS, et al. Mutations in TCF12, encoding a basic helix-loop-helix partner of TWIST1, are a frequent cause of coronal craniosynostosis. *Nat Genet* 2013;45:304-307
10. Bredero-Boelhouwer H, Treharne LJ, Mathijssen IM. A triage system for referrals of pediatric skull deformities. *J Craniofac Surg* 2009;20:242-245
11. Ridgway EB, Weiner HL. Skull deformities. *Pediatr Clin North Am* 2004;51:359-387
12. Neff S, Subramaniam RP. Monro-Kellie doctrine. *J Neurosurg* 1996;85:1195
13. Wagshul ME, Eide PK, Madsen JR. The pulsating brain: A review of experimental and clinical studies of intracranial pulsatility. *Fluids Barriers CNS* 2011;8:5
14. Sainte-Rose C, LaCombe J, Pierre-Kahn A, et al. Intracranial venous sinus hypertension: cause or consequence of hydrocephalus in infants? *J Neurosurg* 1984;60:727-736
15. Gonsalez S, Hayward R, Jones B, et al. Upper airway obstruction and raised intracranial pressure in children with craniosynostosis. *EUR RESPIR J* 1997;10:367-375
16. Hayward R, Gonsalez S. How low can you go? Intracranial pressure, cerebral perfusion pressure, and respiratory obstruction in children with complex craniosynostosis. *J Neurosurg* 2005;102 PEDIATRICS:16-22
17. Driessen C, Joosten KFM, Bannink N, et al. How does obstructive sleep apnoea evolve in syndromic craniosynostosis? A prospective cohort study. *Archives of Disease in Childhood* 2013;98:538-543
18. Gosain AK, McCarthy JG, Glatt P, et al. A study of intracranial volume in Apert syndrome. *PLAST RECONSTR SURG* 1995;95:284-295
19. Anderson PJ, Netherway DJ, Abbott AH, et al. Analysis of intracranial volume in apert syndrome genotypes. *Pediatr Neurosurg* 2004;40:161-164
20. Rijken BFM, Lequin MH, Van Der Lijn F, et al. The role of the posterior fossa in developing Chiari i malformation in children with craniosynostosis syndromes. *J Cranio-Maxillofac Surg* 2015;43:813-819

21. Rijken BF, den Ottelander BK, van Veelen ML, et al. The occipitofrontal circumference: reliable prediction of the intracranial volume in children with syndromic and complex craniosynostosis. *Neurosurg Focus* 2015;38:E9

22. Breakey RWF, Knoops PGM, Borghi A, et al. Intracranial Volume and Head Circumference in Children with Unoperated Syndromic Craniosynostosis. *Plast Reconstr Surg* 2018;142:708e-717e

23. Spruijt B, Joosten KF, Driessen C, et al. Algorithm for the Management of Intracranial Hypertension in Children with Syndromic Craniosynostosis. *Plast Reconstr Surg* 2015;136:331-340

24. Coll G, Arnaud E, Selek L, et al. The growth of the foramen magnum in Crouzon syndrome. *Child's Nerv Syst* 2012;28:1525-1535

25. Di Rocco F, Dubravova D, Ziyadeh J, et al. The foramen magnum in isolated and syndromic brachycephaly. *Child's Nerv Syst* 2014;30:165-172

26. Assadsangabi R, Hajmomenian M, Bilaniuk LT, et al. Morphology of the foramen magnum in syndromic and non-syndromic brachycephaly. *Childs Nervous System* 2015;31:735-741

27. Coll G, Arnaud E, Collet C, et al. Skull base morphology in fibroblast growth factor receptor type 2-related faciocraniosynostosis: a descriptive analysis. *Neurosurgery* 2015;76:571-583; discussion 583

28. Rijken BF, Lequin MH, de Rooi JJ, et al. Foramen magnum size and involvement of its intraoccipital synchondroses in Crouzon syndrome. *Plast Reconstr Surg* 2013;132:993e-1000e

29. Rijken BFM, Lequin MH, Van Veelen MLC, et al. The formation of the foramen magnum and its role in developing ventriculomegaly and Chiari i malformation in children with craniosynostosis syndromes. *J Cranio-Maxillofac Surg* 2015;43:1042-1048

30. Tokumaru AM, Barkovich AJ, Ciricillo SF, et al. Skull base and calvarial deformities: Association with intracranial changes in craniofacial syndromes. *AM J NEURORADIOL* 1996;17:619-630

31. De Jong T, Rijken BFM, Lequin MH, et al. Brain and ventricular volume in patients with syndromic and complex craniosynostosis. *Child's Nerv Syst* 2012;28:137-140

32. Spruijt B, Joosten KF, Driessen C, et al. Algorithm for the Management of Intracranial Hypertension in Children with Syndromic Craniosynostosis. *Plast Reconstr Surg* 2015;136:331-340

33. Al-Saleh S, Riekstins A, Forrest CR, et al. Sleep-related disordered breathing in children with syndromic craniosynostosis. *J Craniomaxillofac Surg* 2011;39:153-157

34. Driessen C, Joosten KF, Bannink N, et al. How does obstructive sleep apnoea evolve in syndromic craniosynostosis? A prospective cohort study. *Arch Dis Child* 2013;98:538-543

35. Driessen C, Joosten KF, Florisson JM, et al. Sleep apnoea in syndromic craniosynostosis occurs independent of hindbrain herniation. *Childs Nerv Syst* 2013;29:289-296

36. Driessen C, Mathijssen IM, De Groot MR, et al. Does central sleep apnea occur in children with syndromic craniosynostosis? *Respir Physiol Neurobiol* 2012;181:321-325

37. Inverso G, Brustowicz KA, Katz E, et al. The prevalence of obstructive sleep apnea in symptomatic patients with syndromic craniosynostosis. *Int J Oral Maxillofac Surg* 2016;45:167-169

38. Zandieh SO, Padwa BL, Katz ES. Adenotonsillectomy for obstructive sleep apnea in children with syndromic craniosynostosis. *Plast Reconstr Surg* 2013;131:847-852

39. Booth CD, Figueroa RE, Lehn A, et al. Analysis of the jugular foramen in pediatric patients with craniosynostosis. *J Craniofac Surg* 2011;22:285-288

40. Florisson JMG, Barmpalios G, Lequin M, et al. Venous hypertension in syndromic and complex craniosynostosis: The abnormal anatomy of the jugular foramen and collaterals. *J Cranio-Maxillofac Surg* 2015;43:312-318

41. Hayward R. Venous hypertension and craniosynostosis. *Childs Nerv Syst* 2005;21:880-888

42. Gray JL, Kang SS, Zenni GC, et al. FGF-1 affixation stimulates ePTFE endothelialization without intimal hyperplasia. *J Surg Res* 1994;57:596-612

43. Collmann H, Sorensen N, Krauss J. Hydrocephalus in craniosynostosis: a review. *Childs Nerv Syst* 2005;21:902-912

44. Cinalli G, Renier D, Sebag G, et al. Chronic tonsillar herniation in Crouzon's and Apert's syndromes: the role of premature synostosis of the lambdoid suture. *J Neurosurg* 1995;83:575-582

45. Cinalli G, Sainte-Rose C, Kollar EM, et al. Hydrocephalus and craniosynostosis. *J Neurosurg* 1998;88:209-214

46. Cinalli G, Chumas P, Arnaud E, et al. Occipital remodeling and suboccipital decompression in severe craniosynostosis associated with tonsillar herniation. *Neurosurgery* 1998;42:66-71; discussion 71-63

47. Strahle J, Muraszko KM, Buchman SR, et al. Chiari malformation associated with craniosynostosis. *Neurosurg Focus* 2011;31:E2

48. Fearon JA, Rhodes J. Pfeiffer syndrome: a treatment evaluation. *Plast Reconstr Surg* 2009;123:1560-1569

49. Thompson DN, Harkness W, Jones BM, et al. Aetiology of herniation of the hindbrain in craniosynostosis. An investigation incorporating intracranial pressure monitoring and magnetic resonance imaging. *Pediatr Neurosurg* 1997;26:288-295

50. Fearon JA, Dimas V, Ditthakasem K. Lambdoid Craniosynostosis: The Relationship with Chiari Deformations and an Analysis of Surgical Outcomes. *Plast Reconstr Surg* 2016;137:946-951

51. Sainz LV, Zipfel J, Kerscher SR, et al. Cerebro-venous hypertension: a frequent cause of so-called "external hydrocephalus" in infants. *Childs Nerv Syst* 2019;35:251-256

52. Thompson DN, Malcolm GP, Jones BM, et al. Intracranial pressure in single-suture craniosynostosis. *Pediatr Neurosurg* 1995;22:235-240

53. Renier D, Lajeunie E, Arnaud E, et al. Management of craniosynostoses. *Childs Nerv Syst* 2000;16:645-658

54. Mathijssen I, Arnaud E, Lajeunie E, et al. Postoperative cognitive outcome for synostotic frontal plagiocephaly. *J Neurosurg* 2006;105:16-20

55. Eley KA, Johnson D, Wilkie AOM, et al. Raised intracranial pressure is frequent in untreated nonsyndromic unicoronal synostosis and does not correlate with severity of phenotypic features. *Plast Reconstr Surg* 2012;130:690e-697e

56. Wall SA, Thomas GP, Johnson D, et al. The preoperative incidence of raised intracranial pressure in nonsyndromic sagittal craniosynostosis is underestimated in the literature. *J Neurosurg Pediatr* 2014;14:674-681

57. van Veelen ML, Eelkman Rooda OH, de Jong T, et al. Results of early surgery for sagittal suture synostosis: long-term follow-up and the occurrence of raised intracranial pressure. *Childs Nerv Syst* 2013;29:997-1005

58. van Veelen ML, Mihajlovic D, Dammers R, et al. Frontobiparietal remodeling with or without a widening bridge for sagittal synostosis: comparison of 2 cohorts for aesthetic and functional outcome. *J Neurosurg Pediatr* 2015;16:86-93

59. Cornelissen MJ, Loudon SE, van Doorn FE, et al. Very Low Prevalence of Intracranial Hypertension in Trigonocephaly. *Plast Reconstr Surg* 2017;139:97e-104e

60. Cornelissen MJ, Loudon SE, van Doorn FEC, et al. Very Low Prevalence of Intracranial Hypertension in Trigonocephaly. *Plast Reconstr Surg* 2017;139:97e-104e

61. Christian EA, Imahiyerobo TA, Nallapa S, et al. Intracranial hypertension after surgical correction for craniosynostosis: a systematic review. *Neurosurg Focus* 2015;38:E6

62. Thomas GP, Johnson D, Byren JC, et al. The incidence of raised intracranial pressure in nonsyndromic sagittal craniosynostosis following primary surgery. *J Neurosurg Pediatr* 2015;15:350-360

63. Thompson DN, Harkness W, Jones B, et al. Subdural intracranial pressure monitoring in craniosynostosis: its role in surgical management. *Childs Nerv Syst* 1995;11:269-275

64. Marucci DD, Dunaway DJ, Jones BM, et al. Raised intracranial pressure in Apert syndrome. *Plast Reconstr Surg* 2008;122:1162-1168

65. Kress W, Schropp C, Lieb G, et al. Saethre-Chotzen syndrome caused by TWIST 1 gene mutations: functional differentiation from Muenke coronal synostosis syndrome. *Eur J Hum Genet* 2006;14:39-48

66. Greene AK, Mulliken JB, Proctor MR, et al. Phenotypically unusual combined craniosynostoses: presentation and management. *Plast Reconstr Surg* 2008;122:853-862

67. Woods RH, Ul-Haq E, Wilkie AO, et al. Reoperation for intracranial hypertension in TWIST1-confirmed Saethre-Chotzen syndrome: a 15-year review. *Plast Reconstr Surg* 2009;123:1801-1810

68. de Jong T, Bannink N, Bredero-Boelhouwer HH, et al. Long-term functional outcome in 167 patients with syndromic craniosynostosis; defining a syndrome-specific risk profile. *J Plast Reconstr Aesthet Surg* 2010;63:1635-1641

69. Abu-Sittah GS, Jeelani O, Dunaway D, et al. Raised intracranial pressure in Crouzon syndrome: incidence, causes, and management. *J Neurosurg Pediatr* 2016;17:469-475

70. Renier D, Sainte-Rose C, Marchac D, et al. Intracranial pressure in craniostenosis. *J Neurosurg* 1982;57:370-377

71. Mathijssen IM, Arnaud E. Benchmarking for craniosynostosis. *J Craniofac Surg* 2007;18:436-442

72. Marchac D, Arnaud E, Renier D. Frontocranial remodeling without opening of frontal sinuses in a scaphocephalic adolescent: a case report. *J Craniofac Surg* 2002;13:698-705

73. de Jong T, van Veelen ML, Mathijssen IM. Spring-assisted posterior vault expansion in multisuture craniosynostosis. *Childs Nerv Syst* 2013;29:815-820

74. Arnaud E, Marchac D, Renier D. Reduction of morbidity of the frontofacial monobloc advancement in children by the use of internal distraction. *Plast Reconstr Surg* 2007;120:1009-1026

75. O'Connor EJF, Marucci DD, Jeelani NO, et al. Ocular advancement in monobloc distraction. *Plast Reconstr Surg* 2009;123:1570-1577

76. Honnebier MB, Cabiling DS, Hetlinger M, et al. The natural history of patients treated for FGFR3-associated (Muenke-type) craniosynostosis. *Plast Reconstr Surg* 2008;121:919-931

77. Deschamps-Braly J, Hettinger P, el Amm C, et al. Volumetric analysis of cranial vault distraction for cephalocranial disproportion. *Pediatr Neurosurg* 2011;47:396-405

78. van der Vlugt JJ, van der Meulen JJ, Creemers HE, et al. Cognitive and behavioral functioning in 82 patients with trigonocephaly. *Plast Reconstr Surg* 2012;130:885-893

79. Kelleher MO, Murray DJ, McGillivary A, et al. Behavioral, developmental, and educational problems in children with nonsyndromic trigonocephaly. *J Neurosurg* 2006;105:382-384

80. Vermeij-Keers C, Mazzola RF, Van der Meulen JC, et al. Cerebro-craniofacial and craniofacial malformations: an embryological analysis. *Cleft Palate J* 1983;20:128-145

81. O'Rahilly R, Gardner E. The initial appearance of ossification in staged human embryos. *Am J Anat* 1972;134:291-301

82. McBratney-Owen B, Iseki S, Bamforth SD, et al. Development and tissue origins of the mammalian cranial base. *Dev Biol* 2008;322:121-132

83. Jiang X, Iseki S, Maxson RE, et al. Tissue origins and interactions in the mammalian skull vault. *Dev Biol* 2002;241:106-116

84. Merrill AE, Bochukova EG, Brugger SM, et al. Cell mixing at a neural crest-mesoderm boundary and deficient ephrin-Eph signaling in the pathogenesis of craniosynostosis. *Hum Mol Genet* 2006;15:1319-1328

85. Chai Y, Jiang X, Ito Y, et al. Fate of the mammalian cranial neural crest during tooth and mandibular morphogenesis. *Development* 2000;127:1671-1679

86. Keil VC, Hartkamp NS, Connolly DJA, et al. Added value of arterial spin labeling magnetic resonance imaging in pediatric neuroradiology: pitfalls and applications. *Pediatr Radiol* 2019;49:245-253

87. Wang J, Licht DJ, Jahng GH, et al. Pediatric perfusion imaging using pulsed arterial spin labeling. *J Magn Reson Imaging* 2003;18:404-413

88. Williams DS, Detre JA, Leigh JS, et al. Magnetic resonance imaging of perfusion using spin inversion of arterial water. *Proc Natl Acad Sci U S A* 1992;89:212-216

89. Detre JA, Leigh JS, Williams DS, et al. Perfusion imaging. *Magn Reson Med* 1992;23:37-45

90. Ferre JC, Bannier E, Raoult H, et al. Arterial spin labeling (ASL) perfusion: techniques and clinical use. *Diagn Interv Imaging* 2013;94:1211-1223

91. Golay X, Petersen ET. Arterial spin labeling: benefits and pitfalls of high magnetic field. *Neuroimaging Clin N Am* 2006;16:259-268, x

92. Alsop DC, Detre JA. Reduced transit-time sensitivity in noninvasive magnetic resonance imaging of human cerebral blood flow. *J Cereb Blood Flow Metab* 1996;16:1236-1249

93. Qiu A, Mori S, Miller MI. Diffusion tensor imaging for understanding brain development in early life. *Annu Rev Psychol* 2015;66:853-876

PART I

BRAIN IMAGING IN NON-OPERATED INFANTS WITH ISOLATED AND SYNDROMIC CRANIOSYNOSTOSIS

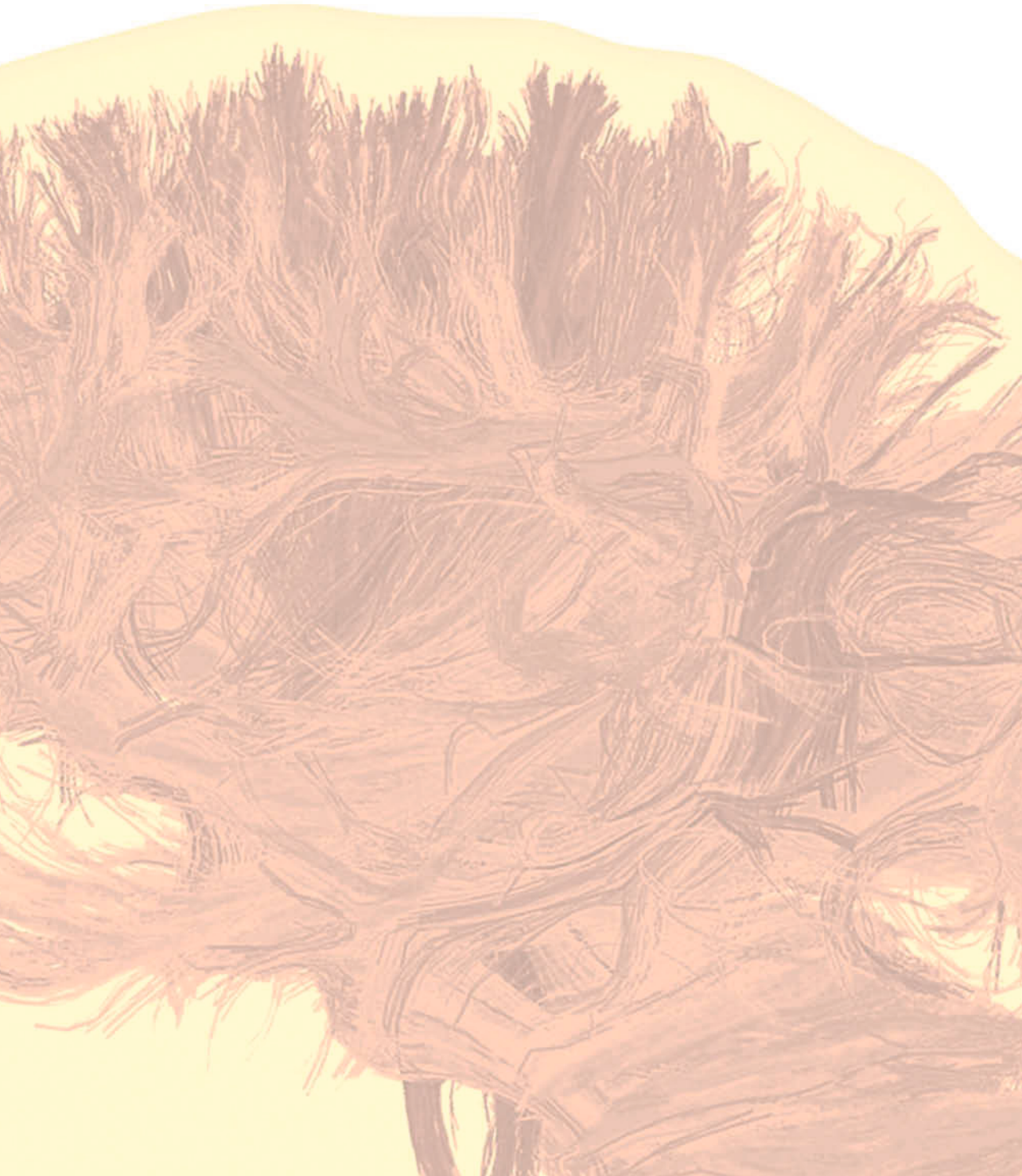

CHAPTER 2

USING PERFUSION CONTRAST FOR SPATIAL NORMALIZATION OF ASL MRI IMAGES IN A PEDIATRIC CRANIOSYNOSTOSIS POPULATION

CATHERINE A. DE PLANQUE

HENK J. M. M. MUTSAERTS

VERA C. KEIL

NICOLE S. ERLER

MARJOLEIN H. G. DREMMEN

IRENE M. J. MATHIJSSEN

JAN PETR

Frontiers in Neuroscience, 2021 Jul 19;15:698007

ABSTRACT

Spatial normalization is an important step for group image processing and evaluation of mean brain perfusion in anatomical regions using arterial spin labeling (ASL) MRI and is typically performed via high-resolution structural brain scans. However, structural segmentation and/or spatial normalization to standard space is complicated when gray/white matter contrast in structural images is low due to ongoing myelination in newborns and infants. This problem is of particularly clinical relevance for imaging infants with inborn or acquired disorders that impair normal brain development.

We investigated whether the ASL MRI perfusion contrast is a viable alternative for spatial normalization, using a pseudo-continuous ASL acquired using a 1.5 T MRI unit (GE Healthcare). Four approaches have been compared: (1) using the structural image contrast, or perfusion contrast with (2) rigid, (3) affine, and (4) nonlinear transformations – in 16 healthy controls [median age 0.83 years, inter-quartile range (IQR) ± 0.56] and 36 trigonocephaly patients (median age 0.50 years, IQR ± 0.30) – a non-syndromic type of craniosynostosis. Performance was compared quantitatively using the real-valued Tanimoto coefficient (TC), visually by three blinded readers, and eventually by the impact on regional cerebral blood flow (CBF) values.

For both patients and controls, nonlinear registration using perfusion contrast showed the highest TC, at 17.51 (CI 6.66–49.38) times more likely to have a higher rating and 17.45–18.88 ml/100 g/min higher CBF compared with the standard normalization.

Using perfusion-based contrast improved spatial normalization compared with the use of structural images, significantly affected the regional CBF, and may open up new possibilities for future large pediatric ASL brain studies.

Keywords: ASL, segmentation, registration, spatial normalization, pediatric, craniosynostosis

INTRODUCTION

Spatial normalization is an important step for brain image processing; it not only enables group analyses but is also required for automatic segmentation of tissue type and brain regions. Functional or physiological MRI acquisitions, such as arterial spin labeling (ASL) perfusion MRI, typically perform nonlinear registration via conventional structural – mostly T1-weighted (T1w) – scans for their higher resolution and structural contrast. However, in situations where the tissue contrast is low and changing, such as in early phases of myelination in newborns and infants, these structural reference scans may not help or even fail normalization.[1-3]

The use of other images with higher tissue-contrast could help registration. As an alternative to spatial normalization via segmentation and registration of structural images, studies use contrast from different MRI modalities. Feng et al. used Diffusion Tensor Imaging (DTI) as a substitute for T1w scans.[4] In DTI images, premyelination is encountered prior to being detectable at T1w or T2w imaging.[5] Similarly, Mutsaerts et al. used cerebral blood flow (CBF) and pseudo-CBF, created from a gray matter (GM) map from segmented T1w image to register individual ASL and T1w volumes instead of using the morphological images for the registration, for example, the ASL control images or M0 scans registered to T1w images in elderly subjects.[6] This approach was especially important in cases where the image contrast difference between GM and white matter (WM) was low in ASL control images or in M0 scans, due to, for example, use of strong background suppression or short TR, respectively. This approach can be potentially extended to direct spatial normalization of ASL to standard space in the pediatric population as ASL studies of the brain show sufficient CBF contrast between GM and WM already in early age despite the potential lack of GM/WM contrast in T1w images.[5]

The problem with spatial normalization in subjects with ongoing myelination is of particular clinical relevance in imaging babies with inborn or acquired disorders impairing normal brain development. Craniosynostosis, referred to the premature fusion of the skull sutures leading to skull and brain deformations, is an example of such disease.[7-10] Trigonocephaly, a non-syndromic type of craniosynostosis that presents within a sliding scale of severity in phenotype and brain imaging, is one of the key components in the decision making for surgical treatment in the first years of life. Imaging of these newborns is essential, and ASL is an MRI technique that could provide cerebral perfusion measurements on both a global and regional level.

Spatial normalization is then necessary to be able to evaluate perfusion in predefined anatomical regions. However, automatic methods for spatial normalization are challenging in young children with craniosynostosis as there are issues with low GM/WM contrast and skull deformity, as explained above.[7, 11] In previous ASL studies in

craniosynostosis patients, regions of interest (ROI) were therefore placed manually, which made spatial normalization escapable.[12] However, this practice is time consuming, and it increases the likelihood of error in delineation and decreases the repeatability across subjects.

To overcome the issues with spatial normalization of T1w images, we propose to use different contrast than from the structural images for the spatial normalization. In this study, we set to investigate if the ASL CBF image contrast can be directly used for spatial normalization in children with trigonocephaly and healthy controls under the age of 18 months. We combined technical and clinical expertise to compare the standard method that uses structural images for the normalization with three different registrations of ASL directly to MNI using rigid, affine, and nonlinear transformations. We hypothesize that direct ASL spatial normalization to the MNI space is possible, that nonlinear registration can be used in this context to improve the normalization quality in young healthy controls and trigonocephaly patients, and that this normalization will have a significant effect on the measured regional CBF. With this study we aim to facilitate the investigation of frontal lobe perfusion in trigonocephaly patients in a clinical setting to assess the value of vault surgery in these patients.

MATERIALS AND METHODS

The Ethics Committee approved this prospective imaging study in patients with trigonocephaly (METC-2018-124), which is part of ongoing work at the Erasmus Medical Center involving protocolized care, brain imaging, clinical assessment, data summary, and evaluation.[13] To participate in this study, informed research consent has been obtained.

Subjects

Preoperative MRI brain scans from 36 children with metopic synostosis for whom a surgical correction was considered were included over a period of 2 years (2018–2020). Surgery was considered only for moderate and severe presentation of metopic synostosis, mainly defined by severe narrowing and a protruding midline ridge of the forehead, hypotelorism (eyes close together), and biparietal widening.[14] Children were less than 2 years of age at the time of the MRI brain study. The control group consisted of sixteen subjects undergoing MRI brain studies for clinical reasons, with the following inclusion criteria: (1) no neurological pathology of the head or neck (e.g., children with intracranial masses, prior neurosurgeries, known myelin disorders); (2) no neurological or psychological morbidity on follow-up; and (3) no residual motion artifacts in the subjects' brain MRI data.

MRI Acquisition

All MRI data were acquired using a 1.5 Tesla MR Unit (General Electric Healthcare, Milwaukee, WI, United States), and the imaging protocol included a three-dimensional spoiled gradient T1w MR sequence. Imaging parameters included slice thickness of 2 mm, no slice gap, a field of view 22.4 cm, matrix size 224 x 224, in plane resolution 1 mm, echo time 3.1 ms and repetition time 9.9 ms. The pseudo-continuous ASL sequences with the following imaging parameters: 3D fast spin-echo spiral readout with a stack of 8 spirals and 3 averages, repetition time 4,604 ms, echo time 10.7 ms, voxel size 3.75 mm x 3.75 mm x 4.0 mm, field of view 24.0 cm x 24.0 cm, labeling duration 1,450 ms, post-labeling delay 1,025 ms, and background suppression. This protocol was identical in both trigonocephaly patients and controls. Both groups underwent deep sedation or sevoflurane-induced anesthesia during the MRI procedure.

Image Processing

Data processing and analysis were performed with ExploreASL, a Matlab-based toolbox (MathWorks, MA, United States) developed to facilitate quality control and analyses for single or multicenter ASL studies.[15-17] This toolbox is based on Statistical Parametric Mapping (SPM) 12 (Wellcome Trust Centre for Neuroimaging, University College London, United Kingdom).[18]

The preprocessing included the default 3D ASL processing of ExploreASL except for the ASL-T1w registration part, which includes the quantification of the M0 and CBF image.[15]

Afterwards, we compared four approaches: (1) normalization via segmentation and spatial normalization of the T1w images (regT1); a direct registration of ASL to MNI using either (2) rigid body (regASLrigid), (3) affine (regASLaffine), or (4) a nonlinear Direct Cosine Transform (DCT) transformation (regASLdct).

For regT1, the T1w image was segmented – to GM, WM, and cerebrospinal fluid – and registered to MNI space with ExploreASL default settings except for using SPM12 with the NITRC 2.3 brain template of 1-year-olds. The 1-year-old template was chosen for all subjects since this was the closest match for the majority of our subjects.[19] The M0 and T1w images were rigidly aligned and applied to ASL to align it with T1w. The spatial normalization of ASL for regT1 was then obtained as the joint transformation of ASL to T1w and T1w to MNI space.

For the regASLrigid, regASLaffine, regASLdct, a pseudo-CBF image was constructed in the MNI space using the GM and WM probability maps from the NITRC template resampled to 1.5 mm x 1.5 mm x 1.5 mm voxels, multiplying them by 60 and 20 ml/min/100 g, respectively, and finally smoothing them to the ASL resolution. The native ASL CBF image was then registered with the pseudo-CBF image using the respective

transformations. The nonlinear DCT consisted of 16 discrete-cosine basis functions along each dimension.[20] For all the above-mentioned transformations, all registration steps were combined in a single joint transformation with a single interpolation from native to standard space.

Quantitative Evaluation

We compared the four normalization methods quantitatively by studying the overlap between the individual CBF image registered to the standard space and a CBF template in the standard space using the Tanimoto similarity coefficient for real-valued vectors, see equation (1) in the work of Anastasiu et al.[21] The Tanimoto coefficient (TC) is a measure of image overlap, ranging from 0% (completely dissimilar) to 100% (identical images). If we assume that perfect registration does not lead to identical images but ones that still retain physiological differences, TC >70% can be regarded as excellent image agreement. We masked the brain in both images and normalized the values in each image to the 97th percentile value while excluding the higher signal values from the computation. Note that we computed the whole-brain TC for continuous perfusion-weighted values (also known as Tanimoto distance) rather than the commonly used measure for binary images. [21]

Qualitative Evaluation

The spatial normalization of ASL images to the MNI space was inspected qualitatively by examining the overlay of CBF and outer WM borders in MNI space with a threshold at 50% WM partial volume. The T1w-based and the three types of ASL-based normalizations were visually scored by three raters: a pediatric neuroradiologist (MD, 7 years of radiology experience), an ASL image processing engineer (JP, 10 years of experience), and a neuroradiologist (VK, 10 years of experience).

The visual alignment of the ASL images in MNI space was categorized into four quality categories: (1) unusable, 2) poor, (3) usable, and (4) excellent. For the evaluation of the results of each normalization method of each subject, the rater rated overviews of normalizations showing 12 axial and 12 sagittal slices. All visual overlay images from both the patient and control groups for all four normalization methods were pseudo-randomized and pseudonymized. The pseudonym was visible to the raters throughout the whole procedure of individual rating and for reaching consensus. The raters were blinded to the method and clinical history of the patients and controls.

Statistical Analyses

Statistical analyses were performed using R (Version 4.0.3; R Core Team, 2020).[22] The descriptive characteristics are presented as mean and SD or as median and inter-quartile range (IQR), depending on whether the data are normally distributed or not. Categorical data are presented as counts. Age differences between patients and controls were assessed using Student's t-test. A chi square test was performed to assess the effect of sex between groups. A significance level of 0.05 was chosen for all tests.

Differences in TC between patients and controls were investigated for each of the normalizations (T1w, rigid-body, affine, and DCT) using a scatterplot and a boxplot.

In addition, to investigate the differences in the consensus rating of different types of normalization, we fitted a Bayesian proportional odds cumulative logit mixed model. Besides the type of registration, the model included the patient's group (patient vs. control) and random intercepts for each subject to take into account the fact that different types of normalization performed in the same child are likely correlated. The results are presented as odds ratios and corresponding 95% credible intervals (CI). To facilitate interpretation of the estimated differences in ratings between the different types of normalization, we plotted the estimated probability of receiving a particular rating for each type of normalization (in patients). To compare the mean CBF in three gyri of the frontal lobe in trigonocephaly patients vs. controls for different normalizations, we fitted a mixed linear model for each of the gyri. A random intercept was included to take into account the fact that measurements of different gyri in the same child are likely correlated. Mean regional CBF that was assessed in an anatomical region of interest cannot be reliably assessed in group analyses in children for whom the spatial normalization failed. To avoid bias in the CBF analysis, we have excluded all children from whom one of the four methods failed to generate CBF map in standard space or from whom the map was rated as unusable in the qualitative analysis. Due to the small sample size, no other variables could be included in the model.

RESULTS

Characteristics

A total of 36 patients with trigonocephaly with a median age of 0.50 years (IQR 0.30) and sixteen control subjects with a median age of 0.83 years (IQR 0.56) were included (**Table 1**). The age was shown to be significantly different (p = 0.006) between patients (mean: 0.60 years) and controls (mean: 0.90 years). Sex was also significantly different between groups (p = 0.03) but had no significant effect on the frontal lobe perfusion in this cohort (p = 0.09).

Table 1. Patient characteristics

	Trigonocephaly (n=36)	Controls (n=16)
Sex (n female)	11 (30.6%)	10 (62.5%)
Age (median± IQR years)	0.50±0.30	0.83±0.56

Quantitative Comparison of Normalization Strategies

From all normalization strategies, regASLdct shows the highest TC score (**Figure 1**). The range of the TC is depicted for patients and controls in **Figure 2**. The overlapping boxplots of the ASL normalization types in the control group, demonstrate that there is little difference between these normalizations with respect to the TC. RegASLdct had the highest TC outcome for patients as well as controls. For patients, regASLaffine had better TC outcomes than regT1, or regASLrigid, whereas for controls regASLrigid performed similar to regASLaffine.

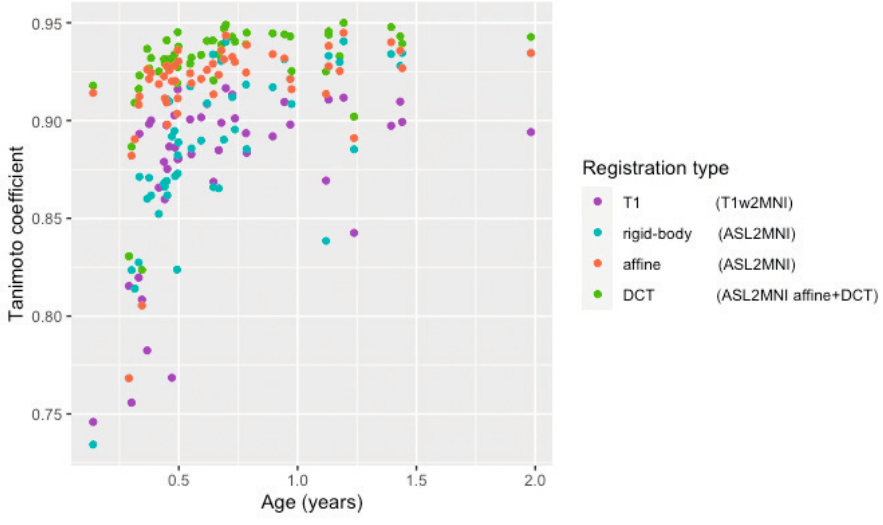

Figure 1. A scatterplot of the Tanimoto coefficient of four registration types of the total cohort in time (age in years).

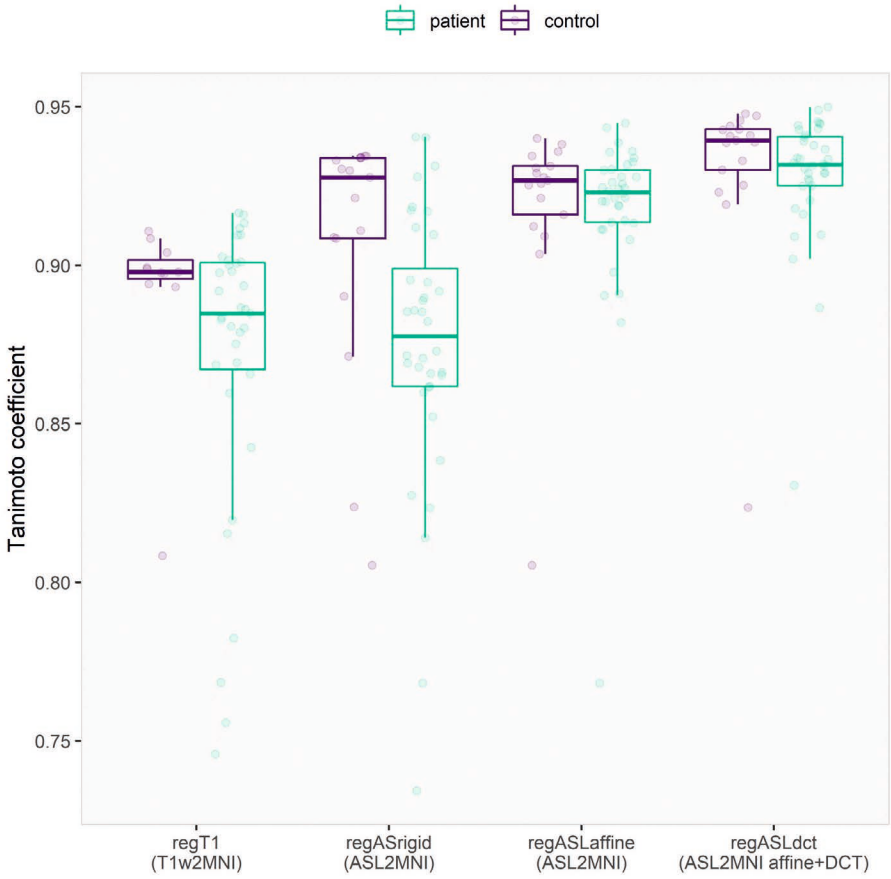

Figure 2. Visualization of the Tanimoto coefficient of the four registration types in patients and controls. The dots represent the original data, while the boxplots show the 25, 50, and 75% quantiles. The whiskers reach to a maximum of 1.5 times the IQR.

Qualitative Comparison of Normalization Strategies

The T1w image, the ASL image, the four normalizations, and the pseudo-image of three trigonocephaly subjects are shown in **Figure 3**. As depicted in **Table 2**, the MRI of a patient with trigonocephaly received higher ratings compared with the MRIs of controls (OR 2.61 CI 0.70–9.95). RegASLrigid has lower odds of receiving a higher rating (OR 0.33 CI 0.14–0.77). The odds of having a higher rating are 2.61 times as large for regASLaffine (CI 1.11–6.25) and 17.51 times as large as for regASLdct (CI 6.66–49.38) compared with the odds of the regT1.

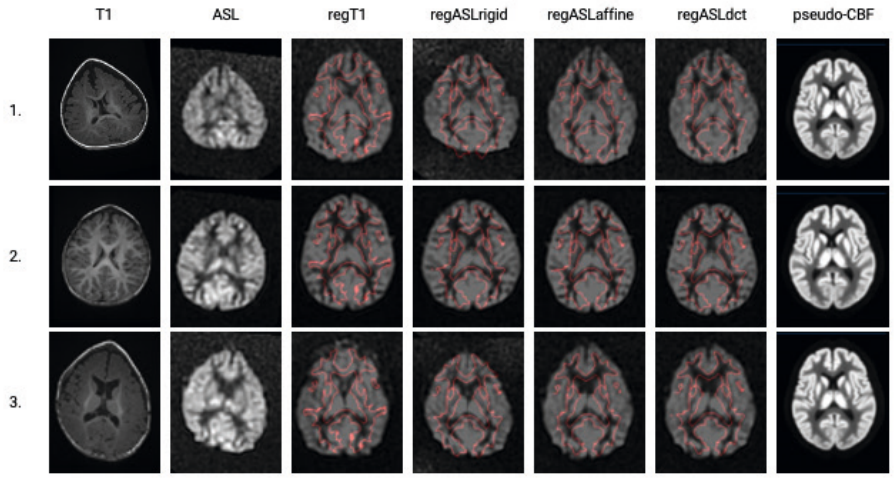

Figure 3. A single axial slice is shown (columns left to right) for the T1-weighted image and the ASL image in their native space before registration and for the results of the four registration methods in the standard space: regT1, regASLrigid, regASLaffine, and regASLdct of three trigonocephaly subjects (rows). In the standard space, a CBF image is shown with borders of the WM from the template (with a threshold at 50%) shown in red. Finally, the pseudo-CBF images of the three trigonocephaly patients are shown.

Table 2. Odds ratios for receiving a higher rating (i.e., the odds are calculated as P(rating>k)/P(rating≤k)

	Odds Ratio	**2.5%**	**97.5%**
trigonocephaly	2.611	0.698	9.954
regASLrigid	0.332	0.143	0.770
regASLaffine	2.608	1.113	6.249
regASLdct	17.508	6.659	49.378

The resulting estimated probabilities for an MRI of a patient to receive a particular rating are visualized in **Figure 4** and reported **in Table 3**. The highest probabilities of a good rating were estimated for regASLdct (0.38, 95% CI 0.19–0.60 for rating 4 and 0.56, 95% CI 0.38–0.72 for rating 3). RegASLaffine had the highest probability of receiving a rating of 3 (0.64, 95% CI 0.49–0.76), and a one in four chance of receiving a rating of 2 (95% CI0.12–0.42). For regT1 and regASLrigid ratings 2 and 3 were most likely (regT1 rating 3: 0.48, 95% CI 0.29–0.66, rating 2: 0.43, 95% CI 0.24–0.61; regASLrigid rating 3: 0.26, 95% CI 0.12–0.44, rating 2: 0.59, 95% CI 0.44–0.72).

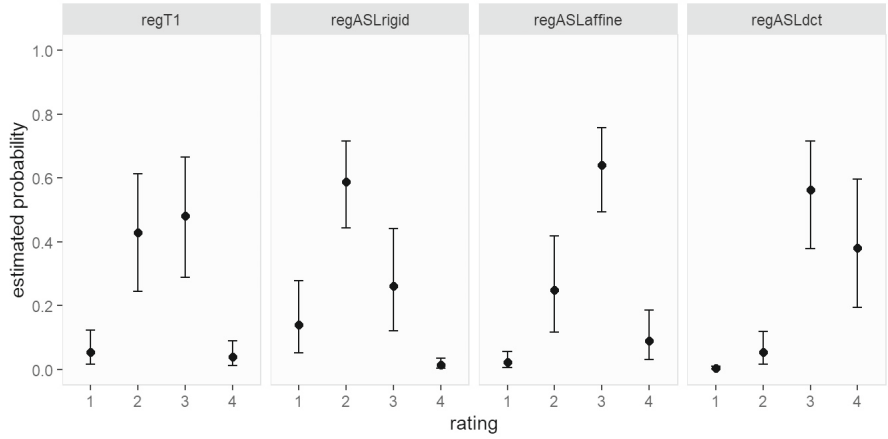

Figure 4. Estimated probability (and corresponding 95% CI) of obtaining a certain rating for each type of registration (for patients).

Table 3. Estimated probability to get a particular rating for each type of registration (and corresponding 95% CI).

rating	regT1	regASLrigid	regASLaffine	regASLdct
1	0.05 [0.02, 0.12]	0.14 [0.05, 0.28]	0.02 [0.01, 0.05]	0.00 [0.00, 0.01]
2	0.43 [0.24, 0.61]	0.59 [0.44, 0.72]	0.25 [0.12, 0.42]	0.05 [0.02, 0.12]
3	0.48 [0.29, 0.66]	0.26 [0.12, 0.44]	0.64 [0.49, 0.76]	0.56 [0.38, 0.72]
4	0.04 [0.01, 0.09]	0.01 [0.00, 0.03]	0.09 [0.03, 0.19]	0.38 [0.19, 0.60]

CBF Comparison of Normalization Strategies

The results of the mixed linear model demonstrate that there was no evidence of a difference in the mean CBF of the frontal lobe between trigonocephaly patients and controls (**Table 4**). Moreover, the mean CBF evaluated in the frontal lobe was significantly higher for direct ASL registration to the MNI space via a pseudoCBF for all three types of registration (regASLrigid, regASLaffine, regASLdct) compared with regT1.

Table 4. Linear mixed model on the three gyri of the frontal lobe of 41 subjects using the Hammers Atlas (mL/100g/min).

Inferior Frontal Gyrus	Value	Std.Error	2.5%	97.5%
(Intercept)	52.81	4.68	43.54	62.08
trigonocephaly patient	8.13	5.34	-2.71	18.97
regASLrigid	9.33	0.90	7.55	11.12
regASLaffine	17.11	0.90	15.32	18.89
regASLdct	17.45	0.90	15.67	19.24
Middle frontal Gyrus				
(Intercept)	50.15	5.07	40.09	60.21
trigonocephaly patient	1.93	5.78	-9.82	13.67
regASLrigid	10.59	1.05	8.51	12.68
regASLaffine	18.94	1.05	16.86	21.02
regASLdct	18.49	1.05	16.40	20.57
Superior Frontal Gyrus				
(Intercept)	45.75	4.63	36.58	54.93
trigonocephaly patient	9.39	5.27	-1.32	20.09
regASLrigid	14.28	1.00	12.29	16.26
regASLaffine	18.99	1.00	17.01	20.98
regASLdct	18.88	1.00	16.90	20.87

DISCUSSION

In this study, we have shown that direct normalization of ASL images to MNI space using ASL CBF as image contrast outperforms spatial normalization based on T1w segmentation in MRI brain studies of both patients and controls who are less than 2 years of age. The nonlinear registration outperformed both rigid and affine registration among the methods using the ASL CBF contrast. While better results in TC of the regASLdct were shown for the control group, the difference between regT1 and regASLdct was even higher in patients in both qualitative analysis and CBF analysis. The CBF values in three gyri of the frontal lobe, which are clinically relevant for trigonocephaly patients, were significantly different compared with the CBF values extracted using the spatial normalization with the regT1 method. This shows the impact of the choice of registration contrast and the importance of this proposed method in a cohort where gray-white matter contrast in structural images is low due to ongoing myelination.

Using the SPM-based segmentation and normalization pipeline in ExploreASL with T1w, our initial attempts to register and segment the brain of trigonocephaly patients

showed poor performance, even though a dedicated template for young children was used.[13] Our normalization was complicated by the ongoing myelination in these young patients. Here, we were able to combine our previously developed CBF-contrast-based registration with a low-degree-of-freedom nonlinear component to improve the registration for the deformed skulls reaching a better registration.[6] In this previous study of Mutsaerts et al., T1w images of elderly patients with frontotemporal dementia were spatially normalized to MNI and ASL was aligned with T1w images using the CBF-GM contrast. The joint transformation of ASL to T1w and T1w to MNI space was then used for spatial normalization of ASL to MNI. In the current study, we extended the previous work by aligning ASL to MNI directly using the CBF vs. GM contrast and investigating, also, the DCT transformation to assess the qualitative and quantitative benefit of this method in a pediatric patient cohort with skull deformations.

Both regT1 and regASLrigid performed poorly on the TC and qualitatively. For the regT1 we attribute this to the relatively low WM-GM contrast of these images. The poor performance of regASLrigid is likely caused by the fact that brain size and shape differ with age. Also, it is challenging to register with MNI with only a rigid registration that preserves size. The regASLaffine and regASLdct registrations show a better alignment. RegASLaffine and regASLdct addresses both issues and therefore performed better in TC and on the qualitative rating. The advantage of regASLdct over regASLaffine is that it can adapt to the nonlinear deformations present in the trigonocephaly patients. Therefore, rigid and affine registrations followed by nonlinear deformations using a linear combination of three-dimensional DCT basis functions were considered sufficient for alignment of the individual data to the template.[20] The quality of the pseudo-CBF image is essential for the registration. Typical values of CBF of 60 and 20 ml/min/100 g in GM and WM, respectively, were used. Even though these values are only rough approximations, and the population and individual values differ largely, they still capture the general differences in contrast between the tissue types, and this approximation was sufficient for the regASLrigid and regASLaffine registration. This, however, was not sufficient for the regASLdct registration with more degrees of freedom. To obtain good results, the regASLdct registration had to be performed in two iterations, where the regional CBF in GM and WM were first approximated from the ASL image after a rough alignment and used to construct a more realistic pseudo-CBF image in the second iteration. While the spatial normalization reached a good quality in most subjects, further improvement could be achieved in the future in large populations using population-specific templates. To address the relatively high deformation variability, the Cerebromatics approach could be used to create a template that covers a range of deformation types and severity. Subgroups other than trigonocephaly patients could also possibly be considered. To address more severe deformations, further deformation algorithms might need to be tested that provide potentially a better performance than the DCT registration.[23]

Ground truth measurement of CBF was not present in this study to ultimately prove the validity of the proposed method for spatial normalization. However, since all methods contained the same preprocessing except for the spatial normalization, we assume that a difference in extracted regional CBF is a sufficient measure of the difference between the methods. Moreover, we assume that the method that performed better at the qualitative and quantitative evaluation of the spatial normalization will also be closer to the ideal normalization.

As the registration of spatial MRI sequences to structural regT1 images of the brain is a major challenge in patients with unmyelinated brains (such as neonates), there are other example studies concerning the use of contrast that is not usual for this population. Because many immature white matter tracts cannot be differentiated with conventional MR images (T1w or T2w) caused by insufficient myelination during the preterm development period, Feng et al. and Yoshida et al. used DTI as a substitute for T1w in a preterm population.[4, 5] Another example, which is also relevant for neonates, is tract based spatial statistics, permitting a voxel-wise statistical analysis of the entire white matter skeleton instead of the usual DTI ROI approach.[24, 25] This study could be an initial impetus for future large cohort pediatric ASL studies using ASL as an unusual contrast.

Imaging of preterm and term-born infants for clinical indications is of great interest. It has been demonstrated that various injuries, due to perinatal risk often leads to damage in selective white matter.[26] De Vis et al. have already demonstrated that CBF progressively increases during the first period of life as synaptogenesis, myelination, and brain functional activity progress.[27] Miranda et al. have observed cerebral perfusion was significantly higher in preterm newborns studied at term-corrected age than in term-born newborns, indicating that brain perfusion may be influenced by developmental and postnatal age.[28] Both studies were based on manual ROI delineations of cortical regions or on manual placement of control points in GM and WM. Using the proposed normalization method provides clinical users an automatic delineation, which could potentially lead to a higher reproducibility and regional accuracy.

Limitations

One main limitation is that we tested whole-brain alignment only, i.e., we have not systematically tested the alignment quality on the level of individual cortical structures. While the method proved to provide usable or excellent spatial normalization and thus should allow the reliable assessment of perfusion in specific regions of the MNI space, a more thorough validation is needed to demonstrate whether this normalization method allows regional CBF evaluation in MNI space using gray and white matter masks. Currently, the method thus allows the study of regional brain perfusion even in the absence of a T1w image, but further validation is needed to fully replace T1w

images in ASL processing when not available. For that reason, more advanced analysis that uses T2-weighted and DTI MR brain images to aid segmentation is planned. Moreover, we aim to study the GM CBF after partial volume correction. However, currently, tissue segmentation from T1w images is not possible for all subjects, which is a hurdle for use of partial-volume correction on an individual basis.[4] Second, while this cohort of 36 preoperative MRI scans of trigonocephaly patients is limited in size, it is the first study on automated ASL evaluation in trigonocephaly patients aged 0–3 years. The craniofacial unit of the Erasmus MC continues with the prospective collection of preoperative MRI scans of craniosynostosis patients for clinical and research perspectives which includes also other patients than those with trigonocephaly. A validation of this methodology on a larger cohort is thus planned, which will also include patients with more severe skull deformations. A third limitation is that our control group consisted of patients who underwent MRI examination for clinical reasons, where the MRI and clinical course showed no cerebral pathology. At last, patients and controls were not age exactly matched. While this might slightly affect the CBF difference and the performance of the normalization between groups, the key findings of this study lie in comparing normalization methods within each group for which this minor age difference bears no importance.

CONCLUSION

In conclusion, when the conventional T1w and T2w contrast between GM and WM are hard to differentiate, spatial normalization is feasible by using the ASL perfusion contrast directly. The choice of contrast for registration has an impact on both the quality of ASL alignment and the extracted regional CBF values. The results of this study may be an important step toward the feasibility of future large pediatric ASL MRI brain studies.

REFERENCES

1. Knickmeyer RC, Gouttard S, Kang C, et al. A structural MRI study of human brain development from birth to 2 years. *J Neurosci* 2008;28:12176-12182
2. Dubois J, Dehaene-Lambertz G, Kulikova S, et al. The early development of brain white matter: a review of imaging studies in fetuses, newborns and infants. *Neuroscience* 2014;276:48-71
3. Holland D, Chang L, Ernst TM, et al. Structural growth trajectories and rates of change in the first 3 months of infant brain development. *JAMA Neurol* 2014;71:1266-1274
4. Feng L, Li H, Oishi K, et al. Age-specific gray and white matter DTI atlas for human brain at 33, 36 and 39 postmenstrual weeks. *Neuroimage* 2019;185:685-698
5. Yoshida S, Oishi K, Faria AV, et al. Diffusion tensor imaging of normal brain development. *Pediatr Radiol* 2013;43:15-27
6. Mutsaerts H, Petr J, Thomas DL, et al. Comparison of arterial spin labeling registration strategies in the multi-center GENetic frontotemporal dementia initiative (GENFI). *J Magn Reson Imaging* 2018;47:131-140
7. de Jong T, Bannink N, Bredero-Boelhouwer HH, et al. Long-term functional outcome in 167 patients with syndromic craniosynostosis; defining a syndrome-specific risk profile. *J Plast Reconstr Aesthet Surg* 2010;63:1635-1641
8. Spruijt B, Joosten KF, Driessen C, et al. Algorithm for the Management of Intracranial Hypertension in Children with Syndromic Craniosynostosis. *Plast Reconstr Surg* 2015;136:331-340
9. Maliepaard M, Mathijssen IM, Oosterlaan J, et al. Intellectual, behavioral, and emotional functioning in children with syndromic craniosynostosis. *Pediatrics* 2014;133:e1608-1615
10. Johnson D, Wilkie AO. Craniosynostosis. *Eur J Hum Genet* 2011;19:369-376
11. Keil VC, Hartkamp NS, Connolly DJA, et al. Added value of arterial spin labeling magnetic resonance imaging in pediatric neuroradiology: pitfalls and applications. *Pediatr Radiol* 2019;49:245-253
12. Doerga PN, Lequin MH, Dremmen MHG, et al. Cerebral blood flow in children with syndromic craniosynostosis: cohort arterial spin labeling studies. *J Neurosurg Pediatr* 2019:1-11
13. de Planque CA, Petr J, Gaillard L, et al. Cerebral Blood Flow of the Frontal Lobe in Untreated Children with Trigonocephaly versus Healthy Controls: An Arterial Spin Labeling Study. *Plast Reconstr Surg* 2022;149:931-937
14. Birgfeld CB, Saltzman BS, Hing AV, et al. Making the diagnosis: metopic ridge versus metopic craniosynostosis. *J Craniofac Surg* 2013;24:178-185
15. Mutsaerts H, Petr J, Groot P, et al. ExploreASL: An image processing pipeline for multi-center ASL perfusion MRI studies. *Neuroimage* 2020;219:117031
16. Mutsaerts HJ, van Osch MJ, Zelaya FO, et al. Multi-vendor reliability of arterial spin labeling perfusion MRI using a near-identical sequence: implications for multi-center studies. *Neuroimage* 2015;113:143-152
17. Mutsaerts HJ, Steketee RM, Heijtel DF, et al. Inter-vendor reproducibility of pseudo-continuous arterial spin labeling at 3 Tesla. *PLoS One* 2014;9:e104108
18. Ashburner J. A fast diffeomorphic image registration algorithm. *Neuroimage* 2007;38:95-113
19. Shi F, Yap PT, Wu G, et al. Infant brain atlases from neonates to 1- and 2-year-olds. *PLoS One* 2011;6:e18746
20. Ashburner J, Friston KJ. Nonlinear spatial normalization using basis functions. *Hum Brain Mapp* 1999;7:254-266

21. Anastasiu DC, Karypis, G. Efficient identification of Tanimoto nearest neighbors. *Int J Data Sci Anal* 2017:153–172

22. Team RC. R: A language and environment for statistical computing. R Foundation for Statistical Computing, Vienna, Austria. ; 2020

23. Klein A, Andersson J, Ardekani BA, et al. Evaluation of 14 nonlinear deformation algorithms applied to human brain MRI registration. *Neuroimage* 2009;46:786-802

24. Smith SM, Jenkinson M, Johansen-Berg H, et al. Tract-based spatial statistics: voxelwise analysis of multi-subject diffusion data. *Neuroimage* 2006;31:1487-1505

25. Duerden EG, Foong J, Chau V, et al. Tract-Based Spatial Statistics in Preterm-Born Neonates Predicts Cognitive and Motor Outcomes at 18 Months. *AJNR Am J Neuroradiol* 2015;36:1565-1571

26. Rutherford M, Counsell S, Allsop J, et al. Diffusion-weighted magnetic resonance imaging in term perinatal brain injury: a comparison with site of lesion and time from birth. *Pediatrics* 2004;114:1004-1014

27. De Vis JB, Petersen ET, de Vries LS, et al. Regional changes in brain perfusion during brain maturation measured non-invasively with Arterial Spin Labeling MRI in neonates. *Eur J Radiol* 2013;82:538-543

28. Miranda MJ, Olofsson K, Sidaros K. Noninvasive measurements of regional cerebral perfusion in preterm and term neonates by magnetic resonance arterial spin labeling. *Pediatr Res* 2006;60:359-363

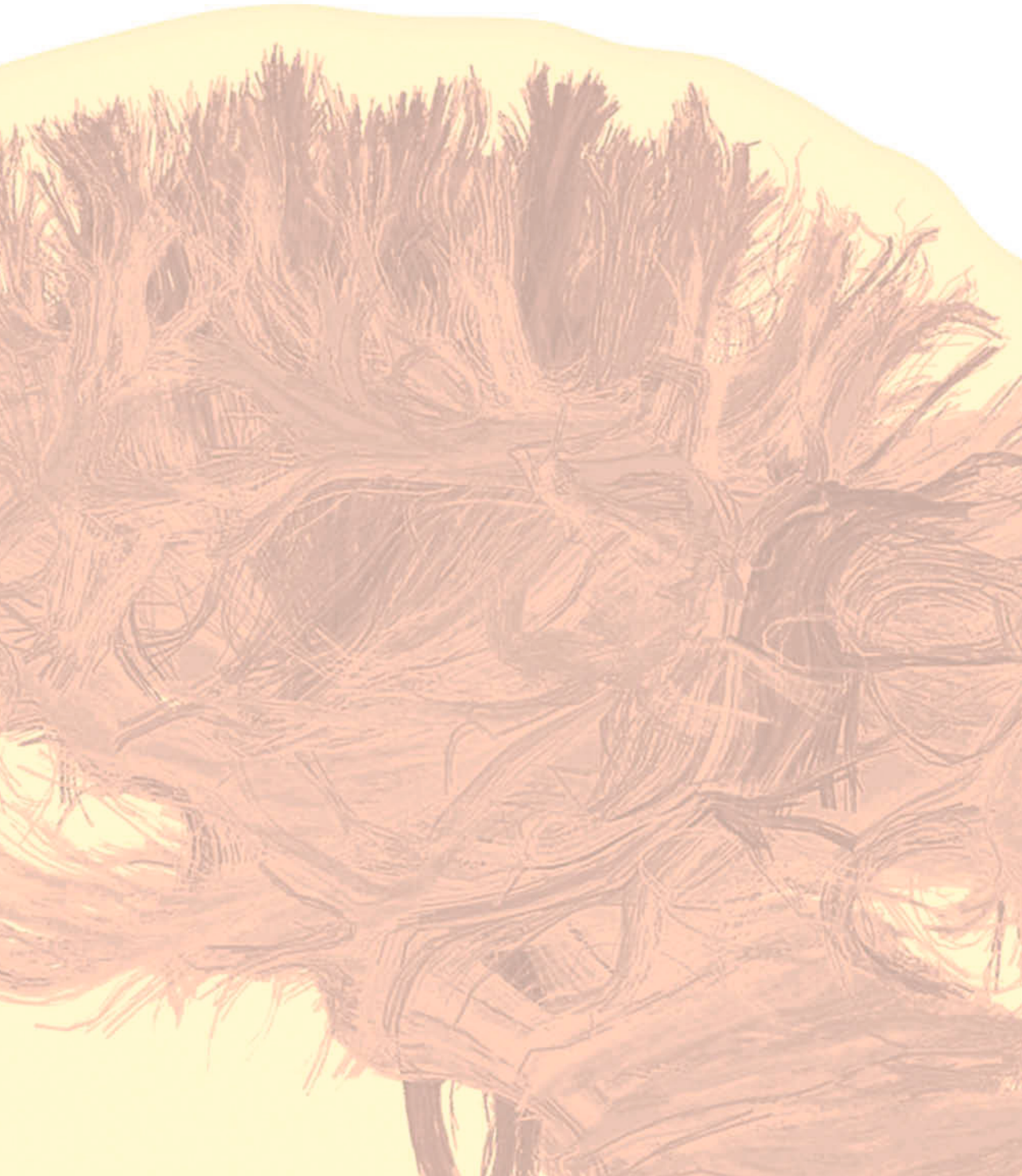

3

CHAPTER 3

CEREBRAL BLOOD FLOW OF THE FRONTAL LOBE IN UNTREATED CHILDREN WITH TRIGONOCEPHALY VERSUS HEALTHY CONTROLS: AN ARTERIAL SPIN LABELING STUDY

CATHERINE A. DE PLANQUE

JAN PETR

LINDA GAILLARD

HENK J. M. M. MUTSAERTS

MARIE-LISE C. VAN VEELEN

SARAH L. VERSNEL

MARJOLEIN H. G. DREMMEN

IRENE M. J. MATHIJSSEN

Journal of Plastic and Reconstructive Surgery, 2022 Apr 1;149(4):931-937

ABSTRACT

Background: Craniofacial surgery is the standard treatment for children with moderate to severe trigonocephaly. The added value of surgery to release restriction of the frontal lobes is unproven, however. In this study, the authors aim to address the hypothesis that the frontal lobe perfusion is not restricted in trigonocephaly patients by investigating cerebral blood flow.

Methods: Between 2018 and 2020, trigonocephaly patients for whom a surgical correction was considered underwent magnetic resonance imaging brain studies with arterial spin labeling to measure cerebral perfusion. The mean value of cerebral blood flow in the frontal lobe was calculated for each subject and compared to that of healthy controls.

Results: Magnetic resonance imaging scans of 36 trigonocephaly patients (median age, 0.5 years; interquartile range, 0.3; 11 female patients) were included and compared to those of 16 controls (median age, 0.83 years; interquartile range, 0.56; 10 female patients). The mean cerebral blood flow values in the frontal lobe of the trigonocephaly patients (73.0 ml/100 g/min; SE, 2.97 ml/100 g/min) were not significantly different in comparison to control values (70.5 ml/100 g/ min; SE, 4.45 ml/100 g/min; $p = 0.65$). The superior, middle, and inferior gyri of the frontal lobe showed no significant differences either.

Conclusions: The authors' findings suggest that the frontal lobes of trigonocephaly patients aged less than 18 months have a normal cerebral blood flow before surgery. In addition to the very low prevalence of papilledema or impaired skull growth previously reported, this finding further supports the authors' hypothesis that craniofacial surgery for trigonocephaly is rarely indicated for signs of raised intracranial pressure or restricted perfusion for patients younger than 18 months.

CLINICAL QUESTION/LEVEL OF EVIDENCE: Risk, II.

INTRODUCTION

Trigonocephaly caused by prenatal closure of the metopic suture is the second most common form of single-suture craniosynostosis.[1] Patients present within a sliding scale of severity in phenotype, depending on the timing of suture closure. It remains a subject of discussion, which degree of severity is clinically relevant for a surgical indication. Nowadays, patients with moderate and severe phenotypes undergo surgical correction of the frontal bones and supraorbital rims, aiming for unrestricted brain development, to reduce the risk of neurodevelopmental disorders and to improve aesthetics. Nevertheless, preoperatively, less than 2 percent of the trigonocephaly patients have papilledema as a sign of intracranial hypertension.[2] Moreover, preoperative trigonocephaly patients show a normal intracranial volume in comparison to healthy, aged-matched controls.[3] Lastly, it was shown that patients with trigonocephaly are at risk of developing mental deficiencies/disorders, behavioral problems, and delays in speech and language, which was also the case for the milder phenotypes which were not operated.[4, 5] Taking all the above together, it remains unknown what the added value of surgery is in trigonocephaly with respect to future brain development.

The exact mechanism of the association between trigonocephaly and suboptimal neurodevelopmental outcome is not fully understood.[6] Although some have suggested that brain development is impaired as a result of the synostosis, others hypothesize that the increased prevalence of neurodevelopmental disorders in these patients is caused by an intrinsic brain disorder. The former hypothesis of restricted brain development caused by synostosis could be reflected in altered cerebral blood flow.[7-10] Brain perfusion in trigonocephaly patients was examined previously with single-photon emission computed tomography, and a lower perfusion was reported in the frontal lobe preoperatively compared to postoperatively and to the rest of the brain.[9, 10] These two studies offered qualitative evaluation of relative perfusion values only, however. Despite the development of more advanced magnetic resonance imaging techniques to measure cerebral perfusion, this original claim has not been reassessed yet. Arterial spin labeling magnetic resonance imaging is a technique that provides injectionfree measurements of absolute brain perfusion with quantitative accuracy and precision comparable to that of H2015 positron emission tomography. [11] Arterial spin labeling has previously been used for several pediatric applications (e.g., vascular diseases, tumors, epilepsy, seizures) to detect cortical hyperperfusion or hypoperfusion.[12] The main advantages of the arterial spin labeling technique are that it measures absolute perfusion and does not require intravenous contrast agent injection.[13] Craniosynostosis patients present a further challenge given the skull deformations of these patients.[8, 14, 15]

The aim of this study was to reassess the previous claims of perfusion changes in craniosynostosis subjects to gain more insight into the hypothesis of brain restriction

by comparing preoperative frontal lobe cerebral blood flow of young children with moderate to severe trigonocephaly with cerebral blood flow of aged-matched, healthy controls. Brain perfusion was assessed in several brain regions, focusing mostly on the frontal lobe because of the shape of the skull in trigonocephaly patients and the increased prevalence of behavior and cognitive disorders. Based on the very low prevalence of papilledema or impaired skull growth in trigonocephaly compared to other craniosynostosis patients, we hypothesized that there would be no abnormalities in frontal lobe perfusion in the first 2 years of life.[2, 3]

PATIENTS AND METHODS

The Ethics Committee of the Erasmus Medical Center approved this prospective imaging study in patients with trigonocephaly (METC-2018-124), which is part of ongoing work at the Dutch Craniofacial Center. This study was conducted according to the principles of the Declaration of Helsinki.

Study Population

Magnetic resonance imaging scans from children with metopic synostosis for whom a surgical correction was considered were included over a period of 2 years (2018 to 2020). Surgery is only considered for moderate and severe presentation, mainly defined by the forehead shape in a bird's eye view and considered present if the lateral orbital rim is visible and the midline ridge is significantly prominent. This is illustrated by Birgfeld et al. in Figure 5.[16] Children were less than 2 years of age at the time of the magnetic resonance imaging brain study. The control group consisted of subjects undergoing magnetic resonance imaging for clinical reasons. These subjects were included when the following conditions were met: (1) the subjects were found to have no neurological pathology of the head and neck area on imaging, (2) the subjects were free of any neurological or psychological morbidity on follow-up, and (3) the subjects' magnetic resonance imaging data were of sufficient quality to be used for research.

Magnetic Resonance Imaging Acquisition

All brain magnetic resonance imaging data were acquired with a 1.5T scanner (General Electric Healthcare, Chicago, Ill.), including pseudocontinuous arterial spin labeling sequence with the following imaging parameters: threedimensional fast spin echo spiral readout with a stack of eight spirals with three signal averages, repetition/echo time of 4604 msec/10.7 msec, voxel size of 3.75 × 3.75 × 4.0 mm3, field of view at 24.0 × 24.0 cm, labeling duration of 1450 msec, postlabeling delay of 1025 msec, five background suppression pulses, and an inversion recovery M0 scan for calibration. This protocol was identical in both trigonocephaly patients and controls. Both groups underwent deep sedation or anesthesia during the magnetic resonance imaging procedure, which included using sevoflurane or propofol.

Arterial Spin Labeling Data Analysis

The arterial spin labeling technique uses water molecules in the blood to measure perfusion. This imaging technique magnetically labels arterial blood water when it flows through the neck, and after a postlabeling delay during which the blood is allowed to flow to distal brain tissue an image of the brain is able to depict this change in magnetization in the blood. Therefore, an arterial spin labeling image is weighted for the cerebral blood flow (i.e., the volume of blood that perfuses 100 g of tissue per minute). Data processing and evaluation were performed with the ExploreASL pipeline and included the basic processing of arterial spin labeling and M0 calibration images as described in the ExploreASL review article.[17] T1-weighted images were excluded from the complete analysis due to insufficient differentiation between white and gray matter. This is common for the age group we studied because of incomplete myelination and precluded successful segmentation and spatial normalization in some of the subjects. To be able to use the structural atlas of brain regions for the evaluation, the arterial spin labeling images were directly aligned with the Montreal Neurological Institute template. In this age group, the brain is of considerably different shape and size than the adult brain. Therefore, a dedicated template, the University of North Carolina 0-1-2 infant atlases for 1-year-olds, was used to replace the adult template.[18] The control images were not of high enough contrast to allow alignment with the mean Montreal Neurological Institute T1-weightedimage; therefore, registration of the individual cerebral blood flow to a standard-space pseudo cerebral blood flow, based on the gray matter and white matter maps of the template, was performed.[19] Because of the relatively high amount of skull deformations in the patient group, rigid or affine registration was not considered sufficient for the alignment of the individual data to the template. Therefore, an affine registration, followed by nonlinear deformations using a linear combination of three-dimensional discrete cosine transform basis functions, was used.[20]

The cerebral blood flow was quantified according to the consensus article by Alsop et al.[11] Regional cerebral blood flow was evaluated in both hemispheres taken together in the superior, middle, and inferior gyri of the frontal lobe. The anatomical regions of interest were taken from Hammer's atlas in the Montreal Neurological Institute space and transformed to the subject's native space using the previously obtained transformation for the spatial normalization.[21] Mean cerebral blood flow values and the frontal lobe, occipital lobe, parietal lobe, temporal lobe, insula, cerebellum, caudate, putamen, and thalamus brain regions were investigated.

Statistical Analyses

Statistical analyses were performed using R version 4.0.3 (R Foundation for Statistical Computing, Vienna, Austria).[22] The descriptive statistics of the patient demographics are presented as mean and SD or as median and interquartile range, depending on if the data are normally distributed or not. Categorical data are presented as counts.

Histograms, boxplots, and the Shapiro-Wilk test were used to confirm that cerebral blood flow was approximately normally distributed. Linear mixed models were used to compare the mean cerebral blood flow in the frontal lobe in trigonocephaly patients versus control subjects. We did not include age or sex in this model due to our limited sample size. A chi-square test was performed to assess the effect of sex on the frontal lobe perfusion. To confirm the validity of our data, we normalized cerebral blood flow data of the frontal lobe by occipital lobe data using the ratio of frontal lobe to occipital lobe. We compared this frontal lobe to occipital lobe ratio between patients and control subjects by using a t test. In addition, we assessed the ratio of the spatial coefficient of variation — a measure of global spatial signal distribution — between the frontal lobe and occipital lobe, comparing the ratios between patients and control subjects using a t test. A significance level of 0.05 was considered for all tests. As a supplement, descriptive data on cerebral blood flow of the other brain regions were set out as mean, standard deviation, standard error, and lower and upper confidence interval.

RESULTS

Patient Characteristics

Thirty-six unoperated patients with trigonocephaly with a median age of 0.50 years (interquartile range, 0.30) and 16 control subjects with a median age of 0.83 years (interquartile range, 0.56) were included in this study, as presented in **Table 1**. During follow-up after the magnetic resonance imaging scans, 18 patients underwent a frontosupraorbital remodeling at a median age of 0.82 years (interquartile range, 0.08). All patients were initially considered for surgical intervention. Eighteen patients were operated on to correct the contour of the forehead, and the remaining patients were not operated on after joint decision making with their parents (n = 18). The follow up median age of the operated trigonocephaly group was 1.63 years (interquartile range, 1.16); the follow-up median age of the trigonocephaly group not operated on was 1.71 years (interquartile range, 0.41).

Table 1. Patient Characteristics.

	Trigonocephaly	Controls
n MRI	36	16
f : m	11:25	10:06
median age (IQR)	0.5(0.3)	0.83(0.56)
n Frontosupraorbital remodellation	18	
f : m	07:11	
median age (IQR)	0.82(0.08)	
Follow-up		
operated trigonocephaly patients median age (IQR)	1.63(1.16)	
non-operated trigonocephaly patients median age (IQR)	1.71(0.41)	

Frontal Lobe Perfusion

By linear mixed model**, Table 2** demonstrates that there was no significant difference in the mean cerebral blood flow of the frontal lobe between trigonocephaly patients (73 ml/100 g/ min) and control patients (70.5 ml/100 g/min, p = 0.65). **Table 3** shows the mean perfusion for the superior, middle, and inferior frontal gyri. None of these three levels was significantly different between the patient and control groups.

Table 2. Linear mixed model on the perfusion of the frontal lobe using the structural atlas (mL/100g/min).

	Trigonocephaly				**Control**				
	mean	SE	lower.ci	upper.ci	mean	SE	lower.ci	upper.ci	p-value
Frontal lobe	73.0	2.97	67.0	78.9	70.5	4.45	61.6	79.4	0.65

Table 3. Linear mixed model on the three gyri of the frontal lobe using the Hammers Atlas (mL/100g/min).

	Trigonocephaly				**Control**			
	mean	SE	lower.ci	upper.ci	mean	SE	lower.ci	upper.ci
Superior frontal gyrus	70.9	2.90	65.1	76.7	68.2	4.34	59.5	76.9
Middle frontal gyrus	68.4	3.09	62.2	74.6	70.1	4.63	60.8	79.4
Inferior frontal gyrus	76.8	2.9	70.9	82.6	75.9	4.5	66.8	84.9

To account for physiological perfusion fluctuations, we chose the occipital lobe as a reference region for normalization. Both frontal/occipital cerebral blood flow ratios between patients and control subjects and the spatial coefficient of variance between patients and control subjects did not show a significant difference (p = 0.10 and p = 0.09, respectively). To demonstrate the range of values, the mean cerebral blood flow of the frontal lobe for each individual in our cohort is shown in **Figure 1.** Finally, sex had no significant effect on the frontal lobe perfusion in this cohort (p = 0.09).

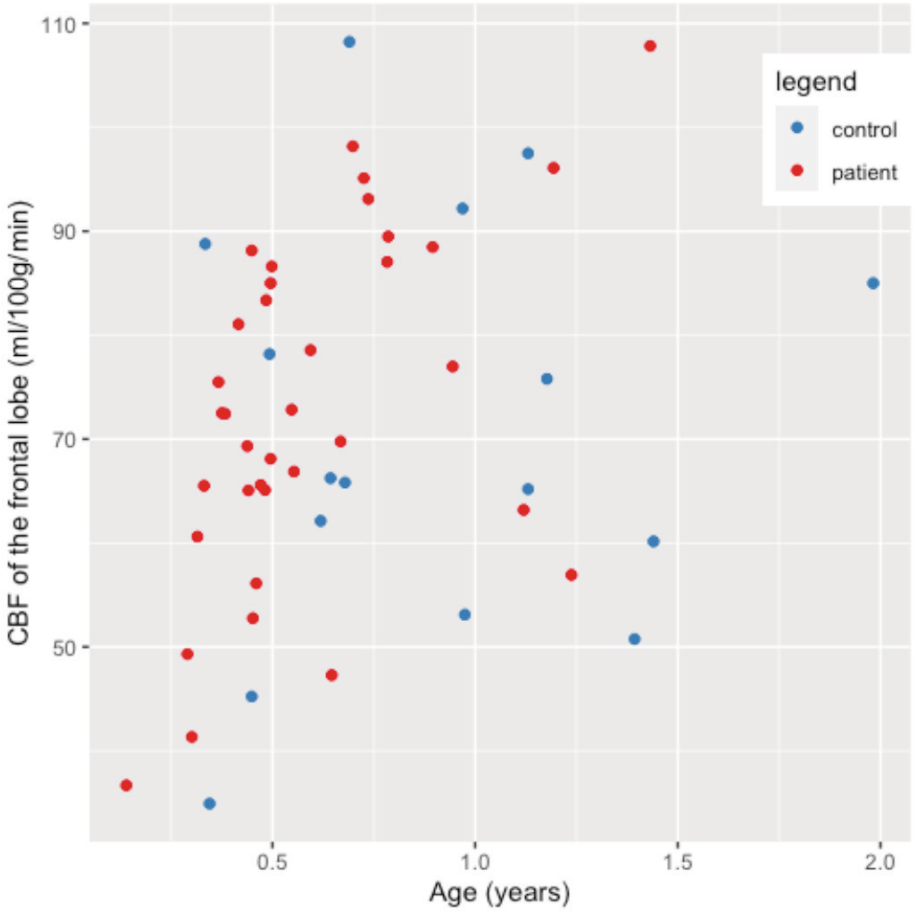

Figure 1. Mean CBF (mL/100g/min) of the frontal lobe of each trigonocephaly patient and control.

Perfusion of Other Brain Regions

We observed no significant difference in trigonocephaly patients as compared to control subjects for the frontal lobe, occipital lobe, parietal lobe, temporal lobe, insula, cerebellum, caudate, putamen, and thalamus. The cerebral blood flow values are summarized in **Table 4, Supplemental Digital Content 1**.

Supplemental table 4. Perfusion per brain region from the structural atlas in mL/100g/min.

	Trigonocephaly					Control				
Brain Region	mean	sd	se	lower.ci	upper.ci	mean	sd	se	lower.ci	upper.ci
Caudate	63.25	14.04	1.65	59.95	66.55	56.20	15.61	2.76	50.57	61.83
Cerebellum	73.96	15.67	1.85	70.28	77.64	66.47	21.88	3.87	58.58	74.36
Frontal lobe	72.97	16.77	1.98	69.03	76.91	70.51	19.97	3.53	63.31	77.71
Insula	79.93	15.96	1.88	76.18	83.68	73.34	21.95	3.88	65.43	81.25
Occipital lobe	80.32	20.95	2.47	75.40	85.25	71.60	18.20	3.22	65.04	78.16
Parietal lobe	77.49	18.37	2.16	73.18	81.81	72.94	17.35	3.07	66.68	79.20
Putamen	78.93	15.20	1.79	75.36	82.50	70.88	25.23	4.46	61.79	79.98
Temporal lobe	71.90	15.91	1.88	68.16	75.64	69.93	19.87	3.51	62.77	77.10
Thalamus	93.24	25.25	2.98	87.30	99.17	80.03	28.15	4.98	69.88	90.18

DISCUSSION

The aim of this study was to investigate cerebral blood flow in the frontal lobe of patients with trigonocephaly as compared to age-matched control subjects. Our findings suggest that there is no significant difference in cerebral blood flow in trigonocephaly patients as compared to healthy control subjects. This is consistent with our hypothesis that there are no abnormalities in frontal lobe perfusion in trigonocephaly patients aged 0 to 18 months. This aligns with previous findings of very low risk to develop raised intracranial pressure in the first 18 months of life in trigonocephaly patients and that trigonocephaly patients have normal intracranial volume compared to control subjects without cerebral pathology.[2, 3] Theoretically, it would be possible to have a normal cerebral blood flow but a raised intracranial pressure, which may be compensated by reduced cerebrovascular resistance. However, as trigonocephaly patients rarely have increased intracranial pressure, we do not expect that this is the reason for a normal cerebral blood flow in our cohort.

The functional indication for surgery of trigonocephaly has been debated among craniofacial surgeons for a few years. Whether premature closure of the metopic suture restricts brain development mechanically and whether craniofacial surgery has a positive effect have never been proven. Our current finding of equal cerebral blood flow in trigonocephaly patients before surgery and controls implies that metopic synostosis does not impair perfusion in the forebrain up to 18 months of age and, thus, rejects the hypothesis of mechanical restriction of brain development. As with the theory that trigonocephaly is mainly an inborn brain disorder, recent studies have shown that some genetic mutations found in patients with trigonocephaly overlap with

those of patients with developmental delay disorders.[6, 23, 24] Further studies into the microstructure of the brain, using diffusion tension imaging, for example, are required to further clarify brain development in trigonocephaly patients and understand the underlying pathophysiology.

Our findings differ from those of previous imaging single-photon emission computed tomography studies in trigonocephaly patients.[9, 10] This can be explained by the development of different, more advanced imaging techniques over the last few years. We used a quantitative method instead of the qualitative comparison. Another reason for the different findings could be the difference in age range (1 to 9 years).[9] Our findings are roughly similar to those of the largest arterial spin labeling study of healthy children to date.[25] Carsin-Vu et al. showed a mean perfusion of 54.6 ml/100 g/min and of 68.4 ml/100 g/min in the frontal lobes of healthy children aged 6 to 11 months (n = 4) and 12 to 23 months (n = 14), respectively.[25] It is difficult to compare our findings with those of other arterial spin labeling studies as there are differences in the methodology of brain region definition (e.g., manual or automatic regions of interest), different arterial spin labeling strategies (i.e., pulsed, pseudocontinuous), and different arterial spin labeling acquisition readout parameters.[25-28] Because of our limited sample size, we did not conduct additional analyses on age and its correlation with cerebral perfusion. As the age range of patients and control subjects was similar, we expected that age would not have had a significant effect on our results.

Using the default statistical parametric mapping– based pipeline in ExploreASL, our initial attempts to register and segment the brain of trigonocephaly patients showed poor performance. Our registration was complicated by the skull malformation and the relatively poor tissue contrast in these young patients. A strength of this study is that we were able to combine our previously developed cerebral blood flow–based registration with a low-degree-of-freedom, nonlinear component to improve the registration for the deformed skulls, thus achieving a better registration.[17]

Our study has several limitations. First, our study focuses on a limited number of patients. It is difficult, therefore, to establish with certainty that no difference exists in cerebral blood flow between trigonocephaly patients and control subjects. We demonstrated that the range of cerebral blood flow in both trigonocephaly patients and control subjects is similar to the range found in previous studies. In our cohort, there was no evidence of a difference in cerebral blood flow between trigonocephaly patients and control subjects. Nevertheless, large cohort studies and, therefore, standardized cerebral blood flow values in pediatric patients are lacking. Arterial spin labeling studies that focus on clinical relevance of differences in cerebral blood flow range are required for a pediatric setting. Before incorporating this concept into clinical decision-making, this study should be further expanded. Validation of cerebral blood flow values in trigonocephaly patients at different age categories compared to an age-

matched healthy pediatric population is important and essential if we want to translate cerebral blood flow values to the clinical treatment or surgical approach.

Second, our control group consisted of patients who underwent magnetic resonance imaging examination for clinical reasons in which magnetic resonance imaging and clinical course showed no cerebral pathology. Patients and controls were not age-matched exactly. There was a small age difference between the groups, which may have produced an additional mean cerebral blood flow difference of −0.3, 0.12, and −0.06 ml/100 g/min (for the three presented models) between the groups, which would have either reduced the group difference or not changed it significantly.[25]

Third, we did not differentiate between gray and white matter when evaluating the mean regional cerebral blood flow due to the absence of T1-weighted image segmentation. Instead, the mean parenchymal cerebral blood flow was assessed per region. Gray matter perfusion is around two times higher than white matter perfusion in pediatric populations, and joint evaluation of gray matter and white matter signals can bias the cerebral blood flow analysis if gray matter and white matter volumes differ significantly between groups.[25, 26, 28] However, such volumetric difference between gray matter and white matter is not expected; thus, we estimate that this had no influence. More advanced analysis is planned that uses T2-weighted and diffusion tension imaging magnetic resonance images to aid the segmentation and study the partial volume- corrected gray matter cerebral blood flow.[29] As the study of Carsin-Vu et al. among pediatric patients found no difference in cerebral blood flow between patients using different types of anesthesia, we did not take these factors into consideration in our analysis.[25] We did not find a significant effect of sex on cerebral blood flow in our cohort ($p = 0.09$). This finding is similar to that of other pediatric arterial spin labeling studies, such as those by Duncan et al. ($p = 0.70$), Wong et al. ($p = 0.683$), and Carsin-Vu et al. ($p = 0.16$), which also demonstrated that sex did not have a significant effect on cerebral blood flow.[25, 27, 30]

CONCLUSIONS

The fact that we were unable to detect abnormalities in cerebral blood flow in untreated moderate to severe trigonocephaly patients less than 18 months of age as compared to control subjects supports a more conservative approach to prevent potential overtreatment of patients with reported very low prevalence of papilledema and impaired skull growth, this finding further supports our hypothesis that craniofacial surgery for trigonocephaly is rarely indicated for signs of raised intracranial pressure or restricted perfusion in patients younger than 18 months. Future studies should focus on assessing outcomes related to Cerebral blood flow, intracerebral hemorrhage, and neurocognition in unoperated versus operated trigonocephaly patients during follow-up.

REFERENCES

1. Cornelissen M, Ottelander B, Rizopoulos D, et al. Increase of prevalence of craniosynostosis. *J Craniomaxillofac Surg* 2016;44:1273-1279
2. Cornelissen MJ, Loudon SE, van Doorn FEC, et al. Very Low Prevalence of Intracranial Hypertension in Trigonocephaly. *Plast Reconstr Surg* 2017;139:97e-104e
3. Maltese G, Tarnow P, Wikberg E, et al. Intracranial volume before and after surgical treatment for isolated metopic synostosis. *J Craniofac Surg* 2014;25:262-266
4. van der Vlugt JJB, van der Meulen J, Creemers HE, et al. Cognitive and behavioral functioning in 82 patients with trigonocephaly. *Plast Reconstr Surg* 2012;130:885-893
5. Kelleher MO, Murray DJ, McGillivary A, et al. Behavioral, developmental, and educational problems in children with nonsyndromic trigonocephaly. *J Neurosurg* 2006;105:382-384
6. Mocquard C, Aillet S, Riffaud L. Recent advances in trigonocephaly. *Neurochirurgie* 2019;65:246-251
7. Grandhi R, Peitz GW, Foley LM, et al. The influence of suturectomy on age-related changes in cerebral blood flow in rabbits with familial bicoronal suture craniosynostosis: A quantitative analysis. *PLoS One* 2018;13:e0197296
8. Doerga PN, Lequin MH, Dremmen MHG, et al. Cerebral blood flow in children with syndromic craniosynostosis: cohort arterial spin labeling studies. *J Neurosurg Pediatr* 2019:1-11
9. Shimoji T, Shimabukuro S, Sugama S, et al. Mild trigonocephaly with clinical symptoms: analysis of surgical results in 65 patients. *Childs Nerv Syst* 2002;18:215-224
10. Sen A, Dougal P, Padhy AK, et al. Technetium-99m-HMPAO SPECT cerebral blood flow study in children with craniosynostosis. *J Nucl Med* 1995;36:394-398
11. Alsop DC, Detre JA, Golay X, et al. Recommended implementation of arterial spin-labeled perfusion MRI for clinical applications: A consensus of the ISMRM perfusion study group and the European consortium for ASL in dementia. *Magn Reson Med* 2015;73:102-116
12. Keil VC, Hartkamp NS, Connolly DJA, et al. Added value of arterial spin labeling magnetic resonance imaging in pediatric neuroradiology: pitfalls and applications. *Pediatr Radiol* 2019;49:245-253
13. Wang J, Licht DJ, Jahng GH, et al. Pediatric perfusion imaging using pulsed arterial spin labeling. *J Magn Reson Imaging* 2003;18:404-413
14. Yerys BE, Herrington JD, Bartley GK, et al. Arterial spin labeling provides a reliable neurobiological marker of autism spectrum disorder. *J Neurodev Disord* 2018;10:32
15. Hales PW, d'Arco F, Cooper J, et al. Arterial spin labelling and diffusion-weighted imaging in paediatric brain tumours. *Neuroimage Clin* 2019;22:101696
16. Birgfeld CB, Saltzman BS, Hing AV, et al. Making the diagnosis: metopic ridge versus metopic craniosynostosis. *J Craniofac Surg* 2013;24:178-185
17. Mutsaerts H, Petr J, Groot P, et al. ExploreASL: An image processing pipeline for multi-center ASL perfusion MRI studies. *Neuroimage* 2020;219:117031
18. Shi F, Yap PT, Wu G, et al. Infant brain atlases from neonates to 1- and 2-year-olds. *PLoS One* 2011;6:e18746
19. Mutsaerts H, Petr J, Thomas DL, et al. Comparison of arterial spin labeling registration strategies in the multi-center GENetic frontotemporal dementia initiative (GENFI). *J Magn Reson Imaging* 2018;47:131-140
20. Ashburner J, Friston KJ. Nonlinear spatial normalization using basis functions. *Hum Brain Mapp* 1999;7:254-266

21. Hammers A, Allom R, Koepp MJ, et al. Three-dimensional maximum probability atlas of the human brain, with particular reference to the temporal lobe. *Hum Brain Mapp* 2003;19:224-247

22. Team RC. R: A language and environment for statistical computing. R Foundation for Statistical Computing, Vienna, Austria. ; 2020

23. Calpena E, Hervieu A, Kaserer T, et al. De Novo Missense Substitutions in the Gene Encoding CDK8, a Regulator of the Mediator Complex, Cause a Syndromic Developmental Disorder. *Am J Hum Genet* 2019;104:709-720

24. Reijnders MRF, Miller KA, Alvi M, et al. De Novo and Inherited Loss-of-Function Variants in TLK2: Clinical and Genotype-Phenotype Evaluation of a Distinct Neurodevelopmental Disorder. *Am J Hum Genet* 2018;102:1195-1203

25. Carsin-Vu A, Corouge I, Commowick O, et al. Measurement of pediatric regional cerebral blood flow from 6 months to 15 years of age in a clinical population. *Eur J Radiol* 2018;101:38-44

26. Tortora D, Mattei PA, Navarra R, et al. Prematurity and brain perfusion: Arterial spin labeling MRI. *Neuroimage Clin* 2017;15:401-407

27. Duncan AF, Caprihan A, Montague EQ, et al. Regional cerebral blood flow in children from 3 to 5 months of age. *AJNR Am J Neuroradiol* 2014;35:593-598

28. Kim HG, Lee JH, Choi JW, et al. Multidelay Arterial Spin-Labeling MRI in Neonates and Infants: Cerebral Perfusion Changes during Brain Maturation. *AJNR Am J Neuroradiol* 2018;39:1912-1918

29. Feng L, Li H, Oishi K, et al. Age-specific gray and white matter DTI atlas for human brain at 33, 36 and 39 postmenstrual weeks. *Neuroimage* 2019;185:685-698

30. Wong AM, Yeh CH, Lin JJ, et al. Arterial spin-labeling perfusion imaging of childhood encephalitis: correlation with seizure and clinical outcome. *Neuroradiology* 2018;60:961-970

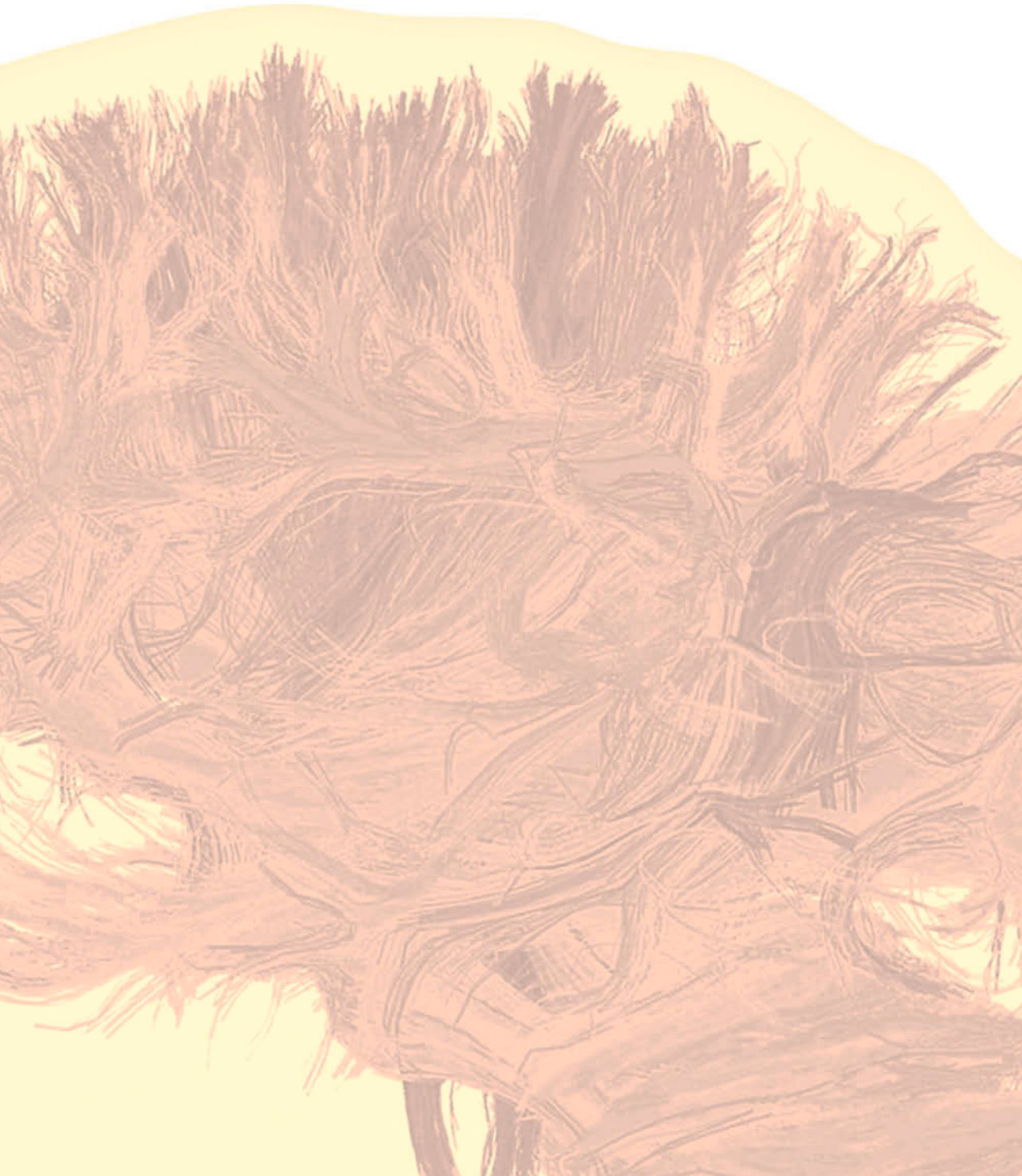

4

CHAPTER

REPLY: DISCUSSION CEREBRAL BLOOD FLOW OF THE FRONTAL LOBE IN UNTREATED CHILDREN WITH TRIGONOCEPHALY VERSUS HEALTHY CONTROLS: AN ARTERIAL SPIN LABELING STUDY

CATHERINE A. DE PLANQUE

JAN PETR

LINDA GAILLARD

HENK J. M. M. MUTSAERTS

MARIE-LISE C. VAN VEELEN

SARAH L. VERSNEL

MARJOLEIN H. G. DREMMEN

IRENE M. J. MATHIJSSEN

Accepted for publication in the Journal of Plastic and Reconstructive Surgery, June 2022

Dear Editor,

We have read the letter to the editor from Long et al. with great interest.[1] The authors of this letter stated two methodological concerns on which we will respond.

The first concern is that objective criteria are missing for true trigonocephaly or benign metopic ridge. We only included moderate to severe trigonocephaly patients according to the definitions of Birgfeld et al[2]. Birgfeld et al. provide both a phenotypical distinction between benign metopic ridge and metopic synostosis in their article, as well as illustrative photographs with corresponding CT-imaging in Figure 1.[2] Cho et al. and Anolik et al. described CT measures to assess severity of metopic synostosis. In both articles the cut-off point to determine surgical indication remains subjective and poor consensus for the intermediate presentation of metopic craniosynostosis is found.[3, 4] In addition, Sisti et al. recently reviewed all literature in Pubmed on trigonocephaly, relating to 15 anthropometric cranial measurements for surgical indications.[5] This study illustrates that most papers have a lack of diagnostic criteria for trigonocephaly.[5] At our center, the decision for surgery is made through shared decision making with parents. In 2021 this resulted in surgery for 14 patients (moderate or severe presentation) and a conservative treatment for 40 patients (18 mild, and 22 moderate or severe presentation).

The second raised concern is the potential blunting effect of sevoflurane on CBF. If it does, a similar effect on both the patients and controls is expected. In our previous ASL study in patients with syndromic craniosynostosis using the same sedation protocol, we found a difference between the groups.[6] This suggests that the normal findings in patients with trigonocephaly reflect normal CBF.

Very few studies have investigated the influence of anesthesia on ASL CBF in the pediatric population. Carsin-Vu et al. included 84 subjects from 6 months to 15 years and showed no significant CBF changes with sevoflurane in comparison with general anesthesia.[7] Kaisti et al. showed in 8 healthy males (age range 20-26) that sevoflurane reduced regional CBF less than propofol.[8]

Without sedation, scanning of one sequence is possible, because of the limited timeframe. However, more sequences, as in our protocol, requires a longer time period. Without sedation, motion artifacts would make it impossible to analyze.

Finally, Long et al. mention that cerebral perfusion is a limited measure of neurodevelopment and that fMRI studies in scaphocephaly patients have shown a difference in functional brain connectivity compared to controls. However, there is still a lot unknown about the optimal way of scanning, reproducibility, and interpretation

of the fMRI results. Finding a difference in connectivity in fMRI studies would be at the same level of evidence as the ASL brain MRI study.[9]

To conclude, our study further supports our hypothesis that surgery for trigonocephaly is rarely indicated functionally. Parents should be informed about the unknown added value of surgery regarding raised intracranial pressure and brain perfusion. Comparative research on outcome of conservative versus surgical treatment of moderate to severe trigonocephaly is needed to establish clinical guidelines.

REFERENCES

1. Long AS, Persing JA, Alperovich M. Discussion: Cerebral Blood Flow of the Frontal Lobe in Untreated Children with Trigonocephaly versus Healthy Controls: An Arterial Spin Labeling Study. *Plastic and reconstructive surgery*. 2022;
2. Birgfeld CB, Saltzman BS, Hing AV, et al. Making the diagnosis: metopic ridge versus metopic craniosynostosis. *J Craniofac Surg*. Jan 2013;24(1):178-85. doi:10.1097/SCS.0b013e3182668 3d100001665-201301000-00042 [pii]
3. Cho MJ, Kane AA, Seaward JR, Hallac RR. Metopic "ridge" vs. "craniosynostosis": Quantifying severity with 3D curvature analysis. *Journal of cranio-maxillo-facial surgery : official publication of the European Association for Cranio-Maxillo-Facial Surgery*. Sep 2016;44(9):1259-65. doi:S1010-5182(16)30107-X [pii] 10.1016/j.jcms.2016.06.019
4. Anolik RA, Allori AC, Pourtaheri N, Rogers GF, Marcus JR. Objective Assessment of the Interfrontal Angle for Severity Grading and Operative Decision-Making in Metopic Synostosis. *Plast Reconstr Surg*. May 2016;137(5):1548-1555. doi:10.1097/PRS.0000000000002052 00006534-201605000-00028 [pii]
5. Sisti A, Bassiri Gharb B, Papay F, Rampazzo A. Anthropometric Cranial Measurements in Metopic Craniosynostosis/Trigonocephaly: Diagnostic Criteria, Classification of Severity and Indications for Surgery. *J Craniofac Surg*. Jan-Feb 01 2022;33(1):161-167. doi:10.1097/ SCS.0000000000008196
6. Doerga PN, Lequin MH, Dremmen MHG, et al. Cerebral blood flow in children with syndromic craniosynostosis: cohort arterial spin labeling studies. *J Neurosurg Pediatr*. Dec 27 2019:1-11. doi:10.3171/2019.10.PEDS19150 2019.10.PEDS19150 [pii]
7. Carsin-Vu A, Corouge I, Commowick O, et al. Measurement of pediatric regional cerebral blood flow from 6 months to 15 years of age in a clinical population. *Eur J Radiol*. Apr 2018;101:38-44. doi:S0720-048X(18)30041-X [pii] 10.1016/j.ejrad.2018.02.003
8. Kaisti KK, Langsjo JW, Aalto S, et al. Effects of sevoflurane, propofol, and adjunct nitrous oxide on regional cerebral blood flow, oxygen consumption, and blood volume in humans. *Anesthesiology*. Sep 2003;99(3):603-13. doi:00000542-200309000-00015 [pii] 10.1097/00000542-200309000-00015
9. Cabrejo R, Lacadie C, Sun A, et al. Functional Network Development in Sagittal Craniosynostosis Treated With Whole Vault Cranioplasty. *J Craniofac Surg*. Jul-Aug 01 2021;32(5):1721-1726. doi:10.1097/SCS.0000000000007505 00001665-900000000-92866 [pii]

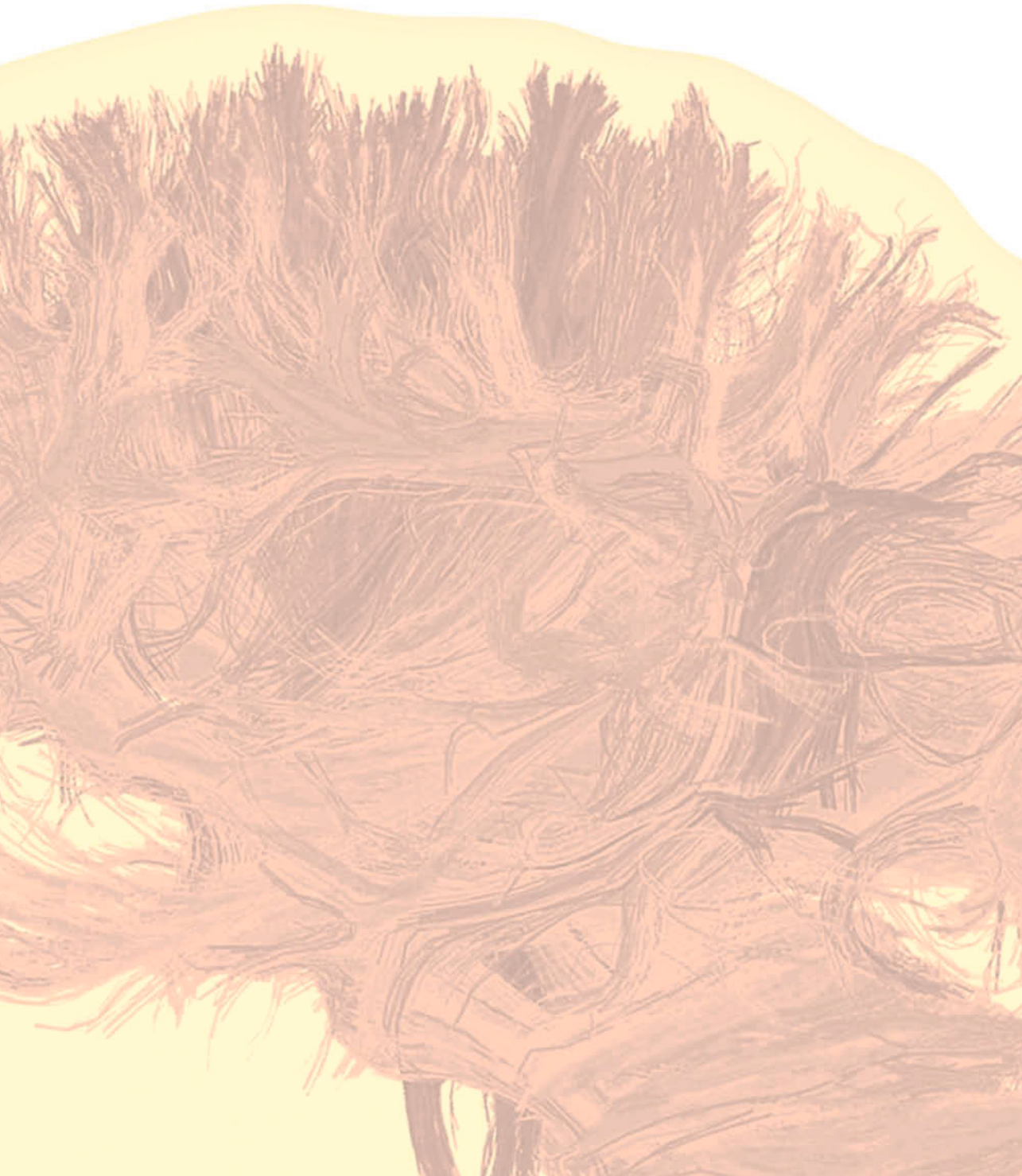

5

CHAPTER 5

A DIFFUSION TENSOR IMAGING ANALYSIS OF FRONTAL LOBE WHITE MATTER MICROSTRUCTURE IN TRIGONOCEPHALY PATIENTS

CATHERINE A. DE PLANQUE

LINDA GAILLARD

HENRI A. VROOMAN

BO LI

ESTHER E. BRON

MARIE-LISE C. VAN VEELEN

IRENE M. J. MATHIJSSEN

MARJOLEIN H. G. DREMMEN

Pediatric Neurology, 2022 Jun;131:42-48.

ABSTRACT

Background: Children with trigonocephaly are at risk for neurodevelopmental disorders. The aim of this study is to investigate white matter properties of the frontal lobes in young, unoperated patients with metopic synostosis as compared to healthy controls using diffusion tension imaging (DTI).

Methods: Preoperative DTI data sets of 46 patients with trigonocephaly with a median age of 0.49 (interquartile range: 038) years were compared with 21 controls with a median age of 1.44 (0.98) years. White matter metrics of the tracts in the frontal lobe were calculated using FMRIB Software Library (FSL). The mean value of tract-specific fractional anisotropy (FA) and mean diffusivity (MD) were estimated for each subject and compared to healthy controls. By linear regression, FA and MD values per tract were assessed by trigonocephaly, sex, and age.

Results: The mean FA and MD values in the frontal lobe tracts of untreated trigonocephaly patients, younger than 3 years, were not significantly different in comparison to controls, where age showed to be a significant associated factor.

Conclusions: Microstructural parameters of white matter tracts of the frontal lobe of patients with trigonocephaly are comparable to those of controls aged 0-3 years.

Keywords: Trigonocephaly, Craniosynostosis, White matter microstructures, Frontal lobe, Diffusion Tensor Imaging, Tract-specific DTI

INTRODUCTION

Trigonocephaly, caused by prenatal closure of the metopic suture, is the second most common form of single-suture craniosynostosis.[1] The presentation of metopic synostosis is highly variable and ranges from a mild phenotype to a severe phenotype with the classic wedge-shaped skull, depending on when the suture closes during gestation. Children with metopic synostosis are at risk for neurocognitive disorders, such as behavioral problems and delays in speech and language development.[2, 3]

Patients with moderate and severe phenotypes undergo surgical correction of the frontal bones and supraorbital rims, with the aim to prevent potential restriction of brain development, to reduce the risk of raised intracranial pressure, and to improve esthetic outcomes. However, the functional indication for surgical intervention has been under debate. Recent studies have shown that the percentage of patients with trigonocephaly with preoperative papilledema as a sign of intracranial hypertension is negligible (<2%).[4] In addition, preoperatively patients with trigonocephaly show a normal intracranial volume similar to that of healthy age-matched controls.[5] Furthermore, cerebral blood flow of the frontal lobes in unoperated patients with trigonocephaly up to the age of 18 months is not significantly different from control patients as shown with arterial spin labelling-magnetic resonance imaging (MRI).[6] Finally, the triangular shape of the forehead tends to improve over time, although it is not known to what extend this self-correction occurs.

To date, the exact underlying pathophysiology of metopic synostosis and its relation with neurocognitive disorders is unclear. There are two predominant theories on the relation between metopic synostosis and potential altered neurodevelopment. One theory states that metopic synostosis is part of a bone malformation of the frontal bones which in turn leads to mechanical restriction of brain development.[7] The second theory proposes an intrinsic brain anomaly in which the exerted pressure by the frontal lobes as driving force of suture patency is failing.[5, 7-9] In line with the latter theory, previous studies have demonstrated that the frontal intracranial volume is smaller in patients with trigonocephaly than in controls and that neurodevelopmental disorders occur in both unoperated patients with a mild trigonocephaly phenotype as well as in operated patients with a severe phenotype.[2, 3, 5] In addition, recent studies have shown an overlap in genetic mutations between patients with trigonocephaly and patients with neurodevelopmental disorders.[10-12] These findings suggest that aberrant neural development, especially of the frontal lobe, is caused by an inborn brain problem, rather than mechanical restriction.

Insight into the microarchitecture of the white matter of the unoperated brain could improve our understanding of the pathophysiology of metopic synostosis and its relation to altered neural development. MRI with diffusion tension imaging (DTI) can

be used to investigate the white matter microarchitecture by analyzing white matter tracts. Recent studies have shown that the microstructure of white matter tracts may be altered in some types of craniosynostosis.[13-17] However, to date, there have been no studies on the microstructure of the white matter in patients with isolated metopic synostosis. Therefore, the aim of this study is to investigate the white matter properties of the frontal lobe in unoperated patients with metopic synostosis as compared to healthy controls using DTI measurements. Based on the early development of white matter structures and on the higher prevalence of neuro-developmental disorders in patients with trigonocephaly, we hypothesize that the white matter microstructure of the frontal lobe is altered early in life. [4, 5]

MATERIAL AND METHODS

We conducted a prospective cohort study, which was approved by the Institutional Research Ethics Board at the Erasmus University Medical Center, Rotterdam, the Netherlands (MEC-2018-124). This study is part of ongoing work at the Dutch Craniofacial Center involving protocolized care, brain imaging, and clinical assessment.

Subjects

Patients were included between 2018 and 2020. We included all unoperated patients with nonsyndromic trigonocephaly, for whom a surgical correction was considered and for whom three-dimensional diffusion-weighted MRI and T1 -weighted MRI scans of the brain were available. We considered patients with a genetic variant (n = 3) of unknown significance as patients with nonsyndromic trigonocephaly. Patients with known pathogenic mutations (e.g., 9p deletion syndrome, Down syndrome, Jacobsen syndrome) or patients born prematurely were excluded from this study. Controls were identified from a historic hospital MRI database of children who had undergone MRI brain studies for clinical reasons between 2010 and 2020. Patients were considered a control if any cerebral and/or skull pathology was absent. Scans of potential controls were reviewed by an expert pediatric radiologist and a neurosurgeon to ensure the absence of any cerebral pathology and/or skull pathology. MRI brain scans of insufficient quality due to motion artefacts were excluded (n = 4).

MRI acquisition

All brain MRI data were acquired with a 1.5-Tesla unit (General Electric Healthcare, Milwaukee, Wisconsin), including a three-dimensional T1 -weighted fast-spoiled gradient-recalled sequence and a DTI sequence. DTI was obtained using a multirepetition single-shot echo-planar sequence with a slice thickness of 3 mm without a gap. Images were obtained in 25 of 35 gradient directions with the following parameters: b-value: 1000s/mm^2; repetition time: 15,000 ms; time to echo: 82.1 ms; field of view: 240 x 240 mm^2; and matrix size: 128 x 128, resulting in a voxel size of 1.8

x 1.8 x 3.0 mm^3. Both groups underwent deep sedation or anesthesia during the MRI procedure using sevoflurane or propofol.

White matter tracts of the frontal lobe

Major white matter tracts coursing completely or partially through the frontal lobe were analyzed: the anterior thalamic radiation (ATR), cingulate gyrus part of the cingulum (CGC), unicate fasciculus (UNC), the forceps minor (FMI), and the inferior fronto-occipital fasciculus (IFO). Tracts of the left and right hemisphere were analyzed separately as previous studies have shown regional asymmetry between hemispheres.[18] Assuming mechanical restriction of the frontal lobe would not affect the occipital lobe, we also assessed the forceps major (FMA). The FMA locates in the occipital region and therefore served as a subject-specific control tract. As an additional measure, we assessed the ratio of FMI/FMA between patients and controls.

DTI metrics

The white matter metrics derived from DTI, voxel by voxel, are mathematically estimated based on three mutually perpendicular eigenvectors, whose magnitude is given by three corresponding eigenvalues. These eigenvalues are used to generate quantitative maps of fractional anisotropy (FA), the derivation of mean diffusivity (MD), radial diffusivity (RD), and axial diffusivity (AD). As the FA, MD, RD, and AD equations are mathematically coupled, we first investigated FA and MD before analyzing the impact of the radial and axial measures of diffusivity. FA represents the amount of diffusional asymmetry in a voxel, which is presented from 0 (infinite isotropy) to 1 (infinite anisotropy). The MD is measured in mm^2/sec.

Data processing

The image processing was performed with the use of the FMRIB Software library (FSL), version 6.0.0, created by the Analysis Group, FMRIB, Oxford, UK (ref). [19] First, the images were modified in a preprocessing step to exclude nonbrain tissue and then to correct for artifacts induced by eddy currents and for translations and/or rotations resulted from head motion. The resulting transformation matrices were used to rotate the gradient direction table to account for rotations applied to the data. The diffusion tensor was fitted at each voxel, and common scalar metrics were subsequently computed.

Second, fully automated probabilistic tractography was performed as described by de Groot et al. on each subject's diffusion data set, using the FSL plugin AutoPtx.[20] The results of the probabilistic tractography were normalized to a scale from 0 to 1 using the total number of successful seed-to-target attempts. Next, we thresholded each pathway, using previously established values (ATR: 0.002, CGC: 0.01, IFO: 0.01, FMA: 0.005, FMI: 0.01, UNC: 0.01; de Groot et al., 2015). Nonzero mean DTI scalar measures were computed within each tract. Average fractional anisotropy and mean diffusivity values were then computed for each fiber bundle.[21]

Quality control

Quality control was performed by visually inspecting each tract for each subject (by BL, with 4 years of diffusion MRI experience). If tracts were segmented inadequately, the subject was excluded from this study. Two representative subjects, one patient with trigonocephaly and one control, are shown in **Figure 1**.

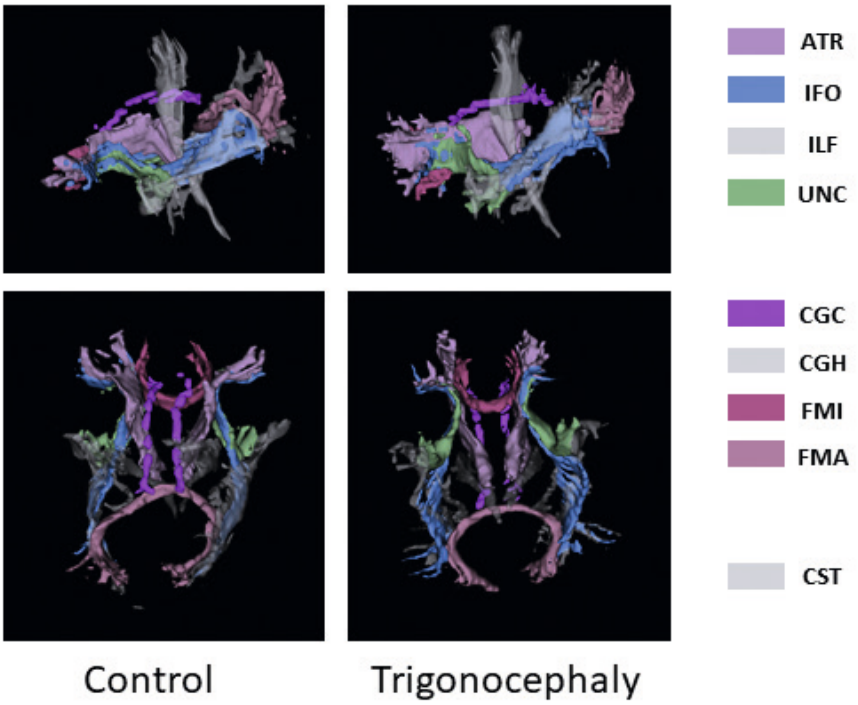

Figure 1. Tractography of the representative patient and control. The tracts used in this study are depicted as colored tracts. These tracts include the anterior thalamic radiation (ATR), the inferior fronto-occipital fasciculus (IFO), uncinate fasciculus (UNC), cingulate gyrus part of the cingulum (CGC), the forceps minor (FMI), and the forceps major (FMA). The gray tracts were not used in this study and include the inferior longitudinal fasciculus (ILF), the hippocampal gyrus associated cingulum (CGH), and the corticospinal tract (CST). In each column, the left and superior views of the tracts are shown.

Statistical analysis

Statistical analysis was conducted using R Studio (version 4.03).[22] Continuous data are presented as mean and standard deviation or as median and interquartile range (IQR), depending on whether the data are being distributed normally or not. Categorical data are presented as counts. Per tract histograms, boxplots and the Shapiro-Wilk test were used to confirm FA and MD were approximately normally distributed. Parametric statistics were used after establishing that the distribution of the data did not violate assumptions of normality. If a normal distribution was violated, several transformations

were investigated. If this transformation did not improve the normal distribution, the untransformed data were used.

FA and MD values in each of the chosen tracts were investigated by box plots and scatterplots. Subsequent linear regression models were used to further examine the FA values and MD values, with patient/control, sex, and age as independent variables. Sex and age have previously been shown to affect FA and MD values.[18, 23-28] 13-Coefficients were calculated (stats package) for each regression. Affected tracts would be further investigated by assessing the diffusivity values AD and RD. The FMA was assessed as a control tract to further validate our results; we compared the FA FMI/FMA ratio between patients and controls and the MD FMI/FMA ratio between patients and controls using a *t* test. The Bonferroni correction was conducted, and a P-value < 0.0025 (P-value = 0.05/20) was considered statistically significant. The effect of age on FA and MD between patients with trigonocephaly and controls was investigated using effect plots.

As an additional analysis, we created subgroups based on age categories, to further correct for any effect due to age. Because of the low number of patients and controls, this is enclosed in **Supplemental Table 1.**

RESULTS

Characteristics

Fourty-six patients with trigonocephaly with a median age of 0.49 years (IQR: 038) and twenty-one control subjects with a median age of 1.44 years (IQR: 0.98) were included in this study as presented in **Table 1.**

Table 1. Descriptives

	Trigonocephaly	Controls
n MRI	46	21
f : m	12:34	14:07
median age (IQR)	0.49 (0.38)	1.44(0.98)

Fractional anisotropy

By linear regression, we found no significant effect of trig-onocephaly or gender on FA values of the investigated white matter tracts (**Table 2**). The effect of age was significant for all tracts, including the control tract FMA *(P* < 0.0025). The FA FMI/FMA ratio between patients and controls did not show a significant difference *(P* = 0.79) as well. We visualized the effect of age on increase of the FA value per tract in patients compared to controls, using scatterplots and effect plots (**Figure 2**) to correct for the age difference between the patient and control group, which confirmed again the nonsignificant difference between patients with trigonocephaly and controls.

Table 2. Linear regression on FA and MD with independent variables age, trigonocephaly and gender. Bonferroni (0,05/20 = 0,0025)

		FA				
		Estimate	**Std. Error**	**CI 2.5%**	**CI 97.5%**	**P-value**
ATR L	(Intercept)	0,25	0,01	0,23	0,26	0
	Age(years)	0,03	0,00	0,02	0,04	0
	Trigonocephaly	0,01	0,01	0,00	0,02	0,05
	Gender(male)	-0,01	0,00	-0,02	0,00	0,09
ATR R	(Intercept)	0,24	0,01	0,23	0,26	0
	Age(years)	0,03	0,00	0,02	0,04	0
	Trigonocephaly	0,01	0,01	0,00	0,02	0,08
	Gender(male)	0,00	0,00	-0,01	0,01	0,43
CGC L	(Intercept)	0,26	0,01	0,23	0,29	0
	Age(years)	0,05	0,01	0,04	0,07	<0,0025
	Trigonocephaly	0,01	0,01	-0,01	0,04	0,22
	Gender(male)	-0,01	0,01	-0,03	0,01	0,25
CGC R	(Intercept)	0,24	0,01	0,21	0,27	0
	Age(years)	0,05	0,01	0,03	0,06	<0,0025
	Trigonocephaly	0,01	0,01	-0,01	0,03	0,40
	Gender(male)	-0,01	0,01	-0,03	0,01	0,47
FMI	(Intercept)	0,33	0,01	0,30	0,36	0
	Age(years)	0,09	0,01	0,07	0,10	0
	Trigonocephaly	0,01	0,01	-0,02	0,03	0,49
	Gender(male)	0,00	0,01	-0,02	0,02	0,87
IFO L	(Intercept)	0,27	0,01	0,26	0,29	0
	Age(years)	0,04	0,00	0,03	0,05	0
	Trigonocephaly	0,00	0,01	-0,01	0,02	0,81
	Gender(male)	-0,01	0,01	-0,02	0,00	0,15

Table 2. Continued.

		FA				
		Estimate	**Std. Error**	**CI 2.5%**	**CI 97.5%**	**P-value**
IFO R	(Intercept)	0,27	0,01	0,25	0,28	0
	Age(years)	0,05	0,00	0,04	0,06	0
	Trigonocephaly	0,00	0,01	-0,01	0,02	0,56
	Gender(male)	-0,01	0,01	-0,02	0,00	0,20
UNC L	(Intercept)	0,25	0,01	0,24	0,26	0
	Age(years)	0,04	0,00	0,03	0,05	0
	Trigonocephaly	0,01	0,01	0,00	0,02	0,06
	Gender(male)	-0,01	0,00	-0,02	0,00	0,02
UNC R	(Intercept)	0,25	0,01	0,23	0,26	0
	Age(years)	0,04	0,00	0,03	0,05	0
	Trigonocephaly	0,01	0,01	0,00	0,02	0,20
	Gender(male)	0,00	0,01	-0,01	0,01	0,50
FMA	(Intercept)	0,31	0,01	0,28	0,33	0
	Age(years)	0,05	0,01	0,04	0,07	<0,0025
	Trigonocephaly	-0,01	0,01	-0,03	0,01	0,32
	Gender(male)	0,00	0,01	-0,01	0,02	0,60

Table 2. Continued.

		MD				
		Estimate	**Std. Error**	**CI 2.5%**	**CI 97.5%**	**P-value**
ATR L	(Intercept)	1,12	0,02	1,07	1,16	0
	Age(years)	-0,07	0,01	-0,09	-0,04	<0,0025
	Trigonocephaly	0,01	0,02	-0,03	0,05	0,71
	Gender(male)	-0,01	0,02	-0,04	0,03	0,75
ATR R	(Intercept)	1,10	0,02	1,05	1,14	0
	Age(years)	-0,07	0,01	-0,09	-0,04	<0,0025
	Trigonocephaly	0,01	0,02	-0,03	0,04	0,76
	Gender(male)	0,00	0,01	-0,03	0,03	0,86
CGC L	(Intercept)	1,09	0,02	1,05	1,13	0
	Age(years)	-0,08	0,01	-0,10	-0,06	<0,0025
	Trigonocephaly	0,02	0,02	-0,01	0,06	0,21
	Gender(male)	0,00	0,01	-0,02	0,03	0,86
CGC R	(Intercept)	1,11	0,02	1,07	1,16	0
	Age(years)	-0,09	0,01	-0,11	-0,06	<0,0025
	Trigonocephaly	0,02	0,02	-0,02	0,06	0,45
	Gender(male)	0,00	0,02	-0,04	0,03	0,84
FMI	(Intercept)	1,21	0,02	1,16	1,25	0
	Age(years)	-0,10	0,01	-0,13	-0,08	<0,0025
	Trigonocephaly	0,01	0,02	-0,03	0,05	0,58
	Gender(male)	-0,01	0,02	-0,04	0,03	0,72
IFO L	(Intercept)	1,15	0,02	1,10	1,20	0
	Age(years)	-0,08	0,01	-0,10	-0,05	<0,0025
	Trigonocephaly	0,05	0,02	0,00	0,09	0,04
	Gender(male)	-0,01	0,02	-0,04	0,03	0,73
IFO R	(Intercept)	1,15	0,02	1,10	1,20	0
	Age(years)	-0,08	0,01	-0,11	-0,06	<0,0025
	Trigonocephaly	0,04	0,02	0,00	0,08	0,07

Table 2. Continued.

		MD				
		Estimate	**Std. Error**	**CI 2.5%**	**CI 97.5%**	**P-value**
	Gender(male)	0,01	0,02	-0,03	0,04	0,68
UNC L	(Intercept)	1,09	0,02	1,06	1,13	0
	Age(years)	-0,06	0,01	-0,08	-0,04	<0,0025
	Trigonocephaly	0,02	0,02	-0,01	0,05	0,11
	Gender(male)	0,00	0,01	-0,03	0,02	0,82
UNC R	(Intercept)	1,10	0,02	1,07	1,14	0
	Age(years)	-0,07	0,01	-0,09	-0,05	<0,0025
	Trigonocephaly	0,02	0,01	0,00	0,05	0,09
	Gender(male)	0,00	0,01	-0,02	0,02	0,99
FMA	(Intercept)	1,17	0,03	1,11	1,24	0
	Age(years)	-0,09	0,02	-0,12	-0,05	<0,0025
	Trigonocephaly	0,01	0,03	-0,04	0,07	0,59
	Gender(male)	0,01	0,02	-0,04	0,05	0,77

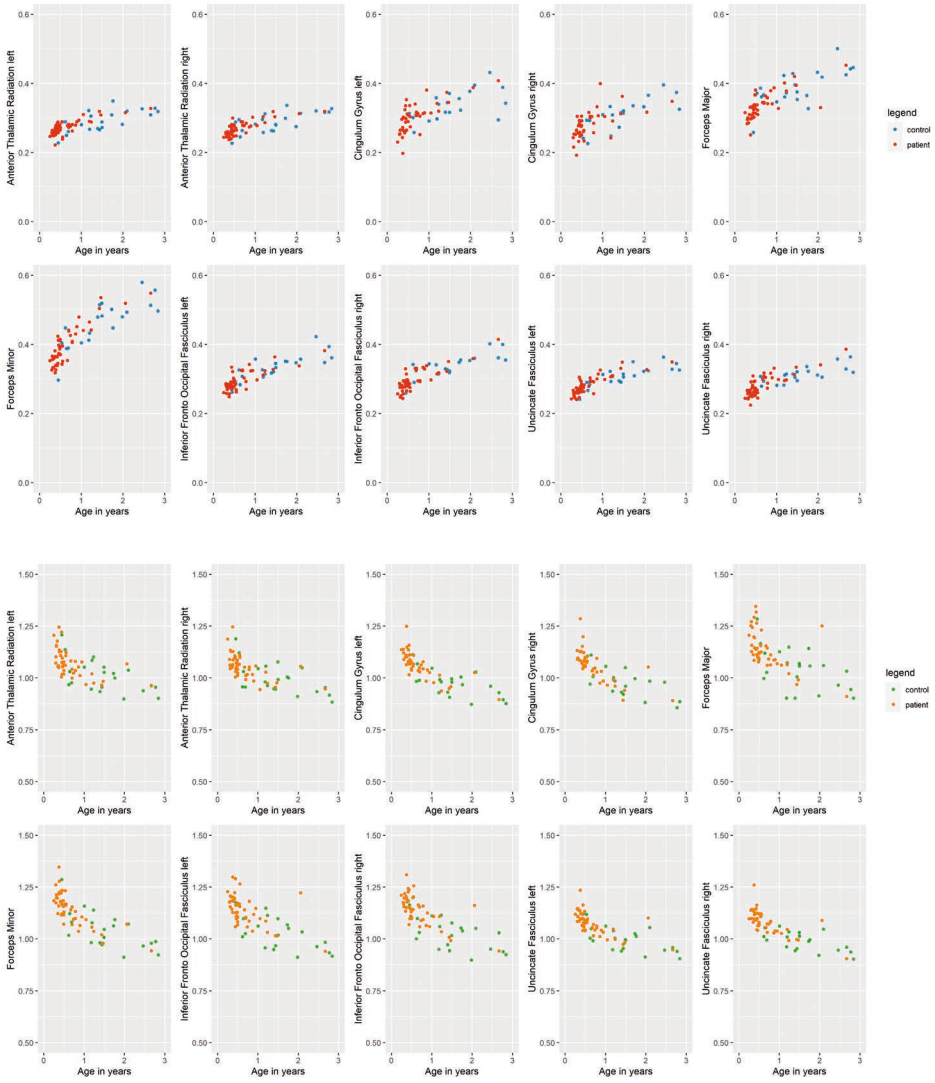

Figure 2. Scatterplots of FA (scalar value ranging between 0 and 1) and MD (mm2/sec). FA, fractional anisotropy; MD, mean diffusivity.

Mean diffusivity

The results of the linear regression on values of MD of the analyzed white matter tracts are shown in **Table 2**, showing the effect of trigonocephaly, age, and gender on the MD values. No significant difference in the MD values was found in the frontal lobe tracts comparing patients to controls. The effect of gender was not significant on the MD values in the different tracts. The effect of age was significant for the left ATR, left and right CGC, FMI, left and right IFO, and the left UNC ($P < 0.0025$). The effect of

age was significant in the reference tract FMA as well. Assessing the MD FMI/ FMA ratio between patients and controls showed no significant difference *(P* = 0.77). Using scatterplots and effect plots for all tracts, the MD in time (age in years) is visualized for patient and controls (**Figure 2**). It shows the decrease of MD in time and the nonsignificant difference between patients and controls.

As there was no significant difference in both FA and MD values of patients as compared to controls, we did not further investigate the diffusivity values RD and AD. An additional analysis to further correct for age with the 21 oldest patients compared to the 21 controls showed no significant difference between patients with trigonocephaly and controls (**Supplemental Table 1**).

Supplemental table 1. Linear regression on FA and a linear regression on MD with independent variables age, trigonocephaly and gender. Bonferroni (0,05/20 = 0,0025)

		FA			MD		
		Estimate	Std. Error	P value	Estimate	Std. Error	P value
ATR R	(Intercept)	0,25	0,01	<0,0025	1,08	0,02	<0,0025
	Age(years)	0,03	0,00	<0,0025	-0,06	0,01	<0,0025
	Trigonocephaly	0,01	0,01	0,03	-0,01	0,02	0,59
	Gender(male)	-0,01	0,01	0,19	0,01	0,02	0,42
ATR L	(Intercept)	0,25	0,01	<0,0025	1,09	0,02	<0,0025
	Age(years)	0,03	0,00	<0,0025	-0,06	0,01	<0,0025
	Trigonocephaly	0,01	0,01	0,04	-0,01	0,02	0,78
	Gender(male)	-0,01	0,01	0,05	0,00	0,02	0,90
CGC L	(Intercept)	0,27	0,01	<0,0025	1,07	0,02	<0,0025
	Age(years)	0,04	0,01	<0,0025	-0,06	0,01	<0,0025
	Trigonocephaly	0,02	0,01	0,19	0,01	0,02	0,65
	Gender(male)	-0,01	0,01	0,63	0,01	0,01	0,45
CGC R	(Intercept)	0,25	0,02	<0,0025	1,08	0,02	<0,0025
	Age(years)	0,04	0,01	<0,0025	-0,07	0,01	<0,0025
	Trigonocephaly	0,02	0,01	0,21	-0,01	0,02	0,78
	Gender(male)	-0,01	0,01	0,29	0,02	0,02	0,38
FMA	(Intercept)	0,32	0,01	<0,0025	1,15	0,03	<0,0025
	Age(years)	0,04	0,01	<0,0025	-0,07	0,02	<0,0025

Supplemental table 1. Continued.

		FA			MD		
		Estimate	Std. Error	P value	Estimate	Std. Error	P value
	Trigonocephaly	-0,01	0,01	0,63	0,01	0,03	0,86
	Gender(male)	0,00	0,01	0,74	0,01	0,03	0,79
FMI	(Intercept)	0,34	0,02	<0,0025	1,18	0,02	<0,0025
	Age(years)	0,08	0,01	<0,0025	-0,09	0,01	<0,0025
	Trigonocephaly	0,01	0,01	0,34	-0,01	0,02	0,80
	Gender(male)	0,00	0,01	0,74	0,00	0,02	0,83
IFO L	(Intercept)	0,28	0,01	<0,0025	1,13	0,03	<0,0025
	Age(years)	0,04	0,01	<0,0025	-0,07	0,02	<0,0025
	Trigonocephaly	0,01	0,01	0,48	0,04	0,02	0,15
	Gender(male)	-0,01	0,01	0,07	0,00	0,02	0,92
IFO R	(Intercept)	0,27	0,01	<0,0025	1,14	0,03	<0,0025
	Age(years)	0,04	0,00	<0,0025	-0,07	0,02	<0,0025
	Trigonocephaly	0,01	0,01	0,24	0,03	0,02	0,20
	Gender(male)	-0,01	0,01	0,10	0,01	0,02	0,60
UNC L	(Intercept)	0,26	0,01	<0,0025	1,07	0,02	<0,0025
	Age(years)	0,04	0,00	<0,0025	-0,05	0,01	<0,0025
	Trigonocephaly	0,02	0,01	0,01	0,01	0,02	0,55
	Gender(male)	-0,01	0,01	0,01	0,01	0,01	0,58
UNC R	(Intercept)	0,26	0,01	<0,0025	1,09	0,02	<0,0025
	Age(years)	0,04	0,00	<0,0025	-0,06	0,01	<0,0025
	Trigonocephaly	0,01	0,01	0,05	0,01	0,01	0,36
	Gender(male)	-0,01	0,01	0,28	0,01	0,01	0,41

**These analyses were run on a subset of 21 oldest trigonocephaly patients (Median age 0.79, IQR 0.52) in comparison to 21 controls (median age 1.44, IQR 0.98).*

RD and AD

In the supplemental figure (**Supplemental Figure 1**), the scatterplots of RD and AD are depicted.

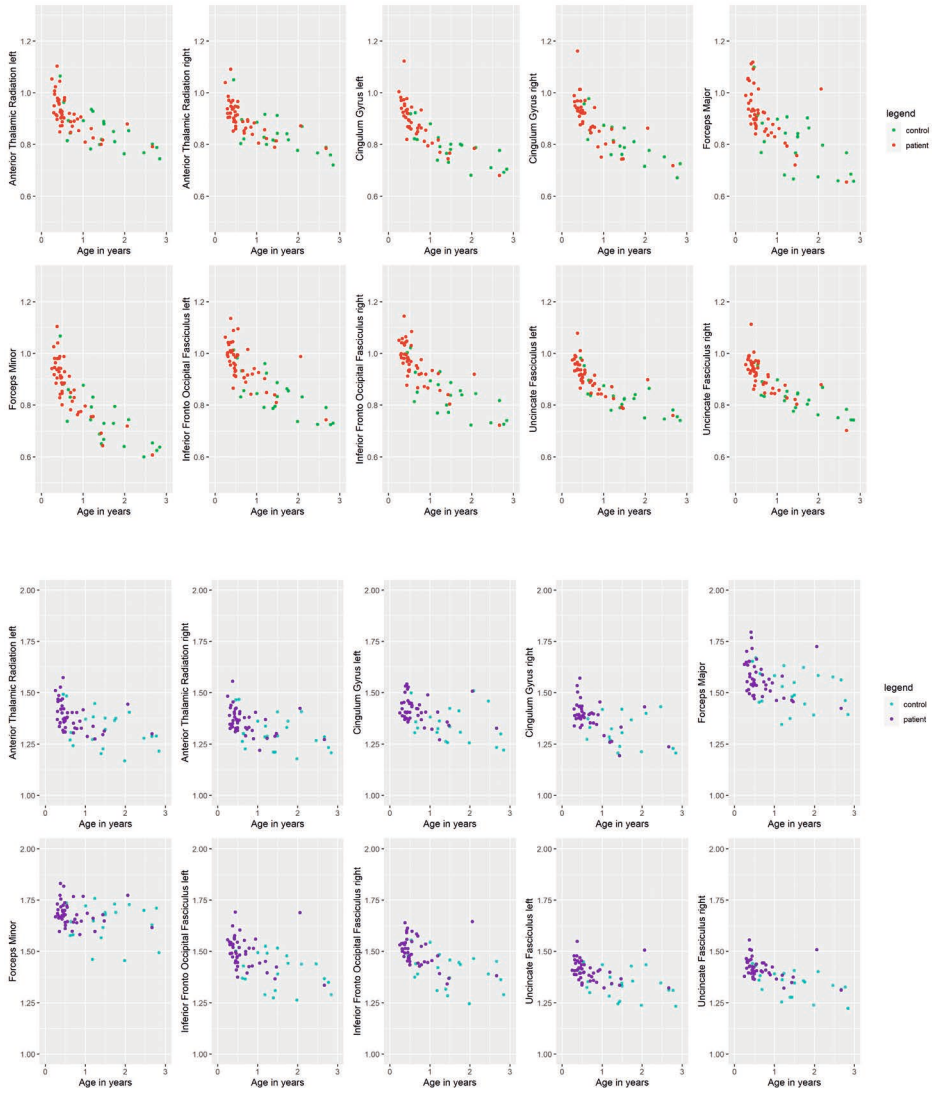

Supplemental Figure 1. Scatterplots of RD and AD (mm^2/sec)

DISCUSSION

In this report, we present, to our knowledge, the first study on automated DTI in patients with trigonocephaly aged 0 to 3 years. Based on the increased prevalence of neurodevelopmental disorders in patients with trigonocephaly, we hypothesized that white matter tracts of the frontal lobe of patients with trigonocephaly would be abnormal from early life onward.[2, 29-31]

In this study, we did not detect a significant difference in the FA or MD values of frontal lobe tracts in young patients with trigonocephaly as compared to controls. A second reason could be that a difference between patients with trigonocephaly and controls could not be shown because the effect was masked by a large age difference between groups.

The exact underlying pathophysiology of metopic synostosis is unclear, with two dominant hypotheses, namely an inborn brain disorder causing the metopic suture to close prematurely vs mechanical restriction in which the closed metopic suture causing impaired development of the frontal lobe.[5, 7-9] In line with the theory that trigonocephaly is an inborn brain disorder, recent studies have shown that some genetic mutations found in patients with trigonocephaly overlap with patients with developmental delay disorders.[10-12] This suggests that aberrant neural development, especially of the frontal lobe, is associated with metopic synostosis. Previous studies have demonstrated that neuro-developmental disorders occur in both unoperated patients with a mild trigonocephaly phenotype as well as in operated patients with a severe phenotype.[2, 3] Mechanical restriction seems unlikely, as surgical intervention has not been proven to improve neuro-cognitive outcomes and the percentage of intracranial hypertension in patients with trigonocephaly is negligible.[2-4]

Several studies have investigated the associations between neurocognitive disorders and trigonocephaly. Studies focused on different aspects of neurocognitive development, including IQ behavior, autism, and characteristics of attention deficit hyperactivity disorder, oppositional deficit hyperactivity Disorder, or conduct disorder.[2, 29-31] These studies strongly suggest that there is an increased risk for patients with trigonocephaly to develop neurocognitive disorders.

Twenty-one to thirty-one percent of patients with trigonocephaly have an IQ < 80-85 as compared to <16% of the norm group. Translating these numbers to our cohort would mean a subset, of 9 to 14 patients of this cohort, would be affected. Although a previous study in preterm neonates used DTI as a predictive tool to assess neurocognitive functioning later in life, our study may have missed the subtle effect of only a subgroup of neurocognitively affected patients with trigonocephaly.[32] However, if we assess the raw data, we cannot distinguish an outlying subgroup of patients with trigonocephaly. It

is difficult to assess neuro-cognitive function and (mild) disorders in neurodevelopment at the age of the patients included in the study (<3 years). Future studies should further assess DTI in older patients with trigonocephaly and its relation with neurocognitive function.

To our knowledge, only one study has investigated DTI in metopic synostosis in a small sample of patients. Cabrejo et al. used DTI to investigate combined sagittal and metopic synostosis patients (n = 5) and found an increased FA value in the cingulate tract of these patients as compared to isolated sagittal synostosis patients (N = 5).[14] However, they did not investigate isolated metopic synostosis, nor did they include normal controls. In contrast to this study, we did not find a significant difference in the cingulate tract or other tracts in patients with metopic synostosis as compared to controls.

Our study has several limitations. Currently, large cohort studies and standardized DTI values and thresholds in healthy infants and young children are missing. In addition, DTI depends on many technical variables, such as the type of scanner used and the amount of diffusion encoding directions. This makes it impossible to compare the values in our study to other pediatric DTI studies. In addition, in this study, we have chosen to use tract-based technology rather than a region-of-interest or whole-brain voxel-based approach. A region-of-interest approach could perhaps be valuable to assess specific local differences. In addition, we obtained controls from a historic cohort of subjects who had undergone an MRI brain scan for clinical reasons. Next, we were unable to fully match the age of patients and controls. Myelination development is greatest during the first years of life, and small differences in age affect FA and MD. However, we did not have enough statistical power to subdivide our cohort into groups of 0-1, 1-2, and 2+ years. In line with this, we observed a significant effect of age on the FA and MD values in both patients and controls. Although we did an additional analysis between patients and controls of similar age in the supplemental table, we were still not able to find any statistically significant difference between patients and controls. Finally, the trigonocephaly cohort consists of 81% male patients, whereas the control group consists of 36% males. However, by linear regression, sex has demonstrated no significant impact on the FA or MD values.

Future perspectives

In this study, we could not identify a significant difference between the main white matter tracts of the frontal lobe in young patients with trigonocephaly and controls. However, one could argue that the potential mechanical restriction of the metopic synostosis and/or intrinsically affected white matter is too subtle to measure/not yet measurable with DTI or arterial spin labelling on this age. We investigated whole tracts as a parameter of white matter microstructure in patients with trigonocephaly. Insight into other brain structures than white matter microstructure, for example, by volumetric

analysis of global or regional gray and white matter structures or cortical microstructure analysis, might improve our understanding of the pathophysiology of metopic synostosis and its possible relation to altered neural development. For the future, the comparison of brain properties of older operated patients with trigonocephaly with brain properties of older nonoperated patients with trigonocephaly could give more information about the substrate of the cognitive and behavioral issues and the added value of surgery.

CONCLUSION

In conclusion, microstructural parameters of white matter tracts of the frontal lobe of patients with trigonocephaly are comparable to those of controls aged 0-3 years. No difference in FA or MD of the frontal lobe white matter microstructure in trigonocephaly was found.

REFERENCES

1. Cornelissen M, Ottelander B, Rizopoulos D, van der Hulst R, Mink van der Molen A, van der Horst C et al. Increase of prevalence of craniosynostosis. J Craniomaxillofac Surg 2016;44:1273-9.
2. van der Vlugt JJB, van der Meulen J, Creemers HE, Verhulst FC, Hovius SER , Okkerse JME. Cognitive and behavioral functioning in 82 patients with trigonocephaly. Plast Reconstr Surg 2012;130:885-93.
3. Kelleher MO, Murray DJ, McGillivary A, Kamel MH, Allcutt D , Earley MJ. Behavioral, developmental, and educational problems in children with nonsyndromic trigonocephaly. J Neurosurg 2006;105:382-4.
4. Cornelissen MJ, Loudon SE, van Doorn FEC, Muller RPM, van Veelen MC , Mathijssen IMJ. Very Low Prevalence of Intracranial Hypertension in Trigonocephaly. Plast Reconstr Surg 2017;139:97e-104e.
5. Maltese G, Tarnow P, Wikberg E, Bernhardt P, Lagerlof JH, Tovetjarn R et al. Intracranial volume before and after surgical treatment for isolated metopic synostosis. J Craniofac Surg 2014;25:262-6.
6. de Planque CA, Petr J, Gaillard L, Mutsaerts H, van Veelen MC, Versnel SL et al. Cerebral Blood Flow of the Frontal Lobe in Untreated Children with Trigonocephaly versus Healthy Controls: An Arterial Spin Labeling Study. Plast Reconstr Surg 2022;149:931-7.
7. van der Meulen J. Metopic synostosis. Childs Nerv Syst 2012;28:1359-67.
8. Moss ML. The pathogenesis of premature cranial synostosis in man. Acta Anat (Basel) 1959;37:351-70.
9. Riemenschneider PA. Trigonocephaly. Radiology 1957;68:863-5.
10. Mocquard C, Aillet S , Riffaud L. Recent advances in trigonocephaly. Neurochirurgie 2019;65:246-51.
11. Reijnders MRF, Miller KA, Alvi M, Goos JAC, Lees MM, de Burca A et al. De Novo and Inherited Loss-of-Function Variants in TLK2: Clinical and Genotype-Phenotype Evaluation of a Distinct Neurodevelopmental Disorder. Am J Hum Genet 2018;102:1195-203.
12. Calpena E, Hervieu A, Kaserer T, Swagemakers SMA, Goos JAC, Popoola O et al. De Novo Missense Substitutions in the Gene Encoding CDK8, a Regulator of the Mediator Complex, Cause a Syndromic Developmental Disorder. Am J Hum Genet 2019;104:709-20.
13. Rijken BF, Leemans A, Lucas Y, van Montfort K, Mathijssen IM , Lequin MH. Diffusion Tensor Imaging and Fiber Tractography in Children with Craniosynostosis Syndromes. AJNR Am J Neuroradiol 2015;36:1558-64.
14. Cabrejo R, Lacadie C, Sun A, Chuang C, Yang J, Brooks E et al. Functional Network Development in Sagittal Craniosynostosis Treated With Whole Vault Cranioplasty. J Craniofac Surg 2021;32:1721-6.
15. Brooks ED, Yang J, Beckett JS, Lacadie C, Scheinost D, Persing S et al. Normalization of brain morphology after surgery in sagittal craniosynostosis. J Neurosurg Pediatr 2016;17:460-8.
16. Beckett JS, Chadha P, Persing JA , Steinbacher DM. Classification of trigonocephaly in metopic synostosis. Plast Reconstr Surg 2012;130:442e-7e.
17. Florisson JM, Barmpalios G, Lequin M, van Veelen ML, Bannink N, Hayward RD et al. Venous hypertension in syndromic and complex craniosynostosis: the abnormal anatomy of the jugular foramen and collaterals. J Craniomaxillofac Surg 2015;43:312-8.
18. Dean DC, 3rd, Planalp EM, Wooten W, Adluru N, Kecskemeti SR, Frye C et al. Mapping White Matter Microstructure in the One Month Human Brain. Sci Rep 2017;7:9759.
19. Jenkinson M, Beckmann CF, Behrens TE, Woolrich MW , Smith SM. Fsl. Neuroimage 2012;62:782-90.

20. de Groot M, Ikram MA, Akoudad S, Krestin GP, Hofman A, van der Lugt A et al. Tract-specific white matter degeneration in aging: the Rotterdam Study. Alzheimers Dement 2015;11:321-30.

21. Muetzel RL, Mous SE, van der Ende J, Blanken LM, van der Lugt A, Jaddoe VW et al. White matter integrity and cognitive performance in school-age children: A population-based neuroimaging study. Neuroimage 2015;119:119-28.

22. Team RC. R: A language and environment for statistical computing. R Foundation for Statistical Computing, Vienna, Austria. 2020.

23. Schneider JF, Il'yasov KA, Hennig J , Martin E. Fast quantitative diffusion-tensor imaging of cerebral white matter from the neonatal period to adolescence. Neuroradiology 2004;46:258-66.

24. Yoshida S, Oishi K, Faria AV , Mori S. Diffusion tensor imaging of normal brain development. Pediatr Radiol 2013;43:15-27.

25. Provenzale JM, Liang L, DeLong D , White LE. Diffusion tensor imaging assessment of brain white matter maturation during the first postnatal year. AJR Am J Roentgenol 2007;189:476-86.

26. Dubois J, Hertz-Pannier L, Dehaene-Lambertz G, Cointepas Y , Le Bihan D. Assessment of the early organization and maturation of infants' cerebral white matter fiber bundles: a feasibility study using quantitative diffusion tensor imaging and tractography. Neuroimage 2006;30:1121-32.

27. Cascio CJ, Gerig G , Piven J. Diffusion tensor imaging: Application to the study of the developing brain. J Am Acad Child Adolesc Psychiatry 2007;46:213-23.

28. Walker L, Chang LC, Nayak A, Irfanoglu MO, Botteron KN, McCracken J et al. The diffusion tensor imaging (DTI) component of the NIH MRI study of normal brain development (PedsDTI). Neuroimage 2016;124:1125-30.

29. Speltz ML, Collett BR, Wallace ER, Starr JR, Cradock MM, Buono L et al. Intellectual and academic functioning of school-age children with single-suture craniosynostosis. Pediatrics 2015;135:e615-23.

30. Speltz ML, Collett BR, Wallace ER , Kapp-Simon K. Behavioral Adjustment of School-Age Children with and without Single-Suture Craniosynostosis. Plast Reconstr Surg 2016;138:435-45.

31. Bellew M , Chumas P. Long-term developmental follow-up in children with nonsyndromic craniosynostosis. J Neurosurg Pediatr 2015;16:445-51.

32. Janjic T, Pereverzyev S, Jr., Hammerl M, Neubauer V, Lerchner H, Wallner V et al. Feed-forward neural networks using cerebral MR spectroscopy and DTI might predict neurodevelopmental outcome in preterm neonates. Eur Radiol 2020;30:6441-51.

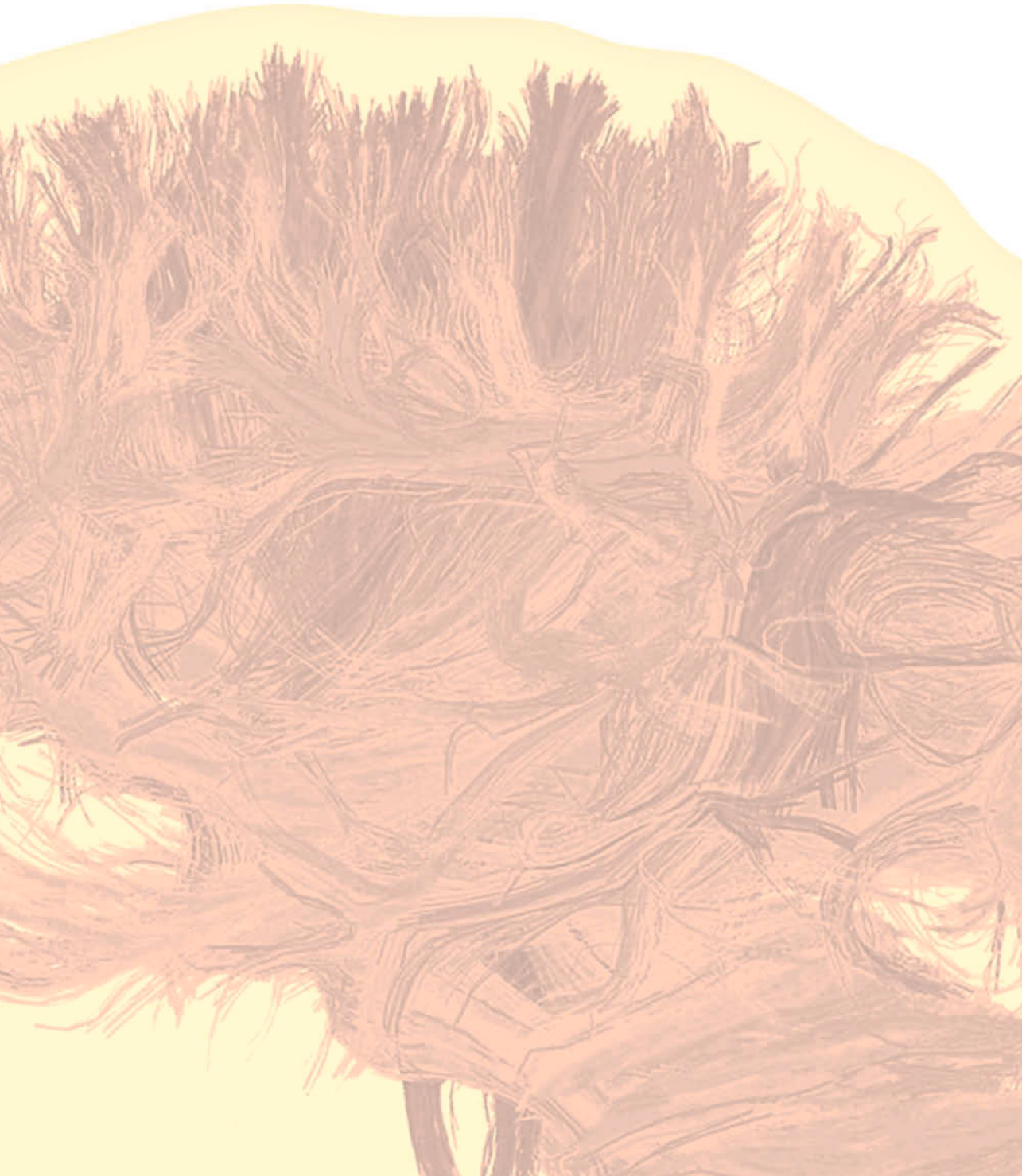

6

CHAPTER

A DIFFUSION TENSOR IMAGING ANALYSIS OF WHITE MATTER MICROSTRUCTURES IN NON-OPERATED CRANIOSYNOSTOSIS PATIENTS

CATHERINE A. DE PLANQUE

JOYCE M. G. FLORISSON

ROBERT C. TASKER

BIANCA F. M. RIJKEN

MARIE-LISE C. VAN VEELEN

IRENE M. J. MATHIJSSEN

MAARTEN H. LEQUIN

MARJOLEIN H. G. DREMMEN

Journal of Neuroradiology 2022 Jun 27.

ABSTRACT

Purpose: In 7 to 15 year old operated syndromic craniosynostosis patients we have shown the presence of microstructural anomalies in brain white matter by using DTI. To learn more about the cause of these anomalies, the aim of the study is to determine diffusivity values in white matter tracts in non-operated syndromic craniosynostosis patients aged 0-2 years compared to healthy controls.

Methods: DTI datasets of 51 non-operated patients with syndromic craniosynostosis with a median [IQR] age of 0.40 [0.25] years, were compared with 17 control subjects with a median of 1.20 [0.85] years. Major white matter tract pathways were reconstructed with ExploreDTI from MRI brain datasets acquired on 1.5 Tesla MRI system. Eigenvalues of these tract data were examined, with subsequent assessment of the affected tracts. Having syndromic craniosynostosis (versus control), gender, age, frontal occipital horn ratio (FOHR) and tract volume were treated as independent variables.

Results: λ_2 and λ_3 of the tracts genu of the corpus callosum and the hippocampal segment of the cingulum bundle show a $\eta^2 > 0.14$ in the comparison patients vs controls, which indicates a large effect on radial diffusivity. Subsequent linear regressions on radial diffusivity of these tracts show that age and FOHR are significantly associated interacting factors on radial diffusivity ($p<0.025$).

Conclusion: Syndromic craniosynostosis shows not to be a significant factor influencing the major white matter tracts. Enlargement of the ventricles show to be a significant factor on radial diffusivity in the tracts corpus callosum genu and the hippocampal segment of the cingulate bundle.

Abbreviations:
AD - Axial Diffusivity
FA – Fractional Anisotropy
FGFR - Fibroblast Growth Factor Receptors
FOHR – Frontal Occipital Horn Ratio
MD - Mean Diffusivity
RD - Radial Diffusivity
sCS - syndromic Craniosynostosis

Keywords: DTI, Diffusion Tensor Imaging, Tractography, Craniosynostosis, Syndrome

INTRODUCTION

Patients with syndromic craniosynostosis (sCS) are at risk of developing intellectual disabilities and problems in behavioural and emotional function. Whether these derangements are caused by disturbances in brain development is unknown.[1] Mutations in genes encoding the fibroblast growth factor receptors (*FGFR*) – which are expressed during early embryonic development – are known to be responsible for the pattern of abnormal skull development in sCS.[2, 3] These gene mutations induce premature fusion of skull sutures and also affect the development of brain tissue and CSF circulation.[4-6] It is known that mutations in *FGFR-1* or *FGFR-2* are associated with decreased myelin thickness,[7] but is this finding a consequence of mechanical distortion of the brain due to abnormal shape, ventriculomegaly and/or cerebellar tonsillar herniation, or does this finding reflect an intrinsic cause?[8-11 12, 13]

Previously, we have reported abnormalities in brain white matter microstructure using MRI DTI in a group of operated sCS patients aged 7 to 15 years. We identified significantly higher white matter mean diffusivity (MD), axial diffusivity (AD) and radial diffusivity (RD) in the cingulate bundle, corpus callosum and cortical spinal tract.[14] These findings suggested the presence of abnormal white matter microstructural tissue properties in sCS patients and now lead us to the purpose of our study: 1) Are these abnormalities already present in young non-operated sCS patients? 2) If so, does it reflect exposure to some mechanically related cause like worsening ventriculomegaly or does such an abnormality have an intrinsic cause?

We hypothesize that abnormalities in white matter architecture are already evident in non-operated children with syndromic craniosynostosis. To test our hypothesis, we used DTI based tracts in young non-operated children with sCS.

MATERIAL AND METHODS

The Institution Research Ethics Board at the Erasmus University Medical Center, Rotterdam, The Netherlands approved this study (MEC-2014-461), which is part of ongoing work at the Dutch Craniofacial Center involving protocolized care, brain imaging, clinical assessment and data summary and evaluation.

Subjects

MRIs from non-operated children with genetically confirmed diagnosis of syndromic craniosynostosis aged under 2 years were included. The cohort consisted of patients with Apert syndrome (mutation in the fibroblast growth factor receptor (*FGFR*) 2 gene), patients with Crouzon-Pfeiffer (mutation in *FGFR* 1 or *FGFR* 2 gene), patients with Muenke syndrome (mutation in *FGFR* 3 gene) and patients with Saethre-syndrome (mutation or deletion in the twist related protein (*TWIST1* gene). Patients with 2 or more affected sutures, but for whom a responsible gene mutation has not been found, were named complex craniosynostosis patients. Controls with the same age range were identified from a historic hospital MRI database of children who had undergone MRI brain studies for clinical reasons between 2010-2020. Patients were considered a control if any cerebral and/or skull pathology was absent. Scans of potential controls were reviewed by an expert pediatric radiologist and a neurosurgeon to ensure the absence of any cerebral pathology and/or skull pathology.

MRI Acquisition

All brain MRI data were acquired with a 1.5 Tesla unit (General Electric Healthcare, Milwaukee, Wisconsin), including three-dimensional (3D) T1-weighted fast spoiled gradient-recalled sequence, high-resolution 3D T2- weighted spin echo sequence, and DTI sequences. DTI was obtained using a multi repetition single-shot echo-planar sequence with a section thickness of 3 mm without a gap. Images were obtained in 25 gradient directions with the following parameters: sensitivity, b: 1000s/mm^2; TR: 15,000ms; TE: 82.1ms; FOV: 240 x 240 mm^2; and matrix: 128 x 128, resulting in a voxel size of 1.8 x 1.8 x 3.0 mm. This protocol was identical in both sCS patients and controls and kept equal throughout the entire study period.

DTI Data Collection

DTI processing was performed using ExploreDTI (http:// exploredti.com/). The processing consisted of correction of subject motion and eddy current distortions, and a weighted linear least-squares estimation of the diffusion tensor with the robust extraction of kurtosis indices with linear estimation (REKINDLE) approach.[15, 16] White matter tracts for fiber tractography included projection fibers (corticospinal tract), commissural fibers (corpus callosum), tracts of the brain stem (medial cerebellar peduncle) and the tracts of the limbic system (fornix and cingulated bundle).

A ROI approach was used for white matter tract analysis, with the *MRI Atlas of Human White Matter* as a guideline.[17] "OR/SEED" and "AND" operators were used when tracts were allowed to pass through, and "NOT" operators were used when tracts were not allowed to pass through. Occasionally, "NOT" operators were used to avoid aberrant or crossing fibers from other bundles. To secure measuring identical parts of the different white matter tracts, 2 AND operators at both ends of a bundle to extract always the same segment of the particular white matter tract were used. We measured the tracts as reported previously.[14]

DTI Metrics

The white matter metrics from DTI, voxel-by-voxel, are mathematically based on 3 mutually perpendicular eigenvectors, whose magnitude is given by 3 corresponding eigenvalues sorted in order of decreasing magnitude as λ_1, λ_2 and λ_3. An ellipsoid is created by the long axis of λ_1 and the small axes λ_2 and λ_3, from where the measured length of the three axes are the eigen values. These eigenvalues are used to generate quantitative maps of fractional anisotropy (FA), the derivation of MD, RD and AD. FA represents the amount of diffusional asymmetry in a voxel, which is presented from 0 (infinite isotropy) to 1 (infinite anisotropy). AD stands for the diffusivity along the neural tract: λ_1. The diffusivity of the minor axes, λ_2 and λ_3, is called the perpendicular or radial diffusivity. The mean of these diffusivity λ_1, λ_2 and λ_3 is known as MD. FA, MD, AD and RD are used as indirect markers of white matter microstructure of these young patients.[18] However, the mathematical coupling in the FA, MD, RD and AD equations means that our statistical approach will first need to assess for differences in the eigenvalues before analysing the impact of summary measures of diffusivity. The following equations were used:

$$FA = \sqrt{\frac{3}{2}} \cdot \frac{\sqrt{(\lambda_1 - MD)^2} + (\lambda_2 - MD)^2 + (\lambda_3 - MD)^2}{\sqrt{\lambda_1^2 + \lambda_2^2 + \lambda_3^2}}$$

$$MD = \frac{(\lambda_1 + \lambda_2 + \lambda_3)}{3}$$

$$RD = \frac{(\lambda_2 + \lambda_3)}{2}$$

$$AD = \lambda_1$$

	unit of measure
FA	scalar value ranging between 0-1
MD	mm²/sec
RD	mm²/sec
AD	mm²/sec

Frontal Occipital Horn Ratio

Since ventriculomegaly is an associated abnormality in sCS patients that can affect DTI metrics, the *Frontal Occipital Horn Ratio* (FOHR) was used as a parameter to correct for ventricular size.[19] FOHR is defined as (frontal horn width + occipital horn width)/biparietal diameter*2 and gives a ratio of ventricle size that can be interpreted independent of age. A FOHR ≥ 0.4 was considered ventriculomegaly.

Reliability and Reproducibility

Inter-observer reliability of tract measurements was determined by comparing the results of two trained raters blinded to subject information. Both performed all structural measurements twice in 10 subjects, 5 patients and 5 control subjects. Interrater reliability was based on 10 repeated ratings and found to be high, as depicted in Rijken et al.[14]

Partial volume effects due to brain deformity and abnormal ventricular size and shape potentially influenced the DTI fiber tractography data in patients with sCS. The FA threshold was set at 0.1, and the maximum angle threshold, at 45°. This DTI fiber tractography protocol has been used in craniosynostosis patients and controls.[14] Of note, even though a FA threshold of 0.2 is commonly used,[20] a threshold of 0.1 made it possible to track all structures in the control group and almost all structures in the sCS group. However, the FA threshold of 0.1 meant that more aberrant tracts were generated and additional AND and NOT ROIs were required to exclude aberrant fibers. Additionally, by extracting particular segments from a white matter tract (by using 2 AND operators), we could measure identical white matter structures and make fair comparisons between patients with sCS and control subjects.[14]

Statistical Analysis

Analyses were carried out using R Studio Version 1.1.442 – © 2009-2018 RStudio, Inc. Parametric statistics were used when the distribution of the data did not violate assumptions of normality. To minimize false positives resulting from multiple tests, multivariate analysis of variance (MANOVA) was used to determine whether patients and controls differed in patterns of λ_1, λ_2 and λ_3 in the examined tracts. For λ_1, λ_2 and λ_3 a η^2 was calculated, in which Cohen's guideline for "high" is $\eta^2 > 0.14$. [21] The significant lambda values gave information from which tract FA or which diffusivity value could be affected in patients versus controls (see above, *DTI Metrics*).

Subsequent analyses used linear regression on corpus callosum genu and hippocampal segment of the left cingulate bundle with sCS/control, sex, FOHR and tractvolume added to the model as independent variables. *ß-C*oefficients were calculated (stats package) for each regression. The Bonferroni correction was conducted and a p-value < 0.025 (p-value = 0.05/2) was considered statistically significant. To investigate these tracts syndrome specifically, we undertook an additional linear regression dividing the

craniosynostosis group in 5 subgroups (Apert, Crouzon, Muenke, Saethre-Chotzen and Complex). Each group was separately compared with the control group.

RESULTS

Patient characteristics

Fifty-one non-operated sCS patients with a median age of 0.40 [IQR0.25] years were included, which involved Apert (n =8), Crouzon-Pfeiffer (n =14), Muenke (n = 8), and Saethre-Chotzen (n = 10) syndromes, and complex craniosynostosis (n = 11). Seventeen control subjects were included with a median age of 1.20 [IQR 0.85] years (**Table 1**). The measured tracts are visualized in **Figure 1**.

Table 1. Patient Characteristics

	Apert	Crouzon-Pfeiffer	Muenke	Saethre-Chotzen	Complex	Total patients	Controls
no. of subjects		14	8	10	11	51	17
M/F sex	4/4	5/9	1/7	5/5	2/9	17/34	5/12
Median age (IQR)	0.28 (0.07)	0.59 (0.37)	0.36 (0.13)	0.50 (0.22)	0.39 (0.22)	0.40 (0.25)	1.20 (0.85)

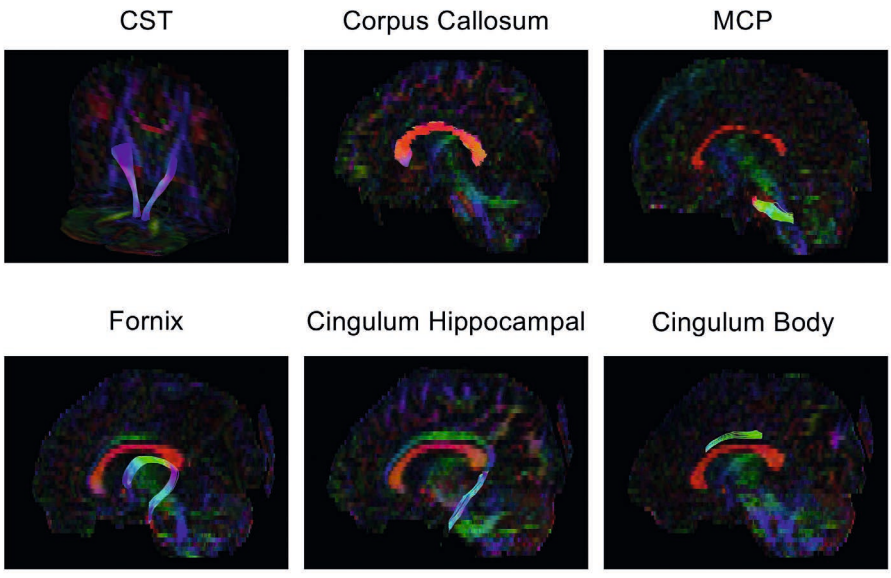

Figure 1. Tractography: midsegment of bilateral corticospinal tracts (CST) and midsagittal views of the corpus callosum, medial cerebellar peduncle (MCP), fornix, cingulum hippocampal segment and cingulum body in a control patient.

Eigen values λ_1, λ_2 and λ_3

Table 2 summarizes the η^2 of λ_1, λ_2, λ_3 by white matter tract. Left and right hemispheres show regional asymmetries. The genu of the corpus callosum, and the hippocampal segment of the left cingulum bundle show a $\eta^2 > 0.14$ in λ_2 or λ_3.

Table 2. Overview of η2 of MANOVAs λ1, λ2 and λ3 in patients vs controls

	λ1	**λ2**	**λ3**
CST left	0,07	0,00	0,01
CST right	0,04	0,00	0,01
Corpus Callosum Genu	0,04	0,13	**0,14**
Corpus Callosum body	0,01	0,07	0,07
Corpus Callosum Splenium	0,01	0,04	0,05
MCP	0,13	0,00	0,00
Fornix Left	0,00	0,00	0,00
Fornix Right	0,01	0,00	0,01
Cingulum Hippocampal left	0,07	**0,14**	0,13
Cingulum Hippocampal right	0,03	0,12	0,07
Cingulum Body left	0,00	0,10	0,08
Cingulum Body right	0,00	0,11	0,06

*For λ1, λ2 and λ3 a η2 was calculated, in which Cohen's guideline for "high" is η2 >0.14

The summary shape of the tensors of each voxel in a 3D ellipsoid is shown in **Figure 2** with the mean λ_1, λ_2, λ_3 of patients and controls for the corpus callosum genu and hippocampal segment of the left cingulate bundle. We see the three major, medium and minor axis of the diffusion displacement. Both ellipsoids show any degree of anisotropy, orientation in 3D space. The control group shows smaller ellipsoids in comparison with sCS patients. The corpus callosum shows a more anisotropic ellipsoid then the cingulate bundle, which has a more Gaussian appearance.

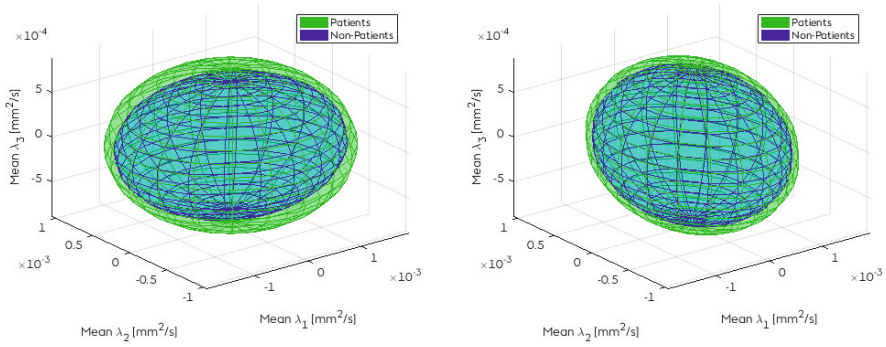

1a. **1b.**

Figure 2. Ellipsoids of the mean λ1, λ2 and λ3 in two tracts: 1a. Corpus Callosum Genu and 1b. Cingulate Bundle Hippocampal Left

Radial diffusivity analyses

Since the genu of the corpus callosum and the hippocampal segment of the left cingulum bundle show a $\eta^2 > 0.14$ in λ_2 and λ_3, subsequent analyses focused on RD (see **Table 3**).

By linear regression we found no significant effect of having syndromic craniosynostosis on RD in the corpus callosum genu and the hippocampal segment of the left cingulate bundle ($p = 0.60$ and $p=0.78$). The effect of age was significant for both tracts ($p<0.025$). A rise of 0.1 FOHR gives a rise of 0.15×10^{-3} mm²/sec in RD for the corpus callosum genu (95% CI $0.1 \times 10^{-3} - 0.2 \times 10^{-3}$ mm²/sec, $p<0.025$) and a rise of 0.07×10^{-3} mm²/sec for the hippocampal segment of the left cingulate bundle (95% CI $0.03 \times 10^{-3} - 0.10 \times 10^{-3}$ mm²/sec, $p = .000$). The effect of gender and the effect of tract volume were not significant on the RD values in the two assessed tracts.

In the **supplemental table 1 and 2**, subsequent linear regressions based on type of syndrome are depicted. None of the specific syndromes in both linear regressions, on RD of the corpus callosum genu and on RD of the hippocampal segment of the left cingulate bundle, showed to be significantly different compared to the control group.

Table 3. Linear regression on RD with independent variables sCS, gender, age, tractvolume and FOHR (Bonferroni 0.05/2 = 0.025)

RD Corpus Callosum Genu

	Estimate*	SE*	2.5% CI*	97.5% CI*	P value < 0.025
Intercept	0,58	0,12	0,34	0,83	<0.025
Syndromic Craniosynostosis	0,02	0,05	-0,07	0,12	0.60
Gender(female)	-0,01	0,03	-0,08	0,05	0.67
Age in years	-0,15	0,04	-0,24	-0,07	<0.025
Tractvolume in mm^3	0,00	0,00	0,00	0,00	0.10
FOHR per 0.10	0,15	0,03	0,10	0,20	<0.025

*all values are x 10^-3

RD Hippocampal Segment of the Left Cingulate Bundle

	Estimate*	SE*	2.5% CI*	97.5% CI*	P value < 0.025
Intercept	0,71	0,08	0,55	0,87	<0.025
Syndromic Craniosynostosis	0,01	0,03	-0,05	0,06	0.78
Gender(female)	0,01	0,02	-0,04	0,05	0.80
Age in years	-0,09	0,03	-0,14	-0,04	<0.025
Tractvolume in mm^3	0,00	0,00	0,00	0,00	0.52
FOHR per 0.10	0,07	0,02	0,03	0,10	<0.025

*all values are x 10^-3
Abbreviations: RD: Radial Diffusivity, FOHR: Frontal Occipital Horn Ratio

Supplemental Table 1. Linear regression on RD Corpus Callosum Genu with independent variables type of syndrome, gender, age, tractvolume and FOHR.

	Estimate*	SE*	2.5% CI*	97.5% CI*	P value
(Intercept)	0.72	0.15	0.41	1.02	0.000
Apert	0.05	0.07	-0.09	0.20	0.484
Crouzon	0.06	0.05	-0.04	0.17	0.233
Muenke	-0.03	0.07	-0.17	0.10	0.609
Saethre-Chotzen	-0.03	0.06	-0.15	0.10	0.668
Complex	0.02	0.06	-0.11	0.14	0.806
Gender(female)	-0.01	0.03	-0.08	0.06	0.692
Age in years	-0.16	0.04	-0.25	-0.07	0.001
Tractvolume in mm3	0	0	0	0	0.093
FOHR per 0.10	0.12	0.03	0.06	0.19	0.001

*all values are x 10^-3

Supplemental Table 2. Linear regression on RD of the hippocampal segment of the left cingulate bundle, with independent variables type of syndrome, gender, age, tractvolume and FOHR.

	Estimate*	SE*	2.5% CI*	97.5% CI*	P value
(Intercept)	0.79	0.09	0.61	0.97	0.000
Apert	0.00	0.04	-0.09	0.09	0.975
Crouzon	0.02	0.03	-0.04	0.09	0.477
Muenke	0.05	0.04	-0.03	0.13	0.188
Saethre-Chotzen	-0.01	0.04	-0.08	0.06	0.779
Complex	0.01	0.04	-0.07	0.08	0.876
Gender(female)	0.00	0.02	-0.04	0.05	0.948
Age in years	-0.09	0.03	-0.14	-0.03	0.002
Tractvolume in mm3	0.00	0.00	0.00	0.00	0.597
FOHR per 0.10	0.06	0.02	0.02	0.11	0.002

*all values are x 10^-3

Abbreviations: RD: Radial Diffusivity, FOHR: Frontal Occipital Horn Ratio

DISCUSSION

In this study of white matter microstructure using DTI, we have focused on significant differences of λ_1, λ_2 and λ_3 in the major white matter tracts of 0-2 years old non operated craniosynostosis patients and controls in the major white matter tracts. Consistent with previous studies of white matter asymmetry,[22] our results show lateralization in lambdas. Syndromic craniosynostosis shows not to be a significant factor influencing the DTI parameters in the assessed major white matter tracts. Age and FOHR shows to be significant factors affecting the RD in the tracts corpus callosum genu and the hippocampal segment of the left cingulate bundle.

Biological effect on increased RD

The corpus callosum is an early myelinated region of the brain, undergoing development in weeks 12 to 16 of pregnancy.[23] During normal brain development and white matter maturation, FA increases and diffusivity (MD, AD and RD) decreases.[24, 25] Although differences in DTI can demonstrate differences in microstructure, the physics of the measurement is nonspecific and could reflect a variety of mechanisms.[22] As water movement is more restricted perpendicular to myelin membranes than it is parallel to these membranes, it is presumed that RD reflects myelin integrity. Furthermore, RD is determined by axon density and/or diameter of the white matter tract.[26, 27]

Our previous study of 7 to 15 years olds with sCS, compared to aged matched controls, found increased RD values in the corpus callosum and cingulate bundle.[14] Could this be an intrinsic cause? The fibroblast growth factor receptors have a role in myelination of the corpus callosum and cingulate gyrus. Wilke et al showed that in craniofacial development, *FGFR2* and *3* are involved in telencephalon development from which the cingulate bundle and corpus callosum arises.[28] *FGFR* genes are critical to cerebral cortex developmental processes including neuronal migration and stabilization of dendritic patterning.[7, 29] Mutations in the *FGFR* gene could potentially result in abnormal dendritic arborisation patterns, measured as increased diffusivity values. *TWIST1* is a transcription factor which is involved in mesodermal differentiation and development.[30] In the current study, we did not find increased diffusivity values in the major white matter tracts in the groups: sCS patients vs controls. Although we did additional analyses comparing specific syndromes to controls (Supplemental Table 1 &2) , we were not able to find any statistically significant difference compared to controls. However, we do not have enough statistical power to assess this question.

Mechanical effect on increased RD

We also used the current study to examine for any potential association between brain white matter microarchitecture changes and ventriculomegaly.[31, 32] We used FOHR as a measure of ventriculomegaly and found that in non-operated sCS patients, compared with controls, there was a significant interaction between RD and FOHR

in sCS in the corpus callosum genu and the hippocampal segment of the cingulate bundle. In this study 0.1 increase in FOHR gives a significant increase of RD. Higher RD values could indicate less defined tissue organization, axonal pathology, reduced myelination or myelin damage.[26, 27] This finding could be related to the mechanical effect of ventriculomegaly. However, it remains unknown if this increase of RD is reversible, if this increase of RD influences cognitive outcome and, if so, which FOHR cut-off point is optimal for performing a third ventriculostomy or shunt insertion to improve the outcome.

Limitations

Our study has several limitations. To date there are no normal ranges of DTI measurements in children under the age of 2 years in literature. DTI is dependent on many technical variables, such as the type of MRI scanner used and the amount of diffusion encoding directions, which makes it extremely difficult to compare absolute DTI values with other DTI studies. Our diffusion protocol may have been overly sensitive. Our use of a 0.1 threshold made it possible to track all structures in the control group and almost all structures in the craniosynostosis group. However, the 0.1 FA threshold meant that more aberrant tracts were generated and additional AND and NOT ROIs were required to exclude aberrant fibers. Though, equal measurements were made between two groups. Also, the sample size was small and, therefore, we may have failed to identify associations when in fact they do exist, and *vice versa*.

Analysing different syndromes of craniosynostosis as one group, will bias the outcome. The spectrum of *FGFR* 2 mutations is widely spread, e.g. cognitive functioning of patients with Apert syndrome is significantly different compared to patients with Crouzon syndrome.[1] As syndromic craniosynostosis differ substantially from each other, it should preferably be analysed per syndrome. However, we did not have the statistical power to interpret potential differences of individual syndrome in comparison to controls, as undertaken in the supplemental tables. That said, the current report is the largest DTI study, to date, in non-operated craniosynostosis patients.

CONCLUSION

Before any surgery, microstructural parameters of white matter tracts of syndromic craniosynostosis patients are comparable to those of controls aged 0-2 years. Enlargement of the ventricles plays a significant role on RD in the corpus callosum genu and the hippocampal segment of the cingulate bundle.

Conflict of interest disclosure

All authors declare no conflict of interests.

Acknowledgements

We thank Eng. L.H. Boogaart and Eng. S. Hoogstraten for visualizing Figure 1.

REFERENCES

1. Maliepaard M, Mathijssen IM, Oosterlaan J, et al. Intellectual, behavioral, and emotional functioning in children with syndromic craniosynostosis. *Pediatrics* 2014;133:e1608-1615
2. Morriss-Kay GM, Wilkie AO. Growth of the normal skull vault and its alteration in craniosynostosis: insights from human genetics and experimental studies. *J Anat* 2005;207:637-653
3. Rijken BF, Lequin MH, Van Veelen ML, et al. The formation of the foramen magnum and its role in developing ventriculomegaly and Chiari I malformation in children with craniosynostosis syndromes. *J Craniomaxillofac Surg* 2015;43:1042-1048
4. Di Rocco C, Frassanito P, Massimi L, et al. Hydrocephalus and Chiari type I malformation. *Childs Nerv Syst* 2011;27:1653-1664
5. Britto JA, Evans RD, Hayward RD, et al. From genotype to phenotype: the differential expression of FGF, FGFR, and TGFbeta genes characterizes human cranioskeletal development and reflects clinical presentation in FGFR syndromes. *Plast Reconstr Surg* 2001;108:2026-2039; discussion 2040-2026
6. Raybaud C, Di Rocco C. Brain malformation in syndromic craniosynostoses, a primary disorder of white matter: a review. *Childs Nerv Syst* 2007;23:1379-1388
7. Furusho M, Dupree JL, Nave KA, et al. Fibroblast growth factor receptor signaling in oligodendrocytes regulates myelin sheath thickness. *J Neurosci* 2012;32:6631-6641
8. Cinalli G, Spennato P, Sainte-Rose C, et al. Chiari malformation in craniosynostosis. *Childs Nerv Syst* 2005;21:889-901
9. Collmann H, Sorensen N, Krauss J. Hydrocephalus in craniosynostosis: a review. *Childs Nerv Syst* 2005;21:902-912
10. Abu-Sittah GS, Jeelani O, Dunaway D, et al. Raised intracranial pressure in Crouzon syndrome: incidence, causes, and management. *J Neurosurg Pediatr* 2016;17:469-475
11. de Jong T, Bannink N, Bredero-Boelhouwer HH, et al. Long-term functional outcome in 167 patients with syndromic craniosynostosis; defining a syndrome-specific risk profile. *J Plast Reconstr Aesthet Surg* 2010;63:1635-1641
12. Tan K, Meiri A, Mowrey WB, et al. Diffusion tensor imaging and ventricle volume quantification in patients with chronic shunt-treated hydrocephalus: a matched case-control study. *J Neurosurg* 2018;129:1611-1622
13. Hattori T, Ito K, Aoki S, et al. White matter alteration in idiopathic normal pressure hydrocephalus: tract-based spatial statistics study. *AJNR Am J Neuroradiol* 2012;33:97-103
14. Rijken BF, Leemans A, Lucas Y, et al. Diffusion Tensor Imaging and Fiber Tractography in Children with Craniosynostosis Syndromes. *AJNR Am J Neuroradiol* 2015;36:1558-1564
15. Tax CM, Otte WM, Viergever MA, et al. REKINDLE: robust extraction of kurtosis INDices with linear estimation. *Magn Reson Med* 2015;73:794-808
16. Veraart J, Sijbers J, Sunaert S, et al. Weighted linear least squares estimation of diffusion MRI parameters: strengths, limitations, and pitfalls. *Neuroimage* 2013;81:335-346
17. Oishi K FA, van Zijl PC, et al. *MRI Atlas of Human White Matter.* Amsterdam: Elsevier; 2010
18. Qiu A, Mori S, Miller MI. Diffusion tensor imaging for understanding brain development in early life. *Annu Rev Psychol* 2015;66:853-876
19. O'Hayon BB, Drake JM, Ossip MG, et al. Frontal and occipital horn ratio: A linear estimate of ventricular size for multiple imaging modalities in pediatric hydrocephalus. *Pediatr Neurosurg* 1998;29:245-249
20. Feldman HM, Yeatman JD, Lee ES, et al. Diffusion tensor imaging: a review for pediatric researchers and clinicians. *J Dev Behav Pediatr* 2010;31:346-356

21. J C. *statistical power analysis for the behavioural sciences*. New York: Lawrence Erlbaum Associates; 1988

22. Dean DC, 3rd, Planalp EM, Wooten W, et al. Mapping White Matter Microstructure in the One Month Human Brain. *Sci Rep* 2017;7:9759

23. Dubois J, Dehaene-Lambertz G, Kulikova S, et al. The early development of brain white matter: a review of imaging studies in fetuses, newborns and infants. *Neuroscience* 2014;276:48-71

24. Lobel U, Sedlacik J, Gullmar D, et al. Diffusion tensor imaging: the normal evolution of ADC, RA, FA, and eigenvalues studied in multiple anatomical regions of the brain. *Neuroradiology* 2009;51:253-263

25. Yap QJ, Teh I, Fusar-Poli P, et al. Tracking cerebral white matter changes across the lifespan: insights from diffusion tensor imaging studies. *J Neural Transm (Vienna)* 2013;120:1369-1395

26. Song SK, Yoshino J, Le TQ, et al. Demyelination increases radial diffusivity in corpus callosum of mouse brain. *Neuroimage* 2005;26:132-140

27. Tasker RC, Westland AG, White DK, et al. Corpus callosum and inferior forebrain white matter microstructure are related to functional outcome from raised intracranial pressure in child traumatic brain injury. *Dev Neurosci* 2010;32:374-384

28. Wilke TA, Gubbels S, Schwartz J, et al. Expression of fibroblast growth factor receptors (FGFR1, FGFR2, FGFR3) in the developing head and face. *Dev Dyn* 1997;210:41-52

29. Huang JY, Lynn Miskus M, Lu HC. FGF-FGFR Mediates the Activity-Dependent Dendritogenesis of Layer IV Neurons during Barrel Formation. *J Neurosci* 2017;37:12094-12105

30. Bildsoe H, Fan X, Wilkie EE, et al. Transcriptional targets of TWIST1 in the cranial mesoderm regulate cell-matrix interactions and mesenchyme maintenance. *Dev Biol* 2016;418:189-203

31. Mangano FT, Altaye M, McKinstry RC, et al. Diffusion tensor imaging study of pediatric patients with congenital hydrocephalus: 1-year postsurgical outcomes. *J Neurosurg Pediatr* 2016;18:306-319

32. Yuan W, McKinstry RC, Shimony JS, et al. Diffusion tensor imaging properties and neurobehavioral outcomes in children with hydrocephalus. *AJNR Am J Neuroradiol* 2013;34:439-445

PART II

BRAIN IMAGING DURING FOLLOW-UP OF OPERATED CHILDREN WITH ISOLATED AND SYNDROMIC CRANIOSYNOSTOSIS

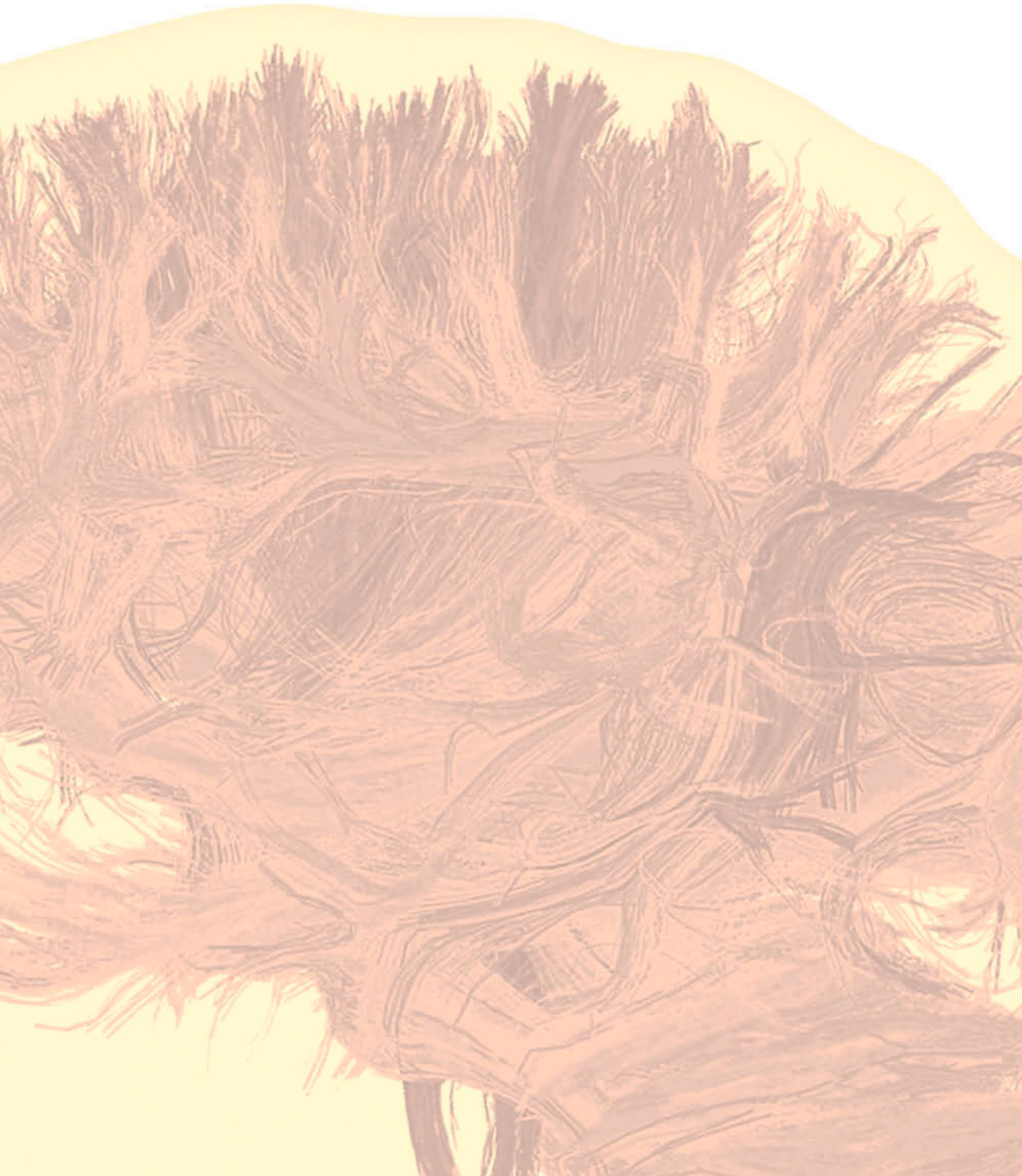

CHAPTER 7

CORTICAL THICKNESS IN CROUZON-PFEIFFER SYNDROME: FINDINGS IN RELATION TO PRIMARY CRANIAL VAULT EXPANSION

ALEXANDER T. WILSON

CATHERINE A. DE PLANQUE

SUMIN S. YANG

ROBERT C. TASKER

MARIE-LISE C. VAN VEELEN

MARJOLEIN H. G. DREMMEN

HENRI A. VROOMAN

IRENE M. J. MATHIJSSEN

PRS Global Open, 2020 Apr 11;8(10):e3204.

ABSTRACT

Background: Episodes of intracranial hypertension are associated with reductions in cerebral cortical thickness (CT) in syndromic craniosynostosis. Here we focus on Crouzon-Pfeiffer syndrome patients to measure CT and evaluate associations with type of primary cranial vault expansion and synostosis pattern.

Methods: Records from 34 Crouzon-Pfeiffer patients were reviewed along with MRI data on CT and intracranial volume to examine associations. Patients were grouped according to initial cranial vault expansion (frontal/occipital). Data were analyzed by multiple linear regression controlled for age and brain volume to determine an association between global/lobar CT and vault expansion type. Synostosis pattern effect sizes on global/lobar CT were calculated as secondary outcomes.

Results: Occipital expansion patients demonstrated 0.02 mm thicker cortex globally (P = 0.81) with regional findings, including: thicker cortex in frontal (0.02 mm, P = 0.77), parietal (0.06 mm, P = 0.44) and occipital (0.04 mm, P = 0.54) regions; and thinner cortex in temporal (-0.03 mm, P = 0.69), cingulate (-0.04 mm, P = 0.785), and, insula (-0.09 mm, P = 0.51) regions. Greatest effect sizes were observed between left lambdoid synostosis and the right cingulate (d = -1.00) and right lambdoid synostosis and the left cingulate (d = -1.23). Left and right coronal synostosis yielded effect sizes of d = -0.56 and d = -0.42 on respective frontal lobes.

Conclusions: Both frontal and occipital primary cranial vault expansions correlate to similar regional CT in Crouzon-Pfeiffer patients. Lambdoid synostosis appears to be associated with cortical thinning, particularly in the cingulate gyri.

INTRODUCTION

The Crouzon-Pfeiffer syndrome is a common form of syndromic craniosynostosis,[1] and mutations in the fibroblast growth factor receptor (*FGFR2*) gene are responsible for phenotypic severity in accelerated cranial suture fusion, facial anomalies, and exorbitism.[2] Clinically, a severe sequela of (CP) syndrome is intracranial hypertension (ICH), which may be due to factors such as cranial growth restriction, venous outflow obstruction, hydrocephalus, and obstructive sleep apnea.[3-5] Hence, cranial vault expansion is commonly performed, and at our center, it involves procedures such as fronto-orbital advancement, biparietal out-fracturing, and occipital expansion.[6] Compared with fronto-orbital advancement, occipital expansion has produced a greater gain in intracranial volume at our center while reducing the incidence of papill-edema and tonsillar herniation.[7]

Cerebral cortical thickness is an important in vivo biomarker for brain development and cognitive ability.[8] [9]As a subcomponent of cortical volume, cortical thickness is a general measure of neuronal density, dendritic arborization, and glial support.[10] Due to advancement in image-processing techniques, its use in recent years across a variety of disciplines has risen and demonstrated it to be of increasing importance in establishing a morphologic link to various pathologic and non-pathologic neuropsychological outcomes.[9, 11-15] More recently it has demonstrated sensitivity to evidence of ICH in the syn-dromic craniosynostosis population.[16] Almost two-thirds of patients with CP syndrome develop ICH and undergo cranial vault expansion,[17] yet they exhibit—on average— global cortical thinning.[16] Since most cases of CP syndrome develop with normal intelligence,[18, 19] we wondered whether the apparent discrepancy between evidence of global cortical thinning and development of normal intelligence could be resolved by a better understanding of lobar cortical findings proximate to skull regions involved in cranial vault expansion procedures. Hence, the primary aim of this study was to compare differences in cortical thickness following frontal versus occipital primary vault expansion in CP syndrome patients. Our secondary aim was to determine whether any relationship between synostosis pattern and cortical thickness exists.

METHODS

The Institution Research Ethics Board at Erasmus University Medical Center, Rotterdam, the Netherlands approved this study (approval no.: MEC-2014-461), which is a part of ongoing work at the Dutch Craniofacial Center and involves protocolized care, brain imaging, clinical assessment, and data summary and evaluation.[6, 20, 21] We reviewed the medical records of CP syndrome patients who were managed at our center between 2008 and 2018. Our usual practice in such patients involves scheduled primary vault expansion in the first year of life. Patients were included in this study if they had cranial magnetic resonance imaging (MRI) data that could be extracted and analyzed from three-dimensional T1-weighted fast spoiled gradient echo sequences. We excluded patients in whom the quality of imaging was not suitable for analysis.

Additional clinical and demographic data collected include sex, age at the time of MRI, birth weight, age at the time of vault expansion, initial type of vault expansion, and synostosis pattern. Initial type of vault expansion was classified as frontal or occipital. Suture-specific synostosis was noted in each patient as a binary variable for each of the 6 major sutures. Partial involvement of a suture was considered as positive. Fundoscopy to assess for papilledema was also performed in all cases by a pediatric ophthalmologist before surgery, 3 months postoperatively, biannually until the age of 4, annually until the age of 6 and then upon indication in older patients. When papilledema was detected, it was followed up with confirmatory fundoscopy and imaging 4–6 weeks later. Data from these examinations were collected to analyze the presence of ICH both pre and postoperatively.

MRI Acquisition

All MRI scans were performed on a 1.5 T scanner (GE Healthcare, MR Signa Excite HD, Little Chalfont, UK) with the imaging protocol, including a three-dimensional fast spoiled gradient echo T1-weighted MR sequence. Imaging parameters for craniosynostosis patients were the following: 2 mm slice thickness, no slice gap; field of view (FOV): 22.4 cm; matrix size: 224 × 224; in plane resolution of 1 mm; echo time : 3.1 ms; and repetition time: 9.9 ms.[22]

MRI was the imaging modality of choice in this study because of its ability to adequately distinguish between tissue densities (white matter, grey matter, and dura) critical to the calculation of cerebral cortical thickness.

Cortical Thickness and Brain Volume

MRI dicom files were exported and converted to neu-roimaging informatics technology initiative (NIfTI)-1 file format on a computer cluster with Scientific Linux as the operating system before analysis with FreeSurfer software modules (v6.0, see https://surfer.nmr.mgh.harvard.edu) developed by the Athinoula A. Martinos Center for Biomedical

Imaging, Massachusetts General Hospital).[23] The processing methodologies used by FreeSurfer have previously been validated and described in detail.[24-26] Maps produced by FreeSurfer are not restricted by voxel resolution of the original data and are therefore able to detect submillimeter changes in cortical thickness as demonstrated by validation against histological analysis (within 0.07 mm and statistically indistinguishable from standard neuropathologic techniques) and manual mea-surements.[27-30]All T1-weighted images from the cohort were processed using the "auto-recon-all" pipeline in FreeSurfer. Estimates of vertex-wise cortical thickness were then generated by hemisphere and by cerebral lobes (ie, frontal, temporal, parietal, occipital, cingulate, and insula) as specified by the "--lobes" argument within the 'mris_annotation2label' command. Left and right hemisphere thickness outputs were averaged to generate a value for global cortical thickness. Similarly, lobar outputs from left and right hemispheres were averaged to generate a whole lobe thickness. Whole brain volume excluding ventricular volume was exported from FreeSurfer as 'BrainSegVolNotVent' via the 'mri_segstats' command.

Statistical Analysis

All data were imported into R statistical software (R Core Team, R version 3.6.1, 2019, Vienna, Austria) for analysis. Multivariate linear regression was first used to determine the level of variance in global thickness attributable to age at the time of MRI, sex, and whole brain volume. Multivariate analysis of covariance (MANCOVA) was then performed to assess these effects by lobe. Finally, multiple linear regression was used to determine associations between type of initial cranial vault expansion and lobar thickness while controlling for age and brain volume. A post-hoc power analysis was also performed to assess the quantitative limits of our current dataset. Cohen's *d* with 95% confidence intervals were calculated as a secondary analysis to determine effect of suture-specific synostosis on underlying cortical lobes. Homogeneity of variance among suture-specific groups was evaluated by Levene's test for age and χ^2 for sex.

RESULTS

Patient Cohort

Following review of medical and imaging records, 43 CP patients were identified. Six patients were excluded from further analysis since they did not undergo any primary vault expansion; either because they did not have synostosis (n = 2) or because of late referral and/or incomplete records (n = 4). An additional 3 patients underwent primary biparietal expansion and were also excluded. In total, 34 CP patients (19 men, 15 women) were therefore included in our cohort (mean ± SD age at the time of MRI of 8.9 ± 4.5 years). The interval between initial vault expansion and MRI was 7.1 ± 4.7 years. ICH was present in 8 (23.5%) patients preoperatively alone, 8 (23.5%) patients postoperatively alone, and 6 (17.6%) patients both pre and postoperatively. In 12 (35.3%) patients, no ICH was present. Birth weight data (range: 2920–4460 g; SD: 408 g) were

also collected, and no patients were found to be of low enough weight (<1500 g) to impact thickness development as reported in previous studies.[31, 32] Additionally, birth weight was found to be evenly distributed between both treatment groups and among all sutural involvement subgroups.

Primary Cranial Vault Expansion

Before assessing any effect of primary cranial vault expansion type on cortical thickness, we determined the level of variance explained by age, sex, and brain volume. Multivariate linear regression showed that these three variables accounted for 40% of the variance in cortical thickness (R^2 = 0.40), with univariate analyses yielding *R2* for age, sex, and brain volume as 0.39, 0.01, and 0.06, respectively. Further evaluation by lobe using MANCOVA yielded a Pillai trace test statistic of 0.64, 0.17, and 0.24 for age, sex, and brain volume, respectively. Univariate results of the MANCOVA test by lobe are available in **Table 1.**

Of the 34 patients, 13 (7 male, 6 female, median age at MRI 5.1 yrs) underwent occipital expansion as a primary procedure. 21 patients (12 men, 9 women, median age at MRI 11.5) underwent primary frontal expansion. Multiple linear regression did not find a correlation between global cortical thickness and primary cranial vault expansion type (**Table 2**). Primary occipital expansion was associated with a 0.02 mm thicker cortex globally (l = 0.02, 95% CI −0.12 to −0.15, *P* = 0.82), as well as thicker frontal (l = 0.02, 95% CI −0.15 to −0.20, *P* = 0.78), parietal (l = 0.06, 95% CI −0.09 to −0.20, *P* = 0.44), and occipital (l = 0.05, 95% CI −0.10 to −0.19, *P* = 0.51) lobar cortices. Also, in the occipital expansion group, there was an association with thinner temporal (l = −0.03, 95% CI −0.16 to −0.10, *P* = 0.68), cingulate (l = −0.04, 95% CI −0.29 to −0.22, *P* = 0.78), and insular (l = −0.09, 95% CI −0.36 to −0.17, *P* = 0.48) cortices. l-coefficients and 95% confidence intervals for each region are shown in **Figure 1**. Lastly, power analysis revealed the need for a cohort size of 59 patients to detect a 0.2 mm change in thickness at a level of 80%. Our cohort in this study was 80% powered to detect a 0.37 mm difference between surgical treatment groups.

Table 1. Univariate Results from MANCOVA Test to Assess Variability Attributable to Age, Sex, and Brain Volume. Brain vol, whole brain volume; df, degrees of freedom; sum sq, sum of squares; mean sq, mean square; η2, eta squared

Frontal	**df**	**Sum sq**	**Mean sq**	**F**	**η^2**
Age	1	0.37174	0.37174	13.7338	0.30632442
Sex	1	0.02775	0.02775	1.0252	0.0228668
Brain vol	1	0.00204	0.00204	0.0756	0.00168102
Residuals	30	0.81202	0.02707		
Temporal					
Age	1	0.27837	0.278374	17.8413	0.37158609
Sex	1	0.00245	0.00245	0.157	0.00327042
Brain vol	1	0.00024	0.000242	0.0155	0.00032037
Residuals	30	0.46808	0.015603		
Parietal					
Age	1	0.15166	0.151659	7.5828	0.2017265
Sex	1	0.00006	0.000056	0.0028	7.98E-05
Brain vol	1	0.00008	0.000083	0.0042	0.00010641
Residuals	30	0.60001	0.02		
Occipital					
Age	1	0.57963	0.57963	33.9775	0.50018553
Sex	1	0.01966	0.01966	1.1522	0.01696539
Brain vol	1	0.04776	0.04776	2.7999	0.04121398
Residuals	30	0.51178	0.01706		
Cingulate					
Age	1	0.64805	0.64805	10.7218	0.25127664
Sex	1	0.00488	0.00488	0.0807	0.00189218
Brain vol	1	0.11283	0.11283	1.8667	0.04374901
Residuals	30	1.81327	0.06044		
Insula					
Age	1	1.30516	1.30516	21.2218	0.38340486
Sex	1	0.22115	0.22115	3.5959	0.0649652
Brain vol	1	0.03279	0.03279	0.5331	0.00963242
Residuals	30	1.84503	0.0615		

Table 2. Linear Regression Results for Global and Lobar Cortical Thickness

	Global			Frontal		
Predictors	Estimates	CI	p	Estimates	CI	p
(Intercept)	2.92	2.55 – 3.29	**<0.001**	3.06	2.56 – 3.55	**<0.001**
Age at MRI	-0.02	-0.04 – -0.00	**0.012**	-0.02	-0.04 – -0.00	**0.036**
Brain volume	0.00	-0.00 – 0.00	0.917	0.00	-0.00 – 0.00	0.937
Occipital expansion	0.02	-0.12 – 0.15	0.815	0.02	-0.15 – 0.20	0.778
Observations	34			34		
R^2 / R^2 adjusted	0.387 / 0.326			0.308 / 0.239		

	Temporal			Parietal		
Predictors	Estimates	CI	p	Estimates	CI	p
(Intercept)	3.21	2.84 – 3.57	**<0.001**	2.66	2.25 – 3.07	**<0.001**
Age at MRI	-0.02	-0.04 – -0.01	**0.004**	-0.01	-0.03 – 0.01	0.211
Brain volume	0.00	-0.00 – 0.00	0.788	0.00	-0.00 – 0.00	0.991
Occipital expansion	-0.03	-0.16 – 0.10	0.680	0.06	-0.09 – 0.20	0.444
Observations	34			34		
R^2 / R^2 adjusted	0.377 / 0.314			0.217 / 0.139		

	Occipital			Cingulate			Insula		
Predictors	Estimates	CI	p	Estimates	CI	p	Estimates	CI	p
(Intercept)	2.70	2.31 – 3.10	**<0.001**	3.51	2.79 – 4.24	**<0.001**	3.34	2.60 – 4.09	**<0.001**
Age at MRI	-0.02	-0.04 – -0.01	**0.008**	-0.03	-0.06 – 0.00	0.062	-0.06	-0.09 – -0.03	**0.001**
Brain volume	-0.00	-0.00 – 0.00	0.245	-0.00	-0.00 – 0.00	0.254	0.00	-0.00 – 0.00	0.193
Occipital expansion	0.05	-0.10 – 0.19	0.511	-0.04	-0.29 – 0.22	0.783	-0.09	-0.36 – 0.17	0.482
Observations	34			34			34		
R^2 / R^2 adjusted	0.528 / 0.481			0.286 / 0.215			0.426 / 0.368		

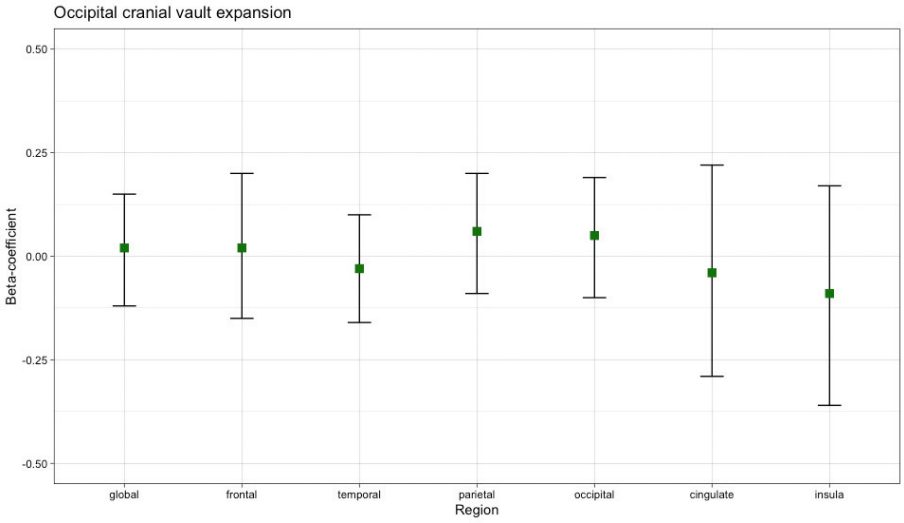

Figure 1. β-coefficients with 95% confidence intervals associated with occipital cranial vault expansion extracted from linear mixed models of each lobe as well as globally.

Synostosis Pattern

Of the 34 patients, 14 suffered from pansynostosis, 7 had bicoronal involvement, 6 had bilambdoid involvement, 4 had isolated sagittal synostosis, and 3 had additional combinations involving multiple sutures. Cohen's *d* effect sizes and 95% confidence intervals for independent involvement of 5 major sutures are shown in **Table 3** along with demographic data for each subgroup. Homogeneity of variance was found to be adequate in each subgroup, as assessed by Levene's test for age (left coronal $P = 0.49$; right coronal $P = 0.57$; sagittal $P = 0.19$; left lambdoid $P = 0.89$; right lambdoid $P = 0.77$) and χ^2 test for sex (left coronal $P = 0.68$; right coronal $P = 0.64$; sagittal $P = 0.63$; left lambdoid $P = 0.98$; right lambdoid $P = 0.98$). For matched syn-ostosis pattern to underlying cortical thickness, the largest effect was observed between coronal sutures and the frontal cortex, with left coronal synostosis yielding an effect size of $d = -0.56$ (95% CI −1.4 to −0.27) and $d = -0.65$ (95% CI −1.49 to −0.19) and right coronal synostosis yielding $d = -0.31$ (95% CI −1.22 to −0.61) and $d = -0.42$ (95% CI −1.34 to −0.50) for left and right frontal lobes, respectively. The overall largest effect sizes were observed between lambdoid suture involvement and the cingulate cortex, with left lambdoid synostosis corresponding to $d = -0.87$ (95% CI −1.65 to −0.10) and $d = -1.00$ (95% CI −1.78 to −-0.21) and right lambdoid synostosis corresponding to $d = -1.23$ (95% CI −2.08 to −0.38) and $d = -1.05$ (95% CI −1.88 to −-0.22) for left and right cingulate cortices respectively. These effects are demonstrated in **Figure 2.**

Table 3. Cohen's *d* Effect Sizes with SD and 95% Confidence Intervals for Suture Involvement on Cortical Thickness by Lobe and Hemisphere.

	Left Coronal	Right Coronal	Sagittal	Left Lambdoid	Right Lambdoid
N	26	28	23	23	25
Male (%)	14 (54%)	15 (54%)	14 (61%)	13 (57%)	14 (56%)
Female (%)	12 (46%)	13 (46%)	9 (39%)	10 (43%)	11 (44%)
Median age (SD)	8.0 (4.7)	8.6 (4.7)	10.7 (3.6)	8.0 (4.6)	8.0 (4.6)
Left frontal					
Cohen's d	−0.56	−0.31	0.03	−0.48	−0.65
Sd	0.20	0.20	0.20	0.20	0.19
Conf.int.lower	−1.40	−1.22	−0.71	−1.24	−1.46
Conf.int.upper	0.27	0.61	0.78	0.28	0.16
Right frontal					
Cohen's d	−0.65	−0.42	0.23	−0.53	−0.59
Sd	0.19	0.19	0.19	0.19	0.19
Conf.int.lower	−1.49	−1.34	−0.52	−1.28	−1.40
Conf.int.upper	0.19	0.50	0.98	0.23	0.21
Left temporal					
Cohen's d	−0.52	−0.06	0.11	−0.56	−0.32
Sd	0.15	0.15	0.15	0.15	0.15
Conf.int.lower	−1.36	−0.98	−0.64	−1.32	−1.12
Conf.int.upper	0.31	0.85	0.85	0.20	0.47
Right temporal					
Cohen's d	−0.24	−0.01	−0.09	−0.43	−0.24
Sd	0.16	0.16	0.16	0.16	0.16
Conf.int.lower	−1.07	−0.92	−0.83	−1.18	−1.04
Conf.int.upper	0.58	0.91	0.66	0.32	0.55
Left parietal					
Cohen's d	−0.42	−0.25	−0.37	−0.05	−0.24
Sd	0.15	0.15	0.15	0.15	0.15
Conf.int.lower	−1.25	−1.17	−1.13	−0.80	−1.03
Conf.int.upper	0.41	0.66	0.38	0.70	0.56
Right parietal					
Cohen's d	−0.37	−0.20	−0.12	−0.30	−0.50
Sd	0.16	0.16	0.16	0.16	0.16

Table 3. Continued.

	Left Coronal	Right Coronal	Sagittal	Left Lambdoid	Right Lambdoid
Conf.int.lower	−1.20	−1.11	−0.87	−1.05	−1.30
Conf.int.upper	0.46	0.72	0.63	0.45	0.30
Left occipital					
Cohen's d	−0.34	−0.10	0.70	−0.07	−0.30
Sd	0.19	0.20	0.19	0.20	0.19
Conf.int.lower	−1.17	−1.02	−0.07	−0.82	−1.10
Conf.int.upper	0.49	0.81	1.47	0.68	0.49
Right occipital					
Cohen's d	−0.31	−0.06	0.78	−0.09	−0.22
Sd	0.19	0.20	0.18	0.20	0.20
Conf.int.lower	−1.13	−0.97	0.01	−0.84	−1.01
Conf.int.upper	0.52	0.86	1.55	0.66	0.58
Left cingulated					
Cohen's d	−0.43	−0.36	0.16	−0.87	−1.23
Sd	0.27	0.27	0.27	0.25	0.24
Conf.int.lower	−1.26	−1.28	−0.59	−1.65	−2.08
Conf.int.upper	0.40	0.56	0.90	−0.10	−0.38
Right cingulated					
Cohen's d	−0.32	−0.11	0.49	−1.00	−1.05
Sd	0.33	0.33	0.32	0.30	0.30
Conf.int.lower	−1.14	−1.03	−0.27	−1.78	−1.88
Conf.int.upper	0.51	0.81	1.25	−0.21	−0.22
Left insula					
Cohen's d	−0.57	−0.27	0.21	−0.30	−0.31
Sd	0.33	0.34	0.34	0.34	0.34
Conf.int.lower	−1.40	−1.19	−0.53	−1.05	−1.10
Conf.int.upper	0.27	0.64	0.96	0.45	0.49
Right insula					
Cohen's d	−0.66	−0.20	0.24	−0.46	−0.30
Sd	0.32	0.33	0.33	0.33	0.33
Conf.int.lower	−1.50	−1.12	−0.51	−1.22	−1.09
Conf.int.upper	0.18	0.72	0.99	0.29	0.50

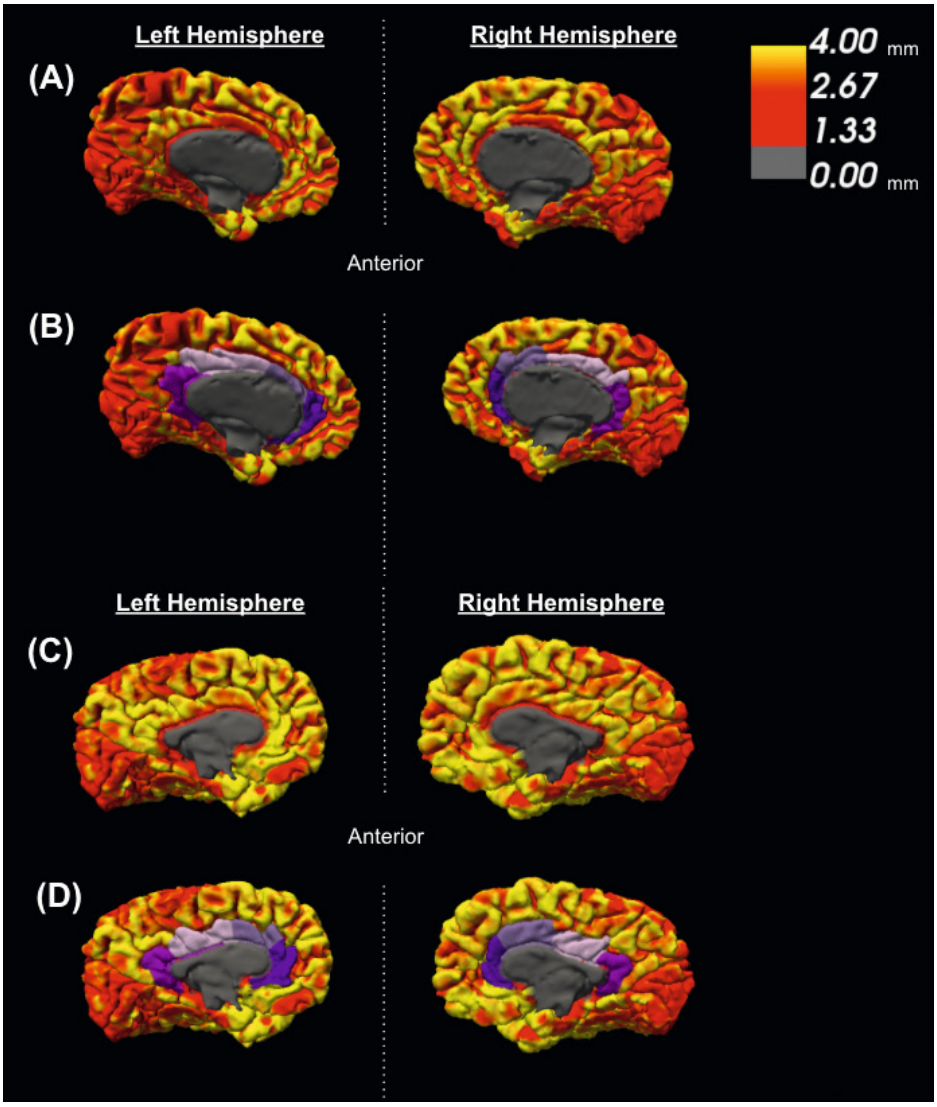

Figure 2. Pial surface heat maps extracted from FreeSurfer with 0–4 mm cortical thickness scale. A, Left and right hemispheres of a 9-year-old CP patient with bilateral lambdoid synostosis. B, Hemispheres of the same patient in A, with cingulate gyri identified in purple. C, Left and right hemispheres of a 7-year-old CP patient with bicoronal synostosis. D, Hemispheres of the same patient in C, with cingulate gyri identified in purple.

DISCUSSION

The primary aim of this study was to determine any association between cortical thickness and frontal versus occipital primary vault expansion in CP syndrome patients. Our secondary aim was to determine any relationship between synostosis pattern and cortical thickness. We hypothesized that cortical lobes beneath growth-restricted regions of the calvaria may be at an increased risk for thinning in CP patients and that targeted vault expansion may confer a protective advantage to these regions. This study failed to find any difference in effect between frontal and occipital primary vault expansions on global or lobar cerebral cortical thickness. In regard to synostosis pattern and cortical thickness, we found that lambdoid synostosis was associated with thinning across all brain regions, but particularly within the cingulate and frontal cortices. This leads us to question our hypothesis of localized growth restriction affecting proximate cortical lobes and consider how cranial shape contributes to pressure elevations and subsequent thinning in distant regions of the brain.

Both frontal and occipital cranial vault procedures resulted in similar cortical thicknesses in this study. Previous work by Spruijt et al evaluated the effect of frontal versus occipital primary vault expansions on occipito frontal head circumference in an Apert and Crouzon cohort and found that occipital-first expansion resulted in greater circumferences and reduced postoperative incidence of papilledema.[7, 16] A recent study has highlighted the importance of papilledema in syndromic craniosynostosis patients, demonstrating an association with global thinning of the cortex.[16] The failure to find a direct association between primary cranial vault expansion type and cortical thickness in this study is most likely due to insufficient power. It is possible that occipital expansion resulted in fewer cases of papilledema than would otherwise be observed; however, the effect of surgery type alone was insufficient to result in detectable cortical thinning. This study was adequately powered to detect only a large difference in cortical thickness (0.37 mm), far exceeding that previously reported as a result of papilledema, between surgical treatment groups. With improved power we would expect more subtle cortical thickness changes to emerge, congruent with previous findings.

Our secondary analysis showed lambdoid synostosis to result in thinning across all brain regions, with pronounced effects in the cingulate and frontal cortices. We expected to observe greater effect sizes between synostoses and corresponding cortical lobes (eg, coronal/frontal, lambdoid/occipital), but interestingly lambdoid involvement was associated with more thinning in the frontal cortex than the occipital. The largest effect sizes observed were those of lambdoid synostoses on the cingulate gyri. To date, lambdoid synostoses have been shown to result in localized brain dysmorphology such as increased rates of cerebellar tonsillar herniation.[33, 34] This is likely due to the disproportionate cerebellar growth, which normally occurs in the

first 2 years of life, in the context of posterior fossa maldevelopment.[35] It may be that the association between lambdoid craniosynostosis and cortical thinning is related to increased ICH rates, which then differentially affects more susceptible cortical regions such as the cingulate gyri. The explanation for why ICH rates may be elevated in lambdoid synostosis is crowding of the posterior fossa leading to venous outflow obstruction and/or accessory venous drainage pathways, which are common in CP syndrome.[36] Furthermore, contralateral growth restriction of the occiput may result in a cranial distortion mirrored by that of the pericallosal artery supplying the cingulate cortex; however, further study is needed to evaluate this possibility.

Coronal suture involvement was also associated with cortical thinning across all brain regions measured; however, its effects were generally small (Cohen's $d < 0.5$) except for frontal lobes. But even in frontal lobes, the effect was not definitive, as 95% confidence intervals included zero at their outer limits. Despite this, it seems that some localized influence does exist, and a more comprehensive explanation is required to resolve these apparent discrepancies. Due to the fact that lambdoid and coronal synostosis both result in significant skull distortion, including flattening of the occiput, scoliosis of the face and turribrachycephaly, dependent upon specific suture combinations, we must consider the influence of overall cranial shape and its contribution to ICH and subsequent cortical changes. It may be that turribrachycephaly contributes to frontal cortical thinning, which occurs in bicoronal and bilambdoid synostosis, while isolated lambdoid suture involvement contributes more heavily to ICH development, disproportionately impacting the cingulate gyri. The idea that cranial shape influences neurodevelopment is supported by previous study in non-syndromic craniosynostosis patients who experienced worse developmental and linguistic outcomes than healthy children or patients with varying forms of single suture synostosis.[37-40] Our results similarly show cortical thickness effect sizes corresponding to these outcomes, with sagittal synostosis resulting in increased cortical thickness across various brain regions, most notably in the occipital lobes.

When interpreting the results of our study, several limitations should be considered. First, 34 patients were included for analysis, which limits the power of our study to draw negative inferences and could explain our failure to discover any cortical changes associated with type of primary cranial vault expansion. Almost all scans were postoperative in this study. Ideally, cortical thickness data pre and postoperatively would be obtained from serial imaging studies; however, this was not possible due to the early age of surgery (median 1.27 years) and the lack of adequate tissue contrast inherent in infant brains on MRI.[41] Additionally, it is possible that other variables unaccounted for in our analysis, which may influence cortical development, could have resulted in reverse confounding, thereby masking any effect of surgical intervention type. Finally, the precision of FreeSurfer processing methodologies may be influenced by cranial dysmorphology. FreeSurfer generates maps using spatial intensity gradients

across tissue classes on MRI data, which allow for greater resolution than voxel size. Previous validation of FreeSurfer has demonstrated cortical thickness measurement to be statistically indistinguishable from traditional neuropathology techniques on histological analysis.[26, 27, 30] Furthermore, FreeSurfer analysis has been applied with accuracy to a variety of neuropathologies, across a variety of ages.[27, 29, 42] In this study we confirmed successful processing through manual inspection of all surfaces generated by the FreeSurfer pipeline on each scan to ensure the reliability of our data.

Despite variable effects of synostosis pattern on regional cortical thickness seen in this study, we observed similar global and regional thicknesses in both frontal-first and occipital-first cranial vault expansion groups. Evaluation of effect size due to suture involvement showed frontal lobe thinning in coronal and lambdoid synostosis cases, suggesting that turribrachycephaly may adversely influence frontal cortex development. Lambdoid synostosis was also associated with a pronounced thinning effect in the cingulate gyri, likely attributable to increased ICH rates due to crowding of the posterior fossa. This explanation seems most likely, given the buried nature of the cingulate cortex as well as its associations with the cerebellum, and frequent tonsillar herniation seen in lambdoid CP cases.[43, 44] Future studies should evaluate the effect of primary cranial vault expansion type as well as synostosis pattern on neuropsychological and functional outcomes such as hearing as well as investigate potential vascular causes of cingulate thinning observed in this study.

REFERENCES

1. Cohen MM, Jr., Kreiborg S. Birth prevalence studies of the Crouzon syndrome: comparison of direct and indirect methods. *Clin Genet* 1992;41:12-15
2. Rutland P, Pulleyn LJ, Reardon W, et al. Identical mutations in the FGFR2 gene cause both Pfeiffer and Crouzon syndrome phenotypes. *Nat Genet* 1995;9:173-176
3. Ghali GZ, Zaki Ghali MG, Ghali EZ, et al. Intracranial Venous Hypertension in Craniosynostosis: Mechanistic Underpinnings and Therapeutic Implications. *World Neurosurg* 2019;127:549-558
4. Spruijt B, Mathijssen IMJ, Bredero-Boelhouwer HH, et al. Sleep Architecture Linked to Airway Obstruction and Intracranial Hypertension in Children with Syndromic Craniosynostosis. *Plast Reconstr Surg* 2016;138:1019e-1029e
5. Cinalli G, Sainte-Rose C, Kollar EM, et al. Hydrocephalus and craniosynostosis. *J Neurosurg* 1998;88:209-214
6. Spruijt B, Joosten KF, Driessen C, et al. Algorithm for the Management of Intracranial Hypertension in Children with Syndromic Craniosynostosis. *Plast Reconstr Surg* 2015;136:331-340
7. Spruijt B, Rijken BFM, den Ottelander BK, et al. First Vault Expansion in Apert and Crouzon-Pfeiffer Syndromes: Front or Back? *Plast Reconstr Surg* 2016;137:112e-121e
8. Burgaleta M, Johnson W, Waber DP, et al. Cognitive ability changes and dynamics of cortical thickness development in healthy children and adolescents. *Neuroimage* 2014;84:810-819
9. S K, Y AD, Rj H, et al. Positive association between cognitive ability and cortical thickness in a representative US sample of healthy 6 to 18 year-olds. *Intelligence* 2009;37:145-155
10. Duncan NW, Gravel P, Wiebking C, et al. Grey matter density and GABAA binding potential show a positive linear relationship across cortical regions. *Neuroscience* 2013;235:226-231
11. Williams VJ, Juranek J, Cirino P, et al. Cortical Thickness and Local Gyrification in Children with Developmental Dyslexia. *Cereb Cortex* 2018;28:963-973
12. Gautam P, Anstey KJ, Wen W, et al. Cortical gyrification and its relationships with cortical volume, cortical thickness, and cognitive performance in healthy mid-life adults. *Behav Brain Res* 2015;287:331-339
13. Alvarez I, Parker AJ, Bridge H. Normative cerebral cortical thickness for human visual areas. *Neuroimage* 2019;201:116057
14. Zink DN, Miller JB, Caldwell JZK, et al. The relationship between neuropsychological tests of visuospatial function and lobar cortical thickness. *J Clin Exp Neuropsychol* 2018;40:518-527
15. Menary K, Collins PF, Porter JN, et al. Associations between cortical thickness and general intelligence in children, adolescents and young adults. *Intelligence* 2013;41:597-606
16. Wilson AT, Den Ottelander BK, De Goederen R, et al. Intracranial hypertension and cortical thickness in syndromic craniosynostosis. *Dev Med Child Neurol* 2020;62:799-805
17. Abu-Sittah GS, Jeelani O, Dunaway D, et al. Raised intracranial pressure in Crouzon syndrome: incidence, causes, and management. *J Neurosurg Pediatr* 2016;17:469-475
18. Fernandes MB, Maximino LP, Perosa GB, et al. Apert and Crouzon syndromes-Cognitive development, brain abnormalities, and molecular aspects. *Am J Med Genet A* 2016;170:1532-1537
19. Maliepaard M, Mathijssen IM, Oosterlaan J, et al. Intellectual, behavioral, and emotional functioning in children with syndromic craniosynostosis. *Pediatrics* 2014;133:e1608-1615
20. Rijken BF, Leemans A, Lucas Y, et al. Diffusion Tensor Imaging and Fiber Tractography in Children with Craniosynostosis Syndromes. *AJNR Am J Neuroradiol* 2015;36:1558-1564

21. Mathijssen IM. Guideline for Care of Patients With the Diagnoses of Craniosynostosis: Working Group on Craniosynostosis. *J Craniofac Surg* 2015;26:1735-1807

22. Rijken BF, Lequin MH, van der Lijn F, et al. The role of the posterior fossa in developing Chiari I malformation in children with craniosynostosis syndromes. *J Craniomaxillofac Surg* 2015;43:813-819

23. Clarkson MJ, Cardoso MJ, Ridgway GR, et al. A comparison of voxel and surface based cortical thickness estimation methods. *Neuroimage* 2011;57:856-865

24. Fischl B, Sereno MI, Dale AM. Cortical surface-based analysis. II: Inflation, flattening, and a surface-based coordinate system. *Neuroimage* 1999;9:195-207

25. Dale AM, Fischl B, Sereno MI. Cortical surface-based analysis. I. Segmentation and surface reconstruction. *Neuroimage* 1999;9:179-194

26. Fischl B, Dale AM. Measuring the thickness of the human cerebral cortex from magnetic resonance images. *Proc Natl Acad Sci U S A* 2000;97:11050-11055

27. Rosas HD, Liu AK, Hersch S, et al. Regional and progressive thinning of the cortical ribbon in Huntington's disease. *Neurology* 2002;58:695-701

28. Kuperberg GR, Broome MR, McGuire PK, et al. Regionally localized thinning of the cerebral cortex in schizophrenia. *Arch Gen Psychiatry* 2003;60:878-888

29. Salat DH, Buckner RL, Snyder AZ, et al. Thinning of the cerebral cortex in aging. *Cereb Cortex* 2004;14:721-730

30. Cardinale F, Chinnici G, Bramerio M, et al. Validation of FreeSurfer-estimated brain cortical thickness: comparison with histologic measurements. *Neuroinformatics* 2014;12:535-542

31. Martinussen M, Fischl B, Larsson HB, et al. Cerebral cortex thickness in 15-year-old adolescents with low birth weight measured by an automated MRI-based method. *Brain* 2005;128:2588-2596

32. Bjuland KJ, Lohaugen GC, Martinussen M, et al. Cortical thickness and cognition in very-low-birth-weight late teenagers. *Early Hum Dev* 2013;89:371-380

33. Chivoret N, Arnaud E, Giraudat K, et al. Bilambdoid and sagittal synostosis: Report of 39 cases. *Surg Neurol Int* 2018;9:206

34. Fearon JA, Dimas V, Ditthakasem K. Lambdoid Craniosynostosis: The Relationship with Chiari Deformations and an Analysis of Surgical Outcomes. *Plast Reconstr Surg* 2016;137:946-951

35. Cinalli G, Renier D, Sebag G, et al. Chronic tonsillar herniation in Crouzon's and Apert's syndromes: the role of premature synostosis of the lambdoid suture. *J Neurosurg* 1995;83:575-582

36. Hayward R. Venous hypertension and craniosynostosis. *Childs Nerv Syst* 2005;21:880-888

37. Korpilahti P, Saarinen P, Hukki J. Deficient language acquisition in children with single suture craniosynostosis and deformational posterior plagiocephaly. *Childs Nerv Syst* 2012;28:419-425

38. Andrews BT, Fontana SC. Correlative vs. Causative Relationship between Neonatal Cranial Head Shape Anomalies and Early Developmental Delays. *Front Neurosci* 2017;11:708

39. Renier D, Lajeunie E, Arnaud E, et al. Management of craniosynostoses. *Childs Nerv Syst* 2000;16:645-658

40. Da Costa AC, Anderson VA, Savarirayan R, et al. Neurodevelopmental functioning of infants with untreated single-suture craniosynostosis during early infancy. *Childs Nerv Syst* 2012;28:869-877

41. Wang F, Lian C, Wu Z, et al. Developmental topography of cortical thickness during infancy. *Proc Natl Acad Sci U S A* 2019;116:15855-15860

42. Nickel K, Tebartz van Elst L, Manko J, et al. Inferior Frontal Gyrus Volume Loss Distinguishes Between Autism and (Comorbid) Attention-Deficit/Hyperactivity Disorder-A FreeSurfer Analysis in Children. *Front Psychiatry* 2018;9:521

43. Badura A, Verpeut JL, Metzger JW, et al. Normal cognitive and social development require posterior cerebellar activity. *Elife* 2018;7

44. Herrojo Ruiz M, Maess B, Altenmuller E, et al. Cingulate and cerebellar beta oscillations are engaged in the acquisition of auditory-motor sequences. *Hum Brain Mapp* 2017;38:5161-5179

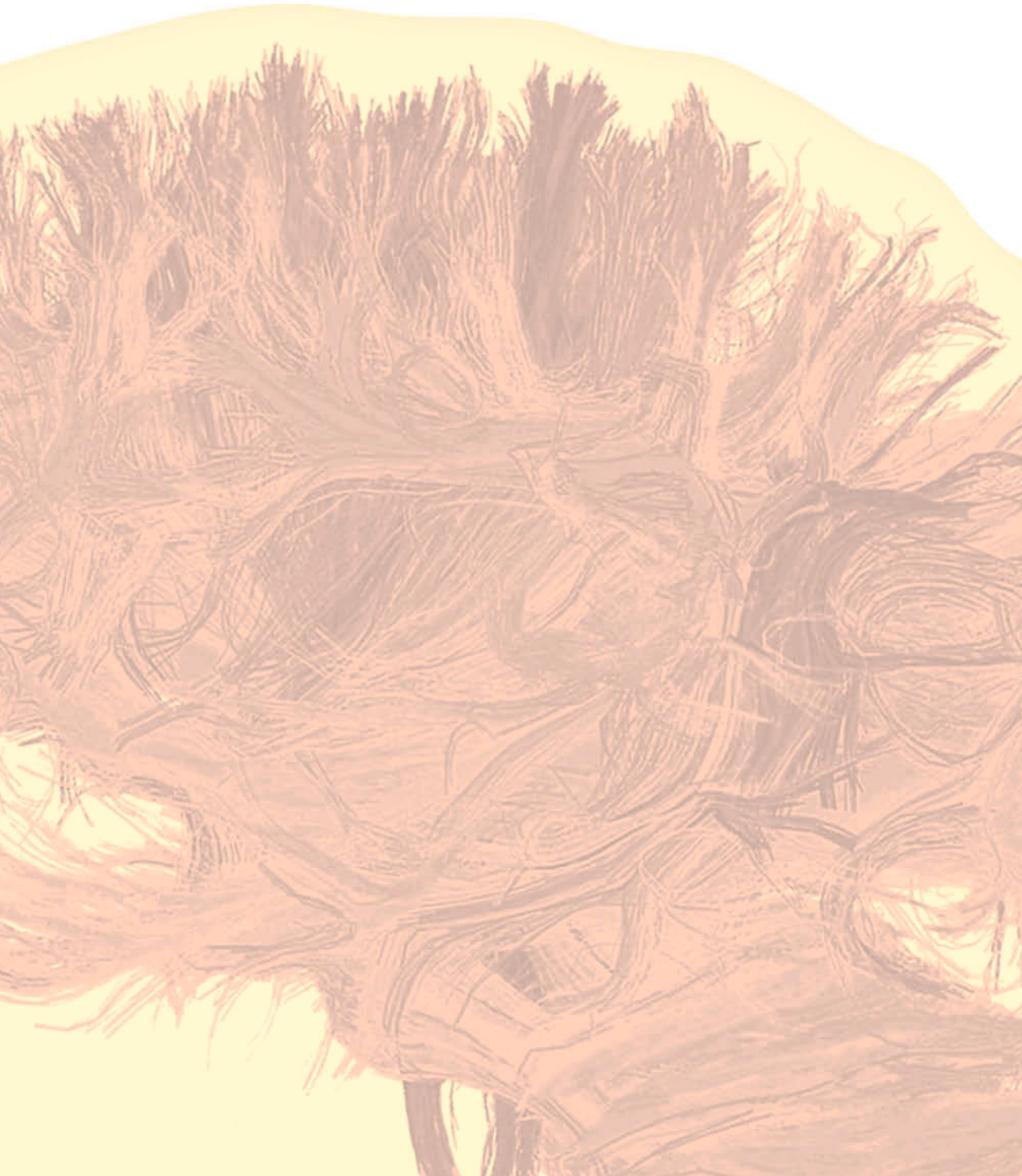

CHAPTER 8

THE COURSE AND INTERACTION OF VENTRICULOMEGALY AND CEREBELLAR TONSILLAR HERNIATION IN CROUZON SYNDROME OVER TIME

PRIYA N. DOERGA

CATHERINE A. DE PLANQUE

NICOLE S. ERLER

MARIE-LISE C. VAN VEELEN

IRENE M. J. MATHIJSSEN

PRS Global Open, 2022 Jan 24;10(1):e3979

ABSTRACT

Background: Children with Crouzon syndrome have a higher incidence of cerebellar tonsillar herniation (TH) and ventriculomegaly than the general population, or children with other craniosynostosis syndromes.

Objective: This retrospective cohort study aimed to determine how ventriculomegaly and TH develop and progress over time and determine associations between ventriculomegaly and TH in Crouzon patients, treated according to our center's protocol.

Methods: Fronto-occipital horn ratio (FOHR) and TH were determined over time using brain-imaging. These data were used to fit a mixed-model to determine associations between them, and with clinical variables, head-circumference, and lambdoid suture synostosis.

Results: Sixty-three Crouzon patients were included in this study. Preoperatively, 28% had ventriculomegaly, and 11% had TH ≥ +5 mm. Postoperatively ventriculomegaly increased to 49%. Over time and with treatment, FOHR declined and stabilized around 5 years of age. TH ≥ +5 mm increased to 46% during follow-up. FOHR and TH were associated: expected FOHR with a TH of either 0 mm versus +8.6 mm at 0 years: 0.44 versus 0.49, and at 5 years: 0.34 versus 0.38; 10% increase of FOHR was associated with 1.6 mm increase in TH. Increased head-circumference was associated with increased FOHR. Lambdoid suture synostosis was associated with +6.9 mm TH increase.

Conclusions: In Crouzon patients, FOHR was large at onset and decreased and stabilized with treatment and time. FOHR was associated with head-circumference and TH. TH was strongly associated with lambdoid suture synostosis and FOHR. Increased head-circumference was associated with an increased FOHR and closed lambdoid sutures before 1 year of age were associated with a +6.92 mm increase in tonsil position.

INTRODUCTION

Crouzon syndrome is a type of syndromic craniosynostosis, with a prevalence of 0.1 per 10,000 live births.[1] There is a lot of overlap between patients with Crouzon and Pfeiffer syndrome, both in phenotype and genetic mutations; we therefore consider them to be a homogenous group of varying severity of the same genetic defect and refer to them all as Crouzon patients. Crouzon syndrome is characterized by mutations in genes for fibroblast growth factor receptors type 1, 2, and 3.[2] Clinically, they often present with multiple suture synostosis, exorbitism, and midface hypoplasia. Crouzon syndrome has a wide spectrum of disease severity, ranging from a mild phenotype to a severe phenotype requiring multiple surgeries to treat intracranial hypertension (ICH), or conditions that cause ICH such as ventriculomegaly or obstructive sleep apnea (OSA).[3-7] Detecting and treating ICH is important because it can cause visual impairment and is thought to affect neurocognitive development.[8]

The wide range of severity and unpredictability of the outcome of surgical treatments in Crouzon syndrome can make treating the individual Crouzon patient difficult. Unexpected problems that can occur are worsening of exorbitism, progressive expansion of ventricles after skull vault expansion, and recurrence of ICH soon after initial treatment.[7] This makes it difficult to decide which treatment is necessary at which moment. Repeat surgeries are related to hydrocephalus, cerebellar tonsillar herniation (TH), and their connection to ICH. Many theories have been postulated about the pathogenesis of TH and how it relates to ventriculomegaly.[9, 10] Although there is no consensus about the sequence in which ventriculomegaly and TH occur, presence of either one is generally taken as a sign indicating a need for a closer follow-up.[7, 11, 12] This study has three main aims: (1) to determine how ventriculomegaly and TH develop and progress over time, (2) to determine how ventriculomegaly and TH relate to one another, (3) to determine which clinical traits, if any, are associated with TH or ventriculomegaly.

METHODS

The medical ethics committee of the Erasmus MC approved this study (MEC2017-1143). This retrospective study gives an overview of children with Crouzon syndrome treated at the Erasmus MC in Rotterdam, the Netherlands, Sophia Children's Hospital, the national referral hospital for patients with syndromic craniosynostosis. It serves an approximately 3.6 million national pediatric population.[13] Patients were included sequentially from June 1994 to October 2019, DNA analysis confirmed Crouzon syndrome.

As part of our clinical protocol,[4] we perform surgical vault expansion before 1 year of age. First choice is occipital expansion with springs, scheduled around the age of 6–5 months. If ventriculomegaly develops before this age, vault expansion is scheduled earlier. When hydrocephalus appears after vault expansion, a shunt or endoscopic third ventriculostomy (ETV) will be considered. If initial ventricular enlargement following a cranial vault expansion is not progressive, an expectant policy is followed. If ICH occurs, a second vault expansion is preferred over shunting. In general, a shunt is avoided before or shortly after cranial vault expansion to prevent skull growth reduction.

Brain Imaging

As per clinical protocol, magnetic resonance imaging (MRI) exams were obtained at first presentation (usually before 1 year old), at 2 and 4 years old, and additionally when clinically indicated. All MRI data were acquired using a 1.5 Tesla MR Unit (General Electric Healthcare, Milwaukee, Wisc.). Images were aligned in sagittal and coronal planes using Philips 3D-modeling in Intellispace software, to ensure measurements were done consistently and in the correct plane.

Computed tomography (CT) scans were acquired using a multidetector CT-scanner (Siemens, Erlangen, Germany). Scan protocol parameters were set to obtain image quality required for clinical interpretation. Patients underwent at least one CT-scan during follow-up before surgery, to determine which cranial sutures were closed. Additional CT-scans were done only when clinically indicated, to minimize radiation exposure.

Fronto-occipital horn ratio (FOHR) was used as parameter for ventricle size. FOHR is calculated as (frontal horn width + occipital horn width)/biparietal diameter*2 and gives a ratio of ventricle size that can be interpreted independent of age.[14, 15] An FOHR ≥ 0.4 was considered ventriculomegaly. FOHR was determined on MRI or CT-scans. Children with hydrocephalus underwent VP-shunt/ETV.

The tonsil position was determined as the position of the lowest cerebellar tonsil in mm above (referred to as negative numbers) the foramen magnum (FM) or below the

FM (TH, referred to as positive numbers; eg, tonsil position of 5 mm or more past the FM: TH ≥ +5 mm), and measured as a continuous variable. Increases in tonsil position referred to increasing downward movement of the cerebellar tonsils. Additionally, TH was divided into two categories: TH < +5 mm and TH ≥ +5 mm below FM.

Presence of abnormal venous anatomy was determined using MRI or CT-scans with angiography. We determined presence of occipital and mastoid emissary veins (0 = normal drainage pattern, 1 = abnormal emissary veins).

Clinical Measurements

Head-circumference was measured using the occipitofrontal circumference, which has shown to be a reliable indicator for intracranial volume.[16, 17] Fundoscopy was performed to screen for ICH as determined by presence of papilledema. Patients were screened preoperatively, at the ages of 2, 4, and 6 years. Polysomnography was used to screen for the presence of OSA, using clinical in-house assessments, and ambulatory sleep studies. Obstructive apnea-hypopnea index (oAHI) was calculated as the number of obstructive and mixed apneas, or obstructive hypopneas with desaturation/arousal, divided by the total sleep duration of one night. The oAHI was used to classify patients in two categories: (1) no/mild (oAHI < 5), and (2) moderate/severe OSA (oAHI ≥ 5). Only head-circumference and early lambdoid suture closure were different on preliminary analysis between children with and without TH ≥ 5 mm and children with and without FOHR ≥ 0.4, and were used for further statistical analysis. Information about the timing and types of surgeries was collected.

Statistical Analysis

Relevant characteristics of the study population are summarized using mean and range, or when appropriate median an interquartile range (IQR), for continuous variables and counts and proportions for categorical variables. To give an overview of the data, we created a heatmap, in which patients were categorized into four groups based on the moment TH ≥ +5 mm developed: (1) patients who developed TH ≥ +5 mm before first vault expansion, (2) patients who had no TH ≥ +5 mm on first MRI, and later developed it, (3) patients who underwent first MRI at a late age and had TH ≥ +5 mm, and (4) patients without TH ≥ +5 mm. For each of these groups, the heatmap shows the frequency of patients with FOHR ≥ 0.4, lambdoid suture synostosis before 1 year of age, papilledema, venous emissary veins, and moderate/severe OSA.

To investigate the association between FOHR and tonsil position, head-circumference, and lambdoid suture synostosis before 1 year of age, we fitted a mixed-model assuming FOHR to follow a beta distribution conditional on the covariates. To allow for nonlinear trajectories over time, we included the children's age using natural cubic splines with three degrees of freedom. Because this leads to difficulties in interpreting the effects of age directly, the effect of age is displayed in figures to facilitate interpretation.

Correlation between repeated measurements of the same child was taken into account by including a random (patient specific) intercept. An analogous model, but assuming a normal distribution, was fitted to investigate the association between tonsil position and FOHR, head-circumference, and lambdoid suture synostosis at the age of less than 1 year. Because FOHR, tonsil position, and head-circumference were measured at different time points, values of the independent variables had to be imputed at the time points the dependent variable was observed. To this end, we estimated both mixed-models in the Bayesian framework, which allowed us to simultaneously impute the missing observations by specifying additional mixed-models for each of the independent variables.

Specifically, the model for FOHR was estimated jointly with random intercept linear mixed-models (with natural cubic splines for age) to impute head-circumference and TH, and the model for TH was fitted jointly with a random intercept beta mixed-model for FOHR and a linear random intercept model for head-circumference (both with a natural cubic spline for age). We assumed vague priors for all parameters. Results of the Bayesian models are presented as posterior mean and 95% credible intervals (CI).

RESULTS

Patient Characteristics

Sixty-three Crouzon patients were included in this study, patient characteristics are presented in **Table 1**, and genetic changes are mentioned in **Supplemental Digital Content 1**, which displays genetic changes present in this cohort of Crouzon patients). Median age at presentation was 0.9 (IQR 0.2–3.0) years; median follow-up at study conclusion was 10.2 (IQR 4.3–15.7) years.

Ventriculomegaly and TH Development and Progress over Time.

Figure 1 shows factors TH ≥ +5 mm and FOHR ≥ 0.4 preoperatively and postoperatively in the 63 children, categorized by the moment at which TH ≥ +5 mm occurred. In patients with both ventriculomegaly and TH ≥ +5 mm (n = 18), TH ≥ +5 mm was detected before ventriculomegaly occurred in one of 18 patients, TH ≥ +5 mm was detected after ventriculomegaly occurred in five of 18 patients, and TH ≥ +5 mm and ventriculomegaly were detected at the same time in 12 of 18 patients. In four patients TH ≥ +5 mm was detected after placement of a VP-shunt; in two patients TH ≥ +5 mm was detected after ETV. Thirteen patients underwent VP-shunting or ETV: 10 patients were initially treated with a vault expansion followed by VP-shunt, and in three patients the order of procedures was the other way around.

Patient-specific trajectories of FOHR and tonsil position are displayed in **Figure 2**. The trajectories show the distinct differences between patients in development and progress of FOHR and tonsil position.

Table 1. Patient characteristics

Crouzon patients	63
M : F	31 : 32
Age at presentation†	0.7 (0.2 – 2.9)
FOHR ≥ 0.4*	31 (18; 13)
TH ≥+5mm*	29 (6; 23)
FOHR ≥ 0.4 and TH ≥+5mm	18
Lambdoid suture synostosis <1yr of age	12
Head circumference < -1.0 SD	22
Papilledema	33
Moderate/severe OSA	18
Surgeries	
No surgery	6
Patients that underwent a single surgery	19
Patients that underwent multiple surgeries	38
Types of surgeries	
Vault expansions‡	59 (46)
Fronto-orbital expansion	15
(Fronto-)biparietal remodellation	20
Occipital expansion classic/spring distraction	24
Midface surgeries‡	26 (18)
Combination vault expansion & midface surgery‡	25 (22)
FM decompressions‡	3 (3)
VP-shunts/ETV and revisions‡	47 (13)
VP-shunt**	8
ETV**	2
VP-shunt + ETV**	3
Endoscopic ventriculostomies‡	6 (4)

Values represent absolute numbers
† Median age (interquartile range) in years
‡ Number of surgeries (number of patients)
* Values represent number of patients (number of patients in whom event occurred preoperatively; number of patients in whom event occurred postoperatively)
** Values represent absolute number of patients
FOHR: fronto-occipital horn ratio, TH: cerebellar tonsillar herniation, OSA: obstructive sleep apnea, FM: foramen magnum, VP-shunt: ventriculoperitoneal shunt, ETV: endoscopic third ventriculostomy

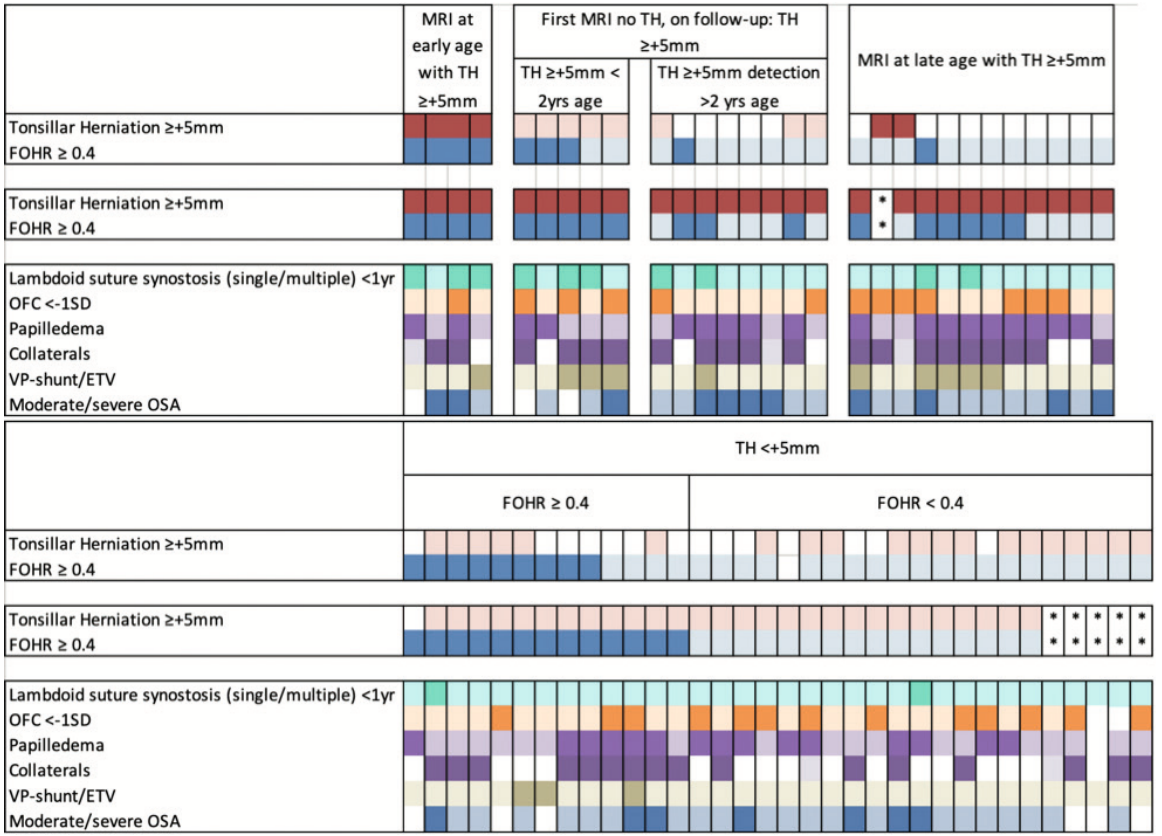

Figure. 1. Heatmap depicting attributes of the 63 Crouzon patients. Patients categorized by presence of TH ≥ +5 mm and/or FOHR ≥ 0.4 before, or after first surgical intervention. Presence of abnormalities in clinical attributes are also displayed. Of each color, the darker shade represents that the abnormalities are present, the lighter shade that the abnormalities are not present, blank squares represent missing values. *Patients who have not undergone skull vault surgery: therefore, only preoperative results displayed. FOHR: fronto-occipital herniation, yr(s): year(s), OFC: occipitofrontal circumference.

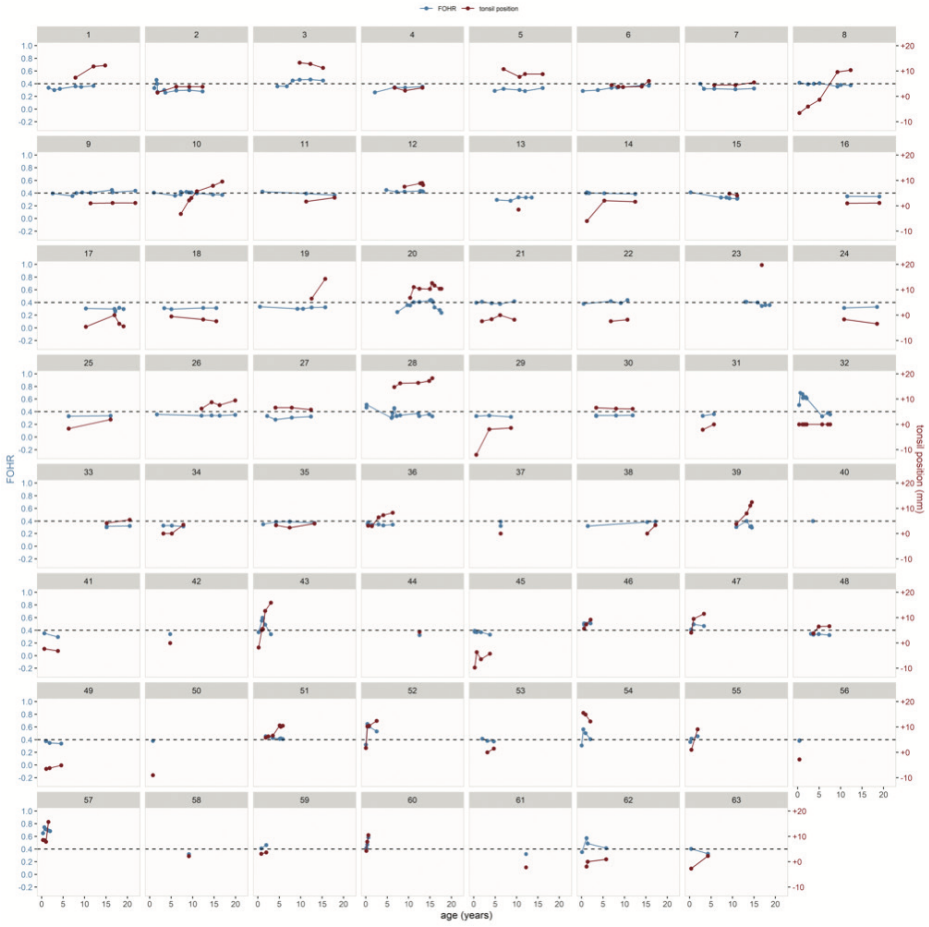

Figure 2. Patient-specific trajectories depicting progression of FOHR and tonsil position over time. Y-axes (left for FOHR, and right for tonsil position) are adjusted so that FOHR values of 0.4 are aligned with a tonsil position of +5 mm.

Relation between Ventriculomegaly and TH

The results of the mixed-model for FOHR are shown in **Table 2**. The odds ratio refers to the change in the ratio FOHR/(1-FOHR) that is associated with a 1-unit change in a covariate. **Table 2** shows that progress of tonsil position is associated with an increase in FOHR (tonsil position: odds ratio = 1.02 (95% CI[1.01–1.03]).

Table 2. Mixed-model for FOHR

			95% CI	
		OR	2.5%	97.5%
(Intercept)		0.756	0.677	0.845
Age at measurement		§		
Tonsil position		1.021	1.012	1.030
Head circumference‡		1.102	1.063	1.140
Closed lambdoid sutures< 1 year		1.103	0.971	1.266
Expected FOHR at 0 and 5 years by specific covariate values*				
Tonsil position†		Expected FOHR	95% CI	
Age 0	Q1: 0.0	0.442	0.415	0.470
	Q3: +8.6	0.486	0.449	0.524
Age 5	Q1: 0.0	0.343	0.327	0.360
	Q3: +8.6	0.384	0.363	0.405
Head-circumference‡				
Age 0	Q1: -0.66	0.434	0.403	0.467
	Q3: 1.39	0.484	0.452	0.516
Age 5	Q1: -0.66	0.336	0.317	0.355
	Q3: 1.39	0.382	0.362	0.400
Closed lambdoid sutures< 1 year				
Age 0	Open	0.462	0.431	0.493
	Closed	0.487	0.456	0.518
Age 5	Open	0.361	0.345	0.378
	Closed	0.385	0.355	0.415

CI: credible interval, OR: odds ratio, FOHR: fronto-occipital horn ratio, Q1: 1st quartile in observed data, Q3: 3rd quartile in observed data

§ The non-linear effect of age at measurement was used in the model, but cannot be represented by a single parameter estimate and the corresponding estimates do not have direct clinical interpretation

† Values represent tonsil position in mm relative to the foramen magnum, where tonsillar herniation past the foramen magnum is represented as positive numbers, and a position above the foramen magnum as negative numbers

‡ in SD

* The other covariates were set to reference/median values (tonsillar position: +3.88 mm, head-circumference: 0.51 SD, lambdoid suture: open)

Figure 3 displays the expected FOHR and corresponding 95% CIs across age for different scenarios with respect to tonsil position, head-circumference and closed lambdoid sutures at the age of less than 1 year. It shows that FOHR starts high during the first 1.5 years of life, declines with treatment and time, and from the age of 5 years remains relatively stable. **Figure 3A** displays the expected FOHR in two scenarios where tonsil position is either 0 mm (first quartile in observed data; Q1) or +8.6 mm (third quartile in observed data; Q3). The other variables were set to the median (head-circumference: 0.51 SD) and reference category (lambdoid sutures: open). It visualizes the difference in FOHR associated with tonsil position at Q1 and Q3: at age 0 an FOHR of 0.44 (Q1 range 95% CI band: [0.42–0.47]) versus 0.49 (Q3 range 95% CI-band: [0.45–0.52]), and at age 5 years an FOHR of 0.34 (Q1 range 95% CI-band [0.33–0.36]) versus 0.38 (Q3 range 95% CI-band [0.36–0.41]).

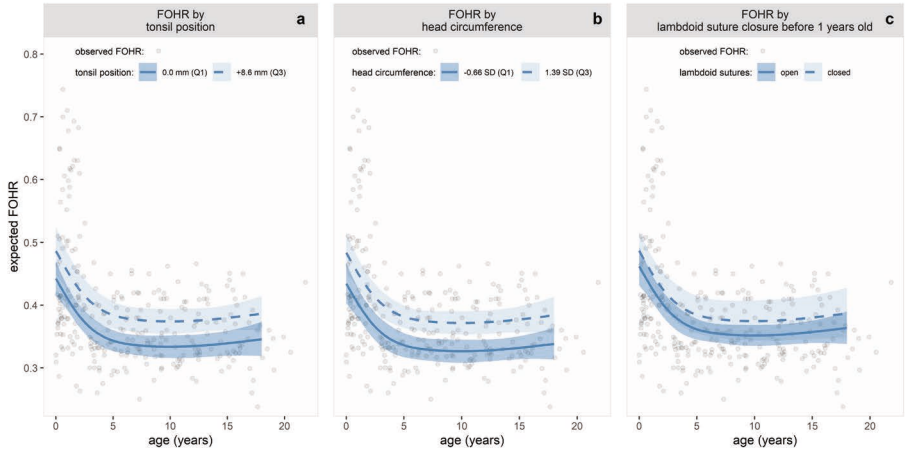

Figure 3. Expected FOHR across age by 3 different covariate values. Expected FOHR and corresponding 95% CI across age, by specific covariate values: FOHR by tonsil position (A); FOHR by head circumference (B); FOHR by lambdoid suture closure before the age of 1 year (C). Variables that are not shown in a particular panel were set to reference/median values (tonsillar position: +3.88 mm, head-circumference: 0.51 SD, lambdoid suture: open).

Results of the mixed-model for tonsil position are given in **Table 3**. Ten percentage-point higher FOHR was associated with a +1. 597 mm increase in tonsil position (95% CI[0.410–3.047]). **Figure 4** visualizes the estimated development of tonsil position over time for different scenarios with regard to FOHR values, head-circumference, and closed lambdoid sutures at the age of less than 1 year. It presents a steep increase in tonsil position during the first 2.5 years of life, after which it slows down. **Figure 4A** shows the expected tonsil position in two scenarios, where FOHR is either 0.33 (Q1) or 0.41 (Q3), and shows an overlap between their 95% CIs. Again, for these scenarios, the other independent variables are set to median or reference values.

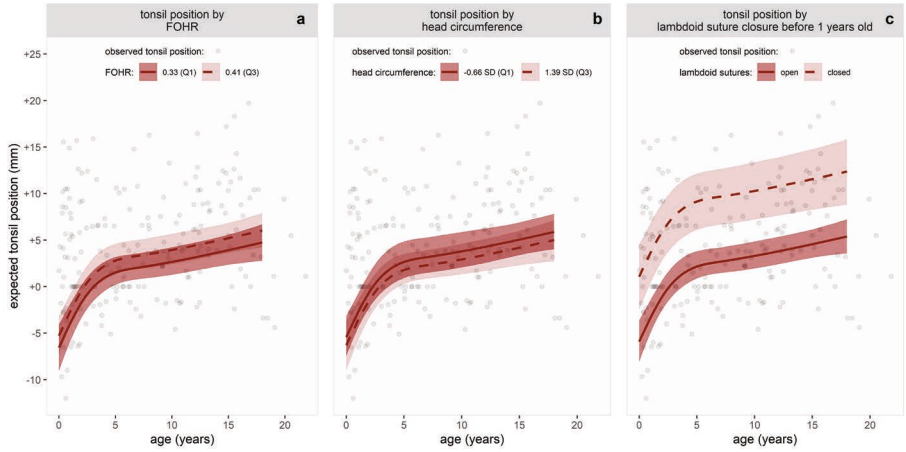

Figure 4. Expected tonsil position across age by 3 different covariate values. Expected tonsillar position and corresponding 95% CI across age, by specific covariate values: Tonsil position by FOHR (A); Tonsil position by head circumference (B); Tonsil position by lambdoid suture before the age of 1 year (C). Variables that are not shown in a particular panel were set to reference/ median values (FOHR: 0.37, headcircumference: 0.51 SD, lambdoid sutures: open).

Closed Lambdoid Sutures and Head-circumference

Figure 3 B, C display the corresponding plots of FOHR for the scenario in which head-circumference varies between its Q1 and Q3, and lambdoid suture closure at the age of less than 1 year is present, or not present. Increase in head-circumference was associated with an increase in FOHR (see Table 2, head-circumference: odds ratio = 1.102 (95% CI[1.063–1.140]). There was no clear evidence for differences in FOHR depending on whether patients presented with closed lambdoid sutures at the age of less than 1 year.

Figure 4 B, C shows the corresponding effects on tonsil position for the scenarios in which head-circumference varied between Q1 and Q3, and lambdoid suture closure before 1 year of age was present or not present. **Table 3** shows that there was no evidence for an association between tonsil position and head-circumference. Closed lambdoid sutures before 1 year of age were associated with a +6.990 mm increase in tonsil position (95% CI [3.614–10.276]).

Table 3. Mixed-model for tonsil position

			95% CI	
		Estimate	2.5%	97.5%
(Intercept)		-11.616	-17.882	-6.232
Age at measurement		§		
FOHR: Per 10% increase		+1.597	+0.410	+3.047
Head circumference‡		-0.424	-1.569	+0.303
Closed lambdoid sutures< 1 year		+6.990	+3.614	+10.276
Expected tonsil position at 0 and 5 years by specific covariate values*				
FOHR		Expected tonsil position	95% CI	
Age 0	Q1: 0.33	-6.558	-9.048	-4.020
	Q3: 0.41	-5.279	-7.233	-3.088
Age 5	Q1: 0.33	+1.518	+0.190	+3.185
	Q3: 0.41	+2.798	+1.347	+4.597
Head-circumference‡				
Age 0	Q1: -0.66	-5.431	-7.459	-3.120
	Q3: 1.39	-6.295	-9.017	-3.648
Age 5	Q1: -0.66	+2.646	+0.929	+4.801
	Q3: 1.39	+1.781	+0.269	+3.517
Closed lambdoid sutures< 1 year				
Age 0	Open	-5.920	-8.086	-3.585
	Closed	+1.079	-2.497	+4.496
Age 5	Open	+2.157	+0.878	+3.806
	Closed	+9.156	+6.105	+12.155

CI: Credible interval, FOHR: fronto-occipital horn ratio, Q1: 1st quartile in observed data, Q3: 3rd quartile in observed data

Values represent tonsil position in mm relative to the foramen magnum, where tonsillar herniation past the foramen magnum is represented as positive numbers, and a position above the foramen magnum as negative numbers.

§ The non-linear effect of age at measurement was used in the model, but cannot be represented by a single parameter estimate and the corresponding estimates do not have direct clinical interpretation

‡ in SD

* The other covariates were set to reference/median values (FOHR: 0.37, head circumference: 0.51 SD, lambdoid sutures: open)

DISCUSSION

In this study focusing on ventriculomegaly and TH in children with Crouzon syndrome, we have identified three main findings. First, we aimed to determine how ventriculomegaly and TH develop and progress over time. We found that ventriculomegaly is present in 29% at onset, the prevalence increases to 49% shortly after skull expansion, mostly in the first 1.5 years, then declines and normalizes over time and following treatment, remaining relatively stable from 5 years of age onward. TH is present in 11% at onset, with time and despite treatment (ie, vault expansion, ETV, or VP-shunting), prevalence increases to 46%, with the biggest increase happening in the first 2.5 years. Second, we aimed to determine how ventriculomegaly and TH relate to one another. We found that FOHR and tonsil position were associated, and that a 10% increase in FOHR was associated with a +1.6 mm increase in tonsil position. Third, we aimed to determine which clinical traits (if any) were associated with TH or ventriculomegaly. We found that FOHR is associated with head-circumference but not with closed lambdoid sutures before 1 year of age, and TH is associated with closed lambdoid sutures before 1 year of age, but not with head-circumference.

The prevalence of 49% of ventriculomegaly is in line with the reported prevalence of 30%–70% in children with Crouzon syndrome.[18-20] The prevalence of %46 of patients with TH ≥ 5+ mm is similarly in line with reported prevalence of %70–%38 in Crouzon patients.[21, 22] In the majority of our patients, ventriculomegaly preceded the development of TH. However, our cohort shows different orders of occurrence of ventriculomegaly and TH, which illustrates the unpredictable nature of developing ventriculomegaly and/or TH.

In line with studies that have shown that premature closure of the lambdoid sutures is associated with development of TH ≥ +5 mm,[23, 24] we found a strong association between closed lambdoid sutures within the first year of life and a +6.990 mm increase in tonsil position (95% CI [3.614–10.276]). We found no evidence for an association between tonsil position and head-circumference.

A study by Coll et al. showed a statistically significant association between the presence of hydrocephalus and TH in Crouzon patients, as determined by a chi-square test.[20] This study expands on that finding by demonstrating that a 10% increase in FOHR was associated with a +1.6 mm increase in tonsil position.

Many theories have been postulated to explain hydrocephalus in syndromic craniosynostosis.[18, 25] However, to date, no unifying theory has been able to explain all variations of manifestations of hydrocephalus and TH.[11, 26] In Crouzon patients, there have been big differences in the prevalence of hydrocephalus and TH ≥ 5+ mm on their

own, but also in how often they occur together between studies using single time-point measurements and serial measurements.[20, 23]

In this report, the great variation in sequence in which ventriculomegaly and TH ≥ +5 mm can occur is exemplified in our relatively large and homogenous group of only Crouzon patients with repeated measurements. Our study showed patients who start with TH ≥ +5 mm and develop ventriculomegaly (n = 1), but also those who start with ventriculomegaly and develop TH ≥ +5 mm (n = 5), those in whom ventriculomegaly and TH ≥ +5 mm are detected at the same time (n = 12), those who start with ventriculomegaly and never get TH ≥ +5 mm (n = 13), and those who have TH ≥ +5 mm and never develop ventriculomegaly (n = 11). These variations exemplify why it is so difficult to predict at onset which clinical course an individual patient will follow and shows the need for individual treatment plans for Crouzon patients.

Figures 3 and 4 show that although FOHR is high at onset, it declines and remains stable from 5 years of age onward. Tonsil position, on the other hand, continues to increase even after the age of 5 years, when FOHR remains stable. This could indicate that TH ≥ +5 mm on its own does not contribute to ventriculomegaly in Crouzon patients. This is supported by our finding that only one in 18 patients who eventually developed both TH ≥ +5 mm and ventriculomegaly developed TH ≥ +5 mm before developing ventriculomegaly. Furthermore, because TH ≥ +5 mm rarely causes neurological deficits, we should question how much of the treatment protocol should be focused on treating/stabilizing TH.[11, 27, 28]

Recent studies show a relationship between ventriculomegaly and increased diffusivity values in white matter tracts of the corpus callosum and cingulate gyrus.[29] This is associated with internalizing and externalizing behavior, showing the importance of treating ventriculomegaly at onset in Crouzon patients.[30, 31]

This study's first limitation is its retrospective aspect. Over time a shift occurred in the availability of brain imaging material. Starting in 2007, we implemented a protocol, including MRI assessment before surgery. Patients who were treated before this time underwent only CT imaging; thus, tonsil position before surgery could not be determined. Most of these patients underwent MRI assessment after first vault surgery.

The second limitation is that we did not have a control group of patients who did not undergo surgical intervention because we aimed to operate on all children before 1 year of age. We therefore cannot determine what changes in FOHR or tonsil position are due to natural progression or due to iatrogenic effects. Similarly, in our small group of patients who underwent VP-drain/ETV, some showed increase in TH; we could not determine if this was despite VP-drain/ETV, or if this was due to iatrogenic effects. These could be topics of interest for future studies.

In conclusion, we found that FOHR was large at onset and that treating ventriculomegaly gives a decrease and stabilization in FOHR over time. FOHR and tonsil position were associated, and a 10% increase in FOHR was associated with a +1.6 mm increase in tonsil position. Increased head-circumference was associated with an increased FOHR and closed lambdoid sutures before 1 year of age were associated with a +6.92 mm increase in tonsil position. Overall, the more common sequence is first occurrence of ventriculomegaly, followed by TH, although we cannot claim a causal relationship.

Supplemental Digital Content - Table 1. Genetic changes present in this cohort of Crouzon patients.

FGFR	Nucleotide Change	Protein Change	n
FGFR1	c.755C>G	Pro252Arg	2
FGFR2	c.314A>G	Tyr105Cys	4
FGFR2	c.799T>C	Ser267Pro	5
FGFR2	c.812G>T	Gly271Val	1
FGFR2	c.826T>C	Phe276Val	2
FGFR2	c.833G>T	Cys278Phe	3
FGFR2	c.962A>T	Asp321Val	1
FGFR2	c.866A>C	Gln289Pro	2
FGFR2	c.868T>C	Trp290Arg	4
FGFR2	c.870G>C	Trp290Cys	1
FGFR2	c.979C>G	Leu372Val	1
FGFR2	c.1012G>C	Gly338Arg	1
FGFR2	c.1018T>C	Tyr340His	1
FGFR2	c.1019A>C	Tyr340Ser	1
FGFR2	c.1024T>A	Cys342Ser	3
FGFR2	c.1024T>C	Cys342Arg	2
FGFR2	c.1025G>A	exon 9	1
FGFR2	c.1026C>G	Cys342Trp	4
FGFR2	c.1032G>A	Ala344Ala(Splicing)	2
FGFR2	c.1040C>G	Ser347Cys	1
FGFR2	c.1061C>G	Ser354Cys	3
FGFR2	c.1069T>G	Leu357Val	1
FGFR2	c.1084+3A>G	Pro361Pro(Splicing)	1
FGFR2	c.1084G>A	Ala362Thr	1
FGFR2	c.1087+1304G>A	Cys342Tyr	8
FGFR2	c.1636G>A	Cys342Tyr	1
FGFR2	c.1694A>G	Glu565Gly	2
FGFR2	c.1851G>C	Leu617Phe	1
FGFR2	c.1922A>G	Lys641Arg	1
FGFR3	c.1172C>A	Ala391Glu	2
		Total	**63**

Nucleotide changes and protein changes that were present in the *FGFR1, FGFR2,* and *FGFR3* genes in our cohort of Crouzon patients. *FGFR*: fibroblast growth factor receptor; A: Adenine; G: Guanine; C: Cytosine; T: Thymine; Pro: Proline; Arg: Arginine; Tyr: Tyrosine; Cys: Cysteine; Ser: Serine; Gly: Glycine; Val: Valine; Phenylalanine; Asp: Aspartic Acid; Gln: Glutamine; Trp: Tryptophan; Leu: Leucine; His: Histidine; Ala: Alanine; Thr: Threonine; Glu: Glutamic Acid. Values represent absolute number of patients.

REFERENCES

1. Cornelissen M, Ottelander B, Rizopoulos D, et al. Increase of prevalence of craniosynostosis. *J Craniomaxillofac Surg* 2016;44:1273-1279
2. Johnson D, Wilkie AO. Craniosynostosis. *Eur J Hum Genet* 2011;19:369-376
3. Maliepaard M, Mathijssen IM, Oosterlaan J, et al. Intellectual, behavioral, and emotional functioning in children with syndromic craniosynostosis. *Pediatrics* 2014;133:e1608-1615
4. Spruijt B, Joosten KF, Driessen C, et al. Algorithm for the Management of Intracranial Hypertension in Children with Syndromic Craniosynostosis. *Plast Reconstr Surg* 2015;136:331-340
5. de Jong T, Bannink N, Bredero-Boelhouwer HH, et al. Long-term functional outcome in 167 patients with syndromic craniosynostosis; defining a syndrome-specific risk profile. *J Plast Reconstr Aesthet Surg* 2010;63:1635-1641
6. Fischer S, Tovetjarn R, Maltese G, et al. Psychosocial conditions in adults with Crouzon syndrome: a follow-up study of 31 Swedish patients. *J Plast Surg Hand Surg* 2014;48:244-247
7. Abu-Sittah GS, Jeelani O, Dunaway D, et al. Raised intracranial pressure in Crouzon syndrome: incidence, causes, and management. *J Neurosurg Pediatr* 2016;17:469-475
8. Abe H, Ikota T, Akino M, et al. Functional prognosis of surgical treatment of craniosynostosis. *Childs Nerv Syst* 1985;1:53-61
9. Chiari H. Ueber Veränderungen des Kleinhirns infolge von Hydrocephalie des Grosshirns. *Deutsche Medicinische Wochenschrift* 1891;17:1172–1175
10. Loukas M, Shayota BJ, Oelhafen K, et al. Associated disorders of Chiari Type I malformations: a review. *Neurosurg Focus* 2011;31:E3
11. Tubbs RS, Lyerly MJ, Loukas M, et al. The pediatric Chiari I malformation: a review. *Childs Nerv Syst* 2007;23:1239-1250
12. Rijken BF, Lequin MH, van der Lijn F, et al. The role of the posterior fossa in developing Chiari I malformation in children with craniosynostosis syndromes. *J Craniomaxillofac Surg* 2015;43:813-819
13. Netherlands S. Jaarraport, Landelijke Jeugdmonitor. 2019
14. Kulkarni AV, Drake JM, Armstrong DC, et al. Measurement of ventricular size: reliability of the frontal and occipital horn ratio compared to subjective assessment. *Pediatr Neurosurg* 1999;31:65-70
15. O'Hayon BB, Drake JM, Ossip MG, et al. Frontal and occipital horn ratio: A linear estimate of ventricular size for multiple imaging modalities in pediatric hydrocephalus. *Pediatr Neurosurg* 1998;29:245-249
16. Rijken BF, den Ottelander BK, van Veelen ML, et al. The occipitofrontal circumference: reliable prediction of the intracranial volume in children with syndromic and complex craniosynostosis. *Neurosurg Focus* 2015;38:E9
17. Breakey RWF, Knoops PGM, Borghi A, et al. Intracranial Volume and Head Circumference in Children with Unoperated Syndromic Craniosynostosis. *Plast Reconstr Surg* 2018;142:708e-717e
18. Cinalli G, Sainte-Rose C, Kollar EM, et al. Hydrocephalus and craniosynostosis. *J Neurosurg* 1998;88:209-214
19. Proudman TW, Clark BE, Moore MH, et al. Central nervous system imaging in Crouzon's syndrome. *J Craniofac Surg* 1995;6:401-405
20. Coll G, Arnaud E, Collet C, et al. Skull base morphology in fibroblast growth factor receptor type 2-related faciocraniosynostosis: a descriptive analysis. *Neurosurgery* 2015;76:571-583; discussion 583

21. Cinalli G, Spennato P, Sainte-Rose C, et al. Chiari malformation in craniosynostosis. *Childs Nerv Syst* 2005;21:889-901

22. Coll G, Arnaud E, Selek L, et al. The growth of the foramen magnum in Crouzon syndrome. *Childs Nerv Syst* 2012;28:1525-1535

23. Cinalli G, Renier D, Sebag G, et al. Chronic tonsillar herniation in Crouzon's and Apert's syndromes: the role of premature synostosis of the lambdoid suture. *J Neurosurg* 1995;83:575-582

24. Fearon JA, Dimas V, Ditthakasem K. Lambdoid Craniosynostosis: The Relationship with Chiari Deformations and an Analysis of Surgical Outcomes. *Plast Reconstr Surg* 2016;137:946-951

25. Sainte-Rose C, LaCombe J, Pierre-Kahn A, et al. Intracranial venous sinus hypertension: cause or consequence of hydrocephalus in infants? *J Neurosurg* 1984;60:727-736

26. Coll G, El Ouadih Y, Abed Rabbo F, et al. Hydrocephalus and Chiari malformation pathophysiology in FGFR2-related faciocraniosynostosis: A review. *Neurochirurgie* 2019;65:264-268

27. Pomeraniec IJ, Ksendzovsky A, Awad AJ, et al. Natural and surgical history of Chiari malformation Type I in the pediatric population. *J Neurosurg Pediatr* 2016;17:343-352

28. Doerga PN, Rijken BFM, Bredero-Boelhouwer H, et al. Neurological deficits are present in syndromic craniosynostosis patients with and without tonsillar herniation. *Eur J Paediatr Neurol* 2020;28:120-125

29. de Planque CA, Tasker RC, et al. Corpus callosum and cingulate bundle white matter abnormalities in non operated craniosynostosis patients - A Diffusion Tensor Imaging Study. *Manuscript submitted for publication 2020*

30. Bubb EJ, Metzler-Baddeley C, Aggleton JP. The cingulum bundle: Anatomy, function, and dysfunction. *Neurosci Biobehav Rev* 2018;92:104-127

31. Lichenstein SD, Verstynen T, Forbes EE. Adolescent brain development and depression: A case for the importance of connectivity of the anterior cingulate cortex. *Neurosci Biobehav Rev* 2016;70:271-287

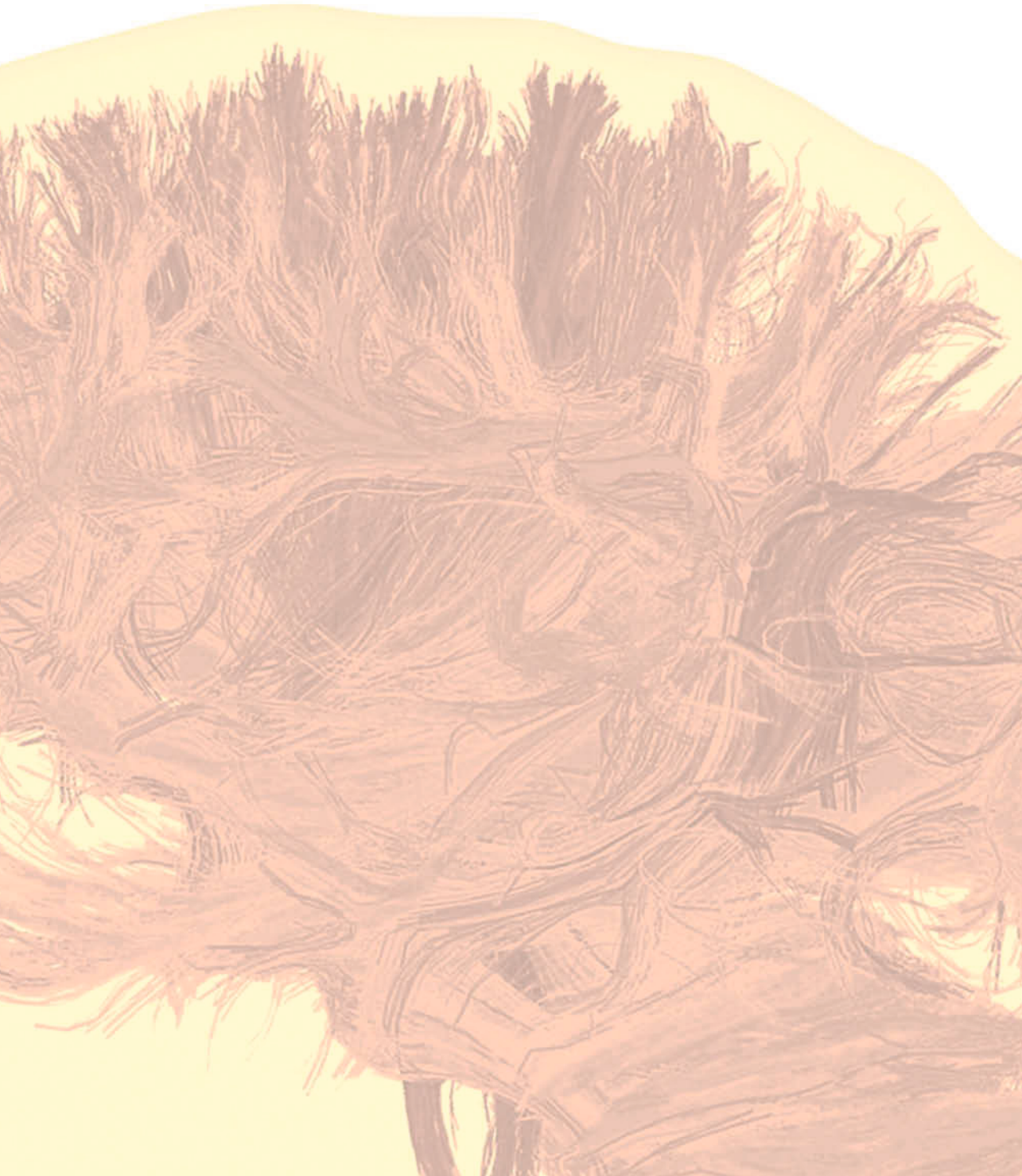

9

CHAPTER

CLINICAL SIGNS, INTERVENTIONS, AND TREATMENT COURSE OF THREE DIFFERENT TREATMENT PROTOCOLS IN PATIENTS WITH CROUZON SYNDROME WITH ACANTHOSIS NIGRICANS

CATHERINE A. DE PLANQUE

STEVEN A. WALL

LOUISE DALTON

GIOVANNA PATERNOSTER

ÉRIC ARNAUD

MARIE-LISE C. VAN VEELEN

SARAH L. VERSNEL

DAVID JOHNSON

JAYARATNAM JAYAMOHAN

IRENE M. J. MATHIJSSEN

Journal of Neurosurgery: Pediatrics, 021 Aug 13;28(4):425-431.

ABSTRACT

Objective: Crouzon syndrome with acanthosis nigricans (CAN) is a rare and clinically complex subtype of Crouzon syndrome. At three craniofacial centers, this multicenter study was undertaken to assess clinical signs in relation to the required interventions and treatment course in patients with CAN.

Methods: A retrospective cohort study of CAN was performed to obtain information about the clinical treatment course of these patients. Three centers participated: Erasmus Medical Centre, Rotterdam, the Netherlands; John Radcliffe Hospital, Oxford, United Kingdom; and Hôpital Necker-Enfants Malades, Paris, France.

Results: Nineteen patients (5 males, 14 females) were included in the study. All children were operated on, with a mean of 2.2 surgeries per patient (range 1–6). Overall, the following procedures were performed: 23 vault expansions, 10 monobloc corrections, 6 midface surgeries, 11 foramen magnum decompressions, 29 CSF-diverting surgeries, 23 shunt-related interventions, and 6 endoscopic third ventriculostomies, 3 of which subsequently required a shunt.

Conclusions: This study demonstrates that patients with the mutation c.1172C>A (p.Ala391Glu) in the FGFR3 gene have a severe disease trajectory, requiring multiple surgical procedures. The timing and order of interventions have changed among patients and centers. It was not possible to differentiate the effect of a more severe clinical presentation from the effect of treatment order on outcome.

Keywords: Crouzon syndrome with acanthosis nigricans; FGFR3; craniosynostosis; craniofacial

INTRODUCTION

Crouzon syndrome accompanied by acanthosis nigricans, a specific skin disorder of hyperkeratosis and hyperpigmentation, represents a clinically and genetically rare entity distinct from the classic Crouzon syndrome and is caused by the mutation c.1172C>A (p.Ala391Glu) in the fibroblast growth factor receptor 3 gene (FGFR3; **Figure 1**).[1] The skin disorder typically occurs later in life.

Figure 1. Photograph of mother and son both with a confirmed c.1172C>A (p.Ala391Glu) mutation in the FGFR3 gene.

The combination of Crouzon syndrome with acanthosis nigricans (CAN) was first described by Suslak et al. and Reddy et al. in 1985.[2, 3] In 1995 Meyers et al. reported the first observation of an FGFR3 transmembrane domain mutation, Ala391Glu, in three unrelated families with CAN.[1]

An overview of 33 published cases of CAN revealed that 39.4% (13/33 cases) presented with choanal atresia at birth, 45.5% (15/33 cases) developed hydrocephalus, and 24.2% (8/33 cases) developed Chiari malformation. In 15.2% (5/33 cases), intellectual impairment and speech delay were present.[4] According to Arnaud-López, CAN patients are clinically more severely affected than Crouzon patients without the skin disorder, whereas mental development in CAN patients seems to be preserved.[4]

In general, the expression of Crouzon syndrome with FGFR1 or FGFR2 mutations ranges from a mild to a severe phenotype. In addition to the presence of multiple suture synostosis, exorbitism, and midface hypoplasia, Crouzon is also characterized by a wide spectrum of functional problems, intracranial hypertension (ICH), or conditions that cause ICH such as progressive ventriculomegaly, tonsillar herniation or the presence of Chiari malformation, and obstructive sleep apnea (OSA).[5-8] Intellect can vary from above normal to substantial cognitive delay.[9]

Little is known about the timing and order of interventions in children with this rare disease. The aim of this multicenter study was to examine the clinical signs, required interventions, and treatment course in children with confirmed FGFR3 CAN.

METHODS

The Research Ethics Review Committees/Internal Review Boards at Erasmus University Medical Centre Rotterdam, the Netherlands, approved this retrospective study, which is a part of ongoing work at the Craniofacial Centre, Erasmus Medical Centre Rotterdam, the Netherlands. John Radcliffe Hospital, Oxford, and Hôpital Necker- Enfants Malades, Paris, France, both full members of the European Reference Network CRANIO, participated in this multicenter retrospective study.

Genetic analysis varies by clinic and over time. Whenever the clinical diagnosis Crouzon syndrome was obvious, targeted sequencing of the FGFR2 gene was undertaken, and when the sequencing was negative, additional screening of the FGFR1 and FGFR3 genes or a panel analysis on craniosynostosis genes was performed.

From 1975 to 2019, patients with CAN were identified and confirmed by DNA analysis of the c.1172C>A (p.Ala391Glu) mutation in the FGFR3 gene. During this period, Erasmus Medical Centre Rotterdam confirmed the genetic diagnosis of 133 Crouzon cases, 6 of which were genetically CAN. Hôpital Necker-Enfants Malades confirmed 185 Crouzon cases, 5 of which had the CAN genetic mutation. Oxford genetically confirmed 8 CAN cases among a cohort of 77 genetically confirmed Crouzon cases.

Data Collection

At all three centers, clinical data were retrospectively collected, including sex, age, phenotype, OSA, progressive ventriculomegaly, tonsillar herniation, and interventions.

Clinical Measurements

Polysomnography was used to screen for the presence of OSA. The obstructive apnea-hypopnea index (OAHI) was used to classify patients into two categories: 1) no/ mild OSA (OAHI ≤ 5) and 2) moderate/severe OSA (OAHI ≥ 5).

Information about the types of surgeries and the chronology of these events was collected. Surgeries were categorized as 1) vault expansion, 2) midface surgery, 3) CSF diverting surgery, 4) respiratory improvement (nonfacial surgery), and 5) other.

Brain Measurements

All measurements were performed on MRI and/or CT studies, which were acquired on a 1.5-T scanner (GE Healthcare, MR Signa Excite HD). The size of the lateral ventricles was evaluated on axial MRI and CT scans. The fronto-occipital horn ratio (FOHR) was calculated as (frontal horn width + occipital horn width)/biparietal diameter × 2. The lateral ventricles were considered enlarged if the FOHR was ≥ 0.4. This resulting ratio of ventricle size can be interpreted independent of age. [10, 11] Hydrocephalus was diagnosed when enlargement of the ventricles was progressive on two MRI or CT scans.

Tonsil position was determined on MRI and/or CT scans as the position of the lowest cerebellar tonsil in millimeters above or below the foramen magnum and was measured as a continuous variable in millimeters. The foramen magnum was defined by the line between the basion and opisthion. A line perpendicular to the foramen magnum line was drawn to the tip of the cerebellar tonsils. A positive position corresponded with tonsillar herniation, whereas a negative measurement indicated a more rostral position of the cerebellar tonsil. Tonsil position was analyzed as a continuous variable. Additionally, the degree of tonsillar herniation below the foramen magnum was divided into two categories: < 5 mm and ≥ 5 mm.[12-14]

Considerations in Decision-Making from a Craniofacial Center Standpoint

At all three centers, ICH is defined by a combination of signs of raised intracranial pressure such as hydrocephalus, papilledema, and indirect signs on radiological imaging or by raised intracranial pressure detected with an invasive measurement.[15] In general, the treatment strategies at the three centers are similar: vault expansion, endoscopic third ventriculostomy (ETV) or ventriculoperitoneal (VP) shunt placement to treat hydrocephalus, midface surgery to improve midface hypoplasia, and foramen magnum decompression (FMD) to relieve brainstem compression. Redo vault expansion is required in cases of ICH. Posterior vault decompression can be combined with an FMD. However, the timing and order of interventions seem to differ among the centers.

Erasmus Medical Centre, Rotterdam, The Netherlands

Erasmus Medical Centre Rotterdam performs vault expansion early as the first treatment. Occipital expansion with springs is the first choice and is scheduled around the patient age of 5 to 6 months. If hydrocephalus develops before this age, vault expansion is scheduled earlier. When hydrocephalus appears after vault expansion, shunt placement or ETV will be considered. If the initial ventricular enlargement

following cranial expansion is not progressive on subsequent scans, a wait and see policy is followed. If ICH occurs, a second vault expansion is preferred instead of shunt insertion. FMD is performed when tonsillar herniation becomes symptomatic or when a syrinx develops. In general, a shunt is avoided before or shortly after cranial vault expansion to prevent growth reduction induced by shunting. In cases of uncontrolled shape development, programmable shunts are used to gradually bring down the ventricle size to prevent over-shunting and skull growth failure.

John Radcliffe Hospital, Oxford, United Kingdom

The Oxford Craniofacial Unit has followed an evolving pathway for these patients. They always identify and treat the primary cause of ICH first. For example, any patient identified with primary hydrocephalus will first be treated with a VP shunt regardless of any additional causes of ICH such as craniocerebral disproportion. In the absence of hydrocephalus, patients with ICH caused by primary craniocerebral disproportion are usually treated with posterior cranial vault distraction followed by frontal surgery. The latter will be in the form of either a standard fronto-orbital advancement and remodeling (FOAR) or, more recently, an FOAR with distraction where appropriate monobloc advancements are used. FMD is performed when needed, that is, only when there is a sign of clinical progression. Oxford does not offer a prophylactic FMD surgery.

Hôpital Necker-Enfants Malades, Paris, France

Management of Crouzon patients at Hôpital Necker- Enfants Malades usually requires multiple surgical interventions. In general, Paris hospital starts with posterior vault expansion before the patient age of 6 months. When central apnea or severe syringomyelia appears, cerebellar tonsillar herniation will be treated, normally around the age of 12 months. A patient will be treated with frontofacial monobloc advancement until they reach an age of at least 18–24 months. Ventricular shunting is preferably avoided or delayed. Consider, for example, that in this study, in 2 of 5 cases with the cloverleaf form of Crouzon, the most severe, a shunt had to be inserted earlier. Primary fronto-orbital advancement or early facial osteotomy Le Fort type III may compromise the subsequent fronto-facial monobloc advancement. However, this salvage secondary monobloc procedure may be undertaken in some instances despite previous anterior osteotomies with a higher morbidity.[16]

RESULTS

Patient Characteristics

Nineteen patients with CAN were included in this study: 6 from Erasmus Medical Centre, 8 from Radcliffe Hospital, and 5 from Hôpital Necker-Enfants Malades. Patient characteristics are presented in **Table 1**. These 19 patients (14 female) presented with exorbitism (n = 15), midface hypoplasia (n = 16), and hypertelorism (n = 8). **Table 1** also shows the presence of choanal atresia, aperture piriformis stenosis, and OSA

and its treatment. OSA was present in 14 patients, 10 of whom had a tracheotomy. Noninvasive therapy was given to 9 patients, and adenotonsillectomy was performed in 13 patients. Four patients had developed papilledema during their lifetimes. Twelve patients developed an FOHR ≥ 0.4, 6 of whom had hydrocephalus. The MRI and/or CT scans of 16 children were available, and we found that 10 children showed tonsillar herniation (≥ 5 mm).

Table 1. Characteristics of patients with Crouzon syndrome and acanthosis nigricans.

Characteristics	No. Of Patients
Total	19
Sex	
Male	5 (26%)
Female	14 (74%)
Age in years at confirmation FGFR3 mutation (median, IQR)	0.98 (6.12)
Follow up age (median, IQR)	10.3 (17.8)
Closed Sutures pattern at birth	
Unilateral coronal	1
Bicoronal	4
Bicoronal metopic	2
Bicoronal partial lambdoid	2
Bicoronal bilambdoid	2
Pansynostosis	3
Unknown	5
Expression pattern	
Exorbitism	15
Midface hypoplasia	16
Hypertelorism	8
Upper Airways	
Choanal Atresia	6
Apertura Piriformis stenosis	9
Obstructive sleep apnea	14
mild	0
moderate	1
severe	13
Treatment Obstructive sleep apnea	
O2	2
Optiflow	1
BiPAP/CPAP	6
Tracheotomy	10
Adenotonsillectomy	13
ICH factors	
Papilledema	4
Ventriculomegaly	12
Progressive ventriculomegaly	6
Tonsillar herniation	10

BIPAP = bilevel positive airway pressure; CPAP = continuous positive airway pressure; FU = follow-up

Surgical Interventions

Table 2 gives an overview of the surgical procedures for all 19 patients**. Figure 2** shows the surgeries divided by medical center location. In **Figure 3**, the chronology of surgeries per patient over time is shown. The 19 patients were of different ages and in different stages of their treatment; therefore, the graphic may not reflect the final number of surgeries for the younger patients before they reach adulthood. Thirteen patients had a first vault expansion before the age of 1 year, and 6 patients had their first after the age of 1. Eleven patients had a redo vault expansion, and 3 of them needed a third vault expansion. Thirteen patients were treated for hydrocephalus; the first intervention was a VP shunt in 8 patients and an ETV in 5 patients. In 3 of these latter 5 patients, ETV failed and a VP shunt was inserted. Eight of 11 patients needed one or more revisions of their shunt. In 8 patients, hydrocephalus was treated before they underwent cranial vault expansion (Netherlands [NL] 1/6, United Kingdom [UK] 4/8, France [FR] 3/5).

Table 2. Overview of surgeries.

Vault expansion	**No. of surgeries (in No. of patients)**
Fronto-supraorbital advancement	7(7)
Fronto parietal expansion	2(2)
Occipital expansion*	9(8)
Occipito parietal expansion, spring distraction	5(4)
Monobloc with distraction**	9(9)
Monobloc without distraction	1(1)
Facial bipartition distraction	1(1)
Foramen Magnum Decompression***	11(9)
Midface surgery	
Le Fort II distraction	1(1)
Le Fort III distraction	4(4)
Bimax	1(1)
Cerebrospinal fluid diverting surgery	
Shunt	23(11)
Endoscopic third ventriculostomy	6(5)
Endoscopic third ventriculostomy converted to shunt	(3)
Respiratory improvement: non-facial surgery	
Tracheotomy	10(10)
Adenotonsillectomy	13(12)
Other	
Cleft Palate Repair	1(1)

* including 5 surgeries in 4 patients combined with Foramen Magnum Decompression
** including 1 mandibular distraction
***including 5 surgeries in 4 patients combined with Occipital Expansion

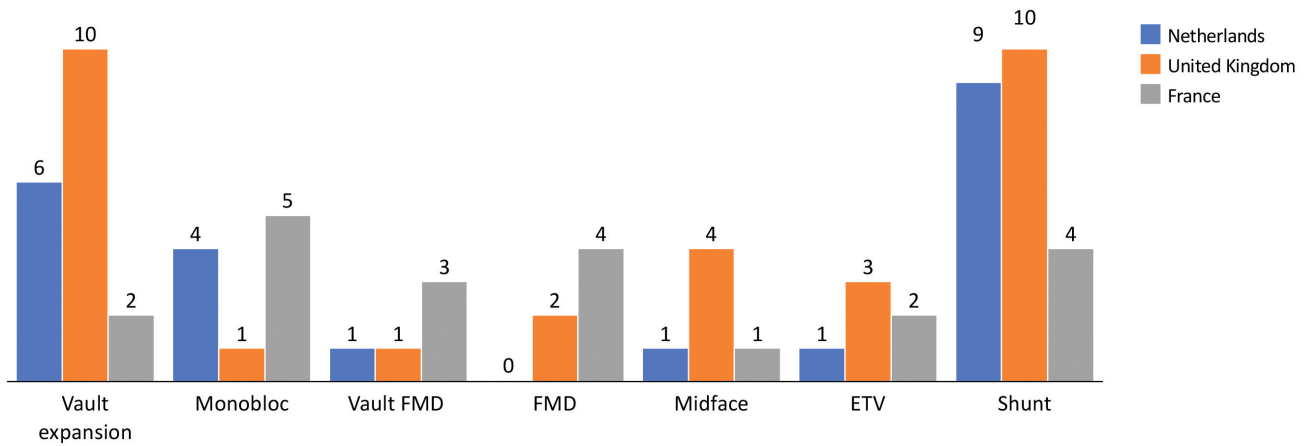

Figure 2. Surgical events per medical center location. Vault FMD = combination vault expansion with FMD; Midface = midface surgery; Shunt = VP shunt

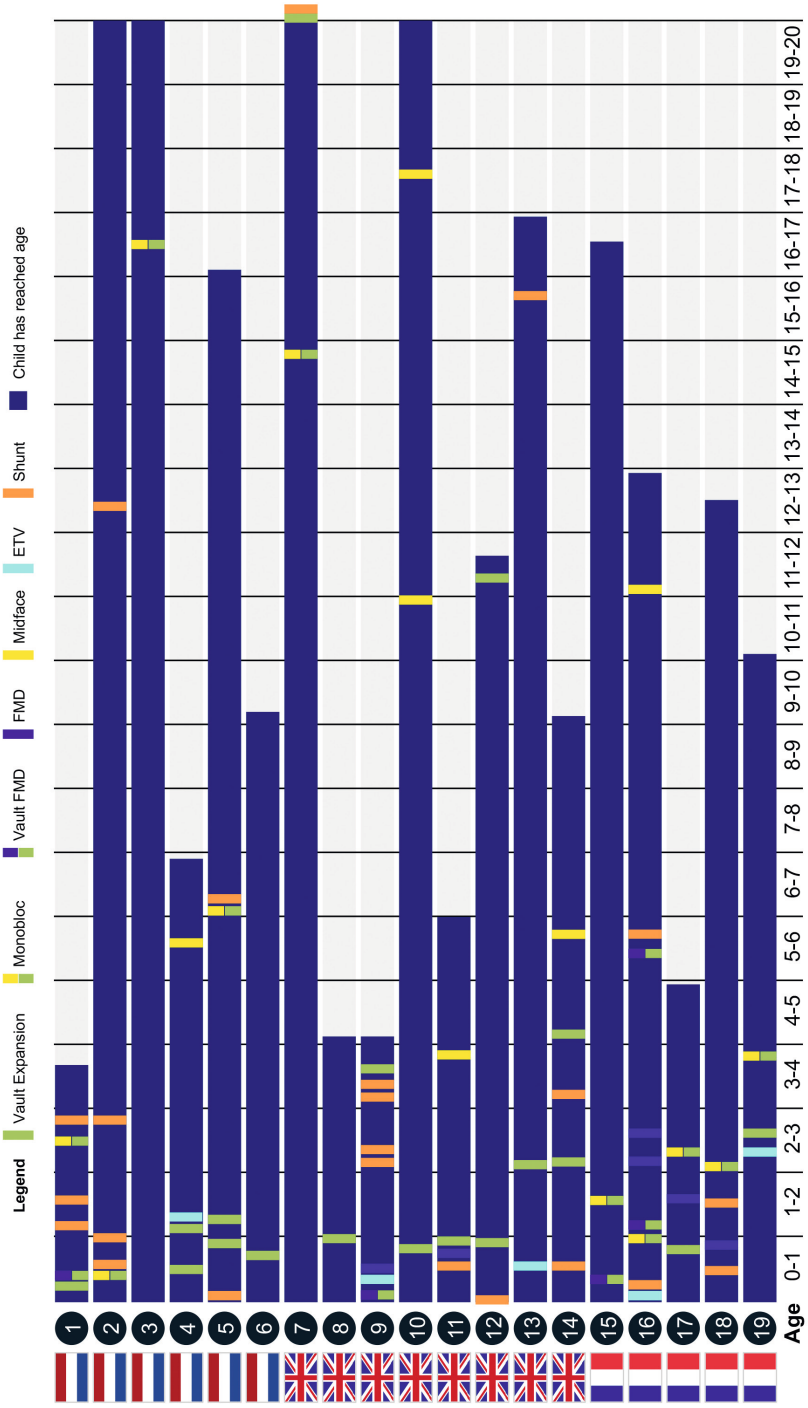

Figure 3. Timeline of events of 19 patients with CAN

Fourteen patients had a monobloc advancement or midface correction (NL 5/6, UK, 4/8, FR 5/5). The UK treated 1 patient with 1 monobloc advancement; the NL and FR treated the majority of their patients with a monobloc advancement. Seven patients underwent an FMD (NL 1/6, UK 2/8, FR 4/5). Five of these 7 patients required treatment for hydrocephalus either before or after the FMD. The timeline of events shows that most children underwent the majority of surgical events in the range of 0–3 years old.

Differences in the timing and order of interventions exist among the centers based on protocol and on the presentation of the patient. Although the order of interventions differed, the total number of interventions per patient was quite similar and the number of skull expansions showed small variations.

Patients receiving a VP shunt first had a mean of 2 skull expansions during follow-up. Each patient receiving a VP shunt after initial skull expansion had a total number of 1.5 vault expansions. Each patient who never received a shunt or never underwent an ETV had 1.3 skull expansions. Among the 9 patients who underwent early (before the age of 1) cranial expansion as the initial intervention, 4 needed subsequent hydrocephalus treatment. The patient numbers were too small for statistical analysis.

DISCUSSION

In this review, we found that CAN follows a complex clinical course mainly dictated by the recurrence of raised intracranial pressure and repeated interventions for hydrocephalus. Treatment strategies differed among the three contributing centers.

All patients in this cohort required multiple surgeries to treat ICH or to treat conditions that cause ICH such as OSA, hydrocephalus, and Chiari malformation.[6, 8] Interventions to improve airway obstruction were often the first intervention in a course of interventions that would follow. In this cohort, 10 of 19 patients needed a tracheostomy, which is more than the 3 tracheostomies in a cohort of 19 patients with Crouzon described by Arnaud et al.[17]

It is difficult to compare our findings with the percentages from other CAN studies because of the small cohorts and case reports in the literature. The treatment of progressive ventriculomegaly in patients in the present cohort is below the range found in CAN studies (43%–75%) and above the published prevalence of progressive ventriculomegaly in Crouzon patients (6%–26%).[1, 4, 18, 19] Shunting and ETV in this cohort are comparable to figures in the Crouzon literature.[8, 20-22] The treatment of hydrocephalus is challenging because of a low success rate with ETV and high shunt failure rate. This may be expected in complex craniosynostosis and is related to young age and multiple cranial surgeries.[6, 8, 21]

Comparable with previous studies of Crouzon patients, half of the patients in our cohort needed a second or third expansion after initial skull expansion.[20] The number of patients requiring midface correction was comparable to other findings.[23] Ten of the 16 patients with available MRI developed tonsillar herniation (63%), which is more than the rate for CAN patients in the literature (24%) but in line with the reported prevalence of Chiari malformation in Crouzon patients (38%–70%).[4, 22, 24] Taken together, all of the data in this study suggest that CAN patients show the same severe clinical course as that in Crouzon patients.

This study is a first effort to collect data from multiple centers on a rare form of complex craniosynostosis. Treatment protocols showed differences among centers and changed over the years. The number of patients and the details on clinical signs and outcome were insufficient to statistically evaluate these protocols. However, some remarks can be made. In general, little has been studied with respect to the timing and order of interventions. Renier et al. suggest avoiding the insertion of a shunt shortly before or after skull expansion because of the anticipated restriction on skull growth.[25] I n t he current study, early shunting seemed to be associated with more skull expansions (2) than late (1.5) or no (1.3) shunting. However, this finding may well reflect the complexity of the patients presenting with hydrocephalus early in their disease course rather than being an effect of any protocol. On the contrary, patients undergoing early cranial expansion (before the age of 1) less frequently entered into a trajectory of hydrocephalus treatment. Again, this finding may reflect the severity of the patients' courses rather than any protocol. Furthermore, this sequence of initial expansion with late or no hydrocephalus treatment may have been at the expense of macrocephaly and turricephaly. Also, the number of shunt revisions was higher after secondary shunting. This finding may be related to inserting a shunt in an already operated field or to local shunt-insertion protocols. FMD is indicated to resolve signs of brainstem compression or a syrinx but may have a role in improving CSF outflow from the fourth ventricle and thus reducing the need for shunting. However, in the current study, the reported shunt/ETV cases were similar in the patients with or without FMD (5/7 vs 8/12). Overall, it seems that the timing and order of interventions may influence the number of surgeries required, but their effect cannot be differentiated from the impact of a severe clinical presentation in this limited number of patients. To answer the question of what timing and which sequence of interventions generate the best functional and cosmetic outcomes with the smallest number of interventions, larger and more detailed studies are necessary. Especially clear definitions of clinical signs and surgical indications and a structural follow-up for skull growth and shape, signs of raised intracranial pressure, and long-term emotional, behavioral, and cognitive development will help to compare and understand different treatment philosophies. International collaborations such as the European Reference Networks can be great facilitators in performing such research.

CONCLUSIONS

In summary, patients with the mutation c.1172C>A (p.Ala391Glu) in the FGFR3 gene follow a severe clinical course with numerous interventions. The timing and order of interventions changed among patients and centers. It was not possible to differentiate the effect of a more severe clinical presentation from the effect of treatment order on outcome. This study further supports a comparison of different treatment philosophies, in which larger sample numbers and a structured multidisciplinary follow-up are required.

REFERENCES

1. Meyers GA, Orlow SJ, Munro IR, et al. Fibroblast growth factor receptor 3 (FGFR3) transmembrane mutation in Crouzon syndrome with acanthosis nigricans. *Nat Genet* 1995;11:462-464
2. Suslak L, Glista B, Gertzman GB, et al. Crouzon syndrome with periapical cemental dysplasia and acanthosis nigricans: the pleiotropic effect of a single gene? *Birth Defects Orig Artic Ser* 1985;21:127-134
3. Reddy BS, Garg BR, Padiyar NV, et al. An unusual association of acanthosis nigricans and Crouzon's disease--a case report. *J Dermatol* 1985;12:85-90
4. Arnaud-Lopez L, Fragoso R, Mantilla-Capacho J, et al. Crouzon with acanthosis nigricans. Further delineation of the syndrome. *Clin Genet* 2007;72:405-410
5. Renier D, Lajeunie E, Arnaud E, et al. Management of craniosynostoses. *Childs Nerv Syst* 2000;16:645-658
6. Spruijt B, Joosten KF, Driessen C, et al. Algorithm for the Management of Intracranial Hypertension in Children with Syndromic Craniosynostosis. *Plast Reconstr Surg* 2015;136:331-340
7. Driessen C, Joosten KF, Bannink N, et al. How does obstructive sleep apnoea evolve in syndromic craniosynostosis? A prospective cohort study. *Arch Dis Child* 2013;98:538-543
8. Abu-Sittah GS, Jeelani O, Dunaway D, et al. Raised intracranial pressure in Crouzon syndrome: incidence, causes, and management. *J Neurosurg Pediatr* 2016;17:469-475
9. Maliepaard M, Mathijssen IM, Oosterlaan J, et al. Intellectual, behavioral, and emotional functioning in children with syndromic craniosynostosis. *Pediatrics* 2014;133:e1608-1615
10. Kulkarni AV, Drake JM, Armstrong DC, et al. Measurement of ventricular size: reliability of the frontal and occipital horn ratio compared to subjective assessment. *Pediatr Neurosurg* 1999;31:65-70
11. O'Hayon BB, Drake JM, Ossip MG, et al. Frontal and occipital horn ratio: A linear estimate of ventricular size for multiple imaging modalities in pediatric hydrocephalus. *Pediatr Neurosurg* 1998;29:245-249
12. Amer TA, el-Shmam OM. Chiari malformation type I: a new MRI classification. *Magn Reson Imaging* 1997;15:397-403
13. Aboulezz AO, Sartor K, Geyer CA, et al. Position of cerebellar tonsils in the normal population and in patients with Chiari malformation: a quantitative approach with MR imaging. *J Comput Assist Tomogr* 1985;9:1033-1036
14. Elster AD, Chen MY. Chiari I malformations: clinical and radiologic reappraisal. *Radiology* 1992;183:347-353
15. Renier D, Sainte-Rose C, Marchac D, et al. Intracranial pressure in craniostenosis. *J Neurosurg* 1982;57:370-377
16. Arnaud E, Haber SE, Paternoster G, et al. [Secondary surgeries in craniosynostosis and faciocraniosynostosis] Chirurgie secondaire des craniostenoses et faciocraniostenoses. *Ann Chir Plast Esthet* 2019;64:494-505
17. Arnaud E, Marchac D, Renier D. Reduction of morbidity of the frontofacial monobloc advancement in children by the use of internal distraction. *Plast Reconstr Surg* 2007;120:1009-1026
18. Cinalli G, Renier D, Sebag G, et al. Chronic tonsillar herniation in Crouzon's and Apert's syndromes: the role of premature synostosis of the lambdoid suture. *J Neurosurg* 1995;83:575-582
19. Collmann H, Sorensen N, Krauss J, et al. Hydrocephalus in craniosynostosis. *Childs Nerv Syst* 1988;4:279-285

20. de Jong T, Bannink N, Bredero-Boelhouwer HH, et al. Long-term functional outcome in 167 patients with syndromic craniosynostosis; defining a syndrome-specific risk profile. *J Plast Reconstr Aesthet Surg* 2010;63:1635-1641

21. Di Rocco F, Juca CE, Arnaud E, et al. The role of endoscopic third ventriculostomy in the treatment of hydrocephalus associated with faciocraniosynostosis. *J Neurosurg Pediatr* 2010;6:17-22

22. Cinalli G, Spennato P, Sainte-Rose C, et al. Chiari malformation in craniosynostosis. *Childs Nerv Syst* 2005;21:889-901

23. Doerga PN, de Planque CA, Erler NS, et al. The Course and Interaction of Ventriculomegaly and Cerebellar Tonsillar Herniation in Crouzon Syndrome over Time. *Plast Reconstr Surg Glob Open* 2022;10:e3979

24. Coll G, Arnaud E, Selek L, et al. The growth of the foramen magnum in Crouzon syndrome. *Childs Nerv Syst* 2012;28:1525-1535

25. Renier D, Arnaud E, Marchac D. [Craniosynostosis: functional and morphologic postoperative results]Craniostenoses: resultats fonctionnels et morphologiques post-operatoires. *Neurochirurgie* 2006;52:302-310

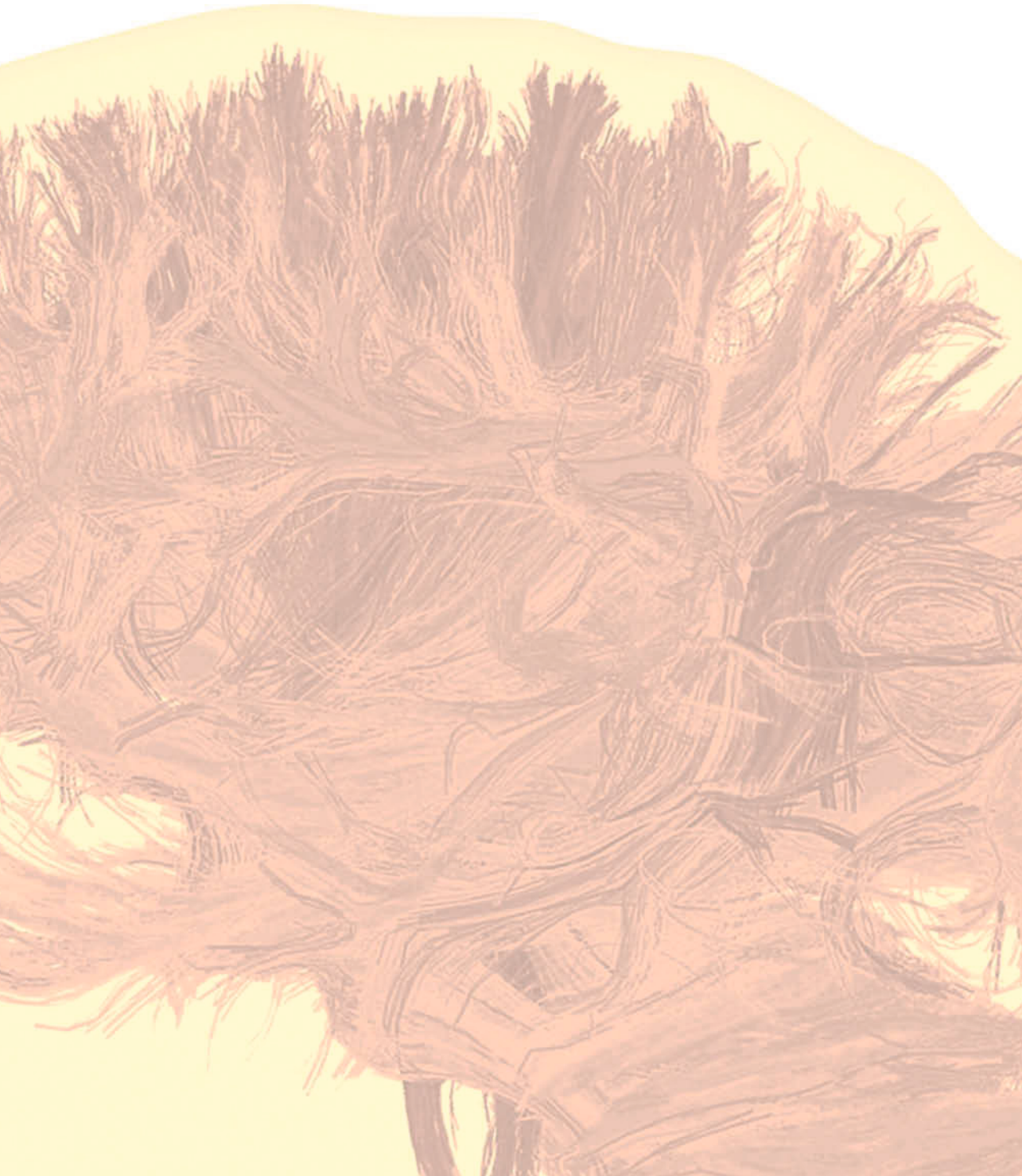

CHAPTER 10

GENERAL DISCUSSION

GENERAL DISCUSSION

This thesis was designed to study the primary genetic cause of abnormal brain development and the secondary effects of ICH on the brain in craniosynostosis patients. Differentiation between primary and secondary brain anomalies in children with craniosynostosis is important to define the best treatment strategy. Identification of primary, inborn disorders of the brain can prevent overtreatment, as it is unlikely that surgery will be of benefit.

We focused on answering the following questions:

- To what extent do primary brain abnormalities exist in non-operated isolated and syndromic craniosynostosis, looking at intracerebral blood flow and brain microstructures? (**Part I**)

- Are there any secondary effects of ICH and treatment on the brain of operated syndromic craniosynostosis patients, focusing on ventriculomegaly, Chiari and cortical thickness? (**Part II**)

We will discuss brain imaging in the pediatric craniosynostosis setting and the questions of the studies of this thesis. Finally, we will have a gander on the future perspectives.

The use of brain imaging in the pediatric setting

Magnetic resonance imaging (MRI) is an excellent tool to image and investigate the brain and is frequently used to design a personalized treatment plan for children with craniosynostosis. However, brain imaging in the first 2 postnatal years is challenging. Myelination is rapidly changing, which makes it hard to differentiate anatomically between grey and white matter on a T1w scan. Also, the skull malformations of the craniosynostosis patients provide an extra anatomical challenge. Because of these challenges, brain imaging studies for the pediatric setting are based on manual Arterial Spin Labeling (ASL) Regions of Interest (ROI) delineations of cortical regions and DTI could only be used by drawing tracts manually.[1-4]

In this thesis, we used a new technique of ASL registration to investigate the pediatric cerebral blood flow (CBF) and we used the new automated FSL as an automatic DTI delineation. These techniques are chosen because of the high reproducibility potential and regional accuracy. Yet, there are different points to remark. Large pediatric ASL studies and therefore standardized CBF values in pediatric patients are lacking. Also, to date, normal ranges of DTI measurements in children under the age of 4 years do not exist in literature. Lastly, both ASL as well as DTI are dependent on many

technical variables, such as the type of MRI scanner and the scanner settings. This makes comparing our studies with other studies challenging.

Part I. To what extent do primary brain abnormalities exist in non-operated isolated and syndromic craniosynostosis, looking at intracerebral blood flow and brain microstructures?

We investigated CBF and white matter integrity in non-operated children with isolated metopic suture synostosis and the white matter integrity in non-operated children with syndromic craniosynostosis.

Isolated metopic suture synostosis

In trigonocephaly patients the functional indication for surgery is debated. Whether premature closure of the metopic suture restricts brain development mechanically, and whether craniofacial surgery has a positive effect on development has never been proven. Previous studies show that operated patients with trigonocephaly are still at risk of developing mental deficiencies, behavioral problems, and delays in speech and language.[5, 6] This suggests surgery is not preventing impairment of cognitive development. However, we do not know what these outcomes will be without surgery. Literature describes that ICH is negligible in trigonocephaly patients (<2%) and that non-operated trigonocephaly patients have a normal intracranial volume compared to controls. [7 8] Also, studies have shown that some genetic mutations found in patients with trigonocephaly overlap with patients with developmental delay disorders, suggesting that the brain could be affected intrinsically.[9-11]

First, we investigated CBF of the frontal lobe in unoperated trigonocephaly patients by ASL. We found similar values in non-operated trigonocephaly patients compared to controls. This implies that metopic synostosis is not related to impaired perfusion in the frontal lobes up to the age of 18 months. In a second study, using DTI, microstructural parameters of white matter tracts of the frontal lobe of trigonocephaly patients were compared to those of controls aged 0-3 years. FA or MD of frontal lobe white matter microstructure in trigonocephaly were similar to controls. Findings from these two studies imply that both local CBF as well as white matter integrity are neither affected by compression of the metopic suture synostosis nor by a genetic cause at this age. However, at this young age the potential differences may have been too subtle or were not yet measurable with ASL or DTI due to the following reasons. First, from 0-2 years the brain is in the main phase of myelination. The timing of myelination is different per brain region and different per individual, which makes it difficult to interpret subtle diffusivity differences between patients and controls. Secondly, including healthy controls for this cohort was challenging because of the young age, what made exact age-matched controls impossible. Thirdly, we investigated whole tracts instead of zooming in to a voxel-based brain matter. Insight in more peripheral, localized, focal

brain properties, e.g. by white matter volume analysis or by voxel-based analysis, will improve our understanding of the pathophysiology of metopic synostosis.

Finally, we may have failed to identify a difference in DTI and ASL, because we excluded syndromic trigonocephaly patients. While specific gene mutations for metopic synostosis are rare, at least 6% of these patients have cytogenetic or chromosal abnormalities.[9] In literature only a minority of trigonocephaly patients develop mental retardation or borderline intellectual functioning. Van der Vlugt et al assessed IQ in 82 trigonocephaly patients. Mental retardation (IQ < 70) was present in 9 percent (n = 7) of the patients, which is elevated compared to the 2.5 percent in the general norm group. Borderline intellectual functioning (IQ 70 - 85) was present in 12 percent of the patients, which is similar to the expected 13.5 percent of the general population.[5] In this study trigonocephaly patients with additional extracranial anomalies had a significantly lower IQ compared to trigonocephaly patients without extracranial anomalies. These patients with other congenital anomalies could have overlapped with syndromic cases.[12] Therefore, early genetic screening of trigonocephaly patients to identify syndromic cases could be relevant for the prediction and follow-up of the neurocognitive development.

Syndromic craniosynostosis

Patients with syndromic craniosynostosis (sCS) show a large variation in intellectual disabilities and behavioural and emotional problems. Children with Apert syndrome or Muenke syndrome show the most cognitive, social, attentional and internalizing problems.[13] Syndromic craniosynostosis patients are at high risk for ICH (9-83% for Apert, 53-64% for Crouzon, 19-43% for Saethre-Chotzen and 0-4% for Muenke syndrome).[14-19] To get more understanding about the pathophysiology of these problems in syndromic craniosynostosis patients we zoomed in on the white matter architecture.

In this thesis we showed that, before any surgery, young syndromic patients have no significant differences in microstructural properties compared to controls. We compared our results (n= 54, age ranges 0-2 years) with the paper on DTI results of older, operated children with sCS (n= 58, age range 6-18 years). Both papers used the same tractography protocol by Rijken et al and both papers found FOHR being a significantly associated factor.[4] Rijken et al. found a similar FA in control subjects in comparison to the operated syndromic craniosynostosis patients. Diffusivity values (MD, RD and AD) of the mean white matter were significantly higher in patients compared with the control group. However, Rijken et al. did not take age into the analyses on operated craniosynostosis patients, while in pediatric DTI studies age is a significant factor for an increase in WM FA and decrease in MD.[20] Also, the control group was not age matched. Therefore, it could be possible that the significant difference between craniosynostosis and controls is in fact caused by the different distribution of age

(6-18 years). However, if we consider the significant difference as a real finding, several reasons can by hypothesized.

Perhaps, microstructural properties are affected by CBF. In unoperated syndromic craniosynostosis patients, Doerga et al showed that these patients with sCS < 1 year old have lower CBF than control subjects.[1] In their study, CBF of these patients normalizes with age and surgical treatment, but with a delay in the usual physiological peak in childhood. Whether this normalization is related to progressing age and maturation or to skull enlargement/ shunt treatment could not be identified. We can try to tie the results of both studies: CBF normalizes in time and diffusivity properties increase. This gives the suggestion that a lower CBF in patients with sCS < 1 years old may influence white matter properties at a later stage. According to this philosophy, a lower CBF in the first years of life provides a lower supply of oxygen, what subsequently leads to an increase in diffusivity properties in the following years. The normalization of CBF in time would be then the new balance with appropriate CBF for a decreased myelin quality. In this case, it would be interesting to investigate if these sCS children have more collateral arteries, a mechanism to accommodate for chronic lack of oxygen. Information on the effects of CBF on the long term is lacking. Literature reports contradicting findings on the relation of CBF and microstructural properties. Aslan et al. and Ouyang et al. observed a paradoxically inverse correlation: higher CBF tended to have a lower FA or AD, where higher CBF tended to have a higher RD.[21, 22] On the contrary, histological studies show highly perfused white matter underlying a highly perfused cortex.[23] This scenario would predict greater white matter integrity with higher CBF. Contradicting findings remain to be reconciled. In conclusion, to understand more about the relation between white matter and CBF in sCS patients, it will be important to assess both values from a corresponding MRI and per patient in the course of time.

Besides age and CBF, also gene mutations may influence microstructural properties over time. Mutations in genes encoding the fibroblast growth factor receptors (*FGFR*) – which are expressed during early embryonic development– are known to be involved in the pattern of abnormal skull development and also known to affect the development of brain tissue in sCS.[24-28] It is known that mutations in *FGFR-1* or *FGFR-2* are associated with decreased myelin thickness[29, 30] and that *FGFR* genes have a major influence on myelination of WM tracts by involving the development of oligodendrocytes.[29, 31, 32] *TWIST 1* (Saethre-Chotzen syndrome), a basic helix-loop-helix (bHLH) domain-containing transcription factor, plays an important role in cortical and mesodermal development.[33, 34] Wilson et all shows cortical surface area is significantly different for FGFR patients in comparison to controls. [35] Taking all of the above together, gene mutations may play a role in microstructural architecture.[16, 18, 36, 37 38, 39]

Finally, it would be of interest to assess which other extrinsic factors other than FOHR, for example OSA and abnormal skull growth, play a role in microstructural properties.

After all, extrinsic factors as FOHR, OSA and abnormal skull growth could be (surgically) treated.

In conclusion: no evidence has been found for intrinsic brain or CBF abnormalities in non-operated patients with isolated metopic suture synostosis aged from 0-2 years. In non-operated syndromic craniosynostosis patients aged 0-2 years, microstructural parameters of the white matter tracts in syndromic patients are comparable to those of controls aged 0-2 years. Enlargement of the ventricles, measured by FOHR, play a significant role on microstructural properties.

Part II. Are there any secondary effects of ICH and treatment on the brain of operated syndromic craniosynostosis patients, focusing on ventriculomegaly, chiari and cortical thickness?

In syndromic patients we see a mechanical distortion of the brain and development of ventriculomegaly and/or cerebellar tonsillar herniation secondary to development of suture synostosis.[16, 18, 36, 37 38, 39] To assess these secondary causes and/or effects of ICH in craniosynostosis patients, we undertook a longitudinal repeated measurement study to investigate the course of ventriculomegaly and the course of tonsillar herniation (TH) in Crouzon-Pfeiffer patients. Enlarged ventricles and the associated increase of intracranial pressure could cause damage to various brain regions, including white and grey matter.[40-42] On the cause of hydrocephalus in syndromic craniosynostosis patients, many theories have been postulated. To date the most accepted theories are 1. venous hypertension caused by impaired venous outflow at the skull base and 2. overcrowded posterior fossa causing tonsillar herniation and inducing obstruction of CSF circulation.[43, 44] However to date, no one unifying theory has been able to explain all variations of manifestations of hydrocephalus and TH. By investigating the course of ventriculomegaly, we discovered ventriculomegaly often presents before surgical treatment. The prevalence of tonsillar herniation increased as patients became older, even after the age of 5 years. Overall, in our study, the more common sequence is first occurrence of ventriculomegaly, followed by TH. One percentage point increase in FOHR was associated with a +1.6mm increase in tonsil position.

The impact of tonsillar herniation seems unpredictable. It can cause symptoms and signs such as a headache, neck pain, ataxia, muscle weakness, altered sensation and dysphagia. Neurological functioning is used as a factor in surgical decision making on treating TH. [45, 46] However, Doerga et al. shows that, in craniosynostosis patients, the absence/presence of symptoms provides no diagnostic certainty in ruling-in or ruling-out normal cerebellar tonsillar position, or TH>5 mm and/or syringomyelia.[47] The question arises how much of the treatment protocol should be focused on treating/stabilizing TH in case it is not progressive and without symptoms.[47-49] It would be helpful to identify a parameter that can predict which patient will develop TH and in

whom it will be progressive and symptomatic. [50] More strict cut off values for shunting in case of ventricular enlargement may be identified.

Previous studies demonstrate varying levels of cortical thinning and grey matter reduction related to the severity of hydrocephalus, in both children and animal models. Increasing ventricle size is associated with decreased neurodevelopment.[51, 52] Wilson et al. show almost two-thirds of patients with Crouzon-Pfeiffer syndrome develop ICH, and they exhibit—on average— global cortical thinning.[35] To prevent and/or treat ICH in patients with Crouzon-Pfeiffer syndrome, patients undergo cranial vault expansion. We studied the potential influence of frontal and occipital primary vault expansions on cortical thickness in the brain regions of the expanded skull. In this study we did not find a difference in the effect between frontal and occipital primary vault expansions and cerebral cortical thickness (regional or global). Next, we looked for local or regional effects related to synostosis pattern. The lambdoid synostosis could have a local effect or a more general effect by playing a role in crowding of the posterior fossa, which could affect venous and CSF outflow obstruction, which subsequently may cause intracranial hypertension in Crouzon patients.[53] In our study we did not observe local effects on the occipital lobes. However, widespread thinning was associated in patients who had synostosis of one or both lambdoid sutures, in which the greatest effect was seen in the cingulate and frontal lobe. These generalized effects and distant regional effects may be an effect of general ICH or this may be because of a varying degree of ICH sensitivity within the cortical regions of the brain. If there is a varying degree of sensitivity to ICH within brain regions, this may have to do with the different timing in myelination per brain region.

Wilson et al. revealed that detection of hydrocephalus or papilledema was independently associated with significant changes in cortical thickness.[35] At the Erasmus MC, fundoscopy and optical coherence tomography (OCT) are commonly used to screen for ICH. Given the correlation between papilledema and cortical thinning, it appears to be important to detect ICH at an earlier stage, even before papilledema can be detected. Because of the complexity of the pathogenesis of ICH in syndromic patients, further assessment on contributing factors is necessary. Moving towards a more preventative approach, screening on ventricular volume or CBF may prove to be valuable. Future studies should investigate these methods of ICH detection.

One of the compensatory mechanisms of ICH is the development or expansion of venous collaterals. The first, not yet published, pilot data of the Erasmus MC craniofacial research group show a strong relation: a high FOHR relates to a high systematic score on collaterals. Collaterals are identified on the first MRI scan and seem not to change over time in this pilot study. Even after shunt placement and improvement of FOHR, collaterals are still identified in the same way as earlier identified on the MRI scan.

This suggest aberrant venous outflow is congenitally defined in these patients, and remain recruited, even in a situation of normalized or treated ICP or ventriculomegaly.

To answer the second question '*Are there any secondary effects of ICH and treatment on the brain of operated syndromic craniosynostosis patients, focusing on ventriculomegaly, chiari and cortical thickness?'* with the studies undertaken in this thesis, ventriculomegaly and TH could be found as a cause of ICH with brain imaging. Screening on CBF reduction in relation to ventriculomegaly may be helpful in the follow up and treatment of ventriculomegaly in these children. We did not find a difference in the effect on cortical thickness (regional or global) comparing frontal and occipital primary vault expansion using brain imaging. Lambdoid suture synostosis showed to have a significant effect on the cortical thickness of the frontal lobe and cingulate gyrus. The possible impact of cortical thinning on neurocognitive development in craniosynostosis patients, needs to be investigated before drawing conclusions with respect to treatment. Also investigating the correlation of cranial shape and cortical thinning would give us information on the functional value of remodeling and reducing excessive height or volume.

Future perspectives

The identification of primary, inborn disorders of the brain as well as the identification of secondary brain disorders, their causes and their impact on outcome could guide us to a better screening policy with earlier and proper treatment to prevent sequelae.

To gain more understanding about the development of the brain in patients with trigonocephaly, future work should focus on several areas. At the age of 0-2 years old, we did not identify a significant difference in brain properties between trigonocephaly patients and controls using DTI and ASL. However, we may have missed subtle anomalies. Next to genetic screening on syndromic trigonocephaly patients, it would be of value to look at new techniques for more detailed analysis. With the new baby free surfer pipeline future studies could assess white matter volumes, cortical thickness volume and the brain by a voxel-based analysis. At this age from 0-2 years old, new opportunities open up in DTI as well. The baby Freesurfer has just been released to allow automated segmentation and surface extraction pipeline for T1-weighted neuroimaging data of infants 0-2 years. [54] In the Erasmus MC an extension of segmentation and skull stripping training datasets using T2w samples is now studied, as well as the registration of the deformed brain. Cortical thickness as well as cortical surface are both still powerful biomarkers that have been used in many clinical studies to assess a variety of neurologic and neurodevelopmental outcomes.[55, 56] Taking all of the above together, new innovative MRI techniques in relation to neurocognitive development assessment could improve risk stratification and expectation management of parents at the initial pre-operative MRI.

Assessing CBF and microstructural white matter properties in older trigonocephaly patients in relation with neurocognitive data would improve our ability to make longitudinal inferences at each stage of development. A study of both neurocognitive data and brain properties of 5-6 years old operated trigonocephaly patients compared with non-operated trigonocephaly patients, will learn us more about the added value of surgery.

In syndromic patients studying the effect of CBF and genetic profile on microstructural properties will give us more information on the pathophysiology and consequently the indication to treat these patients. In the future, it is important to design studies per syndrome and include patients in larger cohorts.

In syndromic craniosynostosis patients we aim to treat/prevent ICH. It would be important to further expand the research on the course of ventriculomegaly and tonsillar herniation. What would be the best severity threshold for FOHR? What role does time of increase and duration of ventriculomegaly have on neurocognitive functioning? Further studies may identify whether stable ventriculomegaly is as harmful as progressive ventriculomegaly, and if so, at what age, duration or cut-off point this should be treated. Knowing these answers, treatment could be aligned with these factors preventing loss of cognitive function.

Which degree of tonsillar herniation will cause symptoms and/or become progressive? In children with syndromic craniosynostosis and involvement of lambdoid sutures, the order of events and causes remain unclear. Is it crowding of the posterior fossa which causes functional stenosis of the aqueduct, with subsequent hydrocephalus and tonsillar herniation? Or is it tonsillar herniation that restricts the outflow of the 4th ventricle what subsequently causes progressive hydrocephalus? What is the role of venous obstruction? Does it generate engorgement thereby adding to posterior fossa crowding? A predictive tool on development of progressive ventriculomegaly for children at their first hospital visit would be of value. This would require a good understanding of the causes and potential interactions.

Also, the potential interaction of ventriculomegaly treatment by ventriculoperitoneal shunt (VPS) on the course of tonsillar herniation needs further study. CSF overdrainage and restricted skull growth as a result of the VPS, are associated with the occurrence of tonsillar herniation in non-synostosis patients and it is likely that the same phenomenon occurs in craniosynostosis patients. This mechanism may add to the finding that while ventricular size decreases over time the incidence of TH increases over time in craniosynostosis patients.

Furthermore, we would like to answer the question: How does ICH impact white matter development in the craniosynostosis brain? As we learned from this thesis,

pronounced thinning effect in the cingulate gyri in Crouzon patients is likely attributable to increased ICH. A study on regional cortical thickness and cortical surface in comparison to neurocognitive outcome would be of value. Also, it would be relevant to investigate what happens with the white matter volume of the cingulate gyrus and corpus callosum in case of ventriculomegaly. If white matter volume gets reduced by the progressive increase of ventriculomegaly by i.e. stretching of the fiber bundles or even because of cortical atrophy, which situation is reversible and what sequelae do we have to prevent? What clinical consequences does reduction of the white matter volume have on neurocognitive development?

Finally, because of the low prevalence of craniosynostosis, craniosynostosis teams worldwide could profit from multicenter prospective studies to elucidate the course of the development of craniosynostosis patients. It is clear that syndromic craniosynostosis differ substantially from each other and need to be analyzed per syndrome. Such larger study groups and a study set up per syndrome can only be realized by cooperation. To compare and understand different treatment philosophies it is essential to obtain clear definitions of clinical signs and surgical indications. A structural follow-up including clinical outcomes such as skull growth and shape, signs of raised ICP and long-term emotional, behavioral, and cognitive development outcomes will contribute to improving treatment for patients with craniosynostosis. International collaborations such as the European Reference Networks can be a great facilitator in performing this research.

REFERENCES

1. Doerga PN, Lequin MH, Dremmen MHG, et al. Cerebral blood flow in children with syndromic craniosynostosis: cohort arterial spin labeling studies. *J Neurosurg Pediatr* 2019:1-11
2. De Vis JB, Petersen ET, de Vries LS, et al. Regional changes in brain perfusion during brain maturation measured non-invasively with Arterial Spin Labeling MRI in neonates. *Eur J Radiol* 2013;82:538-543
3. Miranda MJ, Olofsson K, Sidaros K. Noninvasive measurements of regional cerebral perfusion in preterm and term neonates by magnetic resonance arterial spin labeling. *Pediatr Res* 2006;60:359-363
4. Rijken BF, Leemans A, Lucas Y, et al. Diffusion Tensor Imaging and Fiber Tractography in Children with Craniosynostosis Syndromes. *AJNR Am J Neuroradiol* 2015;36:1558-1564
5. van der Vlugt JJ, van der Meulen JJ, Creemers HE, et al. Cognitive and behavioral functioning in 82 patients with trigonocephaly. *Plast Reconstr Surg* 2012;130:885-893
6. Kelleher MO, Murray DJ, McGillivary A, et al. Behavioral, developmental, and educational problems in children with nonsyndromic trigonocephaly. *J Neurosurg* 2006;105:382-384
7. Cornelissen MJ, Loudon SE, van Doorn FE, et al. Very Low Prevalence of Intracranial Hypertension in Trigonocephaly. *Plast Reconstr Surg* 2017;139:97e-104e
8. Maltese G, Tarnow P, Wikberg E, et al. Intracranial volume before and after surgical treatment for isolated metopic synostosis. *J Craniofac Surg* 2014;25:262-266
9. Mocquard C, Aillet S, Riffaud L. Recent advances in trigonocephaly. *Neurochirurgie* 2019;65:246-251
10. Calpena E, Hervieu A, Kaserer T, et al. De Novo Missense Substitutions in the Gene Encoding CDK8, a Regulator of the Mediator Complex, Cause a Syndromic Developmental Disorder. *Am J Hum Genet* 2019;104:709-720
11. Reijnders MRF, Miller KA, Alvi M, et al. De Novo and Inherited Loss-of-Function Variants in TLK2: Clinical and Genotype-Phenotype Evaluation of a Distinct Neurodevelopmental Disorder. *Am J Hum Genet* 2018;102:1195-1203
12. Jehee FS, Johnson D, Alonso LG, et al. Molecular screening for microdeletions at 9p22-p24 and 11q23-q24 in a large cohort of patients with trigonocephaly. *Clin Genet* 2005;67:503-510
13. Maliepaard M, Mathijssen IM, Oosterlaan J, et al. Intellectual, behavioral, and emotional functioning in children with syndromic craniosynostosis. *Pediatrics* 2014;133:e1608-1615
14. Kress W, Schropp C, Lieb G, et al. Saethre-Chotzen syndrome caused by TWIST 1 gene mutations: functional differentiation from Muenke coronal synostosis syndrome. *Eur J Hum Genet* 2006;14:39-48
15. Marucci DD, Dunaway DJ, Jones BM, et al. Raised intracranial pressure in Apert syndrome. *Plast Reconstr Surg* 2008;122:1162-1168
16. de Jong T, Bannink N, Bredero-Boelhouwer HH, et al. Long-term functional outcome in 167 patients with syndromic craniosynostosis; defining a syndrome-specific risk profile. *J Plast Reconstr Aesthet Surg* 2010;63:1635-1641
17. Woods RH, Ul-Haq E, Wilkie AO, et al. Reoperation for intracranial hypertension in TWIST1-confirmed Saethre-Chotzen syndrome: a 15-year review. *Plast Reconstr Surg* 2009;123:1801-1810
18. Abu-Sittah GS, Jeelani O, Dunaway D, et al. Raised intracranial pressure in Crouzon syndrome: incidence, causes, and management. *J Neurosurg Pediatr* 2016;17:469-475
19. de Jong T, Rijken BF, Lequin MH, et al. Brain and ventricular volume in patients with syndromic and complex craniosynostosis. *Childs Nerv Syst* 2012;28:137-140

20. Cancelliere A, Mangano FT, Air EL, et al. DTI values in key white matter tracts from infancy through adolescence. *AJNR Am J Neuroradiol* 2013;34:1443-1449

21. Aslan S, Huang H, Uh J, et al. White matter cerebral blood flow is inversely correlated with structural and functional connectivity in the human brain. *Neuroimage* 2011;56:1145-1153

22. Ouyang M, Liu P, Jeon T, et al. Heterogeneous increases of regional cerebral blood flow during preterm brain development: Preliminary assessment with pseudo-continuous arterial spin labeled perfusion MRI. *Neuroimage* 2017;147:233-242

23. Madden DJ, Bennett IJ, Burzynska A, et al. Diffusion tensor imaging of cerebral white matter integrity in cognitive aging. *Biochim Biophys Acta* 2012;1822:386-400

24. Morriss-Kay GM, Wilkie AO. Growth of the normal skull vault and its alteration in craniosynostosis: insights from human genetics and experimental studies. *J Anat* 2005;207:637-653

25. Rijken BF, Lequin MH, Van Veelen ML, et al. The formation of the foramen magnum and its role in developing ventriculomegaly and Chiari I malformation in children with craniosynostosis syndromes. *J Craniomaxillofac Surg* 2015;43:1042-1048

26. Di Rocco C, Frassanito P, Massimi L, et al. Hydrocephalus and Chiari type I malformation. *Childs Nerv Syst* 2011;27:1653-1664

27. Britto JA, Evans RD, Hayward RD, et al. From genotype to phenotype: the differential expression of FGF, FGFR, and TGFbeta genes characterizes human cranioskeletal development and reflects clinical presentation in FGFR syndromes. *Plast Reconstr Surg* 2001;108:2026-2039; discussion 2040-2026

28. Raybaud C, Di Rocco C. Brain malformation in syndromic craniosynostoses, a primary disorder of white matter: a review. *Childs Nerv Syst* 2007;23:1379-1388

29. Furusho M, Dupree JL, Nave KA, et al. Fibroblast growth factor receptor signaling in oligodendrocytes regulates myelin sheath thickness. *J Neurosci* 2012;32:6631-6641

30. Azim K, Raineteau O, Butt AM. Intraventricular injection of FGF-2 promotes generation of oligodendrocyte-lineage cells in the postnatal and adult forebrain. *Glia* 2012;60:1977-1990

31. Chen ZF, Behringer RR. twist is required in head mesenchyme for cranial neural tube morphogenesis. *Genes Dev* 1995;9:686-699

32. el Ghouzzi V, Le Merrer M, Perrin-Schmitt F, et al. Mutations of the TWIST gene in the Saethre-Chotzen syndrome. *Nat Genet* 1997;15:42-46

33. Qin Q, Xu Y, He T, et al. Normal and disease-related biological functions of Twist1 and underlying molecular mechanisms. *Cell Res* 2012;22:90-106

34. Bildsoe H, Fan X, Wilkie EE, et al. Transcriptional targets of TWIST1 in the cranial mesoderm regulate cell-matrix interactions and mesenchyme maintenance. *Dev Biol* 2016;418:189-203

35. Wilson AT, Den Ottelander BK, De Goederen R, et al. Intracranial hypertension and cortical thickness in syndromic craniosynostosis. *Dev Med Child Neurol* 2020;62:799-805

36. Cinalli G, Spennato P, Sainte-Rose C, et al. Chiari malformation in craniosynostosis. *Childs Nerv Syst* 2005;21:889-901

37. Collmann H, Sorensen N, Krauss J. Hydrocephalus in craniosynostosis: a review. *Childs Nerv Syst* 2005;21:902-912

38. Tan K, Meiri A, Mowrey WB, et al. Diffusion tensor imaging and ventricle volume quantification in patients with chronic shunt-treated hydrocephalus: a matched case-control study. *J Neurosurg* 2018;129:1611-1622

39. Hattori T, Ito K, Aoki S, et al. White matter alteration in idiopathic normal pressure hydrocephalus: tract-based spatial statistics study. *AJNR Am J Neuroradiol* 2012;33:97-103

40. Zhang S, Ye X, Bai G, et al. Alterations in Cortical Thickness and White Matter Integrity in Mild-to-Moderate Communicating Hydrocephalic School-Aged Children Measured by Whole-Brain Cortical Thickness Mapping and DTI. *Neural Plast* 2017;2017:5167973

41. Fletcher JM, McCauley SR, Brandt ME, et al. Regional brain tissue composition in children with hydrocephalus. Relationships with cognitive development. *Arch Neurol* 1996;53:549-557

42. Olopade FE, Shokunbi MT, Siren AL. The relationship between ventricular dilatation, neuropathological and neurobehavioural changes in hydrocephalic rats. *Fluids Barriers CNS* 2012;9:19

43. Cinalli G, Sainte-Rose C, Kollar EM, et al. Hydrocephalus and craniosynostosis. *J Neurosurg* 1998;88:209-214

44. Sainte-Rose C, LaCombe J, Pierre-Kahn A, et al. Intracranial venous sinus hypertension: cause or consequence of hydrocephalus in infants? *J Neurosurg* 1984;60:727-736

45. Fuller JC, Sinha S, Caruso PA, et al. Chiari malformations: An important cause of pediatric aspiration. *Int J Pediatr Otorhinolaryngol* 2016;88:124-128

46. Aitken LA, Lindan CE, Sidney S, et al. Chiari type I malformation in a pediatric population. *Pediatr Neurol* 2009;40:449-454

47. Doerga PN, Rijken BFM, Bredero-Boelhouwer H, et al. Neurological deficits are present in syndromic craniosynostosis patients with and without tonsillar herniation. *Eur J Paediatr Neurol* 2020

48. Pomeraniec IJ, Ksendzovsky A, Awad AJ, et al. Natural and surgical history of Chiari malformation Type I in the pediatric population. *J Neursurg Pediatr* 2016;17:343-352

49. Tubbs RS, Lyerly MJ, Loukas M, et al. The pediatric Chiari I malformation: a review. *Childs Nerv Syst* 2007;23:1239-1250

50. Doerga PNdP, C.A.; Erler, N.E. ; van Veelen, M.L.C.; Mathijssen, I.M.J. . The course and interaction of ventriculomegaly and cerebellar tonsillar herniation in Crouzon syndrome over time. *submitted for publication* 2020

51. Paturu M, Triplett RL, Thukral S, et al. Does ventricle size contribute to cognitive outcomes in posthemorrhagic hydrocephalus? Role of early definitive intervention. *J Neurosurg Pediatr* 2022;29:10-20

52. Gmeiner M, Wagner H, Schlogl C, et al. Adult Outcome in Shunted Pediatric Hydrocephalus: Long-Term Functional, Social, and Neurocognitive Results. *World Neurosurg* 2019;132:e314-e323

53. Hayward R. Venous hypertension and craniosynostosis. *Childs Nerv Syst* 2005;21:880-888

54. Zollei L, Iglesias JE, Ou Y, et al. Infant FreeSurfer: An automated segmentation and surface extraction pipeline for T1-weighted neuroimaging data of infants 0-2 years. *Neuroimage* 2020;218:116946

55. McCauley SR, Wilde EA, Merkley TL, et al. Patterns of cortical thinning in relation to event-based prospective memory performance three months after moderate to severe traumatic brain injury in children. *Dev Neuropsychol* 2010;35:318-332

56. Almeida LG, Ricardo-Garcell J, Prado H, et al. Reduced right frontal cortical thickness in children, adolescents and adults with ADHD and its correlation to clinical variables: a cross-sectional study. *J Psychiatr Res* 2010;44:1214-1223

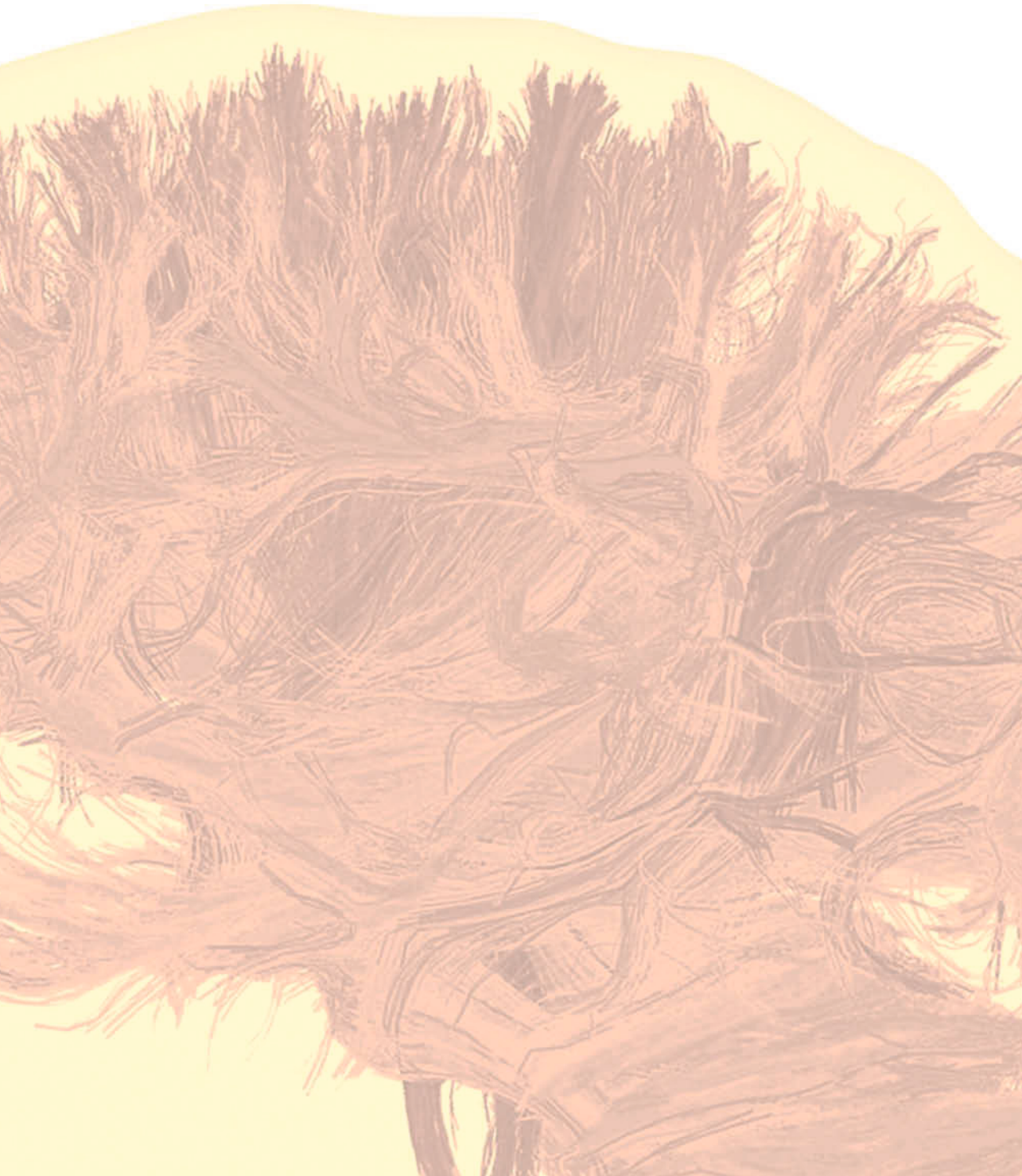

CHAPTER 11

SUMMARY

SUMMARY

Craniosynostosis patients are at risk for developing emotional, behavioral and cognitive disabilities. While the most important aim of surgical treatment is to strive for reducing the risk of developing intracranial hypertension (ICH), it remains unknown what the added value of surgery is with respect to neurocognitive outcome. Is brain development in craniosynostosis mainly affected by intrinsic brain abnormalities or by the potential effect of ICH through compression and subsequent reduced perfusion? This chapter will summarize the most important findings and the clinical implications following from this thesis.

Our first aim was to assess cerebral blood flow in children with craniosynostosis. The ongoing myelination in newborns and infants gives a low gray-white matter contrast on structural brain MRI images, which makes measuring cerebral blood flow in young craniosynostosis patients complicated. In **Chapter 2** we perform the first step of a new technical set up using the arterial spin labeling (ASL) cerebral blood flow (CBF) image as a contrast for spatial normalization instead of the structural image. Validating this new approach for the pediatric setting, ASL CBF contrast shows to be a viable alternative for use in spatial normalization when structural images have poor contrast.

After validating this approach, we further explore cerebral blood perfusion of the frontal lobe in non-operated trigonocephaly patients compared to controls, in **Chapter 3.** Our findings suggest that the frontal lobes of trigonocephaly patients aged under 18 months old have a normal CBF before surgery. In addition to the previously reported very low prevalence of papilledema or impaired skull growth, this finding further supports our hypothesis that craniofacial surgery for trigonocephaly is rarely indicated for signs of raised intracranial pressure or restricted perfusion for patients younger than 18 months. In **Chapter 4** we respond to a letter to the editor regarding this article. We go into detail about the concern that objective criteria are missing for wat constitutes true trigonocephaly or benign metopic ridge and we elaborate on the potential effect of sevoflurane.

With **Chapter 5** microstructural characteristics of the frontal lobe in non-operated trigonocephaly patients aged 0 to 3 years are analyzed. In this study we do not identify significant differences of microstructural parameters of the white matter frontal lobe between trigonocephaly patients and controls. This suggests both the absence of mechanical restriction of the synostosed metopic suture as well as the absence of intrinsically affected white matter. However, at this age, differences could be too subtle to measure with DTI or ASL.

In **Chapter 6** we perform a prospective diffusion tensor imaging MRI study in non-operated syndromic craniosynostosis patients aged 0-2 years. Before any surgery, microstructural parameters of white matter tracts of syndromic craniosynostosis patients are comparable to those of controls aged 0-2 years.

Subsequent analyses show that age and FOHR are associated factors. Enlargement of the ventricles plays a significant role on RD in the corpus callosum genu and the hippocampal segment of the cingulate bundle.

In **Chapter 7** the cortical thickness of the brain in Crouzon syndrome is assessed in relation to the area of vault expansion. This study does not find any difference in effect between frontal and occipital vault expansion on global and lobar cerebral cortical thickness. Lambdoid synostosis is shown to be associated with thinning across all brain regions, but particularly within the cingulate and frontal cortices. This leads us to question our hypothesis of localized growth restriction affecting underlying cortical lobes and to consider more how lambdoid synostosis contributes to intracranial pressure elevation and subsequent thinning in distant regions of the brain by causing e.g. a crowded posterior fossa and enlarged ventricles.

In **Chapter 8** the course of ventriculomegaly and cerebellar tonsillar position over time and its potential associations in children with Crouzon syndrome are investigated. We find that ventricular size in Crouzon patients is large at onset but decreases and stabilizes with treatment over time. Ventricular size is shown to be associated with head-circumference and tonsillar herniation. Irrespective of treatment, both the incidence of patients with tonsillar herniation as well as the severity of tonsillar herniation (in millimeter) itself show to increase over time, is strongly associated with lambdoid suture synostosis and ventricular size. Treatment aimed to correct ventriculomegaly is effective and may prevent tonsillar herniation in the long term, while (posterior) vault expansion appears to have little effect on the development of tonsillar herniation.

At last, **Chapter 9** dives into the rare and severe course of patients with Crouzon syndrome and acanthosis nigricans. Three European craniofacial centres have undertaken this multicentre study to assess clinical signs in relation to the required interventions and treatment course of these patients. This study reveals patients with the mutation c.1172C>A (p.Ala391Glu) in FGFR 3 gene follow a severe clinical course, requiring numerous interventions. Timing and order of interventions differs between patients and centers, but no obvious difference in outcome was related to this.

In conclusion this thesis shows the complexity of the course of patients with craniosynostosis. To answer the question if brain development in craniosynostosis is led by intrinsic brain abnormalities or the potential effect of ICH: the brain development is affected by both intrinsic genetic causes as well as the effect of ICH and its interconnected problems, such as hydrocephalus and tonsillar herniation. Further research is necessary to understand the clinical course and outcome in patients of non-syndromic craniosynostosis as well as the clinical course and outcome in patients with syndromic craniosynostosis. Finally, future studies should focus on to optimize the individual surgical treatment and to predict the clinical neurocognitive outcome.

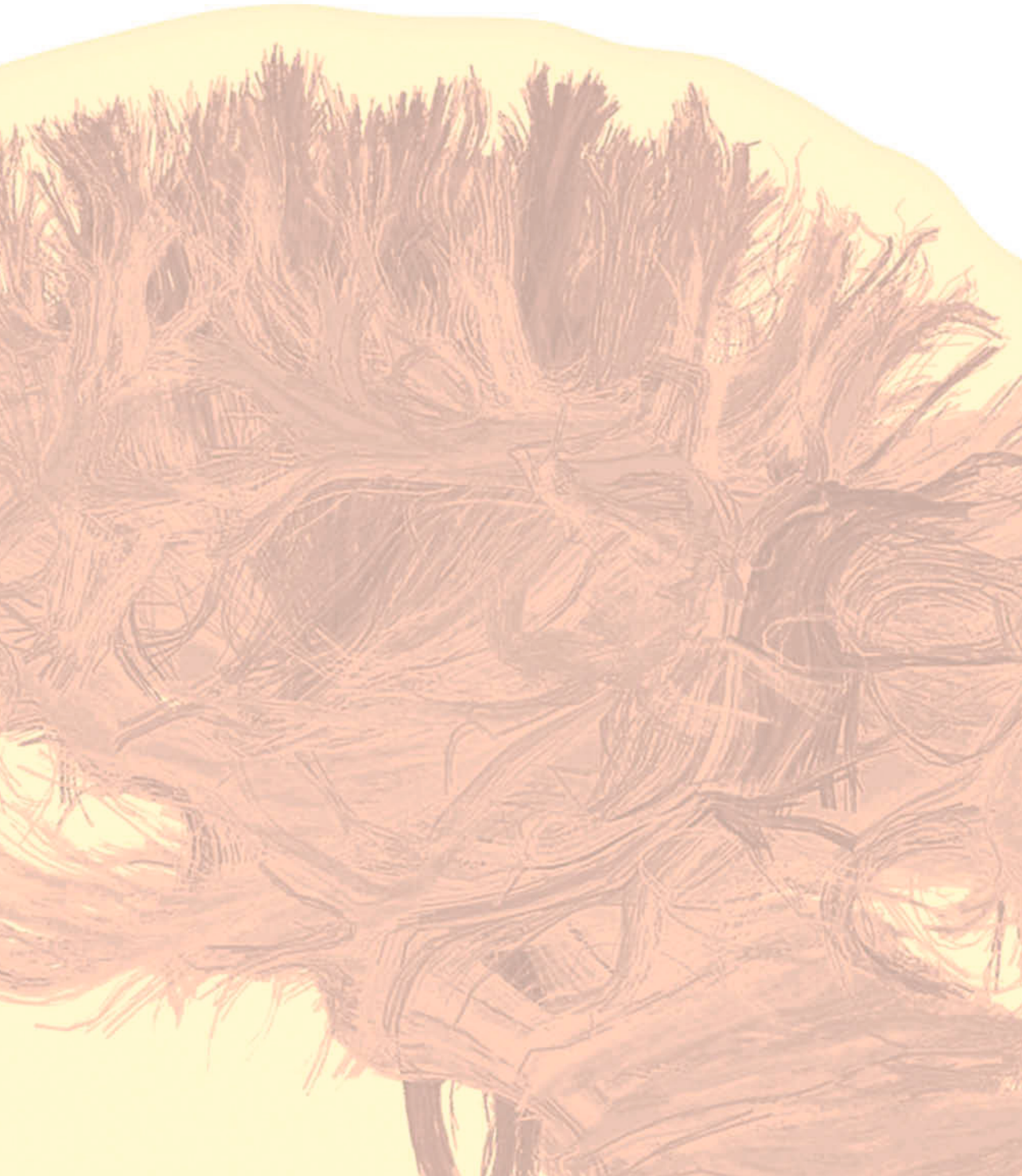

CHAPTER 12

NEDERLANDSE SAMENVATTING

NEDERLANDSE SAMENVATTING

Voor patiënten met craniosynostose is er een risico op het ontwikkelen van emotionele, gedrags- en cognitieve beperkingen. Hoewel het belangrijkste doel van de chirurgische behandeling is om het risico op het ontwikkelen van intracraniële druk te verminderen, blijft het onbekend wat de toegevoegde waarde van chirurgie is met betrekking tot de neurocognitieve uitkomst. Wordt de hersenontwikkeling bij kinderen met craniosynostose geleid door intrinsieke pre-existente genetische hersenafwijkingen of door het potentiële effect van verhoogde intracraniële druk? Dit hoofdstuk vat de belangrijkste bevindingen en de klinische implicaties van dit proefschrift samen.

Ons eerste doel was om de cerebrale doorbloeding te beoordelen bij kinderen met trigonocefalie. Het myeliniserende brein geeft bij pasgeborenen en jonge kinderen weinig contrast op structurele MRI-beelden van de hersenen, wat het meten van de cerebrale bloedstroom niet tot nauwelijks mogelijk maakt. In **hoofdstuk 2** voeren we de eerste stap uit naar een nieuwe technische manier, waar we het Arterial Spin Labeling (ASL) Cerebral Blood Flow (CBF) beeld als contrast gebruiken in plaats van het structurele anatomische beeld. Door deze nieuwe techniek voor de pediatrische setting te valideren, blijkt het ASL CBF-contrast een werkend alternatief te zijn wanneer structurele afbeeldingen een slecht contrast hebben.

In **hoofdstuk 3** gebruiken we deze nieuwe techniek om de cerebrale doorbloeding van de frontale kwab bij nog niet-geopereerde kinderen met trigonocefalie te onderzoeken in vergelijking tot een controlegroep. Onze bevindingen wijzen erop dat de frontale kwab van kinderen met trigonocefalie jonger dan 18 maanden een normale cerebrale doorbloeding hebben vóór de operatie. Na de eerder gepubliceerde zeer lage prevalentie van papiloedeem of verminderde schedelgroei, ondersteunt deze bevinding onze hypothese dat craniofaciale chirurgie voor kinderen met trigonocefalie jonger dan 18 maanden zelden geïndiceerd is door tekenen van verhoogde intracraniële druk of beperkte doorbloeding. In **hoofdstuk 4** reageren we op een brief aan de redactie gericht op dit bovenstaande artikel. We gaan in detail in op de zorg van de auteurs dat objectieve criteria ontbreken voor wat we klinisch beschouwen als een milde vorm tot de ernstige vorm van een wigschedel. Hierna gaan we in op het potentiële effect van narcose op de studie.

In **hoofdstuk 5** worden microstructurele kenmerken van de witte stof van de frontale kwab bij nog niet-geopereerde kinderen met trigonocefalie van 0 tot 3 jaar geanalyseerd middels Diffusion Tensor Imaging (DTI) MRI. In deze studie identificeren we geen significante verschillen in microstructurele parameters van de frontale kwab tussen kinderen met trigonocefalie en controles. Dit suggereert zowel de afwezigheid van een mechanische beperking door het te vroeg sluiten van de voorhoofdsnaad,

als de afwezigheid van pre-existente intrinsieke witte stof afwijkingen. Echter, op deze jonge leeftijd kunnen de verschillen te subtiel zijn om te meten met de brein MRI-technieken ASL of DTI.

In **hoofdstuk 6** voeren we een prospectieve DTI MRI studie uit bij nog niet geopereerde kinderen met syndromale craniosynostose met een leeftijd van 0-2 jaar. De uitkomsten laten zien dat voor de operatie de microstructurele parameters van de witte stof van patiënten met syndromale craniosynostose vergelijkbaar zijn met die van de controlegroep. Verder laten analyses zien dat leeftijd en FOHR geassocieerde factoren zijn. Hieruit concluderen we dat vergroting van het ventriculaire systeem een belangrijke rol speelt op de micro structurele eigenschappen van het corpus callosum genu en het hippocampus segment van de bundel van het cingulum.

In **hoofdstuk 7** wordt de corticale dikte van de hersenen bij kinderen met Crouzon-syndroom beoordeeld in relatie tot het gebied van schedel expansie. Met deze studie vinden we geen verschil in effect tussen een schedel verruimende operatie vanuit het voorhoofd en een schedel verruimende operatie vanuit het achterhoofd op de cerebrale corticale dikte. Lambdoid naad synostose, het te vroeg sluiten van de achterhoofdsnaad, blijkt geassocieerd te zijn met het dunner worden van corticale dikte in alle hersengebieden, maar vooral in de cingulate gyri en de cortex van de frontaal kwabben. Dit past niet bij de hypothese dat lambdoid naad synostose haar onderliggende corticale lobben aantast, maar meer bij de hypothese dat lambdoid naad synostose een gegeneraliseerde hersendrukverhoging veroorzaakt met het daaropvolgende dunner worden van de corticale dikte in verschillende hersengebieden.

In **hoofdstuk 8** wordt het verloop van ventriculomegalie (vergroting van de hersenkamers), en cerebellaire tonsillaire positie (stand van de kleine hersenen), in de tijd bij kinderen met het Crouzon syndroom onderzocht. We vinden dat de grootte van de ventrikels bij Crouzon-patiënten in het begin vaak te groot is, maar na verloop van tijd afneemt en stabiliseert, mede door behandeling. De grootte van de ventrikels blijkt geassocieerd te zijn met hoofdomtrek en tonsillaire herniatie. Ongeacht de behandeling vertoont tonsillaire herniatie zowel in incidentie als in ernst in de tijd toe te nemen, en is sterk geassocieerd met lambdoid naad synostose en met de grootte van de ventrikels. Behandeling gericht op het corrigeren van ventriculomegalie is effectief en kan op lange termijn een tonsillaire herniatie voorkomen, terwijl posterieure schedelexpansie weinig effect lijkt te hebben op het ontstaan van tonsillaire herniatie.

Ten slotte zoomen we in **hoofdstuk 9** in op het zeldzame en ernstige beloop van patiënten met het Crouzon-syndroom met het huidbeeld acanthosis nigricans. Drie Europese craniofaciale centra (Oxford, Parijs, Rotterdam) hebben samen deze studie uitgevoerd om de klinische symptomen te beoordelen in relatie tot de vereiste

interventies en het behandeltraject van deze patiënten. Deze studie laat zien dat patiënten met de mutatie c.1172C>A (p.Ala391Glu) in het FGFR 3-gen een ernstig klinisch beloop volgen, waarvoor multipele interventies nodig zijn. Timing en volgorde van interventies verschilt per patiënt en per centrum, maar er was geen duidelijk verschil te zien in uitkomst voor de patiënt.

Concluderend laat dit proefschrift de complexiteit zien van het beloop van patiënten met craniosynostose. Als antwoord op de vraag of de hersenontwikkeling van een kind met craniosynostose wordt geleid door intrinsieke pre-existente genetische hersenafwijkingen of door het potentiële effect van verhoogde intracraniële druk: de hersenontwikkeling wordt beïnvloed door zówel intrinsieke pre-existente genetische oorzaken als door het effect van verhoogde intracraniële druk met diens onderling verbonden problemen, zoals progressieve ventriculomegalie en tonsillaire herniatie. Meer kennis is nodig voor patiënten met unisuturale niet syndromale craniosynostose en voor patiënten met syndromale vormen van craniosynostose. Dit gezien de significante verschillen in uitkomst en in beloop tussen al deze typen van craniosynostose. Verder onderzoek is nodig om de individuele chirurgische behandeling te optimaliseren en de klinische neurocognitieve uitkomst te voorspellen.

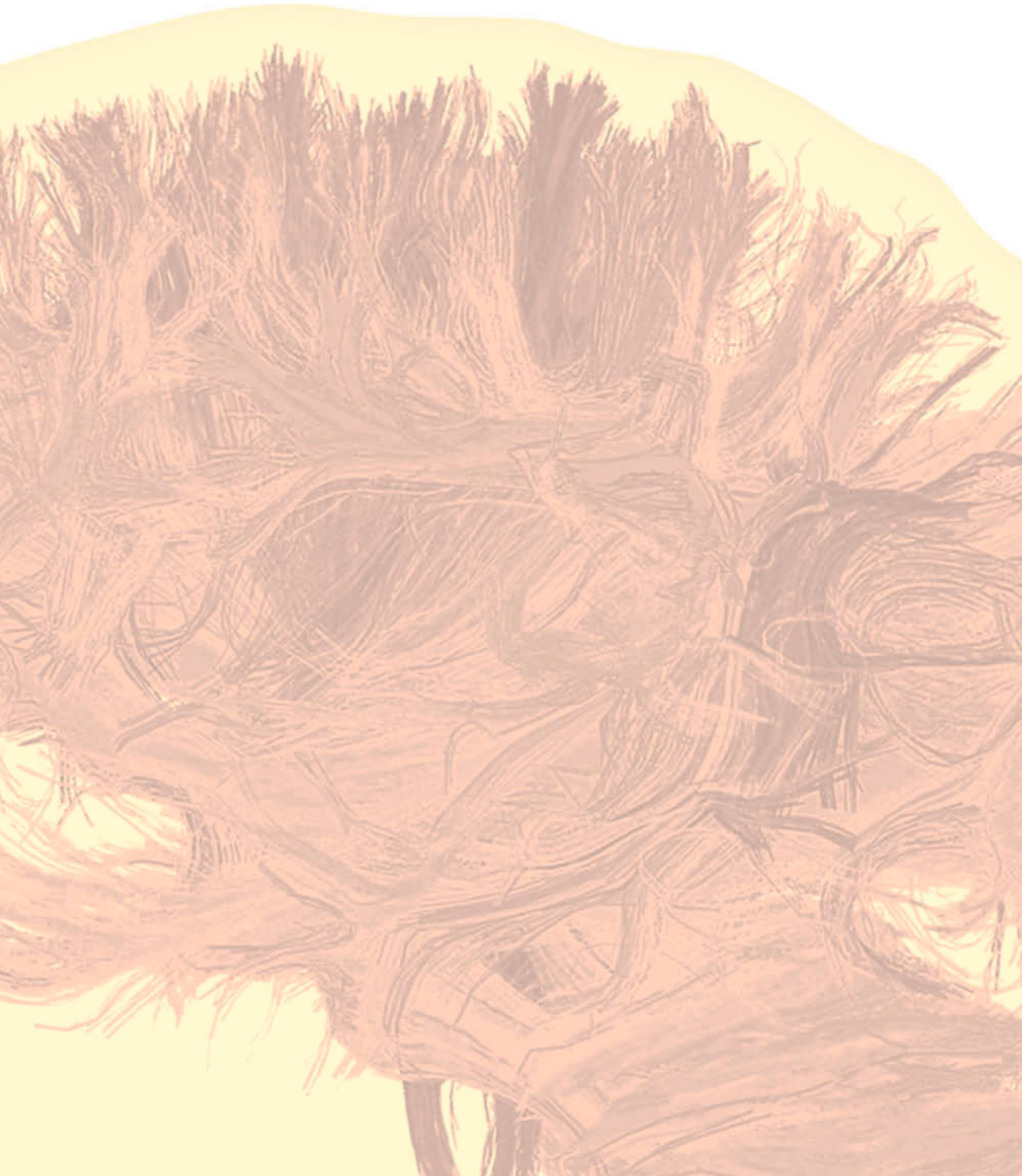

APPENDICES

LIST OF OTHER PUBLICATIONS

Risk factors for revision carpal tunnel release.
Westenberg R, Oflazoglu K, De Planque CA, Jupiter JB, Eberlin KR, Chen NC
Journal of Plast Reconstr Surg 2020 May;145(5):1204-1214.

Dorsal subluxation of the Proximal Interphalangeal Joint after volar base fracture of the middle phalanx.
Oflazoglu K , De Planque CA, Guitton TG, Rakhorst H, Chen N
Journal Hand (N Y) 2022 Jan;17(1):60-67.

Cervical Spinal Cord Compression and Sleep-Disordered Breathing in Syndromic Craniosynostosis.
Den Ottelander B, De Goederen R, De Planque CA, Baart SJ, van Veelen MLC, Corel LJA, Joosten KFM, Mathijssen IMJ, Dremmen MHG
American Journal of Neuroradiology. 2021 Jan;42(1):201-205.

Does the association between abnormal anatomy of the skull base and cerebellar tonsillar position also exist in syndromic craniosynostosis?
Den Ottelander B, De Planque CA, van Veelen MLC, Dremmen MHG, Vrooman HA, Mathijssen IMJ .
Journal of Plast Reconstr Aesthet Surg 2022 Feb;75(2):797-805.

Prenatal ultrasound parameters of twins with sagittal suture craniosynostosis question mechanical constraint as the leading cause.
Cinca KP, de Planque CA, Peters NCJ, Versnel SL, Mathijssen IMJ,
Accepted in the Journal of Craniofacial Surgery 2022

PHD PORTFOLIO

Summary of PhD training and teaching

Name PhD student: Catherine Annemiek de Planque
Erasmus MC Department: Plastic and Reconstructive Surgery and Hand Surgery
PhD Period: April 2018 – April 2021
Promotor: Prof. Dr. IMJ Mathijssen
Co Promotor: Dr. MLC van Veelen

PhD training	**Year**	**Workload (hours)**
General academic skills		
Systematic Literature Retrieval (PubMed 1+2) Course	2018	15
Systematic Literature Retrieval in Multiple Databases Course	2018	5
Introduction in R (NIHES PhD) Course	2018	10
Datacamp Introduction in R Course	2018	10
Endnote Course	2018	5
Scientific Integrity Course	2018	10
Basiscursus Regelgeving en Organisatie (BROK) 92%	2018	28
Open Clinica Course	2018	10
CE08 - Repeated Measurements (NIHES PhD)	2018	40
Microsurgery training	2018	200
Teaching		
Suture techniques-course for TU delft students	2018	20
Anatomy of hand and upper extremity (2-4th year medical students)	2018	60
Coach Microsurgery Course	2018	20
Supervising 4 students during their Master thesis	2018-2021	100
Other		
Research Suite: Use Case Craniosynostosis, I&T department, Erasmus MC	2018-2019	100
Redesigning OpenClinica Database	2018	50
Next Generation Women Leaders by McKinsey&Company	2022	24

Committees

Koers23, Wendbare Organisatie	2018	20
Nationale Denktank –McKinsey& Company	2018	640
Traumaplatform Conference 2019, Voorzitter	2018-2019	150
Bestuur Traumaplatform Foundation	2019-2022	100
NFU Werkgroep Circulaire Economie	2010	50
Taskforce een Duurzaam Erasmus MC	2019-2021	100

Oral Presentations

American Association for Hand Surgery, Phoenix, Arizona, USA	2018	40
Seminar 'Extreme Extremities', Traumaplatform Symposium, Davos, Zwitserland	2018	40
Presentatrice Erasmus MC Collegetour	2019	20
TED Talk: "Duurzaamheid in de zorg"	2019	20
XVIIIth meeting of the international society of craniofacial surgery Paris, Frankrijk	2019	40
International Society for Magnetic Resonance in Medicine, Toronto, Canada	2021	40

CURRICULUM VITAE

Catherine Annemiek de Planque (29-10-1991) was born and raised in Bussum, The Netherlands. She finished secondary education at the Gemeentelijk Gymnasium Hilversum in 2010.

Having many interests, she started with studying Law at the University of Groningen. After successfully completing one year of law degree, she switched to the study of Medicine at the University of Groningen. During her studies she performed research at the Hand and Upper Extremity Service, Orthopaedics at the Harvard Medical School, Massachusetts General Hospital, Boston, US (supervisor: Professor J.B. Jupiter and Dr. N. C. Chen). She graduated from Medical School in 2018. Straight afterwards she commenced work on her PhD supervised by Professor Dr. I.M.J. Mathijssen and Dr. M.L.C. van Veelen at the Erasmus Medical Centre (Erasmus MC), Rotterdam. This research was focused on brain imaging in craniosynostosis patients. During her PhD studies, she got the opportunity to participate in a four month fulltime program of the National Thinktank, led by McKinsey & Company. The theme of the program was: "How could we accelerate the transition towards a circular economy?" Being inspired by this program, she was able to use her acquired knowledge towards sustainable health care by starting sustainability projects in the Erasmus MC and participating in the Taskforce Sustainability of the Erasmus MC. During the COVID pandemic she lived in Copenhagen, Denmark.

After three years study of research, she started working as a doctor at the General Surgery Department in the Onze Lieve Vrouwe Gasthuis (OLVG) hospital Amsterdam (supervisor: Dr. M.F. Gerhards). Having decided for personal reasons that her future is in the Netherlands and abroad, she switched to work as doctor at the Pediatric Department in the OLVG hospital in Amsterdam (supervisor: Drs. M.E. Op de Coul). With ten months of experience in surgery and five months of experience in pediatrics, she started her residency becoming a general practitioner.

DANKWOORD

Dit proefschrift is tot stand gekomen dankzij de bijdrage van velen. In de afgelopen jaren heb ik vanuit alle windstreken hulp gekregen van collega's, familie en vrienden, waarvoor ik mijn dank wil betuigen.

In de eerste plaats mijn promotor. Prof. Dr. I.M.J. Mathijssen. Beste Irene, ik ben zeer dankbaar voor de ruimte die je mij hebt gegeven gedurende mijn promotietraject. Je gaf me de vrijheid om mijn eigen weg te bewandelen en eigen ideeën uit te voeren. En daar ging ik. Tijdens mijn sollicitatiegesprek voor dit PhD traject vroeg ik je naar de mogelijkheden om te participeren in de Nationale Denktank tijdens mijn PhD. Je gaf me deze mogelijkheid. Met veel plezier heb ik een half jaar fulltime meegewerkt aan de Denktank. Ook mocht ik de technische uitdaging aangaan om een stap in de transitie van handmatig meten naar automatisch meten te bewerkstelligen. En gedurende de jaren kwamen zo vele projecten langs: meedenken met de UseCase Cranio, mij inzetten in de Taskforce Duurzaamheid, een TED talk geven over Duurzaamheid in de zorg en Erasmus College Tour presenteren. Ik heb mij zo op een bijzondere wijze persoonlijk en wetenschappelijk kunnen ontwikkelen. Promovendi zoals ik (snel enthousiast over vele onderwerpen) zijn niet de makkelijkste groep om onder je vleugels te hebben. En toch heb ik altijd op je scherpe kritische blik en je support kunnen rekenen. Je hebt veel tijd voor me genomen en ik heb veel van je geleerd. Dank je wel voor het vertrouwen.

Mijn copromotor Marie-Lise. Jouw neurochirurgische blik en vaste begeleiding voor dit proefschrift heb ik als zeer plezierig ervaren. Een kritische mentor, maar ook een mentor waar tijd was om de dag, de uitdagingen bij het opzetten van het craniofaciaal centrum of de situatie thuis met vacuümtentjes ter voorbereiding van beklimming van de Kilimanjaro, te bespreken. Met veel plezier kijk ik hierop terug. Veel dank voor jouw hulp, advies en de mogelijkheid om in jouw kielzog te promoveren. Succes de aankomende tijd met het kinderhersencentrum!

Marjolein, met jouw expertise als kinderradioloog, heb je mij vanaf moment één geholpen mijn radiologische promotietraject te volbrengen. Je nam de tijd om mij MRI's en CT's te leren begrijpen, te meten, en om menig 'simpel chirurgisch geschreven' manuscript vanuit radiologisch oogpunt te corrigeren. Een onmisbare bijdrage aan de meerderheid van de in dit proefschrift beschreven studies. Dank daarvoor!

Aan mijn promotiecommissie ben ik veel dank verschuldigd. Dank u wel voor uw interesse en de tijd die u heeft genomen om mijn proefschrift te beoordelen. Ik kijk ernaar uit om met u van gedachten te wisselen over de inhoud.

Hartelijk dank aan alle ouders en patiënten, die ten behoeve van de wetenschap, hun persoonlijke ziekenhuisdata en scans beschikbaar stelden.

Alle medeauteurs. Dank voor jullie waardevolle input, zonder welke dit proefschrift niet tot stand was gekomen.

Vijftiende verdieping genoten; Robbin, Xavier, Steph, Bianca, Mark, Ralph, Pleun, Saranda, Sumin, Jaap, Joris, Babette, Linda en Alex. Dank jullie wel voor een heerlijke tijd op de vijftiende! Of we alledaags onze dag startten met een goede kop koffie om het leven te bespreken, we les gaven tussen de anatomische preparaten, in een escape room stonden, wonnen tijdens de Erasmus PhD pubquiz of roetsjten door de sneeuw in Oostenrijk, het was een feest om met jullie deze jaren te beleven! Succes met de aankomende stappen!

En Linda in het bijzonder, wat was onze samenwerking waardevol! Wat hebben we samen mooie publicaties geschreven. Dank je wel!

Henk-Jan en Jan, dank voor jullie samenwerking op het gebied van ASL. Dankzij jullie expertise en pipeline konden we een automatiseringsslag maken in het gebruik van ASL MRI bij kinderen met craniosynostose en hebben we zowel een technisch als klinisch paper samen kunnen schrijven!

Henri en Esther, dank jullie wel voor alle tijd en het realiseren van een automatiseringsslag in het gebruik van DTI MRI bij kinderen met craniosynostose. Samen hebben we toch heel wat tijd doorgebracht met sparren, trekken, duwen, vastlopen, runnen, en soms zelfs terug naar start. Om zo van voor af aan alles opnieuw te proberen. Dankzij jullie werk hebben we prachtige publicaties teweeggebracht!

Nicole, dankzij jouw tijd en energie zijn de analyses van dit proefschrift van statistisch goede kwaliteit. Dank voor je flexibiliteit om te overleggen, moeilijke R scripts opnieuw te runnen en samen de ventriculomegaly dataset van boven tot onder statistisch te bekijken!

Manja en Esther, vele uren heb ik, tegenover elkaar zittend en samen kijkend door de microscoop, van jullie mogen leren om kundig te worden in de microchirurgie. Met veel plezier! Ik verheugde me elke keer weer om op het skillslab te mogen zijn!

Usecase groep Marcel, Raoul en Darryl, met veel plezier kijk ik terug op onze meetings en op onze laatste eindsprint: de hackathon, die ervoor zorgde dat data veilig en waardevol uit HIX gehaald kunnen worden. Dit in plaats van het handmatige overschrijf(monniken)werk wat we als PhD-ers nog vaak doen. Dankzij jullie stappen

kunnen de komende PhD-ers vraagstukken met grote hoeveelheid data nauwkeurig oplossen!

Leden van de Taskforce, Lex, Hans-Peter, Frans, Karin, Rob, Laura en Alie. Wat was het een avontuur om met jullie de Taskforce op te zetten! We genoten van elkaars realisme, pessimisme, optimisme en de ambitie binnen de groep om projecten te realiseren! Het ga jullie goed, ik sta achter jullie!

Maarten, Nicole en Team Metabolic. Ik heb genoten om samen met jullie het bijzondere IC project neer te zetten. Een IC-duurzaamheidsrapport om trots op te zijn! Door deze trein op te zetten en te laten rijden komen er veel duurzaamheidsprojecten van de grond!

Carin, als secretaresse van Irene, help je PhD-ers ook nog eens hun promotie tot een goed einde te brengen. Het gaf me vertrouwen om alle stappen samen met jou te doorlopen! Dank je wel voor al je hulp!

Robin, wat een voorkant! In Denemarken hadden we onze eerste Teams meeting, ik weet het nog heel goed! Dat was achteraf misschien ietwat vroeg en wat naïef enthousiast, maar wat was het leuk om meermaals te sparren over de voorkant van het boek. En wat ben ik nu blij met het resultaat. Met een knipoog naar Denemarken! Dank je wel!

Dr. Gerhards en Drs. Op de Coul, dank jullie wel voor het vertrouwen dat jullie mij gaven in het OLVG om als anios Chirurgie en later als anios Kindergeneeskunde aan de slag te gaan. Wat heb ik veel mogen leren en bovenal wat heb ik het naar mijn zin gehad!

Job, Prof. Dr. Doornberg, inspirator, wat is je onuitputtelijke energie aanstekelijk! Ik vind het waardevol en bovenal gezellig om te sparren over de toekomst van de traumazorg, te leren over buitenland avonturen, te dromen over een Traumaplatform-marathon in Boston, of om een marathon te langlaufen in Davos!

Wout, ik moet nog steeds denken aan het moment op Ameland dat jullie mij vroegen plaats te nemen in het 3-koppige Traumaplatformbestuur. Jouw lach is aanstekelijk, of we op een Waddeneiland staan, in de sneeuw of in de kroeg! Je bent de realist, en houdt ons met beide benen op de grond! Jij maakt het traumaplatform tot wat het is!

TEAM Traumaplatform, Lars, Merel, Caroline, Coen en Nils-Jan, wat was het leuk om samen met jullie een weekend Ameland op te tuigen! Met veel plezier denk ik terug aan de opstijgende F16's, waanzinnige presentaties en onze triatlon op Ameland! Succes jongens, jullie zijn goud waard!

Denktankers, wat hebben we veel met en van elkaar geleerd! Onze denktank periode heeft ons een hecht team gemaakt en zo hebben we vaak aan een half woord genoeg! Als we elkaar zien, praten we verder over onze dromen, impact maken, en hoe we het verschil kunnen maken in de wereld! Allemaal ministers van duurzaamheid in de dop! En bovenal, dierbare vrienden!

Kære Guacasquad og Danske Paella, tiden i København er mig kær!

Foxies, al 12 jaar delen we lief en leed, wat gaat de tijd snel! Dat er nog heel veel mooie momenten zullen volgen!

Schiergroep, ik hoop dat we nog vele jaren ons zomerse weekenden door kunnen zetten! Wat een bijzonder pad bewandelt iedereen!

Joen, wat heb je dit proefschrift aan de zijlijn zien groeien! Verhalen over ratten, paranimfen, kreeft, werken aan het Quecha opklap tafeltje, tussentijdse champagne momenten, je was erbij! En vandaag gaan we het vieren!

Professor Zwierstra, er zijn maar een paar mensen die, op de momenten dat je bij een tweesprong komt in je leven, je de goede weg wijzen. U bent een van die personen.

Lief Pension Riant, jullie zijn hier ook een vermelding waard. Altijd op de achtergrond aanwezig, altijd op de hoogte en er is altijd tijd voor ontspanning, een kop thee of voor tranen van het lachen. Wat een feest om jullie dichtbij te hebben! Zin om dit samen met jullie te vieren!

Lieve familie Boogaart, van jullie leer ik dat dromen mag en dat ze met doorzettingsvermogen werkelijkheid kunnen worden!

Lieve Oma, naamgenoot, wie weet bent u erbij en anders laat ik gauw de foto's zien!

Lieve tante Madelien en oom Jim, veel dank voor het helpen schrijven van 'mooi Engels' en het leren presenteren. *"And last, but not least, I can bake you a delicious apple pie!"*

Lieve tantes en ooms, nichten en neven, dank voor al het sparren over de toekomst!

Lieve Willemijn, sans doute, wat ben ik blij je dichtbij te hebben en van je te leren! Van de vroegere disneyliedjes, tot speeches en levenslessen! Je gezelligheid en wijze raad zijn me dierbaar!

Lieve Acettie en Piena, lieve paranimfen, lieve powervrouwen, een dijk van vertrouwen geeft het om jullie vandaag aan mijn zijde te hebben. Pien, ik weet zeker dat je alle moeilijke medische vragen met verve gaat beantwoorden, mocht het nodig zijn. En Acettie, we zien elkaar op de Magere Brug!

Lieve Bart en lieve Maud, lieve broer en zusje, (bijna) mijn hele leven zijn jullie een bepalende factor geweest in de persoon die ik geworden ben. Jullie bewandelen je eigen paden en toch weten we elkaar te vinden. Ik ben trots op jullie! Het boek is af! Ik verheug me om dit samen met jullie te vieren!

Lieve Pap en Mam, zonder jullie was ik er überhaupt niet geweest, maar los daarvan was dit proefschrift zonder jullie niet tot stand gekomen. Ik voel me zeer bevoorrecht en dankbaar dat ik in zo'n warm nest ben opgegroeid en alle kansen en mogelijkheden heb gekregen om te worden wie ik nu ben.

Lieve Pap, jouw wijsheid en kritische vragen geven me energie om het beste uit mezelf te halen. Je hebt me doorzettingsvermogen en ambitie meegegeven. Je bent mijn beste en hoogst gewaardeerde adviseur. Dankjewel daarvoor. De Sound of Music zal niet aanstaan vandaag… toch ben ik benieuwd ;)

Lieve Mam, dank voor alle liefde en vertrouwen die ik van jou heb gekregen! Jij leert me om met beide benen op de grond te staan en tevreden te zijn. En de mens te zien zoals hij of zij is. Dit alles neem ik nu dagelijks mee, zeker ook in het huisartsen vak! Met blijdschap kijk ik terug op alle tijd, warmte, liefde en stabiliteit die je mij hebt gegeven.
Lieve mam, omdat jij altijd het beste voor mij wilt.
Dit proefschrift is voor jullie.

Lieve Luuk, het boek is af! Het proefschrift dat Delft, Copenhagen, Rotterdam, Trondheim, Spitsbergen, Rotterdam, opnieuw Copenhagen, Kingston upon Hull, en Amsterdam heeft meegemaakt. Op vele plekken op de wereld zijn er stukken PhD geschreven. Dit PhD traject heeft de ruimte gegeven om samen een onvergetelijke tijd in Kopenhagen te hebben, waar de liefde voor het buitenland extra is aangewakkerd! Dank je wel voor de vele uren luisterend oor, je adviezen en humor, die deze PhD mede mogelijk hebben gemaakt!
Jouw positiviteit en grenzeloze energie om projecten op te pakken en de wereld te ontdekken is groot! Ik verheug me om samen met jou dromen waar te maken en de wijde wereld in te gaan: waar de wind ons heen blaast!
Luuk, ben trots op jou en hou van jou!